BERGISCHE
UNIVERSITÄT
WUPPERTAL

Photosymbiotic Sea Slugs as Holobiont Model Systems

Symbiont Diversity, Microbiome Dynamics, and Responses to Metal Stress

DISSERTATION

zur Erlangung des Doktorgrades (Dr. rer. nat)
der Fakultät fur Mathematik und Naturwissenschaften
der Bergischen Universität Wuppertal

angefertigt am

Lehrstuhl für Zoologie und Biologiedidaktik

vorgelegt von
Corinna Sickinger

Wuppertal, 2025

Erstgutachterin: Prof'in Dr. Angelika Preisfeld, Bergische Universität Wuppertal

Zweitgutachter: Prof. Dr. Gregor Christa, Bergische Universität Wuppertal

"Je mehr du weißt, desto mehr weißt du, dass du nichts weißt."

Aristoteles

Contents

Summary **1**

Introduction **3**

Results **13**

1 Diversity of Symbiodiniaceae (Dinophyceae) in the Sea Slug Clade Cladobranchia (Nudibranchia) **16**
1.1 Abstract . . . 16
1.2 Introduction . . . 17
1.3 Materials and Methods . . . 19
1.4 Results . . . 22
1.5 Discussion . . . 25
1.6 Conclusion . . . 28

2 Collectin-12 – A Promising Symbiont Recognition Receptor in *Berghia stephanieae* (Á. Valdés, 2005) **36**
2.1 Abstract . . . 36
2.2 Introduction . . . 37
2.3 Materials and Methods . . . 39
2.4 Results . . . 43
2.5 Discussion . . . 43
2.6 Conclusion . . . 46

3 The Phototactic Behavior of the Kleptoplastic Sea Slug *Elysia viridis* (Montagu, 1804) is not Connected to the Photosynthetic Activity of Kleptoplasts **50**
3.1 Abstract . . . 50
3.2 Introduction . . . 51
3.3 Materials and Methods . . . 52
3.4 Results . . . 54
3.5 Discussion . . . 57
3.6 Conclusion . . . 59

4 Photosymbiosis Shapes the Microbiome of the Saccoglossan Sea Slug *Elysia viridis* (Montagu, 1804) **63**
4.1 Abstract . . . 63
4.2 Introduction . . . 64
4.3 Methods . . . 66
4.4 Results . . . 67
4.5 Discussion . . . 70
4.6 Conclusion . . . 73

5 Microbiome Origin and Stress-Related Changes in Bacterial Abundance of the Photosymbiotic Sea Slug *Berghia stephanieae* (Á. Valdés, 2005) 81
5.1 Abstract . . . 81
5.2 Introduction . . . 82
5.3 Methods . . . 84
5.4 Results . . . 86
5.5 Discussion . . . 91
5.6 Conclusion . . . 96

6 Nickel and Cobalt Disrupt the Microbiome and Metabolic Function of the Photosymbiotic Sea Slug *Berghia stephanieae* (Á. Valdés, 2005) 105
6.1 Abstract . . . 105
6.2 Introduction . . . 106
6.3 Materials and Methods . . . 108
6.4 Results . . . 111
6.5 Discussion . . . 117
6.6 Conclusion . . . 120
6.6.1 Additional File 6 . . . 121

7 Cobalt and Nickel Inhibit the Ontogenesis of the Cladobranch Sea Slug *Berghia stephanieae* (Á. Valdés, 2005) 128
7.1 Abstract . . . 128
7.2 Introduction . . . 128
7.3 Materials and Methods . . . 129
7.4 Results . . . 130
7.5 Discussion . . . 133
7.6 Conclusion . . . 134

Discussion 138

Outlook 151

Bibliography 152

Acknowledgements 187

Declaration of Authorship 189

List of Figures

1 Evolution of photosymbiosis in Heterobranchia 4
2 Morphology and microscopic details of *Elysia viridis*. 5
3 Evolution of functional kleptoplasty in Sacoglossa 6
4 Morphology and microscopic details of *Berghia stephanieae*. 7
5 Evolution of photosymbiosis in Cladobranchia. 8
6 Holobiont concept. 9

1.1 A variety of cladobranch species 17
1.2 Relative abundance of Amplicon Sequence Variances (ASVs) and Defining Intragenomic Variant (DIV) profiles of different cladobranch species. 23
1.3 Boxplots showing Shannon diversity indices of Symbiodiniaceae in various cladobranch species. 24
1.4 Non-Metric Multidimensional Scaling (NMDS) analysis based on Bray-Curtis distance matrix. 26

2.1 *Berghia stephanieae* (Á. Valdés, 2005) and close-up of the cerata. 37
2.2 *In situ* HCR protocol. 41
2.3 Preliminary spatial transcriptomic data for *B. stephanieae*. 44
2.4 *In situ* HCR results in sections of *B. stephanieae.* 45

3.1 Scheme of the experimental phototaxis setup. 54
3.2 Relative time of individuals of *Elysia viridis* spent in the illuminated and shaded area. 55
3.3 Number of changes of individuals of *Elysia viridis* between areas 56

4.1 Principal Coordinate Analysis (PCoA) plot of alpha- and beta-diversity and Venn diagrams comparing core microbiome composition of *E. viridis* under different feeding conditions. 68
4.2 Core microbiome of *E. viridis* under different feeding conditions. 69
4.3 Taxonomy-based functional profiling of bacterial communities of *E. viridis* under different feeding conditions. 70

5.1 Relative frequency of the most abundant bacterial families of *E. diaphana* and *B. stephanieae* kept under different feeding and light conditions. 87
5.2 Core microbiome of *E. diaphana* and *B. stephanieae* kept under different husbandry conditions. 89
5.3 Venn diagrams comparing core microbiome composition of *E. diaphana* and *B. stephanieae*. 89
5.4 Principal Coordinate Analysis (PCoA) plot of alpha- and beta-diversity of *E. diaphana* and *B. stephanieae* under different husbandry conditions. 90
5.5 Taxonomy-based functional profiling of bacterial communities of *E. diaphana* and *B. stephanieae* under different husbandry conditions. . . . 92

6.1 Alpha- and beta-diversity of *B. stephanieae*'s microbiome exposed to different nickel and cobalt concentrations. . . . 113
6.2 Core microbiome of *B. stephanieae* treated with different cobalt or nickel concentrations. . . . 114
6.3 Venn diagrams comparing core microbiome composition of *B. stephanieae* exposed to different nickel and cobalt concentrations. . . . 115
6.4 Taxonomy-based functional profiling of bacterial communities of *B. stephanieae* exposed to different Ni and Co concentrations. . . . 116

7.1 Egg mass of *B. stephanieae* and close-up of egg mass with eggs in the multicell stage . . . 131
7.2 Egg development under cobalt exposure. . . . 132
7.3 Egg development under nickel exposure. . . . 133
7.4 Successful symbiont recognition and maintenance in the sea anemone *Exaiptasia diaphana* . . . 141
7.5 Potential bacterial sulfate reduction in *E. viridis* treated with Monolinuron. . . . 145
7.6 Potential bacterial nitrogen cycle in fed and starved *B. stephanieaea*. . . . 146

List of Tables

1.1 Clade and genus names of the 12 genera described and accepted for the family Symbiodiniaceae 18

6.1 Concentration of cobalt and nickel used for the toxicity range finding test and ICP OES analysis. Concentrations correspond to elemental cobalt measured with ICP OES. For each group n = 5. 109
6.2 Concentration of cobalt and nickel used for microbiome analysis. Concentrations correspond to elemental cobalt measured with ICP OES. . 109

7.1 Concentration of cobalt and nickel used for the egg toxicity test and the regarding group names. 130

Summary

This dissertation explores the complex and fascinating biology of photosymbiotic sea slugs, molluscs that have independently evolved a form of photosymbiosis. Photosymbiosis is a nutritional symbiosis in which a heterotrophic host partners with a photosynthetic organism, gaining organic carbon and other metabolites derived from photosynthesis in exchange for shelter, nutrients, and protection. Situated at the intersection of symbiosis research, microbiome ecology, and ecotoxicology, this dissertation combines molecular, ecological, and behavioural approaches to better understand the dynamics of these multipartite associations and their vulnerability to environmental stress. Two model systems are central to the work: the kleptoplastic sacoglossan *Elysia viridis* (Montagu, 1804), which sequesters and maintains algal chloroplasts, and the cladobranch *Berghia stephanieae* (Á. Valdés, 2005), which incorporates intact dinoflagellate symbionts of the family Symbiodiniaceae from its cnidarian prey.

The research begins by situating photosymbiosis within a broader evolutionary and ecological context. Photosymbiosis is shown to be a recurring strategy among marine heterobranch gastropods. These associations are highly diverse and shaped by the identity of the symbionts, the physiology of the host, and the surrounding ecological conditions. By framing sea slugs within the holobiont concept, the dissertation emphasises that photosymbiosis does not occur in isolation but is part of a larger network of interactions, including symbiotic bacteria, contributing to host function and health. To investigate the diversity and stability of photosymbiosis in Cladobranchia, high-throughput metabarcoding of the slugs' photobionts (Symbiodiniaceae) was employed. The results reveal genus- and species-specific patterns, with stable symbioses, meaning a maintenance of the photobiont for more than two weeks, most consistently linked to the Symbiodiniaceae genus *Cladocopium*, whereas unstable symbiosis (maintenance of the photobiont for some days) tend to involve *Symbiodinium* or *Breviolum*. Building on this, molecular analyses of *Berghia stephanieae* identify Collectin-12, a C-type lectin, as a candidate receptor involved in photobiont recognition. Spatial transcriptomic and *in situ* analyses demonstrate its expression in tissues housing symbionts, suggesting a potential role in symbiont uptake and pointing to a conserved immune mechanism shared with cnidarians. The behavioural ecology of photosymbiosis is addressed through phototaxis experiments in *Elysia viridis*. While kleptoplastic slugs generally prefer illuminated areas, this preference does not correlate with the photosynthetic state of the chloroplasts. Even under conditions where photosynthesis was chemically blocked, the slugs continued to orient towards light. These findings challenge the view that photobehavior evolved to optimise photosynthetic performance of kleptoplasts, suggesting instead that it reflects daily periodic activity patterns or food-searching strategies, thereby questioning the extent to which kleptoplasty functions as an adaptive nutritional strategy. The microbiome dimension of the holobiont is investigated in both *Elysia*

viridis and *Berghia stephanieae*. Distinct microbial communities are shown to be associated with different symbiotic states, feeding conditions, and environmental contexts, underscoring the dynamic role of bacteria in shaping holobiont physiology. Shifts in microbiome composition are highlighted as potential early indicators of stress, with implications for both ecological understanding and biomonitoring applications. Finally, the dissertation examines the impact of metal pollution, focusing on nickel and cobalt, elements of growing economic importance due to their role in battery production. Controlled exposure experiments reveal that these metals disrupt the microbiome and bacterial metabolic pathways of *Berghia stephanieae*, while also impairing embryonic development and ontogenesis. Early life stages proved particularly vulnerable, raising concerns about population-level consequences. These findings demonstrate not only the ecological sensitivity of photosymbiotic holobionts but also their potential utility as sentinel species for detecting environmental contamination.

Taken together, this dissertation provides a comprehensive and integrative view of photosymbiotic sea slugs as model systems for understanding symbiosis, host–microbe interactions, and environmental stress responses. By linking molecular recognition, symbiont diversity, microbiome ecology, behaviour, and toxicology, it advances our knowledge of how multipartite symbioses evolve, how they contribute to ecological success, and how they may be disrupted by human activity. In doing so, it positions photosymbiotic sea slugs as powerful but vulnerable models for studying the resilience of marine holobionts in a changing world.

Introduction

Photosymbiosis

Photosymbiosis describes a nutritional symbiosis between a heterotrophic host and a phototrophic partner, wherein the host provides symbionts with physical protection, as well as carbon dioxide and nitrogen, in exchange for photosynthetically derived metabolites such as sugars and amino acids (Dean et al., 2016; Decelle, 2013; Yee et al., 2025). This form of symbiosis plays a crucial role in marine ecosystems, especially in oligotrophic environments. In such environments, photosymbiosis allows animals to supplement or even completely replace heterotrophic nutrition through autotrophic input, significantly increasing their adaptability and survival. The mixotrophic holobiont, formed by this association, can overcome nutrient limitations by recycling and remineralising particulate organic matter internally. As a result, photosymbiosis is particularly advantageous in nutrient-deficient tropical and subtropical waters, supporting the productivity and ecological success of diverse marine lineages, including planktonic foraminifera and corals, by combining heterotrophic and autotrophic nutritional strategies (Caron, 2000; Norris, 2000; Stoecker et al., 2009)

At its core, photosymbiosis represents a spectrum of interactions ranging from facultative, short-lived associations to obligate, long-term dependencies (Emery et al., 2024; Killam et al., 2023; Liao et al., 2025; Sørensen et al., 2020). It can involve whole phototrophic cells (endosymbiosis), as in many coral–algae systems, or the retention of isolated plastids (organelle-level symbiosis), as seen in some marine invertebrates (Hu et al., 2020; Maselli et al., 2021; Ochsenkühn et al., 2017; Rauch et al., 2017; Van Steenkiste et al., 2019). The nutritional contribution of the symbiont varies considerably depending on the host and environmental context. Still, in some cases, it can cover the host's energy demands entirely, and even exceed them under optimal conditions (Muscatine et al., 1984; Thomas et al., 2023; Tremblay et al., 2012).

Photosymbiosis is phylogenetically widespread, having evolved independently in several metazoan lineages. Documented host groups include cnidarians, sponges, flatworms, molluscs, ascidians, and even amphibians, with photobionts drawn from diverse groups such as cyanobacteria, green algae, diatoms, and dinoflagellates (Melo Clavijo et al., 2018). Most well-known examples occur in marine environments, especially coral reef systems, although a few freshwater cases, such as in the freshwater sponge order Spongillida, are known (Pröschold & Darienko, 2020). The establishment and maintenance of photosymbiosis require extensive physiological and morphological adaptations. Many host organisms exhibit increased body surface area, specialised tissue structures, or light-accessing behaviours to enhance the exposure of symbionts to sunlight. For example, some molluscs possess highly branched digestive glands, while certain cnidarians such as the sea anemone *Lebrunia neglecta* Duchassaing & Michelotti, 1860 extend symbiont-rich tentacles during daylight (Moore & Gosliner, 2011; Norton et al., 1992; Venn et al., 2008). To mitigate light and thermal stress, hosts produce protective compounds like mycosporine-like amino acids (MAAs) and fluorescent proteins (Roth, 2014; Shick & Dunlap, 2002),

or regulate light exposure behaviorally via tissue retraction and vertical migration (Djeghri et al., 2019; Sorek et al., 2014).

Within the marine gastropod clade Heterobranchia, photosymbiosis has evolved independently at least twice, giving rise to two fundamentally different strategies: chloroplast retention (kleptoplasty) in Sacoglossa and whole-cell dinoflagellate symbiosis in Cladobranchia (Händeler et al., 2009; Rola et al., 2022). These lineages diverged early within Panpulmonata, yet both evolved mechanisms to exploit autotrophic resources in nutrient-poor marine environments (Klussmann-Kolb et al., 2008). Phylogenetic analyses suggest that these photosymbiotic traits arose independently from non-photosymbiotic ancestors, driven by ecological opportunity and morphological preadaptations such as a branched digestive gland system (Moore & Gosliner, 2011; Rola et al., 2022).

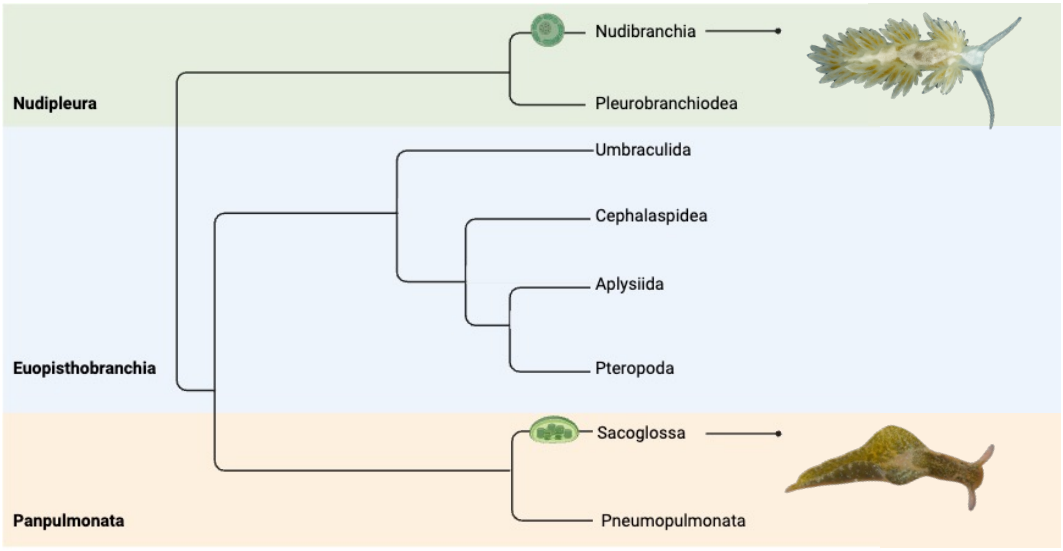

FIGURE 1: Evolution of photosymbiosis in Heterobranchia. Photosymbiosis with Symbiodiniaceae is indicated by a round algae icon, and kleptoplasty is indicated by a chloroplast icon. Phylogeny is based on Wägele et al., 2003.

Kleptoplasty in Sacoglossa

Kleptoplasty, the functional retention of chloroplasts within animal cells, is a special form of photosymbiosis. Unlike classical endosymbioses involving unicellular algae, kleptoplasty refers to the intracellular sequestration of chloroplasts, known as "kleptoplasts", from algal prey. This phenomenon can be found in sacoglossan sea slugs (Gastropoda: Heterobranchia), a specialised clade of marine herbivores that feed primarily on green algae (N. Curtis et al., 2005; Händeler & Wägele, 2007). After ingestion, the chloroplasts are incorporated into epithelial cells of the digestive gland, where they can remain photosynthetically active for days, weeks, or even months, depending on both the host species and the algal source (Rauch et al., 2018; Fig. 2). Based on these differences in retention ability, sacoglossans are classified into three functional groups: non-retaining (NR), short-term retaining (StR), and long-term retaining (LtR) species (Händeler et al., 2009). For example, kleptoplast photosynthesis persists for extended periods without additional feeding in *Elysia timida* (Risso, 1818) and *Elysia chlorotica* A. Gould, 1870, while *Elysia viridis* (Montagu, 1804) a species which is usually not able to incorporate kleptoplasts, can exhibit either

short- or long-term retention depending on the algal species consumed (Cruz et al., 2020; Rauch et al., 2018).

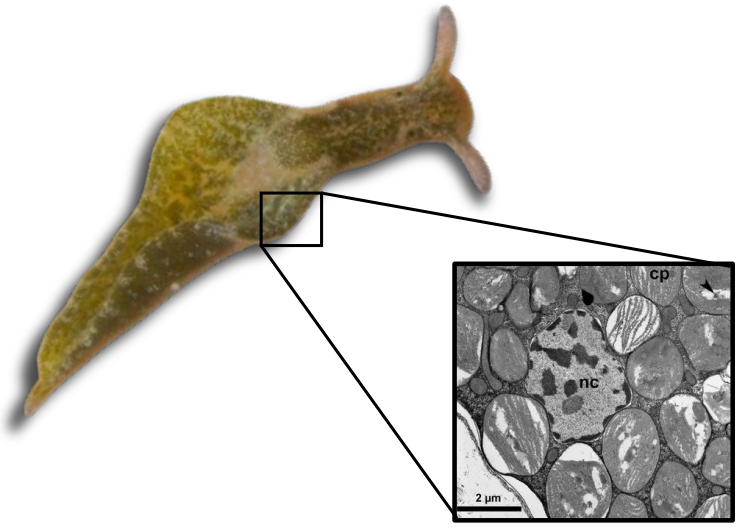

FIGURE 2: Morphology of *E. viridis* and microscopic details showing location of kleptoplast in the host cell. nc: nucleus, cp: chloroplast. The microscopic image was taken from Martin et al., 2015 with permission.

Within Sacoglossa, kleptoplasty likely evolved as a derived trait and exhibits notable variation in both physiological integration and evolutionary occurrence (Fig.3). Phylogenetic analyses indicate that the ability to sequester chloroplasts is ancestral to the group, with long-term retention having evolved independently in multiple lineages through gradual physiological adaptations (Christa et al., 2015). These adaptations include modified cellular architecture in digestive tissues, delayed lysosomal fusion, and molecular strategies for mitigating oxidative stress (De Vries et al., 2014; Laetz et al., 2017a).

The functional role of kleptoplasts in host metabolism remains debated. Early radioisotope studies suggested that photosynthetically fixed carbon can be incorporated into host tissues and may support reproduction or survival during starvation (Cruz et al., 2020; Trench et al., 1974). Behavioural observations support a functional role (Cartaxana et al., 2018; Weaver & Clark, 1981). For instance, *E. timida* displays phototactic behaviour, orienting its body toward light to presumably optimise photosynthetic output (Schmitt & Wägele, 2011). Such observations lead to the assumption that kleptoplasty is an actively maintained trait rather than a passive consequence of herbivory. However, the absence of algal nuclei and thus the genes required for chloroplast maintenance raises questions about how kleptoplasts remain functional over extended periods (Rauch et al., 2015). Some researchers have proposed that kleptoplasts serve primarily as temporary energy storage devices rather than fully integrated organelles (Frankenbach et al., 2021, 2023; Laetz et al., 2017b). Recent ultrastructural and transcriptomic analyses in the LtR species *Elysia crispata* Mörch, 1863 show that kleptoplasts are housed within a specialised host-derived organelle-like structure, referred to as a "kleptosome" (Allard et al., 2025). This finding resolves the long-standing debate over whether plastids are enclosed by host membranes after uptake, providing strong evidence that kleptoplasts are indeed integrated into the host cell environment. One of the key challenges in maintaining intracellular plastids is to prevent their degradation through the normal endosomal–lysosomal pathway. Typically, this pathway is regulated by the transition from

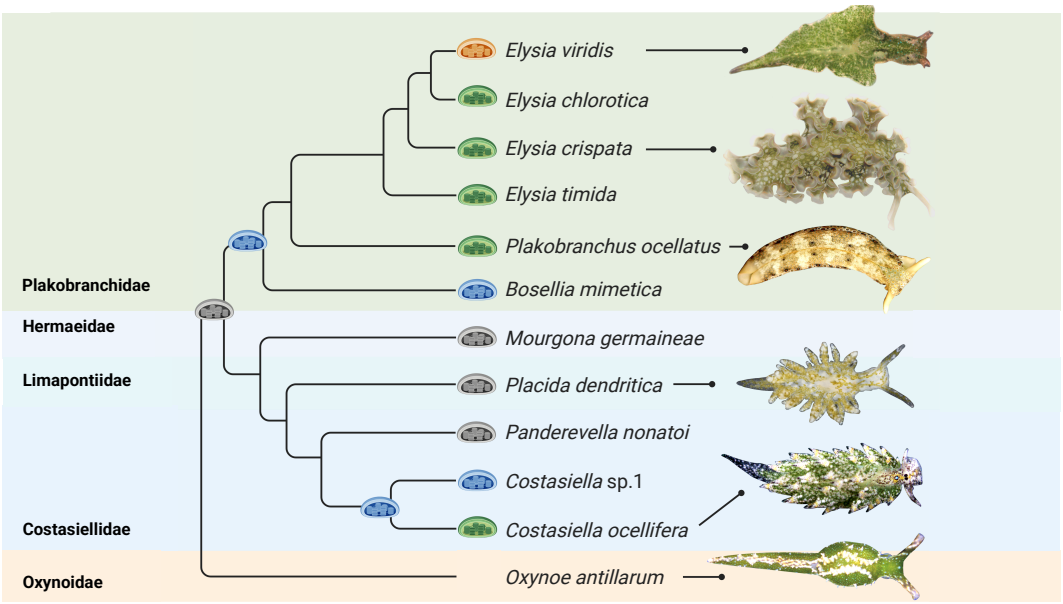

FIGURE 3: Evolution of functional kleptoplasty in Sacoglossa. Mode of kleptoplasty is indicated by chloroplast icons in different colours: grey - non-retaining (NR); blue - short-term retaining (StR); dark green - long-term retaining (LtR), and orange - NR, StR or LtR depending on the food algae. Modified after Kodžoman et al., 2023.

RAB5, an early endosomal marker, to RAB7, which promotes vesicle fusion with lysosomes and subsequent digestion (Chen et al., 2004). In kleptoplastic tissues, however, RAB7 has been observed at plastid membranes already during feeding, suggesting that plastid turnover is an ongoing process rather than being fully suppressed, in contrast to what is known from cnidarian–algal symbioses (Baştürk et al., 2025). Interestingly, not all plastids show RAB7 localisation, which may reflect different stages of plastid processing: newly incorporated plastids remain free of RAB7, while older ones gradually become marked for degradation. These observations point to a dynamic balance in kleptoplasty, where plastid persistence is not achieved by complete inhibition of degradation, but by a regulated equilibrium between initial retention and subsequent digestion.

Photosymbiosis in Cladobranchia

In contrast to sacoglossan sea slugs, cladobranch sea slugs incorporate entire photosynthetically active cells of the dinoflagellate family Symbiodiniaceae into the epithelial cells of their digestive gland system. These symbionts are acquired horizontally, either directly from the environment, as observed in *Melibe engeli* Risbec, 1937, or indirectly through the consumption of photosymbiotic cnidarian prey, as in *Berghia stephanieae* (Á. Valdés, 2005) and various species of *Phyllodesmium* (Burghardt & Wägele, 2014; Kempf, 1984; Rudman, 1981; Wägele, 2004). After ingestion, the algal cells are selectively phagocytosed into the host's digestive epithelial cells, which extend throughout the body and into dorsal appendages on the back of the slug's body, so-called cerata (Fig. 4). There, the symbionts can remain photosynthetically active for variable periods of time (Burghardt, Schrödl, & Wägele, 2008; Burghardt et al., 2005; Kempf, 1991; Monteiro et al., 2019). In *B. stephanieae*, for example, intact Symbiodiniaceae cells are phagocytosed and transiently maintained in the digestive gland, but the association is unstable: the symbionts are typically lost within days

unless replenished through feeding on photosymbiotic cnidarians (Melo Clavijo et al., 2022; Monteiro et al., 2019). In contrast, closely related taxa such as *Phyllodesmium longicirrum* (Bergh, 1905) can establish stable photosymbioses that last for weeks to months and, under sufficient light, support growth and even reproduction in the absence of heterotrophic food sources (Burghardt, Schrödl, & Wägele, 2008; Rudman, 1981, 1991).

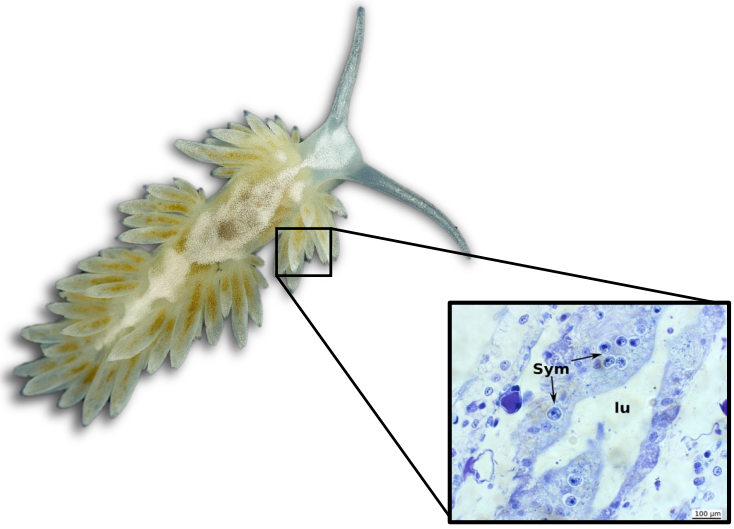

FIGURE 4: Morphology of *B. stephanieae* and histological cross-section through a cerata showing the host cells of the cerata bearing the photobiont. nc: nucleus, cp: chloroplast. The microscopic image was taken from Rola et al., 2022 with permission.

The Symbiodiniaceae symbionts themselves exhibit remarkable diversity in genetic, physiological, and ecological traits. Formerly grouped under the single genus *Symbiodinium*, this family is now divided into multiple genera, including *Symbiodinium*, *Cladocopium*, *Durusdinium*, *Fugacium*, and *Breviolum* based on molecular phylogenies (Guiry, 2024; LaJeunesse et al., 2018). These clades differ significantly in characteristics such as cell size, chlorophyll concentration, photoprotective pigment synthesis, thermal tolerance, and photosynthetic efficiency, which influence both free-living ecology and symbiotic compatibility (Brading et al., 2013; Hennige et al., 2009; LaJeunesse, 2002; LaJeunesse et al., 2018). Metabarcoding and Symbiodiniaceae profiling based on ITS2 have shown that *B. stephanieae*, for instance, associates primarily with *Breviolum minutum* (LaJeunesse, J.E.Parkinson & J.D.Reimer) J.E.Parkinson & LaJeunesse, 2018, a genus known for its broad ecological range and frequent occurrence in cnidarian hosts (Bayliss et al., 2019; Melo Clavijo et al., 2022).

The evolutionary origins of photosymbiosis in Cladobranchia remain only partially resolved (Fig. 5). Not all species with access to photosymbiotic prey establish symbioses, and morphological traits often associated with symbiosis, such as highly branched digestive glands and enlarged, light-exposed cerata, are not universally present among symbiotic taxa (Moore & Gosliner, 2011). The ability to form photosymbioses is scattered across multiple cladobranch superfamilies, including Aeolidioidea, Fionoidea, Arminoidea, and Dendronotoidea, indicating multiple independent evolutionary origins (Johnson & Gosliner, 2012; Moore & Gosliner, 2014; Moore & Gosliner, 2011; Wägele & Willan, 2000).

A key yet still underexplored aspect of these associations is the recognition and incorporation of photobionts by the host. In cnidarians, recognition involves pattern

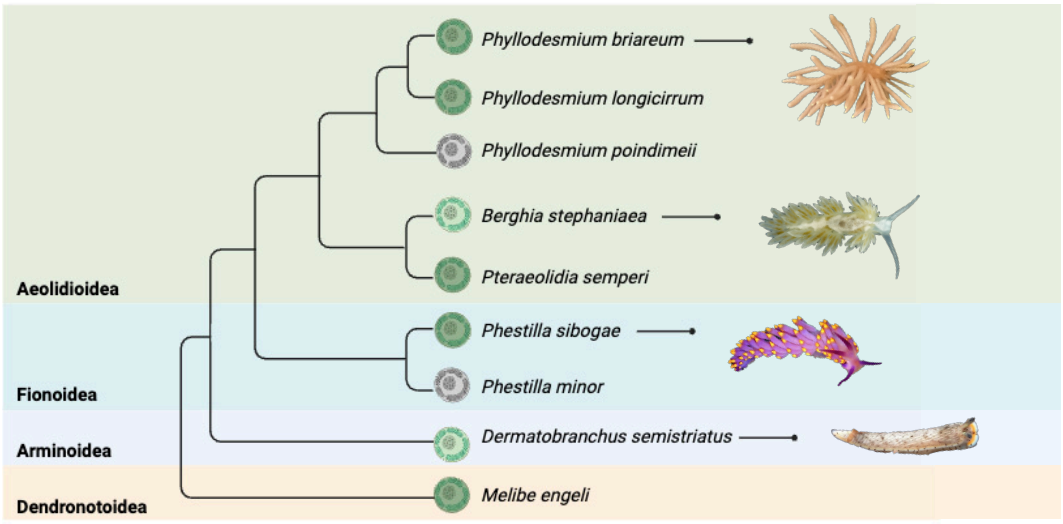

FIGURE 5: Evolution of photosymbiosis in Cladobranchia. Mode of photosymbiosis is indicated by algae icons in different colours: grey - non; light green - unstable, and dark green - stable. Phylogeny is based on Goodheart et al., 2018 and Karmeinski et al., 2021.

recognition receptors (PRRs) of the host cell, such as scavenger receptor class B (SR-B) and scavenger receptor class E (SR-E), thrombospondin type-1 repeat domain-containing proteins (TSRs) and C-type lectins, which bind to microbe-associated molecular patterns (MAMPs) on the algal surface, triggering immune modulation and consequently phagocytosis of the photobiont (Davy et al., 2012). Transcriptomic studies in photosymbiotic heterobranchia, such as in different sacoglossan *Elysia* species and the cladobranch *B. stephanieae*, have identified several candidate PRRs which may play a similar role in photobiont-specific recognition in sea slugs (Melo Clavijo et al., 2020, 2022; Mendoza et al., 2023).

Holobiont Concept

The holobiont concept describes a host organism and its associated microbial and symbiotic partners as a single, functionally integrated biological entity (Baedke et al., 2020; Rohwer et al., 2002). Originally proposed in the context of microbiome studies, the term has gained particular attention in coral reef biology, where it helps explain the tight metabolic and functional integration between reef-building cnidarians and their complex symbiotic communities (Fig. 6). In this context, the coral holobiont typically includes the animal host, intracellular photosynthetic dinoflagellates (Symbiodiniaceae), bacterial and archaeal microbiota, viruses, and sometimes even fungi (Bourne et al., 2016; Peixoto et al., 2017; Rosenberg et al., 2007). These components interact dynamically and are crucial to the host's health, resilience, and ecological function. For instance, Symbiodiniaceae provide the majority of the coral's fixed carbon via photosynthesis, while microbial associates are involved in nitrogen cycling, sulfur metabolism, and protection against pathogens (Peixoto et al., 2017; Raina et al., 2009; Venn et al., 2008). The holobiont framework thus shifts the focus from a single-species perspective to a more systemic view of organismal function and adaptation, allowing a better understanding of host responses, including symbiont dynamics or symbiont loss (bleaching) as responsive actors to environmental stress (Bourne et al., 2009; Weis et al., 2008).

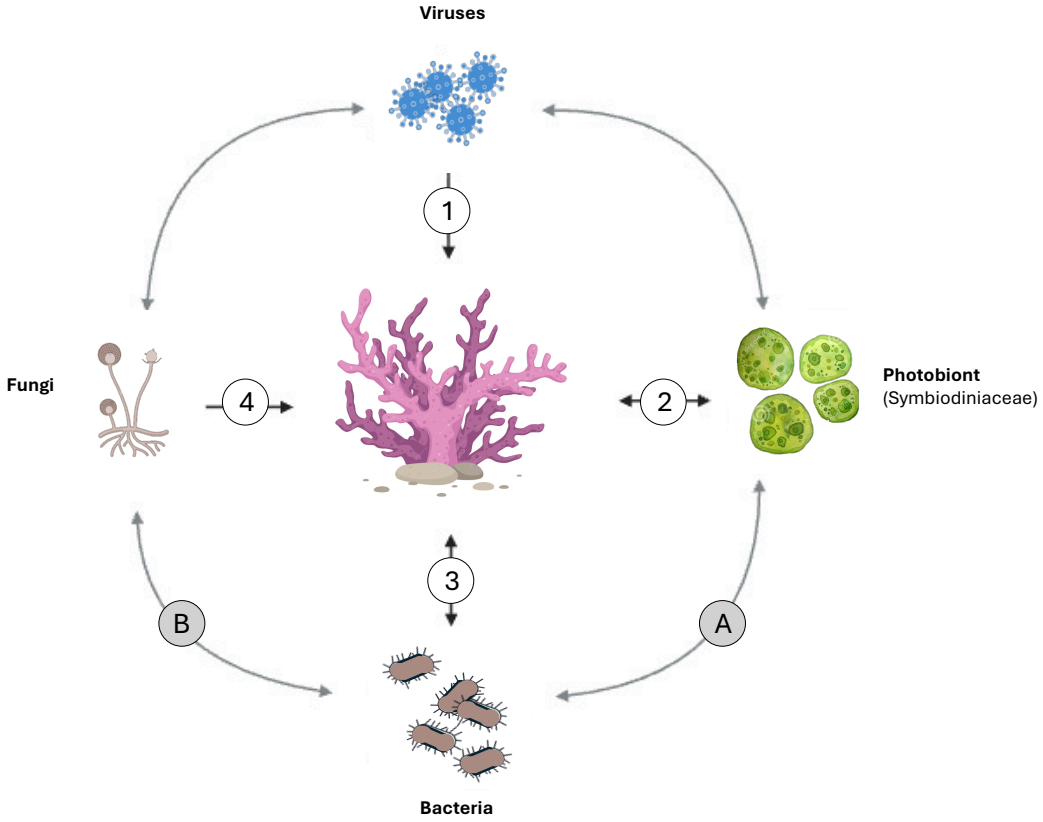

FIGURE 6: Holobiont concept highlighting possible roles and relationships between corals and their symbionts (Peixoto et al., 2017). (1) Gen transfer and natural phage therapy; (2) Main carbon source and DMSP supplier for coral/coral provides shelter and protection; (3) Nutrient cycling (S, C and N) for coral, pathogen control, DMSP degradation/coral provides shelter and protection; (4) Antimicrobial activity. (A) Bacteria provide N/photobiont provides C and S through DMSP production; (B) Bacteria provide C and S through DMSP catabolism/Nutrient exchange.

Transferring the holobiont framework to other animal systems offers promising opportunities to investigate symbiosis from an integrative perspective (Dittami et al., 2021). Marine heterobranch slugs, though morphologically and phylogenetically distinct from cnidarians, represent a particularly compelling example. Their photosynthetic partnerships, whether based on retained plastids or intact algal cells, are embedded within a broader network of microbial associations that together form a dynamic and interactive system. In this context, the host and its phototrophic partners constitute only part of a complex consortium that also includes diverse bacterial, archaeal, viral, and potentially fungal associates, all of which may contribute to nutrient cycling, metabolic supplementation, immune modulation, and symbiont regulation. Morphological and behavioural traits that promote light capture or enhance symbiont stability can thus be interpreted not as isolated adaptations, but as elements of a coordinated system shaped by the interplay of host, photobionts, and associated microbes. Importantly, microbial community structure is increasingly recognised as a sensitive indicator of host health, stress response, and overall system stability (Bourne et al., 2009; Peixoto et al., 2017). Shifts in microbial community structure can signal stress or impending dysbiosis well before visible symptoms appear, making microbiome analyses a valuable tool not only for ecological

and physiological insight, but also for assessing organismal health and environmental resilience (Stévenne et al., 2021).

Pollution by Toxic Heavy Metals

Metals are naturally occurring elements defined by their metallic properties, including high electrical and thermal conductivity, malleability, and, in the case of toxic heavy metals and metalloids, high atomic weight or density (Jeong et al., 2023). In recent years, these metals have become a major global concern due to their persistence, non-degradable nature, and potential to accumulate in food webs (Córdoba-Tovar et al., 2022; Laoye et al., 2025; Oros, 2025). Unlike organic pollutants, which can degrade over time, metals remain in soils, sediments, and aquatic systems, where they may bioaccumulate in organisms and biomagnify through trophic levels, ultimately reaching humans (Córdoba-Tovar et al., 2022; Kumar et al., 2022; Naz et al., 2025). Industrialisation, mining, smelting, fossil fuel combustion, and intensive agriculture have dramatically increased the release of toxic metals such as cadmium, lead, mercury, nickel, and cobalt into the environment (Dagdag et al., 2023; Gautam et al., 2016; Masindi & Muedi, 2018; Real et al., 2024). This has raised concerns not only for human health, where metal exposure is linked to neurological, developmental, and carcinogenic effects, but also for ecosystem stability and biodiversity (Ajala et al., 2025; Kumar et al., 2022). In aquatic invertebrates, for instance, metals can impair growth, reproduction, and survival by inducing oxidative stress and disrupting metabolic pathways. Because metals cannot be destroyed and continue to circulate between air, water, soil, and organisms, even low-level contamination can pose long-term risks (Gashkina, 2024; Jeong et al., 2023; Sousa et al., 2024). These issues have positioned toxic metals as one of the most pressing pollution threats globally, particularly in regions undergoing rapid industrial and resource extraction activities (Hou et al., 2025).

Nickel (Ni) and cobalt (Co) are naturally occurring metals that play essential roles as micronutrients in various biological systems. Nickel serves as a cofactor in specific metalloenzymes such as Urease, while cobalt is a central component of vitamin B_{12}, which is critical for DNA synthesis and cellular metabolism (Martens et al., 2002; Mulrooney & Hausinger, 2003). Under natural conditions, these metals enter marine systems via processes such as weathering, volcanic activity, and riverine input (Saravanan et al., 2024). However, elevated concentrations can be toxic, impairing enzymatic activity, disrupting ion regulation, inducing oxidative stress, and affecting growth and reproduction in a wide range of marine organisms (Correia et al., 2025; J. S. Meyer et al., 2020; Saili et al., 2021).

Global demand for nickel and cobalt has risen sharply over the past two decades, primarily due to their essential role in rechargeable batteries for electric vehicles, consumer electronics, and renewable energy storage systems (European Commission, 2018; US Geological Survey, 2023). This growth has not only intensified the demand for seabed mining but has also led to an expansion of terrestrial mining activities, particularly in tropical coastal regions where lateritic nickel and cobalt deposits occur. Major extraction sites are located in Indonesia, the Philippines, and New Caledonia, which together supply a significant portion of the world's production (Devezas, 2025). In these regions, ore processing and waste disposal often occur close to the shoreline, increasing the risk of metal-rich effluents entering coastal waters. In tropical islands and archipelagos, mining activities frequently coincide

with sensitive marine habitats such as coral reefs, seagrass beds, and mangrove ecosystems (The Metals Company, 2023). Runoff from mined areas can carry fine sediments, processing chemicals, and dissolved metals directly into adjacent bays and lagoons, leading to elevated concentrations of nickel and cobalt in seawater and sediments, as already documented, for example, in New Caledonia (Fernandez et al., 2006; Merrot et al., 2019; Noël et al., 2015). These inputs can alter benthic community structure, smother filter-feeding organisms, and cause bioaccumulation of metals in food webs, with potential impacts on fisheries and biodiversity (Gall et al., 2015; Gao et al., 2013; Purser et al., 2016).

Ecotoxicological studies indicate that both metals can impair key physiological processes in marine organisms, including reproduction, growth, and immune function (Dos Reis et al., 2024; Ou et al., 2023; Saili et al., 2021). Among tested species, the tropical copepod *Acartia sinjiensis* Mori, 1940 and the sea urchin *Diadema antillarum* (Philippi, 1845) appear particularly sensitive to nickel, with chronic effect concentrations as low as 2.9 µg/L in early sea urchin life stages and an effect concentration (EC10) of 5.5 µg/L for copepod larval development (Gissi et al., 2018, 2020). In the case of cobalt, the diatom *Ditylum brightwellii* Grunow, 1885 has been reported as especially vulnerable, with an average lethal concentration (LC50) of 300 µg/L after 96 hours (Saili et al., 2021). While cobalt is less extensively studied than nickel, both have been shown to induce oxidative stress, disrupt ion regulation, and affect enzyme activity at environmentally relevant concentrations (Ates et al., 2016; Blewett & Leonard, 2017; Blewett et al., 2016, 2018; Sun et al., 2020). Early life stages, such as embryos and larvae, often display heightened sensitivity, raising concerns about long-term population-level effects (Connor, 1972; Gopalakrishnan et al., 2007; Noetzel et al., 2025). In phototrophic or photosymbiotic invertebrates, such as corals and certain gastropods, metal exposure may further disrupt the delicate balance between host and symbiont, potentially leading to bleaching or loss of photosynthetic efficiency (Biscéré et al., 2018; Rodriguez et al., 2016). Because many of these species have restricted ranges and low dispersal capacities, recovery from contamination events can be slow or incomplete.

Given the projected continuation of nickel and cobalt mining in coastal tropical regions, there is an urgent need to better understand their ecological impacts, particularly on sensitive and functionally important organisms. Holobiont-based model systems integrating host physiology and microbiome composition offer valuable tools to detect early signs of stress and to assess the long-term consequences of metal exposure on marine ecosystem health.

Aims and Scope of the Present Dissertation

Understanding the complex interactions between marine heterobranch sea slugs, their photosynthetic partners, and associated microbial communities requires an integrative research approach. While photosymbiosis and kleptoplasty in gastropods have been the focus of several physiological and ecological studies, comparatively little is known about the role of the microbiome in these associations, how it responds to environmental stressors, and whether it can be used as a sensitive indicator of host condition. This thesis addresses these gaps by combining microbiome profiling, behavioural analysis, and controlled stress experiments in two model systems: the kleptoplastic sacoglossan *Elysia viridis* and the photosymbiotic cladobranch *Berghia stephanieae*.

By examining holobiont structures under varying symbiotic states, evaluating behavioural responses related to light acquisition, and assessing the impact of heavy metal exposure on both adults and early life stages, this work aims to broaden the holobiont perspective in photosymbiotic sea slugs. In doing so, it seeks to provide insights into the ecological significance of their multipartite associations and to explore their potential as bioindicator species for monitoring environmental change.

This dissertation seeks to find answers to the following questions:

I. How can photosymbiotic sea slugs serve as model organisms for studying the molecular mechanisms, ecological implications, and behavioural aspects of photosymbiosis?
Chapter 1, Chapter 2 and Chapter 3.

II. How do photosymbiotic sea slugs function as holobiont model systems for investigating the structure and diversity of their associated symbionts, and how are these communities shaped by host species, symbiotic state, and ecological context?
Chapter 1, Chapter 4 and Chapter 5

III. What are the effects of metal exposure (nickel and cobalt) on the microbiome structure and stability of *Berghia stephanieae* and its eggs, and can microbiome analyses serve as sensitive indicators for environmental stress and animal welfare? Chapter 6 and Chapter 7.

Results

Chapter 1

Diversity of Symbiodiniaceae (Dinophyceae) in the Sea Slug Clade Cladobranchia (Nudibranchia)

Corinna Sickinger, Michael Brück, Sabrina Bleidißel, Gilles Gasperoni, Sascha Tierling, Cessa Rauch, Angelika Preisfeld and Gregor Christa

Published: 2 December 2025, *Organisms Diversity & Evolution* 25, 517–529 (2025)
https://doi.org/10.1007/s13127-025-00688-9

This study investigates the diversity of algal symbionts (Symbiodiniaceae) in Cladobranchia sea slugs, particularly in the genus *Phyllodesmium*, which maintain long-term associations with their algae symbiont. Using ITS2 metabarcoding, we discovered that *Phyllodesmium* species predominantly host the Symbiodiniaceae genus *Cladocopium*, with genus- and species-specific symbiont profiles.

Chapter 2

Collectin-12 - A Promising Symbiont Recognition Receptor in *Berghia stephanieae* (Á. Valdés, 2005)

Corinna Sickinger, Rebecca Lopez-Anido, Sofia Paz Sedano, Gregor Christa, Angelika Preisfeld and Jessica Goodheart

Unpublished data

This study explores the role of Collectin-12 as pattern recognition receptor in the photosymbiotic sea slug *Berghia stephanieae*. Spatial transcriptomics and *in situ* hybridisation revealed that Collectin-12 is expressed mainly in the digestive gland tissue hosting photobionts, but not in regions storing nematocysts, suggesting a potential role in photobiont recognition.

Chapter 3

The Phototactic Behaviour of the Kleptoplastic Sea Slug *Elysia viridis* (Montagu, 1804) is not Connected to the Photosynthetic Activity of Kleptoplasts

Corinna Sickinger, Elisa Weimann, Johannes Wenning and Gregor Christa

Published: 18 November 2025, *Marine Biology Research* 21(8–10), 417–426
https://doi.org/10.1080/17451000.2025.2577445

This study examined whether the phototactic behaviour of the sacoglossan sea slug *Elysia viridis* is linked to enhancing the photosynthetic activity of its retained chloroplasts (kleptoplasts). In side-choice experiments under different light conditions and treatments, the slugs consistently preferred illuminated areas regardless of feeding state or photosynthetic inhibition.

Chapter 4

Photosymbiosis Shapes the Microbiome of the Saccoglossan Sea Slug *Elysia viridis* (Montagu, 1804)

Corinna Sickinger, Katarina Kodzoman, Angelika Preisfeld and Gregor Christa

Unpublished data

This study investigated how kleptoplast presence and functionality affect the microbiome of the sacoglossan sea slug *Elysia viridis*. Comparing slugs with functional kleptoplasts, inhibited photosynthesis, and no kleptoplasts, we found significant shifts in microbial composition and metabolic pathways depending on kleptoplast presence and activity.

Chapter 5

Microbiome Origin and Stress-Related Changes in Bacterial Abundance of the Photosymbiotic Sea Slug *Berghia stephanieae* (Á. Valdés, 2005)

Corinna Sickinger, Sofie Marie Brackwehr, Jenny Melo Clavijo, Gilles Gasperoni, Sascha Tierling, Angelika Preisfeld and Gregor Christa

Published: 14 June 2024, *Symbiosis* Volume 93, pages 177–192, (2024)
https://doi.org/10.1007/s13199-024-00995-3

This study examined the microbiome of the sea slug *Berghia stephanieae* and its cnidarian prey *Exaiptasia diaphana* to explore how bacterial communities shift under light and starvation stress. The slug's microbiome differed markedly from that of its prey, suggesting vertical transmission rather than environmental acquisition.

Chapter 6

Nickel and Cobalt Disrupt the Microbiome and Metabolic Function of the Photosymbiotic Sea Slug *Berghia stephanieae* (Á. Valdés, 2005)

Corinna Sickinger, Jana Kosky, Andriy Tkach, Alicia Thiel, Julia Bornhorst , Gregor Christa and Angelika Preisfeld

Published: 17 January 2026, *Marine Environmental Research* 216, 107845 (2026)
https://doi.org/10.1016/j.marenvres.2026.107845

This study investigated how exposure to nickel and cobalt affects the microbiome of the cladobranch sea slug *Berghia stephanieae*. Both metals caused concentration-dependent behavioural stress as well as significant shifts in microbial composition and metabolic activity.

Chapter 7

Cobalt and Nickel Inhibit the Ontogenesis of the Cladobranch Sea Slug *Berghia stephanieae* (Á. Valdés, 2005)

Corinna Sickinger, Jana Kosky, Alicia Thiel, Julia Bornhorst, Gregor Christa and Angelika Preisfeld

Unpublished data

This study examined the effects of nickel and cobalt on the embryonic and larval development of the sea slug *Berghia stephanieae*. Both metals caused developmental delays and decreased hatching success, with cobalt exerting a negative impact on egg survival at lower concentrations than nickel.

Chapter 1

Diversity of Symbiodiniaceae (Dinophyceae) in the Sea Slug Clade Cladobranchia (Nudibranchia)

Corinna Sickinger[1], Michael Brück[1], Sabrina Bleidißel[1], Gilles Gasparoni[2], Sascha Tierling[2], Cessa Rauch[3], Angelika Preisfeld[1] and Gregor Christa[4]

[1]*Institute for Zoology and Didactics of Biology, University of Wuppertal, Wuppertal, Germany*
[2]*Department of Genetics, Saarland University, Saarbrücken, Germany*
[3]*Department of Natural History, University of Bergen, Bergen, Norway*
[4]*Department of Evolution and Biodiversity, University of Wuppertal, Wuppertal, Germany*

Published: 2 December 2025, *Organisms Diversity & Evolution* 25, 517–529 (2025)
https://doi.org/10.1007/s13127-025-00688-9

1.1 Abstract

In members of Cladobranchia sea slugs, unique adaptations to incorporate cnidocysts and algal symbionts from their cnidarian prey have evolved. However, many aspects underpinning the recognition and maintenance of these stolen cellular components are still unclear. Regarding the algal symbionts, little is known about the exact Symbiodiniaceae species and their abundance and diversity in Cladobranchia. Yet, understanding the diversity of Symbiodiniaceae inside the slugs can help better understand the symbionts' role in establishing and maintaining the symbiosis. We analysed the Symbiodiniaceae diversity across multiple Cladobranchia genera and species, focusing on the genus *Phyllodesmium*, which contains most of the known cladobranchs in a long-term symbiosis with the algae. Using high-throughput metabarcoding of the Symbiodiniaceae ITS2 region, we found that species of the genus *Phyllodesmium* harboured primarily *Cladocopium*, showing a genus-specific Symbiodiniaceae profile. Within a cladobranch genus, we also uncovered species-specific intragenomic variants of the respective symbiodiniacean genus. Our results reveal a previously unexplored diversity of algal symbionts in Cladobranchia and that *Cladocopium* might be particularly relevant for establishing long-term symbiosis. *Cladocopium* exhibits enhanced carbon fixation capabilities in symbiosis with corals, which may thus facilitate the symbiosis from the symbionts' side. Consequently, studying symbiont diversity and abundance in Cladobranchia is essential for understanding

the mechanism of symbiosis initiation and maintenance.

Keywords Cladobranchia · Symbiodiniaceae · metabarcoding · photosymbiosis · SymPortal

1.2 Introduction

Cladobranchia (Nudibranchia) are often called the "butterflies of the sea" due to their elaborate morphology and vivid colouration (see Fig. 1.1). These sea slugs are specialised feeders, primarily preying on cnidarians, with a particular emphasis on taxa within the classes Anthozoa and Hydrozoa (Goodheart et al., 2017; Wägele & Klussmann-Kolb, 2005). Most cladobranch species possess the remarkable ability to sequester cnidocysts from their cnidarian prey (Goodheart & Bely, 2017). These cnidocysts are transported through the digestive gland system to the distal ends of the cerata (dorsal appendages characteristic of these nudibranchs). Within the cerata, the cnidocysts are phagocytosed by specialised cells that form the cnidosac, where they are retained, matured, and repurposed as a defensive mechanism against potential predators (Goodheart et al., 2018; Obermann et al., 2012).

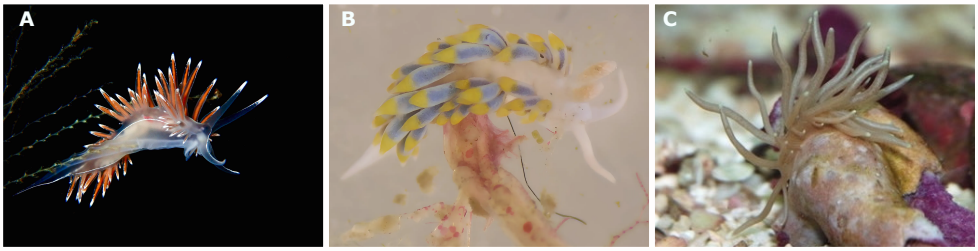

FIGURE 1.1: Cladobranchia are known for their striking and often very colourful morphology, such as *Coryphella lineata* (Lovén, 1846) (A), *Berghia coerulescens* (Laurillard, 1832) (B) and *Phyllodesmium briareum* (Bergh, 1896) (C). Images were taken by Cessa Rauch (A) and Sabrina Bleidißel (B and C).

Many cladobranch species additionally phagocytose the prey's algal symbionts (Symbiodiniaceae) into the epithelial cells of the digestive gland system. In some species, the algae are immediately digested intracellularly. Yet, in members of the cladobranch superfamilies Arminoidea Iredale and O'Donoghue (1923), Fionoidea Gray (1827), and Aeolidioidea Gray (1827), the algal symbionts remain photosynthetically active inside the new host for some days to months (Wägele et al., 2010). This so-called photosymbiosis evolved independently in each family, and recent observations suggest that the symbiont recognition processes may partially resemble those known from their cnidarian prey (Melo Clavijo et al., 2022). Little is known about the mechanisms by which the slugs retain the symbionts and whether any nutrient exchange occurs between the slug and its algal symbionts (Rola et al., 2022), which is key for a successful photosymbiosis in cnidarians. Cladobranch species are generally categorised based on the period during which the algae remain active in the slugs' cytosol. Species that harbour the algae for a couple of weeks possess an unstable photosymbiosis and do not seem to benefit from the photosynthesis performed by the acquired photobionts (Monteiro et al., 2019). These species cannot maintain their biomass when relying solely on the photobionts as a nutritional

source, and even excrete the photobionts after a couple of days. Species that maintain the symbionts for up to several months are in a stable symbiosis, such as *Melibe engeli* Risbec, 1937 or *Phyllodesmium briareum*, and can rely to a certain degree solely on their photobionts, including growth and long-term reproduction without any reduction in the quantity or quality of their egg masses (Burghardt, Stemmer, & Wägele, 2008; Burghardt & Wägele, 2014; Burghardt et al., 2005).

While nutrient exchange is central to establishing long-term symbiosis, the specific Symbiodiniaceae species acquired from the cnidarian prey may also play a critical role in initiating the association. Symbiodiniaceae is divided into twelve phylogenetic genera (often referred to as clades; see Table 1.1) based on their molecular, morphological, physiological, and ecological differences, and are further subdivided into multiple subclades or types (Guiry, 2024; LaJeunesse et al., 2018; Nitschke et al., 2020). The different Symbiodiniaceae genera are associated with functional differences, including thermal tolerance, photosynthetic performance, and advantages for host growth. These Symbiodiniaceae properties are particularly relevant for coral reef restoration, as certain subclades exhibit greater thermal tolerance than others and might help the corals facing global warming (Howells et al., 2020). For instance, members of the genus *Cladocopium* are physiologically diverse, with some adapted to a wide range of temperatures and irradiances (LaJeunesse et al., 2018). In cnidarians, *Cladocopium* symbionts are often associated with corals that highly depend on their symbiont (Davies et al., 2020; Martinez et al., 2022). This tight connection might be based on the high CO_2 fixation and translocation ability of *Cladocopium* to the animal host (Stat et al., 2008). However, the growth of juvenile colonies of the coral *Acropora tenuis* (Dana, 1846) harbouring *Durusdinium* was faster than when bearing *Cladocopium* (Yuyama & Higuchi, 2014) Moreover, representatives of the genus *Symbiodinium*, reported for a variety of soft and hard corals, but also for the upside-down jellyfish *Cassiopea* sp. (Lampert, 2016; Ravindran et al., 2022), tend to become parasitic to the coral host as observed in *Acropora cytherea* (Dana, 1846), which resulted in health reduction of the coral host, probably based on an insufficient nutritional input from the symbiont to the coral (Lesser et al., 2013; Rouzé et al., 2016; Stat et al., 2008). Hence, it appears that the physiological properties of the symbiodiniacean strain in combination with a particular host are relevant to establish a mutualistic symbiosis.

TABLE 1.1: Clade and genus names of the 12 genera described and accepted for the family Symbiodiniaceae following the classification of the World Register of Marine Species (WORMS) and Algae Base (Guiry, 2024)

Clade	**Genus**	**Authorities**
A	*Symbiodinium*	LaJeunesse, 2017
B	*Breviolum*	J.E.Parkinson & LaJeunesse, 2018
C	*Cladocopium*	LaJeunesse & H.J.Jeong, 2018
D	*Durusdinium*	LaJeunesse, 2018
E	*Effrenium*	LaJeunesse & H.J. Jeong, 2018
F	*Fugacium*	LaJeunesse, 2018
Fr3	*Freudenthalidium*	M.Nitschke, C.Brandão & C.Fidalgo, 2020
G	*Gerakladium*	LaJeunesse, 2018
H	*Halluxium*	Calado, Craveiro & Frommlet, 2020
no clade name	*Miliolidium*	Pochon & LaJeunesse, 2021
no clade name	*Philozoon*	Geddes, 1882
no clade name	*Zooxanthella*	K. Brandt, 1881

To better understand the diversity of Symbiodiniaceae in corals and other photosymbiotic animals, SymPortal, an analytical framework for coral algal symbiont NGS ITS2 profiling, was developed (Hume et al., 2019), enabling the identification of symbionts based on metabarcoding of the Symbiodiniaceae ITS2 region. SymPortal leverages the multicopy nature of the ribosomal RNA gene in *Symbiodiniaceae*—with hundreds to thousands of ITS2 copies per genome—that independently accumulate mutations. This intragenomic sequence diversity can then be used for fine-scale taxonomic identification (Hume et al., 2018). SymPortal utilizes this diversity and identifies unique sets of intragenomic ITS2 sequence variants (defining intragenomic variants; DIVs), to establish taxonomic units known as ITS2 type profiles representing specific Symbiodiniaceae taxa (Gardner et al., 2019).

To date, only a few studies have investigated the diversity of symbiodiniacean species within Cladobranchia. A comprehensive analysis of the stable photosymbiotic *Pteraeolidia semperi* (Bergh, 1870) species complex revealed a geographically dependent composition of *Symbiodinium*, *Cladocopium*, and *Durusdinium* (Yorifuji et al., 2015). *Breviolum*, *Cladocopium*, and *Durusdinium* were mainly identified in *Phyllodesmium lizardense* Burghardt, Schrödl, and Wägele, 2008 (stable photosymbiosis), whereas *Symbiodinium* was only occasionally detected (FitzPatrick et al., 2012). In the non-photosymbiotic species *Aeolidiella alba* Risbec, 1928 and *Phestilla lugubris*, the symbiodiniaceans *Breviolum* and *Cladocopium* were identified (Wecker et al., 2015). Using the SymPortal metabarcoding approach, *Breviolum* subclade B1 was recently identified as the symbiont in *Berghia stephanieae* (Á. Valdés, 2005) (unstable photosymbiosis), which the slugs acquired from their food source, *Exaiptasia diaphana* (Rapp, 1829) (Melo Clavijo et al., 2022). To address the knowledge gap in Symbiodiniaceae diversity in Cladobranchia and to understand whether slugs with stable photosymbiosis harbour certain algae, we analysed 16 cladobranch species, focusing on the genus *Phyllodesmium*, using a combined approach including the SymPortal framework.

1.3 Materials and Methods

Sample collection and DNA extraction

Slugs were collected between 2000 and 2022 from Australia, Indonesia, Egypt, the Philippines, Italy, France, and Norway and originated from the collection of Sabrina Bleidißel and Gregor Christa (Additional file 1: Table 1). The animal material was fixed in 98% ethanol and stored at -20 °C. Each sample was shock-frozen in liquid nitrogen and then carefully broken up using a mortar. Following the manufacturer's instructions, DNA from each sample was extracted using the DNeasy Plant Kit (Qiagen, Germany) or the E.Z.N.A. Invertebrate DNA Kit (Peqlab, USA). Information on cnidarian food sources and the photosymbiotic relationship between sea slugs and Symbiodiniaceae was obtained from the literature (Additional file 1: Table 1). The photosymbiosis was then categorised as non-photosymbiotic (immediate digestion), unstable (maintenance for some days), or stable (maintenance for more than two weeks).

Molecular identification of Symbiodiniacaea

For the molecular identification of Symbiodiniaceae, the ribosomal Internal Transcribed Spacer 2 (ITS2) region was amplified using primers containing Illumina adapters (underlined) targeting parts of the 5.8S and 23S regions as well as the entire

ITS2 rRNA gene: ITS-Dino-fwd (5'-TCTTTCCCTACACGACGCTCTTCCGATCT GTGAATTGCAGAACTCCGTG-3') (Pochon et al., 2001), ITS2-Dino-rev2 (5'-GTGACTGGAGTTCAGACGTGTGCTCTTCCGATCT CCTCCGCTTACTTATATGCTT-3') (Stat et al., 2009). Using these primers, an adapter PCR was performed in a total volume of 20 µL: 5 µL template cDNA, 10 µL DreamTaq Green PCR Master Mix (2X) (Thermo Fisher, USA), and 2 µL of 10 µM of each primer. Each sample was adjusted to 20 µL with distilled and sterilised water. The PCR amplification was performed with 30 cycles of denaturation at 94°C for 1 min, annealing at 54°C for 1 min, and extension at 72°C for 1 min. The initial denaturation and final elongation were 95°C for 15 min and 72°C for 10 min, respectively. The PCR products were cleaned with Agencourt AMPure XP magnetic beads (Beckman Coulter, USA). Subsequently, an indexing PCR was performed to add Illumina sequencing adapters containing TrueSeq indices. Index PCR was conducted in a 20 µL volume using 5 µL of the previously purified adapter PCR product, 10 µL Q5® High-Fidelity 2X Master Mix (New England Biolabs, USA), 1 µL of 10 µM of the respective forward and reverse index primer, and 3 µL distilled and autoclaved water. Amplification was performed in a 3-step reaction with an initial denaturation of 5 min at 95 °C, 8 cycles of 1 min at 94 °C denaturation, 1 min at 52 °C annealing, and 1 min at 70 °C for elongation, followed by 10 min of final elongation at 70 °C. Indexed PCR products were cleaned using the Agencourt AMPure XP magnetic beads. Final DNA concentrations were quantified on a QubitTM 4 Fluorometer using the dsDNA-HS kit (Thermo Fisher, USA), pooled equimolarly, and sent to the University of Saarbrücken for sequencing on an Illumina MiSeq platform. Sequencing was conducted with a 2x250 bp paired-end approach according to the manufacturer's instructions. Raw reads were deposited at GenBank under Bioproject PRJNA1244770 (Additional file 1: Table 1).

Simbiodiniaceae assignment

The quality of raw reads was inspected using fastqc, and sequences were then quality-trimmed using BBDuk implemented in BBMerge v38.91 (Bushnell et al., 2017) with qtrim=rl, trimq=20, and minlen=100 parameters. Subsequently, filtered sequences were imported into QIIME 2 v.2021.4 (Bolyen et al., 2019), setting the p-trunc to 140, and were denoised with a maximum error rate of 2 using the DADA2 plugin (Callahan et al., 2016). The taxonomic assignment of Amplicon Sequence Variances (ASVs) was obtained using the RefSeq database extracted from SymPortal (Hume et al., 2019). Additionally, using the SymPortal analytical framework (SymPortal.org) defining intragenomic variant (DIV) profiles were identified (Hume et al., 2019). Raw, demultiplexed MiSeq reads were directly processed through the SymPortal pipeline. Sequence quality control was conducted as part of the SymPortal pipeline using Mothur 1.39.5 (Schloss et al., 2009), the BLAST+ suite (Camacho et al., 2009), and the minimum entropy decomposition method (Eren et al., 2015). ITS2 type profiles (representative of putative Symbiodiniaceae taxa or genotypes) were predicted and characterised by specific sets of DIVs.

We applied these two complementary approaches to assess Symbiodiniaceae diversity. The use of ASVs enables high-resolution discrimination of sequence data at the level of single-nucleotide differences, which is particularly useful for identifying diversity at the genus level (e.g., *Cladocopium*, *Durusdinium*, or *Symbiodinium*) (Cunning et al., 2017; Fujise et al., 2018). This approach is particularly valuable for identifying broad distribution patterns across various hosts or geographic regions. However, the ASV method treats all sequence variants equally, regardless of whether they represent intragenomic copies of a single symbiont strain or distinct

taxa, which can lead to an overestimation of diversity (Apprill & Gates, 2007; Thornhill et al., 2007). To address this, we also applied the DIV concept as implemented in SymPortal. This approach allows for subclade-level resolution by identifying characteristic combinations of intragenomic ITS2 variants, so-called ITS2-type profiles, that are representative of specific Symbiodiniaceae strains (LaJeunesse, 2002; Smith et al., 2017). It explicitly accounts for the multicopy structure of the ITS2 region in Symbiodiniaceae and leverages within-genome diversity to distinguish between intra- and intergenomic variation, without requiring additional markers such as psbAncr (Smith et al., 2017; Thornhill et al., 2007). As previously shown, even a one-base-pair difference in the dominant ITS2 sequence may reflect great evolutionary divergences (Thornhill et al., 2014), highlighting the importance of fine-scale resolution. Our decision to use both approaches in parallel was based on the distinct strengths of each method: ASVs enable reproducible, marker-independent classification at higher taxonomic levels, while DIV profiles provide deeper resolution within individual clades and are particularly suited for detecting ecologically relevant symbiont strains. This combined strategy not only confirmed expected diversity patterns at the genus level but also revealed subtle differences within subclades—differences (LaJeunesse et al., 2018; Sampayo et al., 2009).

Alpha and Beta diversity

Alpha and beta diversity calculations and statistical analyses were performed in QIIME2 v2023.9 (Bolyen et al., 2019) and R v4.0.3 (R Core Team, 2021), with differences considered significant at p <0.05. To describe and compare the alpha diversity across samples, we used the Shannon index that quantifies species richness and evenness, with higher values indicating a more diverse and evenly distributed symbiont community within a sample (Shannon, 1948). Differences in Shannon diversity were evaluated by one-way analysis of variance (ANOVA, Girden, 1992) or if data deviated from normality and/or homogeneity of variance by Kruskal-Wallis-Test (Kruskal & Wallis, 1952). A Non-Metric Multidimensional Scaling (NMDS) plot showing the variation in community composition among food source, sea slug genera, and country based on Bray-Curtis distance values was compiled in R v4.0.3 using the packages vegan (Dixon, 2003) and ggplot2 (Wickham, 2016). The Bray-Curtis distance quantifies compositional dissimilarity between samples based on the presence and relative abundance of shared symbiont taxa, with values ranging from 0 (identical communities) to 1 (entirely dissimilar communities) (Bray & Curtis, 1957). To assess the effects of food source, genus, country, and photosymbiotic status on the symbiont composition, a Permutational Multivariate Analysis of Variance (PERMANOVA, M. J. Anderson, 2014) was performed based on the Bray-Curtis dissimilarities using the adonis2 function from the vegan package in R v4.0.3, with 999 permutations. PERMANOVA tests were carried out for each factor individually to evaluate whether there were significant differences in the community structure between groups. To account for potential differences in group dispersion, the betadisper function was used to test the homogeneity of multivariate dispersions. Significant differences between the individual groups were subsequently analysed using a pairwise PERMANOVA.

1.4 Results

The diversity of Symbiodiniaceae within cladobranch sea slugs was analysed across the 28 specimens from 16 species, considering their geographical origin, photosymbiotic status, and food source using qiime2 and the SymPortal analytical framework (Fig. 1.2). Overall, 272.383 ITS sequences were obtained, with an average of 8.769 sequences per sample.

Cladocopium is the dominant symbiont in *Phyllodesmiun*

The analysis of Symbiodiniaceae ASV and DIV profiles revealed differences between cladobranch genera and the photosymbiotic state of the sea slugs (Additional file 1: Table 2-5). In non-symbiotic species such as *Coryphella lineata*, three different Symbiodiniaceae genera were detected in the ASV profile, with *Breviolum* (42.8%) being the most abundant, followed by *Symbiodinium* (29.6%) and *Cladocopium* (27.4%). Only 0.2% of the sequences were assigned to *Durusdinium* (Fig. 1.2A). In contrast, species collected in Italy with unstable photosymbiosis, *Aeolidiella alderi* (Cocks, 1852), *Spurilla neapolitana* (Delle Chiaie, 1841), and *Berghia coerulescens*, predominantly harboured ASVs identified as *Symbiodinium*, with *Breviolum* being only present to 10.9% in *B. coerulescens*. However, *Spurilla neapolitana* from France displayed a different pattern, containing *Breviolum* (55%), *Symbiodinium* (16.6%), and *Cladocopium* (23.3%). In species with stable photosymbiosis, such as *Pteraeolidia ianthina* and *Phyllodesmium*, the dominant photobiont in our ASV profile was *Cladocopium*. *Pteraeolidia ianthina* collected in Australia also contained *Durusdinium* (34.7%), whereas the individual from Egypt additionally harboured *Symbiodinium* (11%). Most *Phyllodesmium* specimens displayed an ASV symbiont community exclusively composed of *Cladocopium*, regardless of their collection location. A notable exception is *Phyllodesmium macphersonae* (Burn, 1962), which predominantly harboured *Durusdinium* (84.1%), while *Cladocopium* was present only at lower levels (15.9%).

The analysis of DIV profiles using SymPortal showed a species-specific composition with less diversity in symbiodiniaceae genera in cladobranchs with stable symbiosis (Fig. 1.2). The non-photosymbiotic *Coryphella lineata* exhibited a highly diverse DIV profile containing four different ITS2 types: A1bo (7%), A4 (20%), B1 (31%), and C1-C1b-C1c (11%). The four cladobranch species exhibiting an unstable photosymbiosis showed no divergence between their ASV and DIV profiles. *Aeolidiella alderi* and *Spurilla neapolitana* collected in Italy exclusively harboured the ITS2 type A1bo of *Symbiodinium*, while *Berghia coerulescens* also contained type B2 at a relative abundance of 6%. In contrast, *Spurilla neapolitana* from France displayed a more diverse DIV profile, comprising *Breviolum* B1 (41%), *Symbiodinium* A4 (17%), and *Cladocopium* C1-C1b-C1c (17%).

Both specimens of *Pteraeolidia ianthina* showed a dominance of *Cladocopium*, consistent with their ASV profiles. The individual from Australia harboured two distinct ITS2 types of *Cladocopium* (C1-C1b-C1c (22%) and C3 (14%)) as well as the *Durusdinium* type D51 (19%). In contrast, the Egyptian specimen contained only the *Cladocopium* type C1-C1b-C1c at 57% and *Symbiodinium* A1 at 14%.

Stable photosymbiotic species of the genus *Phyllodesmium* showed a maximum of two different ITS2 types. Interestingly, while *P. macphersonae* exhibited a more diverse ASV profile with a proportion of *Cladocopium* and *Durusdinium*, its DIV profile exclusively contained ITS2 type D5. Minor differences were also observed for example, for *Phyllodesmium rudmani* Burghardt and Gosliner, 2006 sample number 9, which exhibited a DIV profile consisting mainly of C1378 (13%) and C1381

(16%) without *Durusdinium*, *Breviolum* or *Symbiodinium* as indicated in the ASV profile. Several *Phyllodesmium* species showed a species-dependent DIV profile, such as *Phyllodesmium crypticum* Rudman, 1981, which had a homogeneous profile consisting of C1-C1b-C1c, or *Phyllodesmium magnum* Rudman, 1991, which exclusively harboured C65/C65a independent of their collection site. Similarly, both *Phyllodesmium lembehensis* Burghardt, Schrödl, and Wägele, 2008 and *Phyllodesmium koehleri* Burghardt, Schrödl, and Wägele, 2008 exclusively harbored ITS2 type C1381, without any *Durusdinium*, *Breviolum*, or *Symbiodinium*. *P. briareum* 2 and 3, which were collected in the Philippines showed a similar DIV profile with C2665 and C1.

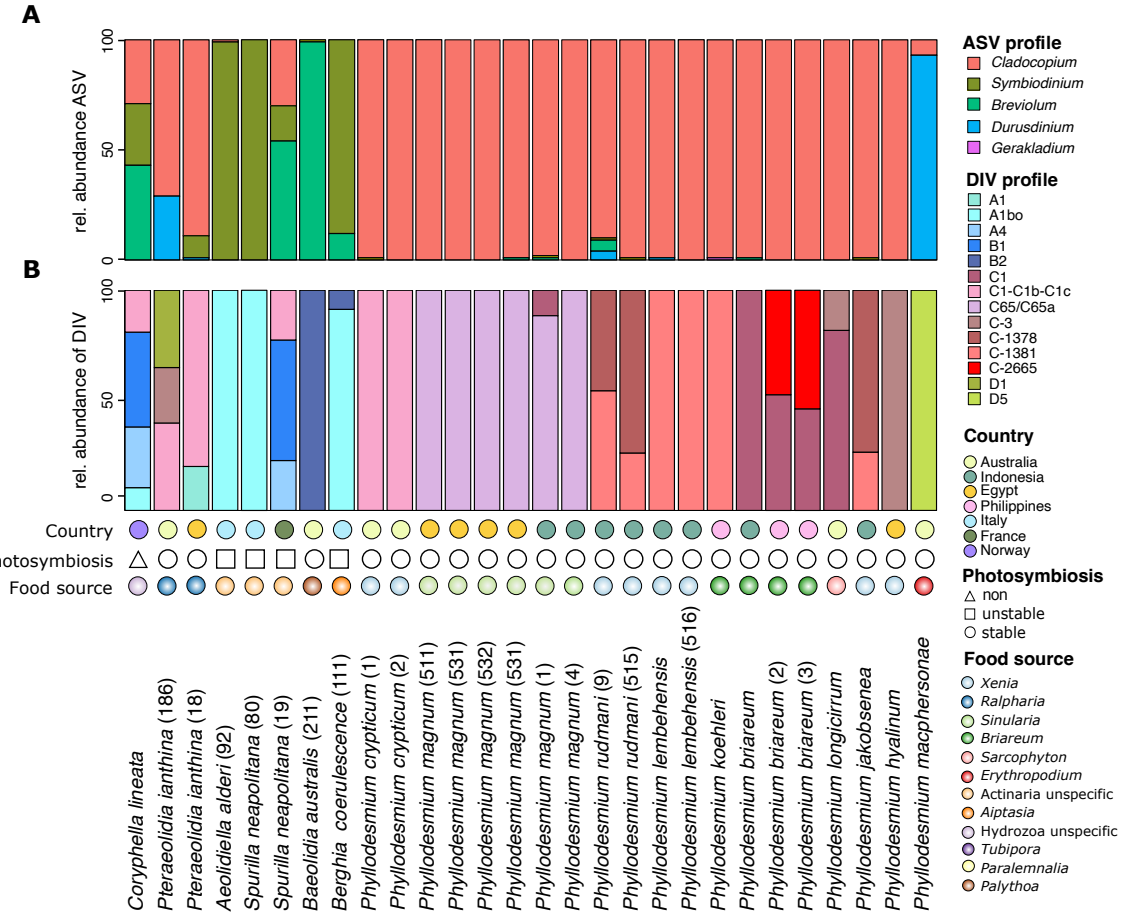

FIGURE 1.2: Relative abundance of Amplicon Sequence Variances (ASVs) (A) and Defining Intragenomic Variant (DIV) (B) profiles of different cladobranch species. Coloured squares indicate ASV or DIV profile; coloured circles indicate either geographic origin (country) or main food source, and shape the status of photosymbiosis (stable, unstable, absent)

Alpha and Beta diversity

Phyllodesmium briareum 2 had the highest alpha diversity, with Shannon indices of 3.94. In contrast, *Aeolidiella alderi* showed the lowest value at 0.62 (see Supplementary Material File 1: Table 6 and 7). Grouping by family revealed significant differences, specifically between Facelinidae (*Pteraeolidia ianthina*) and Aeolidiidae (*Aeolidiella alderi, Berghia coerulescens, Baeolidia australis* (Rudman, 1982) and *Spurilla neapolitana*) ($p = 0.036$), showing that Facelinidae had significantly higher alpha diversity. Further, Myrrhinidae (*Phyllodesmium* spp.) had significantly higher Shannon

indices compared to specimens of the family Aeolidiidae (*Aeolidiella alderi, Berghia coerulescens, Baeolidia australis* and *Spurilla neapolitana*) (p = 0.01) (Fig. 1.3A). Among countries, species from Italy had significantly lower Shannon indices compared to Indonesia (p = 0.026) and the Philippines (p = 0.017 (Fig. 1.3B). We also found a food-source-based difference in alpha diversity with species feeding on Actinaria having a significantly lower Shannon index compared to Hydrozoa-feeding (p = 0.0048116) and Octocorallia-feeding (p = 0.0044188) species (Fig. 1.3C). Neither the food source genus nor the photosymbiotic state (non, unstable, stable) yielded significant differences regarding the Shannon index.

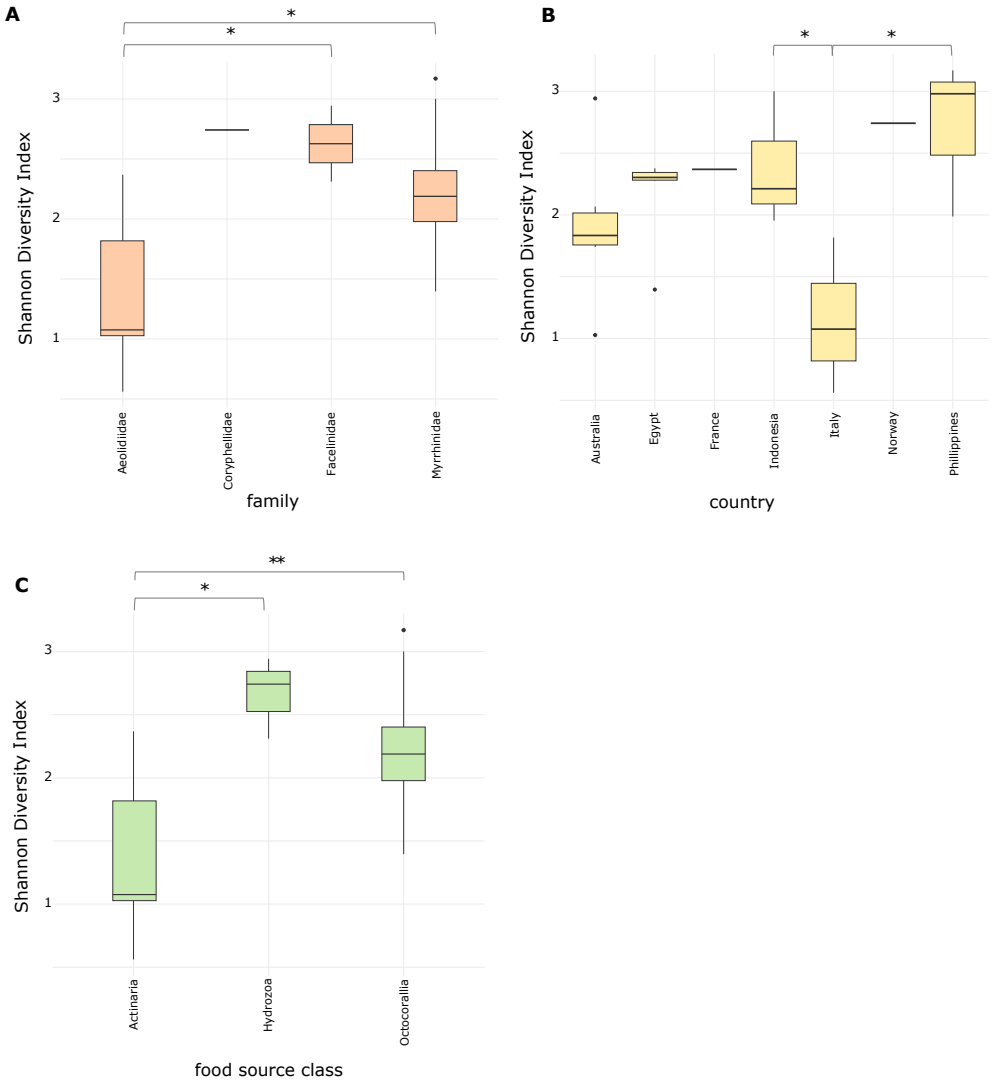

FIGURE 1.3: Boxplots showing Shannon diversity indices of Symbiodiniaceae in various cladobranch species grouped for family (A), country (B) and food source (class) (C). Significant differences between groups are indicated by asterisks (*p <0.05; **p <0.005).

The Bray-Curtis distance analysis and the NMDS ordination revealed a distinct cluster of the food source genus *Sinularia*, which is also reflected in the clustering pattern of the genus *Phyllodesmium* (here *Phyllodesmium magnum*) (Fig. 1.4A). Additionally, some *Phyllodesmium* species clustered with *Pteraeolidia ianthina*, suggesting similarities in their symbiont composition (Fig. 1.4B). Interestingly, most *Phyllodesmium* species clustered together independent of their country of origin, such as *Phyllodesmium magnum* (from Indonesia and Egypt) or *Phyllodesmium briareum* (from

the Philippines or Indonesia) (Fig. 1.4C). However, the species *Spurilla neapolitana*, known for its unstable photosymbiosis, collected in Italy, did not cluster with its conspecifics from France but instead grouped with the other unstable species, *Aeolidiella alderi* and *Berghia coerulescens*, which were also collected in Italy. The NMDS ordination based on geographic origin did not show a clear separation of samples by country, indicating that symbiont community composition is not primarily structured by geographic location. The specimen of *Spurilla neapolitana* collected in France clustered with the only non-photosymbiotic species, *Coryphella lineata* collected in Norway.

A permutational multivariate analysis of variance (PERMANOVA) was conducted using Bray-Curtis distances (see Supplementary Material File 1: Tables 8 and 9) to assess differences in symbiont composition. The analysis revealed that only the factor food source genus had a significant effect on the overall symbiont community structure ($F = 1.7056$, $p = 0.002^{**}$, $R^2 = 0.50083$). A pairwise PERMANOVA revealed significant differences between the groups *Xenia* - *Sinularia* ($F = 4.8293389$, $p = 0.0180000^{*}$, $R^2 = 0.28695951$), *Rapharia* - *Sinularia* ($F = 10.3199873$, $p = 0.0270000^{*}$, $R^2 = 0.63235266$), *Sinularia* - *Briareum* ($F = 7.2199804$, $p = 0.0270000^{*}$, $R^2 = 0.50773490$) and *Sinularia* - Actinaria unspecific ($F = 6.3090635$ $p = 0.0170000^{*}$, $R^2 = 0.47404263$). None of the factors, genus, country, or photosymbiotic status, significantly affected the Bray-Curtis distances between samples. The PERMANOVA results for genus ($F = 0.996$, $p = 0.466$, $R^2 = 0.221$), country ($F = 0.873$, $p = 0.743$, $R^2 = 0.166$), and photosymbiotic status ($F = 0.791$, $p = 0.861$, $R^2 = 0.059$) indicate that variation within groups exceeds any potential group-level differences.

1.5 Discussion

This study is the first to examine the Symbiodiniaceae diversity in several species of Cladobranchia using a metabarcoding approach, providing a foundation for future research. Our results revealed genus-specific patterns in symbiont composition among Cladobranchia, with *Cladocopium* being the most abundant symbiont in slugs with a stable photosymbiosis, particularly in *Phyllodesmium*. We also found a species-specific set of DIVs with C1, C65, and C-1381 as most abundant, particularly in *Phyllodesmium*. *Cladocopium* is known for its broad host range, associating not only with corals and other cnidarians but also with clams, flatworms, foraminifera, and sponges (Fay et al., 2009; Hikosaka-Katayama et al., 2012; Hill et al., 2011; Lee et al., 2020; Riewluang & Wakeman, 2023; Vega de Luna et al., 2019). Specific subclades of *Cladocopium*, such as *Cladocopium sodalum* LaJeunesse & C.C. Butler, 2023 (ITS2 type C3) or *C. proliferum* LaJeunesse, C.C. Butler, Nitschke & van Oppen, 2023 (ITS2 type C1), exhibit stress tolerance and contribute significantly to carbon fixation and release (Abrego et al., 2008; Butler et al., 2023; van Oppen & Berkelmans, 2006). In contrast, species with a stable photosymbiosis of the families Facelinidae and Aeolidiidae only showed a portion of *Cladocopium* symbionts and predominantly incorporated *Symbiodinium* and *Breviolum*, similar to species with an unstable or no photosymbiosis. Representatives of the genera *Symbiodinium* and *Breviolum* are widespread in corals which prefer shallow, light-flooded waters such as *Litophyton arboretum* Forskål, 1775, *Erythropodium caribaeorum* (Duchassaing de Fonbressin & Michelotti, 1860) or *Paralemnalia eburnean* Kükenthal, 1913 (Barneah et al., 2004; Goulet & Coffroth, 2004; Goulet et al., 2008). Several types of *Symbiodinium* are known to adapt to high or fluctuating light conditions and continuously produce

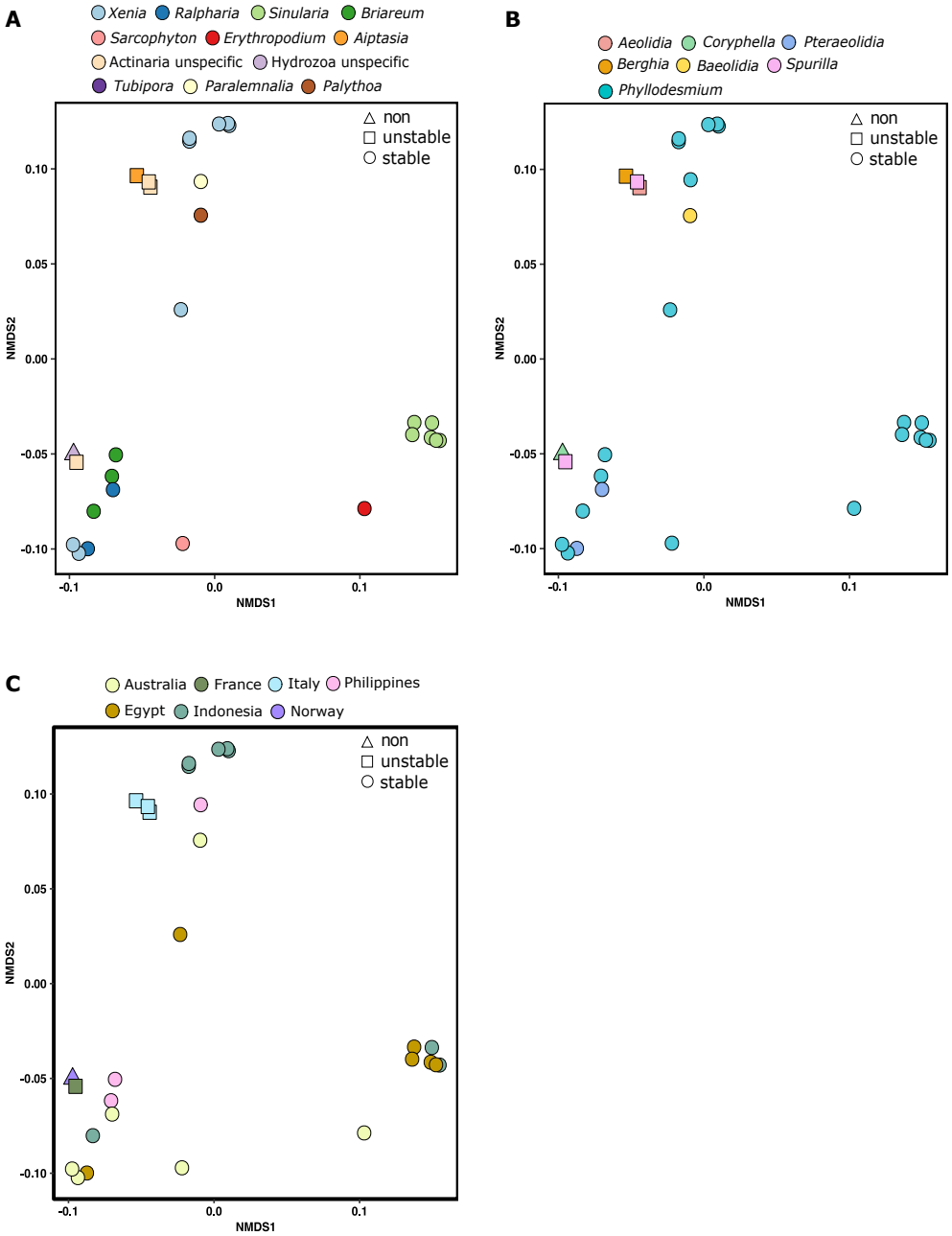

FIGURE 1.4: Non-Metric Multidimensional Scaling (NMDS) analysis based on Bray-Curtis distance matrix. Colour represents either food source genus (A), cladobranch genus (B) or country (C). Shape represents photosymbiosis status

UV-absorbing mycosporine-like amino acids (MAAs) (Banaszak et al., 2006; LaJeunesse, 2002). These compounds, which absorb light in the UVA and UVB range (310–362 nm), play a crucial role in photoprotection by acting as antioxidants and reducing damage caused by singlet oxygen (Hoegh-Guldberg & Jones, 1999; Rosic & Dove, 2011). In response, *Symbiodinium* exhibit enhanced capabilities for alternative photosynthetic electron transport pathways. They can dissociate their antenna complexes from the reaction centers of photosystem II under high light conditions, which helps cnidarians hosting *Symbiodinium* to tolerate better intense light exposure (Reynolds et al., 2008). However, several coral hosts show a reduction in health when harbouring symbionts of the genus *Symbiodinium* that may result from the host

not receiving sufficient nutritional input from this symbiont lineage (Rouzé et al., 2016; Stat et al., 2008). On the contrary, polyps of the upside-down jellyfish *Casiopea* sp. showed the highest survival rate when harbouring exclusively *Symbiodinium*, and adult *Casiopea* sp. showed a stable photosymbiosis without any reduction in health when incorporating *Symbiodinium* (Lampert, 2016). An exception to all other species examined was *Phyllodesmium macphersonae*, in which predominantly *Durusdimium* was found. The genus *Durusdinium* includes extremophile species adapted to strong temperature and turbidity fluctuations, such as the widespread ITS2 type D1-4 (Swain et al., 2017). Symbioses with these symbionts are particularly resistant to dissociation, such as coral bleaching. Studies have shown that corals in high-temperature environments often host a higher abundance of *Durusdinium*, considered the most thermally tolerant among Symbiodiniaceae clades (Abrego et al., 2009; Bay et al., 2016; Jones et al., 2008). Additionally, corals often shift their symbiont communities following bleaching events, replacing their original symbionts (clades A, B, C, or F) with *Durusdinium*, a strategy known as symbiont shuffling thought to enhance resilience against future bleaching and improve survival under rising ocean temperatures (Hume et al., 2016; Thinesh et al., 2019; van Oppen & Berkelmans, 2006).

Thus, the physiological and ecological properties assigned to different Symbiodiniaceae genera and types, such as the parasitic characteristics of *Symbiodinium*, appear to be more host-specific than being attributed to the symbiont (Goulet et al., 2019). As most specimens in our study that incorporated *Symbiodinium*—partially or exclusively—exhibited unstable or no photosymbiosis, this genus may not be suitable for establishing a stable photosymbiosis in Cladobranchia. In contrast, *Cladocopium* may be a more suitable photobiont for cladobranch slugs. Experiments involving cladobranch species with an unstable photosymbiosis, in which a different Symbiodiniaceae genus, such as *Cladocopium*, is introduced instead of *Symbiodinium*, would be exciting to determine whether the physiological traits of the algae facilitate the evolution of stable photosymbiosis in Cladobranchia.

While the presence of a suitable symbiont may play a role in enabling photosymbiosis in Cladobranchia, our data did not reveal a consistent association between the photosymbiotic state or geographic origin and the occurrence of specific Symbiodiniaceae clades. Yet, the food source seems to influence the diversity of symbiodiniaceans within Cladobranchia. Cladobranchia acquire their symbionts horizontally by feeding on cnidarians and incorporating the photobionts of their prey into the cells of their digestive gland system (Rola et al., 2022). However, the diet of most species examined here remains poorly documented. For example, the food source of *Phyllodesmium macphersonae* has only been documented by photographs in the slug's natural habitats, without confirmation through molecular analyses or laboratory experiments. Additionally, many slugs are polyphagous, so the symbiont community's composition in the slugs might be a mix of different food organisms. To better understand symbiont acquisition and composition in Cladobranchia, future studies should also focus on sampling and analysing the cnidarian prey to determine whether the abundance and diversity of the symbionts are conserved in the slugs after preying on the food source. This would also contribute to a better understanding of the symbiont communities associated with cnidarian prey. For example, while *Phyllodesmium briareum* is known to feed on both *Briareum asbestinum* (Pallas, 1766) and *Briareum violaceum* (Quoy & Gaimard, 1833), Symbiodiniaceae have only been characterised in *B. asbestinum* from Mexico (Ramsby & Goulet, 2019). For most cnidarian species serving as potential food sources for Cladobranchia, the composition of associated Symbiodiniaceae remains unknown.

Our combined approach, using ASVs and DIVs, provided detailed insight into the diversity of Symbiodiniaceae in Cladobranchia. Yet, in some cases, a discrepancy between ASVs and DIVs occurred. For instance, in *Phyllodesmium macphersonae* we identified a proportion of *Cladocopium* ASV, but exclusively obtained ITS2 type D5 (*Durusdinium*) regarding its DIV profile. This discrepancy likely reflects the higher sensitivity of ASV-based methods to low-abundance sequences, including potential background noise or minor co-occurring types. In contrast, the DIV approach focuses on the dominant, intragenomically consistent ITS2 variant patterns that define biologically relevant symbiont taxa (Apprill & Gates, 2007; Thornhill et al., 2007). Therefore, we suggest that future studies combine both approaches to obtain the maximum information regarding symbiont diversity and abundance in Cladobranchia.

1.6 Conclusion

Our study presents the first comprehensive analysis of Symbiodiniaceae diversity across multiple Cladobranchia species using ITS2 metabarcoding. It enhances our understanding of photosymbiosis in marine slugs and underscores the role of symbiont diversity in shaping ecological and evolutionary dynamics within Cladobranchia. Species with stable photosymbiosis (*Pteraeolidia ianthina* and *Phyllodesmium* spp.) primarily harbour *Cladocopium*, known for its high CO_2 fixation and thermal tolerance, while those with unstable or no photosymbiosis (*Coryphella lineata*, *Aeolidiella alderi*, *Spurilla neapolitana* and *Berghia coerulescence*) host *Symbiodinium* and *Breviolum*. We observed a correlation between symbiont profile and food source, with *Cladocopium* being more common in species with a stable photosymbiosis, suggesting it may promote symbiosis stability in Cladobranchia. However, whether these physiological traits directly facilitate the evolution of stable photosymbiosis remains to be investigated. The physiological and ecological properties associated with different Symbiodiniaceae genera, such as the parasitic tendencies of *Symbiodinium*, appear to be host-specific and context-dependent rather than solely determined by the symbiont itself. Our study provides a starting point for future research to explore whether introducing alternative Symbiodiniaceae genera can improve symbiont retention in species with unstable photosymbiosis.

Availability of data and materials

Data have been deposited with links to BioProject accession number PRJNA1244770 in the NCBI BioProject database https://www.ncbi.nlm.nih.gov/bioproject/?term=PRJNA1244770 with SRA accession numbers listed in Additional File 1: Table 1.

Acknowledgments

We thank Christina Lo Porto and Jasmin Kirch for their excellent technical assistance in conducting local deep sequencing.

Funding

No funds, grants, or other support were received.

Author Contributions

CS and GC planned the experiments. SB, CR, and GC sampled the material. CS, MB, and GC conducted the experiments, and GG and ST performed the sequencing. CS and GC processed, analysed, and visualised the data. All authors discussed and interpreted the results, wrote and revised the final version of the manuscript.

Ethics declarations

The authors declare no conflicts of interest.

Supplementary Materials

The supplementary material is included in the digital version of this paper.

Additional File 1

— Table 1. Metadata. — Table 2. Sequencing stats. — Table 3. ASV profile relative frequency. — Table 4. ASV profile absolute frequency. — Table 5. DIV sequences relative frequency. — Table 6. DIV profile absolute frequency. — Table 7. Shannon index. — Table 8. Shannon statistic. — Table 9. Bray-Curtis distance matrix. — Table 10. Bray-Curtis statistics.

References

Abrego, D., Ulstrup, K. E., Willis, B. L., & van Oppen, M. J. (2008). Species–specific interactions between algal endosymbionts and coral hosts define their bleaching response to heat and light stress. *Proceedings of the Royal Society B: Biological Sciences*, *275*(1648), 2273–2282.

Abrego, D., Van Oppen, M. J., & Willis, B. L. (2009). Onset of algal endosymbiont specificity varies among closely related species of *Acropora* corals during early ontogeny. *Molecular Ecology*, *18*(16), 3532–3543.

Anderson, M. J. (2014). Permutational multivariate analysis of variance (PERMANOVA). *Wiley Statsref: Statistics Reference Online*, 1–15.

Apprill, A. M., & Gates, R. D. (2007). Recognizing diversity in coral symbiotic dinoflagellate communities. *Molecular Ecology*, *16*(6), 1127–1134.

Banaszak, A. T., Santos, M. G. B., LaJeunesse, T., & Lesser, M. (2006). The distribution of mycosporine-like amino acids (MAAs) and the phylogenetic identity of symbiotic dinoflagellates in cnidarian hosts from the Mexican Caribbean. *Journal of Experimental Marine Biology and Ecology*, *337*(2), 131–146.

Barneah, O., Weis, V., Perez, S., & Benayahu, Y. (2004). Diversity of dinoflagellate symbionts in Red Sea soft corals: Mode of symbiont acquisition matters. *Marine Ecology Progress Series*, *275*, 89–95.

Bay, L. K., Doyle, J., Logan, M., & Berkelmans, R. (2016). Recovery from bleaching is mediated by threshold densities of background thermo-tolerant symbiont types in a reef-building coral. *Royal Society Open Science*, *3*(6), 160322.

Bergh, R. (1870). Malacologische untersuchungen. in: C. semper, reisen im archpel der philippinen. *Wiss. Res.*, *2*(14), 603–645.

Bergh, R. (1896). Eolidiens d'amboine. *Revue Suisse de Zoologie*, *4*(2), 385–394.

Bolyen, E., Rideout, J. R., Dillon, M. R., Bokulich, N. A., Abnet, C. C., Al-Ghalith, G. A., Alexander, H., Alm, E. J., Arumugam, M., Asnicar, F., et al. (2019). Reproducible, interactive, scalable and extensible microbiome data science using QIIME 2. *Nature Biotechnology*, *37*(8), 852–857.

Bray, J. R., & Curtis, J. T. (1957). An ordination of the upland forest communities of southern Wisconsin. *Ecological Monographs*, *27*(4), 326–349.

Burghardt, I., Evertsen, J., Johnsen, G., & Wägele, H. (2005). Solar powered seaslugs - Mutualistic symbiosis of aeolid nudibranchia (Mollusca, Gastropoda, Opisthobranchia) with *Symbiodinium*. *Symbiosis*.

Burghardt, I., & Gosliner, T. M. (2006). *Phyllodesmium rudmani* (Mollusca: Nudibranchia: Aeolidoidea), a new solar powered species from the Indo-West Pacific with data on its symbiosis with zooxanthellae. *Zootaxa*, *1308*(1), 31–47.

Burghardt, I., Schrödl, M., & Wägele, H. (2008). Three new solar-powered species of the genus *Phyllodesmium* Ehrenberg, 1831 (Mollusca: Nudibranchia: Aeolidioidea) from the tropical Indo-Pacific, with analysis of their photosynthetic activity and notes on biology. *Journal of Molluscan Studies*, *74*(3), 277–292.

Burghardt, I., Stemmer, K., & Wägele, H. (2008). Symbiosis between *Symbiodinium* (Dinophyceae) and various taxa of Nudibranchia (Mollusca: Gastropoda), with analyses of long-term retention. *Organisms Diversity & Evolution*, *8*(1), 66–76.

Burghardt, I., & Wägele, H. (2014). The symbiosis between the 'solar-powered'nudibranch *Melibe engeli* Risbec, 1937 (Dendronotoidea) and *Symbiodinium* sp. (Dinophyceae). *Journal of Molluscan Studies*, *80*(5), 508–517.

Burn, R. (1962). Descriptions of victorian nudibranchiate Mollusca, with a comprehensive review of the Eolidacea. *Memoirs of the National Museum of Victoria, Melbourne*, *25*, 95–128.

Bushnell, B., Rood, J., & Singer, E. (2017). BBMerge–accurate paired shotgun read merging via overlap. *PloS one*, *12*(10), e0185056.

Butler, C. C., Turnham, K. E., Lewis, A. M., Nitschke, M. R., Warner, M. E., Kemp, D. W., Hoegh-Guldberg, O., Fitt, W. K., van Oppen, M. J., & LaJeunesse, T. (2023). Formal recognition of host-generalist species of dinoflagellate (*Cladocopium*, Symbiodiniaceae) mutualistic with Indo-Pacific reef corals. *Journal of Phycology*, *59*(4), 698–711.

Callahan, B. J., McMurdie, P. J., Rosen, M. J., Han, A. W., Johnson, A. J. A., & Holmes, S. P. (2016). DADA2: High-resolution sample inference from Illumina amplicon data. *Nature Methods*, *13*(7), 581–583.

Camacho, C., Coulouris, G., Avagyan, V., Ma, N., Papadopoulos, J., Bealer, K., & Madden, T. L. (2009). BLAST+: Architecture and applications. *BMC Bioinformatics*, *10*, 1–9.

Cocks, W. (1852). New species of mollusca. *Naturalist*, *2*(1).

Cunning, R., Gates, R. D., & Edmunds, P. J. (2017). Using high-throughput sequencing of ITS2 to describe *Symbiodinium* metacommunities in St. John, US Virgin Islands. *PeerJ*, *5*, e3472.

Dana, J. D. (1846). *United states exploring expedition during the years 1838-1842: Atlas zoophytes* (Vol. 7). Lea; Blanchard.

Davies, S. W., Moreland, K. N., Wham, D. C., Kanke, M. R., & Matz, M. V. (2020). *Cladocopium* community divergence in two *Acropora* coral hosts across multiple spatial scales. *Molecular Ecology*, *29*(23), 4559–4572.

Delle Chiaie, S. (1841). Descrizione e notomia degli animali invertebrati della sicilia citeriore: Osservati vivi negli anni 1822-1830/da s. delle chiale. *Museum of Comparative Zoology–Biodiversity Heritage Library digitization project*.

Dixon, P. (2003). VEGAN, a package of R functions for community ecology. *Journal of Vegetation Science*, *14*(6), 927–930.

Duchassaing de Fonbressin, P., & Michelotti, G. (1860). Mémoire sur les Coralliaires des Antilles.

Eren, A. M., Morrison, H. G., Lescault, P. J., Reveillaud, J., Vineis, J. H., & Sogin, M. L. (2015). Minimum entropy decomposition: Unsupervised oligotyping for sensitive partitioning of high-throughput marker gene sequences. *The ISME Journal*, *9*(4), 968–979.

Fay, S., Weber, M., & Lipps, J. (2009). The distribution of *Symbiodinium* diversity within individual host Foraminifera. *Coral Reefs*, *28*, 717–726.

FitzPatrick, S., Liberatore, K., Garcia, J., Burghardt, I., Colman, D., Moquin, S., Takacs-Vesbach, C., & Shepherd, U. (2012). *Symbiodinium* diversity in the soft coral *Heteroxenia* sp. and its nudibranch predator *Phyllodesmium lizardensis*. *Coral Reefs*, *31*, 895–905.

Forskål, P. (1775). *Descriptiones animalium, avium, amphibiorum, piscium, insectorum, vermium: Quae in itinere orientali observavit*. ex officina Mölleri.

Fujise, L., Nitschke, M. R., Frommlet, J. C., Serôdio, J., Woodcock, S., Ralph, P. J., & Suggett, D. J. (2018). Cell cycle dynamics of cultured coral endosymbiotic microalgae (*Symbiodinium*) across different types (species) under alternate light and temperature conditions. *Journal of Eukaryotic Microbiology*, *65*(4), 505–517.

Gardner, S. G., Camp, E. F., Smith, D. J., Kahlke, T., Osman, E. O., Gendron, G., Hume, B. C., Pogoreutz, C., Voolstra, C. R., & Suggett, D. J. (2019). Coral microbiome diversity reflects mass coral bleaching susceptibility during the 2016 El Niño heat wave. *Ecology and Evolution*, *9*(3), 938–956.

Girden, E. R. (1992). *ANOVA: Repeated measures*. Sage.

Goodheart, J. A., Bazinet, A. L., Valdés, Á., Collins, A. G., & Cummings, M. P. (2017). Prey preference follows phylogeny: Evolutionary dietary patterns within the marine gastropod group Cladobranchia (Gastropoda: Heterobranchia: Nudibranchia). *BMC Evolutionary Biology*, *17*, 1–14.

Goodheart, J. A., & Bely, A. E. (2017). Sequestration of nematocysts by divergent cnidarian predators: Mechanism, function, and evolution. *Invertebrate Biology*, *136*(1), 75–91.

Goodheart, J. A., Bleidißel, S., Schillo, D., Strong, E. E., Ayres, D. L., Preisfeld, A., Collins, A. G., Cummings, M. P., & Wägele, H. (2018). Comparative morphology and evolution of the cnidosac in Cladobranchia (Gastropoda: Heterobranchia: Nudibranchia). *Frontiers in Zoology*, *15*, 1–18.

Goulet, T. L., & Coffroth, M. A. (2004). The genetic identity of dinoflagellate symbionts in Caribbean octocorals. *Coral Reefs*, *23*, 465–472.

Goulet, T. L., Lucas, M. Q., & Schizas, N. V. (2019). Symbiodiniaceae genetic diversity and symbioses with hosts from shallow to mesophotic coral ecosystems. *Mesophotic Coral Ecosystems*, 537–551.

Goulet, T. L., Simmons, C., & Goulet, D. (2008). Worldwide biogeography of *Symbiodinium* in tropical octocorals. *Marine Ecology Progress Series*, *355*, 45–58.

Guiry, M. D. (2024). How many species of algae are there? A reprise. Four kingdoms, 14 phyla, 63 classes and still growing. *Journal of Phycology*, *60*(2), 214–228.

Hikosaka-Katayama, T., Koike, K., Yamashita, H., Hikosaka, A., & Koike, K. (2012). Mechanisms of maternal inheritance of dinoflagellate symbionts in the acoelomorph worm *Waminoa litus*. *Zoological Science*, *29*(9), 559–567.

Hill, M., Allenby, A., Ramsby, B., Schönberg, C., & Hill, A. (2011). *Symbiodinium* diversity among host clionaid sponges from caribbean and pacific reefs: evidence of heteroplasmy and putative host-specific symbiont lineages. *Molecular Phylogenetics and Evolution*, *59*(1), 81–88.

Hoegh-Guldberg, O., & Jones, R. J. (1999). Photoinhibition and photoprotection in symbiotic dinoflagellates from reef-building corals. *Marine Ecology Progress Series*, *183*, 73–86.

Howells, E. J., Vaughan, G., Work, T. M., Burt, J., & Abrego, D. (2020). Annual outbreaks of coral disease coincide with extreme seasonal warming. *Coral Reefs*, *39*, 771–781.

Hume, B. C., D'Angelo, C., Burt, J. A., & Wiedenmann, J. (2018). Fine-scale biogeographical boundary delineation and sub-population resolution in the *Symbiodinium* thermophilum coral symbiont group from the Persian/Arabian Gulf and Gulf of Oman. *Frontiers in Marine Science*, *5*, 138.

Hume, B. C., Smith, E. G., Ziegler, M., Warrington, H. J., Burt, J. A., LaJeunesse, T., Wiedenmann, J., & Voolstra, C. R. (2019). SymPortal: A novel analytical framework and platform for coral algal symbiont next-generation sequencing ITS2 profiling. *Molecular Ecology Resources*, *19*(4), 1063–1080.

Hume, B. C., Voolstra, C. R., Arif, C., D'Angelo, C., Burt, J. A., Eyal, G., Loya, Y., & Wiedenmann, J. (2016). Ancestral genetic diversity associated with the rapid spread of stress-tolerant coral symbionts in response to Holocene climate change. *Proceedings of the National Academy of Sciences*, *113*(16), 4416–4421.

Jones, A. M., Berkelmans, R., van Oppen, M. J., Mieog, J. C., & Sinclair, W. (2008). A community change in the algal endosymbionts of a scleractinian coral following a natural bleaching event: Field evidence of acclimatization. *Proceedings of the Royal Society B: Biological Sciences*, *275*(1641), 1359–1365.

Kruskal, W. H., & Wallis, W. A. (1952). Use of ranks in one-criterion variance analysis. *Journal of the American Statistical Association*, *47*(260), 583–621.

Kükenthal, W. (1913). *Alcyonaria des Roten Meeres*. K. k. Hof-u. Staatsdr., Hölder.

LaJeunesse, T. (2002). Diversity and community structure of symbiotic dinoflagellates from Caribbean coral reefs. *Marine Biology*, *141*, 387–400.

LaJeunesse, T., Parkinson, J. E., Gabrielson, P. W., Jeong, H. J., Reimer, J. D., Voolstra, C. R., & Santos, S. R. (2018). Systematic revision of Symbiodiniaceae highlights the antiquity and diversity of coral endosymbionts. *Current Biology*, *28*(16), 2570–2580.

Lampert, K. P. (2016). *Cassiopea* and its zooxanthellae. *The cnidaria, past, present and future: The world of medusa and her sisters*, 415–423.

Laurillard, C. L. (1832). *In: Iconographie du règne animal de g. cuvier, ou représentation d'après nature de l'une des espèces les plus remarquables, et souvent non encore figurées, de chaque genre d'animaux. avec un texte descriptif mis au courant de la science: Ouvrage pouvant servir d'atlas à tous les traités de zoologie* (Vol. 4). JB Baillière.

Lee, S. Y., Jeong, H. J., & Lajeunesse, T. (2020). *Cladocopium infistulum* sp. nov. (Dinophyceae), a thermally tolerant dinoflagellate symbiotic with giant clams from the western Pacific Ocean. *Phycologia*, *59*(6), 515–526.

Lesser, M., Stat, M., & Gates, R. (2013). The endosymbiotic dinoflagellates (*Symbiodinium* sp.) of corals are parasites and mutualists. *Coral Reefs*, *32*, 603–611.

Lovén, S. L. (1846). *Index molluscorum: Litora scandinaviæ occidentalia habitantium. faunæ prodromum*. PA Norstedt.

Martinez, S., Grover, R., & Ferrier-Pagès, C. (2022). Symbiont starvation affects the stability of the coral–Symbiodiniaceae symbiosis. *Frontiers in Marine Science*, *9*, 979563.

Melo Clavijo, J., Sickinger, C., Bleidißel, S., Gasparoni, G., Tierling, S., Preisfeld, A., & Christa, G. (2022). The nudibranch *Berghia stephanieae* (Valdés, 2005) is not able to initiate a functional symbiosome-like environment to maintain *Breviolum minutum* (JE Parkinson & LaJeunesse 2018). *Frontiers in Marine Science*.

Monteiro, E. A., Güth, A. Z., Banha, T. N., Sumida, P. Y., & Mies, M. (2019). Evidence against mutualism in an aeolid nudibranch associated with Symbiodiniaceae dinoflagellates. *Symbiosis*, *79*, 183–189.

Nitschke, M. R., Craveiro, S. C., Brandão, C., Fidalgo, C., Serôdio, J., Calado, A. J., & Frommlet, J. C. (2020). Description of *Freudenthalidium* gen. nov. and *Halluxium* gen. nov. to formally recognize clades Fr3 and H as genera in the family Symbiodiniaceae (Dinophyceae). *Journal of Phycology*, *56*(4), 923–940.

Obermann, D., Bickmeyer, U., & Wägele, H. (2012). Incorporated nematocysts in *Aeolidiella stephanieae* (Gastropoda, Opisthobranchia, Aeolidoidea) mature by acidification shown by the pH sensitive fluorescing alkaloid Ageladine A. *Toxicon*, *60*(6), 1108–1116.

Pallas, P. S. (1766). *Elenchus zoophytorum sistens generum adumbrationes generaliores et specierum cognitarum... descriptiones etc*. Varrentrapp.

Pochon, X., Pawlowski, J., Zaninetti, L., & Rowan, R. (2001). High genetic diversity and relative specificity among *Symbiodinium*-like endosymbiotic dinoflagellates in soritid foraminiferans. *Marine Biology*, *139*, 1069–1078.

Quoy, J. R. C., & Gaimard, J. P. (1833). *Zoologie IV: Zoophytes. In:Zoologie. Voyage de la corvette l'Astrolabe : exécuté par ordre du roi, pendant les années 1826-1827-1828-1829* (Vol. 5). J. Tastu, editeur-imprimeur.

R Core Team. (2021). *R: A Language and Environment for Statistical Computing*. R Foundation for Statistical Computing. Vienna, Austria.

Ramsby, B. D., & Goulet, T. L. (2019). Symbiosis and host morphological variation: Symbiodiniaceae photosynthesis in the octocoral *Briareum asbestinum* at ambient and elevated temperatures. *Coral Reefs*, *38*(2), 359–371.

Rapp, W. (1829). *Ueber die Polypen im Allgemeinen und die Actinien insbesondere* (Vol. i-iv: 1-62).

Ravindran, C., Lawrance, I., & Vasanth, A. J. (2022). Endosymbiotic *Symbiodinium* clades occurrence and influence on coral growth and resilience during stress. *Symbiosis*, *86*(3), 261–272.

Reynolds, J. M., Bruns, B. U., Fitt, W. K., & Schmidt, G. W. (2008). Enhanced photoprotection pathways in symbiotic dinoflagellates of shallow-water corals and other cnidarians. *Proceedings of the National Academy of Sciences*, *105*(36), 13674–13678.

Riewluang, S., & Wakeman, K. C. (2023). Biodiversity of symbiotic microalgae associated with meiofaunal marine acoels in Southern Japan. *PeerJ*, *11*, e16078.

Risbec, J. (1937). Note préliminaire au sujet de nudibranches néo-calédoniens. *Bulletin de Museé National d'Histoire Naturelle, Paris, Ser*, *2*(9), 159–164.

Risbec, J. (1928). *Contribution a l'etude des nudibranches neo-caledoniens* (Vol. 2). Société d'éditions géographiques, maritimes et coloniales.

Rola, M., Frankenbach, S., Bleidissel, S., Sickinger, C., Donath, A., Frommlet, J. C., Greve, C., Serôdio, J., Preisfeld, A., Melo Clavijo, J., et al. (2022). Cladobranchia (Gastropoda, Nudibranchia) as a promising model to understand the molecular evolution of photosymbiosis in animals. *Frontiers in Marine Science*, *8*, 745644.

Rosic, N. N., & Dove, S. (2011). Mycosporine-like amino acids from coral dinoflagellates. *Applied and Environmental Microbiology*, *77*(24), 8478–8486.

Rouzé, H., Lecellier, G., Saulnier, D., & Berteaux-Lecellier, V. (2016). *Symbiodinium* clades A and D differentially predispose *Acropora cytherea* to disease and *Vibrio* spp. colonization. *Ecology and Evolution*, *6*(2), 560–572.

Rudman, W. (1981). The anatomy and biology of alcyonarian-feeding aeolid opisthobranch molluscs and their development of symbiosis with zooxanthellae. *Zoological Journal of the Linnean Society*, *72*(3), 219–262.

Rudman, W. (1982). The taxonomy and biology of further aeolidacean and arminacean nudibranch molluscs with symbiotic zooxanthellae. *Zoological Journal of the Linnean Society*, *74*(2), 147–196.

Rudman, W. (1991). Further studies on the taxonomy and biology of the octocoral-feeding genus *Phyllodesmium* Ehrenberg, 1831 (Nudibranchia: Aeolidoidea). *Journal of Molluscan Studies*, *57*(2), 167–203.

Sampayo, E., Dove, S., & LaJeunesse, T. (2009). Cohesive molecular genetic data delineate species diversity in the dinoflagellate genus *Symbiodinium*. *Molecular Ecology*, *18*(3), 500–519.

Schloss, P. D., Westcott, S. L., Ryabin, T., Hall, J. R., Hartmann, M., Hollister, E. B., Lesniewski, R. A., Oakley, B. B., Parks, D. H., Robinson, C. J., et al. (2009). Introducing mothur: Open-source, platform-independent, community-supported software for describing and comparing microbial communities. *Applied and Environmental Microbiology*, *75*(23), 7537–7541.

Shannon, C. E. (1948). A mathematical theory of communication. *The Bell System Technical Journal*, *27*(3), 379–423.

Smith, E. G., Ketchum, R. N., & Burt, J. A. (2017). Host specificity of *Symbiodinium* variants revealed by an ITS2 metahaplotype approach. *The ISME Journal*, *11*(6), 1500–1503.

Stat, M., Morris, E., & Gates, R. D. (2008). Functional diversity in coral–dinoflagellate symbiosis. *Proceedings of the National Academy of Sciences*, *105*(27), 9256–9261.

Stat, M., Pochon, X., Cowie, R. O., & Gates, R. D. (2009). Specificity in communities of *Symbiodinium* in corals from Johnston Atoll. *Marine Ecology Progress Series*, *386*, 83–96.

Swain, T. D., Chandler, J., Backman, V., & Marcelino, L. (2017). Consensus thermotolerance ranking for 110 *Symbiodinium* phylotypes: An exemplar utilization of a novel iterative partial-rank aggregation tool with broad application potential. *Functional Ecology*, *31*(1), 172–183.

Thinesh, T., Meenatchi, R., Jose, P. A., Kiran, G. S., & Selvin, J. (2019). Differential bleaching and recovery pattern of southeast Indian coral reef to 2016 global mass bleaching event: Occurrence of stress-tolerant symbiont *Durusdinium* (Clade D) in corals of Palk Bay. *Marine Pollution Bulletin*, *145*, 287–294.

Thornhill, D. J., Lajeunesse, T., & Santos, S. R. (2007). Measuring rDNA diversity in eukaryotic microbial systems: How intragenomic variation, pseudogenes, and PCR artifacts confound biodiversity estimates. *Molecular Ecology*, *16*(24), 5326–5340.

Thornhill, D. J., Lewis, A. M., Wham, D. C., & LaJeunesse, T. (2014). Host-specialist lineages dominate the adaptive radiation of reef coral endosymbionts. *Evolution*, *68*(2), 352–367.

Valdés, Á. (2005). A new species of *Aeolidiella* Bergh, 1867 (Mollusca: Nudibranchia: Aeolidiidae) from the Florida Keys, USA. *Veliger*, *47*(3), 218–223.

van Oppen, M. J., & Berkelmans, R. (2006). The role of zooxanthellae in the thermal tolerance of corals: A 'nugget of hope' for coral reefs in an era of climate change. *Proceedings of the Royal Society B: Biological Sciences*.

Vega de Luna, F., Dang, K.-V., Cardol, M., Roberty, S., & Cardol, P. (2019). Photosynthetic capacity of the endosymbiotic dinoflagellate *Cladocopium* sp. is preserved during digestion of its jellyfish host *Mastigias papua* by the anemone *Entacmaea medusivora*. *FEMS Microbiology Ecology*, *95*(10), fiz141.

Wägele, H., & Klussmann-Kolb, A. (2005). Opisthobranchia (Mollusca, Gastropoda)–more than just slimy slugs. Shell reduction and its implications on defence and foraging. *Frontiers in Zoology*, *2*, 1–18.

Wägele, H., Raupach, M. J., Burghardt, I., Grzymbowski, Y., & Händeler, K. (2010). Solar powered seaslugs (Opisthobranchia, Gastropoda, Mollusca): Incorporation of photosynthetic units: A key character enhancing radiation? *Evolution in action: Case studies in adaptive radiation, speciation and the origin of biodiversity*, 263–282.

Wecker, P., Fournier, A., Bosserelle, P., Debitus, C., Lecellier, G., & Berteaux-Lecellier, V. (2015). Dinoflagellate diversity among nudibranchs and sponges from French Polynesia: Insights into associations and transfer. *Comptes Rendus. Biologies*, *338*(4), 278–283.

Wickham, H. (2016). *ggplot2: Elegant Graphics for Data Analysis*. Springer-Verlag New York.

Yorifuji, M., Takeshima, H., Mabuchi, K., Watanabe, T., & Nishida, M. (2015). Comparison of *Symbiodinium* dinoflagellate flora in sea slug populations of the *Pteraeolidia ianthina* complex. *Marine Ecology Progress Series*, *521*, 91–104.

Yuyama, I., & Higuchi, T. (2014). Comparing the effects of symbiotic algae (*Symbiodinium*) clades C1 and D on early growth stages of *Acropora tenuis*. *PLoS One*, *9*(6), e98999.

Chapter 2

Collectin-12 – A Promising Symbiont Recognition Receptor in *Berghia stephanieae* (Á. Valdés, 2005)

Corinna Sickinger[1], Rebecca Lopez-Anido[2], Sofia Paz Sedano[2], Gregor Christa[3], Angelika Preisfeld[1] and Jessica Goodheart[2]

[1]*Institute for Zoology and Didactics of Biology, University of Wuppertal, Wuppertal, Germany*
[2]*Invertebrate Zoology, American Museum of Natural History, New York City, USA*
[3]*Department of Evolution and Biodiversity, University of Wuppertal, Wuppertal, Germany*

2.1 Abstract

The cladobranch sea slug *Berghia stephanieae* exhibits a unique biological strategy by incorporating both nematocysts and symbiotic microalgae (photobionts) from its cnidarian prey. While the anatomical localisation of these components is well documented, the molecular mechanisms by which *B. stephanieae* recognises and incorporates its photobionts remain poorly understood. The detection and subsequent incorporation of potential symbionts is a crucial step in this process. Research on photosymbiotic Cnidarians has emphasised the importance of unique photobiont surface molecules, so-called microbe-associated molecular patterns (MAMPs), in recognition by pattern recognition receptors (PRRs) on the host cell's membrane. In Cnidarians, specific PRRs can recognise symbiont-specific MAMPs to initiate the phagocytosis of potential symbionts. In this study, we investigated the potential role of the C-type lectin Collectin-12 in *B. stephanieae's* endosymbiosis. To do so, we analysed gene expression patterns using spatial transcriptomics and *in situ* hybridisation chain reaction (HCR) in both starved and refed slugs. Our results show that Collectin-12 is predominantly expressed in the digestive gland and proximal cerata regions, sites of photobiont localisation, but absent in the distal cnidosac, which is responsible for nematocyst storage. These findings indicate a possible role for Collectin-12 in photobiont recognition, potentially analogous to innate immune recognition pathways observed in cnidarians. The increased expression in refed slugs further implies a dynamic regulation in response to photobiont presence. This study is the first step towards identifying a specific PRR involved in algal recognition in a cladobranch sea slug, highlighting conserved molecular mechanisms underlying metazoan photosymbiosis.

Keywords symbiont recognition · Photosymbiosis · spatial transcriptomics · *in situ* hybridisation chain reaction

2.2 Introduction

Many cladobranch sea slugs possess the remarkable ability to incorporate two biologically distinct components from their cnidarian prey: Nematocysts and microalgae of the family Symbiodiniaceae Fensome, Taylor, Norris, Sarjeant, Wharton & Williams, 1993 (Goodheart et al., 2018; Wägele et al., 2010). Nematocysts, venomous stinging organelles, are transported to and stored in the cnidosac, a specialised structure at the distal tip of the cerata, where they can be reused for defence (Fig.2.1). Additionally, some species phagocytose the microalgae of their food source, called photobiont, into epithelial cells of the digestive gland in the proximal region of the cerata, maintaining them photosynthetically active for extended periods (Rola et al., 2022).

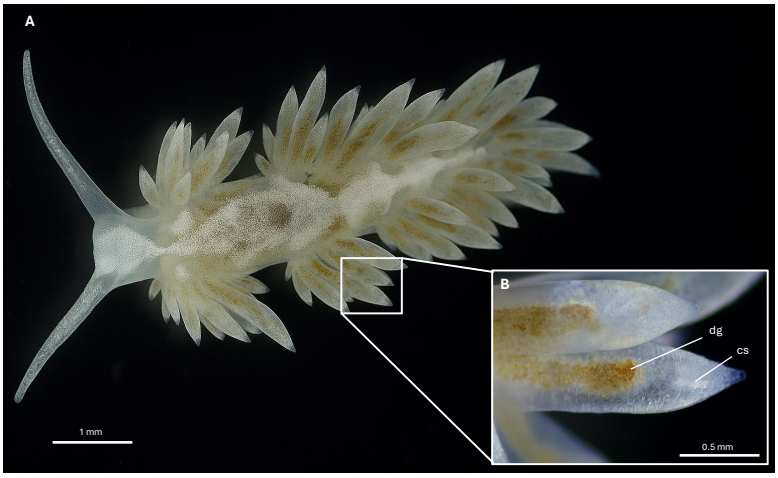

FIGURE 2.1: *Berghia stephanieae* (A) and close up of the cerata with the cnidosac at the distal end and the digestive gland system containing the photobionts at the proximal end (B). cs = cnidosac, dg = digestive gland.

Despite the evolutionary relevance of this incorporation strategy, the underlying molecular mechanisms of recognition and maintenance in the slug host remain poorly understood. The photosymbiosis found in Cnidaria, especially Anthozoa, is probably the best-studied endosymbiotic relationship between a heterotrophic host and a phototrophic symbiont (Davy et al., 2012; Rosset et al., 2021; Weis et al., 2008). The host has to recognise and ingest the specific photobiont, a foreign organism, which comes with considerable risks, as it requires a modification of the immune system and, in the case of false recognition, carries the risk of introducing pathogens into the host's cells (Emery et al., 2024; McFall-Ngai et al., 2013). In cnidarians, a well-studied mechanism to distinguish specific symbionts from pathogens, and to regulate the immune system accordingly, is the interaction between specific surface molecules of the photobiont called microbe-associated molecular patterns (MAMPs) and pattern recognition receptors (PRRs) of the host (Davy et al., 2012; Mansfield & Gilmore, 2019). In this system, MAMPs of the phototrophic microorganism are recognised by PRRs located on the host's cell membrane. If the host cell recognises the microbe as a suitable symbiont, phagocytosis is initiated, a signalling cascade

regulating the immune system is triggered, and specific activator proteins, which induce the early phagosome formation by the recruitment of Rab5 are produced. As a result, the symbiont is incorporated into the host cell. The resulting membrane, referred to as a symbiosome, surrounds the photobiont intracellularly and is crucial for the nutrient exchange between host and photobiont (Malcolm & April, 2012). One of the best-supported mechanisms for symbiont recognition in dinoflagellate-cnidarian symbioses involves interactions between lectins in PRRs of the host and surface glycans on the potential symbiont. The use of the glycan-lectin signalling is backed by evidence of a wide variety of glycans on dinoflagellates and a high number of lectin genes in the host genomes (Davy et al., 2012; Jimbo et al., 2005; Kvennefors et al., 2008; Tivey et al., 2020; Wood-Charlson & Weis, 2009). Interestingly, comparative genomic studies suggest that an expansion of lectin gene families even correlates with symbiotic capabilities in cnidarians (Hamada et al., 2018; Shinzato et al., 2011).

Berghia stephanieae (Á. Valdés, 2005) is capable of incorporating both nematocysts and the microalga *Breviolum minutum* (LaJeunesse, J.E.Parkinson & J.D.Reimer) J.E.Parkinson & LaJeunesse, 2018 from its prey, *Exaiptasia diaphana* (Rapp, 1829). The microalgae remain photosynthetically active for a short period. However, no stable symbiosome is formed, likely due to an unrepressed immune response and the absence of phagosome maturation arrest, leading to the eventual digestion and expulsion of the algae after a few days (Melo Clavijo et al., 2022). Although *B. stephanieae* does not establish a mutualistic and stable photosymbiosis, microscopy studies show that the microalgae are still taken up intracellularly in the digestive gland system, and the question remains how the microalgae *Breviolum minutum* is recognised by the slug cell (Borgstein et al., 2024a; Melo Clavijo et al., 2022; Monteiro et al., 2019). Bulk differential gene expression analyses of the cladobranch sea slug *B. stephanieae* revealed the upregulation in expression of several genes annotated as PRRs, including a variety of C-type lectins (Goodheart et al., 2025; Melo Clavijo et al., 2022). One expression upregulated C-type lectin, named Collectin-12, is known for its role in innate immunity and broad-spectrum recognition of MAMPs such as bacterial lipopolysaccharides and fungal components in vertebrates (Ma et al., 2015; Zhang et al., 2020). In cnidarians, other C-type lectins similar to Collectin-12, such as Millectin, PdC-Lectin or AtTL-2 have been described to bind to the microalgae in vivo, indicating a strong role in symbiont recognition (Kuniya et al., 2015; Kvennefors et al., 2008, 2010; Zhou et al., 2018). This suggests that Collectin-12 might play a potential role in symbiont recognition.

In this study, we performed spatial transcriptomic analysis as well as *in situ* hybridisation chain reaction (HCR) on starved and refed specimens of *B. stephanieae* to locate the expression pattern of Collectin-12 in the slugs tissue. If Collectin-12 is involved in the recognition of photobionts, we would expect its expression to be upregulated in the proximal regions of the cerata, around the digestive gland, where the microalgae are located. As a positive control, we included the previously characterised cnidosac-specific gene Collagen alpha-1(VIII) (UNK10) (Goodheart et al., 2024, 2025), which may play a role in extracellular matrix maintenance and tissue organisation (Q. Li et al., 2024).

2.3 Materials and Methods

To investigate the spatial expression of putative photobiont recognition genes, we chose COLEC12, a C-type lectin (jg39838; annotated as Collectin-12) due to its up-regulated expression in the proximal cerata tissue based on the genome and transcriptome data available for *B. stephanieae* (Goodheart et al., 2024; Melo Clavijo et al., 2022).

Spatial Transcriptomics

We used a spatial-transcriptomics dataset of an adult animal and cerata with preliminary clusters of *B. stephanieae* created by Jessica Goodheart and Rebecca Lopez-Anido using a Visium Spatial Transcriptomics Platform (10xGenomics) to validate the spatial expression of COLEC12 in the cerata. The *Space Ranger* pipelines (version 1.1.0; 10xGenomics) were used to map Illumina short read data to the genome of *B. stephanieae*. The computational tool for single-cell omics *scvi-tools* (Gayoso et al., 2022) was used to perform cluster analysis and K-means clustering were visualised in Loupe Browser (10xGenomics).

Sample preparation for HCR

Berghia stephanieae were maintained in 1 L glass containers with lids, filled with artificial seawater (ASW) at 25 °C. The light intensity was set to 30 µmol photons m^{-2} s^{-1}, following a 12 h / 12 h day-night cycle. The water was replaced once a week with freshly prepared ASW (salinity: 33 PSU, temperature: 25 °C). Slugs were fed three times per week with small *E. diaphana* anemones (7 mm foot and 4 mm oral disk or 4 mm foot and 3 mm oral disk). Previous transcriptomic analyses revealed the strongest expression of COLEC12 in starved and refed B. stephanieae (Melo Clavijo et al., 2022). Thus, for the *in situ* HCR, two adult *B. stephanieae* specimens per group were chosen: one group was starved for one week before fixation, the second group was also starved for one week, then refed with a small *E. diaphana* anemone and fixed one hour after feeding.

Fixation

Adult specimens of *B. stephanieae* were relaxed at -20°C until fully immobile, which required approximately 30 to 50 minutes. Freezing was avoided to preserve tissue integrity. Relaxed specimens were subsequently fixed overnight at 4°C in 4% PFA prepared in DEPC-treated 1× phosphate-buffered saline (PBS) under a fume hood. A fixative-to-tissue ratio of approximately 10:1 was maintained, using 1.5 mL of fixative per specimen.

Embedding

Following fixation, specimens were rinsed three times for 5 minutes each in DEPC-PBS (1×) at room temperature. Dehydration was performed through a graded methanol series consisting of 25%, 50%, and 75% methanol in DEPC-PBS (1×), each for 5 minutes, followed by three washes in 100% methanol for 5 minutes each. Samples were then stored in 100% methanol at -20°C until further processing. For paraffin embedding, fixed specimens stored in methanol were first rehydrated by two successive washes in 100% ethanol (1–2 minutes each). The samples were then cleared in 100% histosol under a fume hood for three consecutive incubations of 20 minutes each. Tissue was subsequently transferred into a tissue cassette and transitioned

into paraffin wax using a series of increasing wax concentrations. The cassette was incubated in a 50% histosol–50% paraffin wax solution for 30 minutes, followed by overnight incubation in 100% paraffin wax at 60°C. The following day, the samples underwent additional wax infiltration with four changes of 100% paraffin wax, each for 1 hour at 60°C. For embedding, specimens were carefully transferred into appropriately sized metal moulds using pre-warmed forceps. The mould was filled with molten paraffin wax, and the tissue was positioned to ensure optimal orientation for sectioning. Mixing the wax with warm forceps helped prevent layering artefacts. The paraffin blocks were allowed to partially solidify (30–50%) at room temperature before being transferred to 4°C for complete solidification. Embedded samples were stored at 4°C until sectioning.

Sectioning

Paraffin-embedded specimens were carefully trimmed using a razor blade to remove excess wax and expose the tissue. Sectioning was performed using a microtome (Thermo Epredia™ HM 340E Electronic Rotary Microtome, Fisher Scientific), with the blade replaced before each session to ensure precise and clean cuts. The section thickness was set to 6 µm. Adhesion slides (Fisherbrand™ Superfrost™ Plus Microscope Slides, Fisher Scientific) were labelled in advance, and sections were carefully transferred onto them. To facilitate adhesion, the sections were floated on a thin layer of DEPC-treated water applied between the slide and the sample using a micropipette. The slides were then placed on a slide warmer at 37°C for 15–20 minutes to promote tissue adherence. After drying, excess water was carefully removed using a Kimwipe tissue, and the slides were transferred to a slide holder wire basket. The slides were then incubated at 37°C overnight to ensure complete drying. The following day, dried slides were stored in a labelled slide box at 4°C until further processing.

Throughout the entire sample preparation, all tools and surfaces were decontaminated with RNase Zap to prevent RNA degradation, and RNA-safe techniques were practised to maintain sample integrity.

HCR probe design

UNK10 (jg13556; annotated as Collagen alpha-1(VIII)) was chosen as a positive control (Goodheart et al., 2024). For both, UNK10 and COLEC12 protein IDs were retrieved from *B. stephanieae* genome annotations and corresponding transcript sequences were identified using the Integrative Genomics Viewer (IGV) (Robinson et al., 2011). The transcript with the greatest length and minimal variation was selected, ensuring a sequence of at least 1000 bp to generate sufficient probes. Further, the transcript sequence was analysed using the Expasy translation tool (Gasteiger et al., 2005) to determine the appropriate reading frame, identified as the longest uninterrupted open reading frame. Translation in Geneious Prime was adjusted accordingly, ensuring the frame was in the 5′–3′ orientation. If the sequence was in the 3′–5′ orientation, a reverse complement was generated before proceeding. The non-coding regions were trimmed, leaving approximately 200 nucleotides on either side. HCR probes were designed using the HCR 3.0 probe maker (Kuehn et al., 2022), which was run via the command line. The software was installed within a dedicated Conda environment, ensuring compatibility with required dependencies

(biopython, bio, blast, numpy, pandas, openpyxl). Probe sequences were submitted to the IDT Pool Submission Format via the IDT website, and 50 pmol oPools^{TM} Oligos with no 5′ modifications were ordered for each probe.

In situ Hybridisation chain reaction

In situ HCR was performed on paraffin-embedded sections of *B. stephanieae* (Choi et al., 2018; Criswell & Gillis, 2020). The procedure was carried out over three consecutive days, involving hybridisation with target-specific probes, amplification using fluorophore-labelled hairpins, and counterstaining with DAPI (Fig. 2.2).

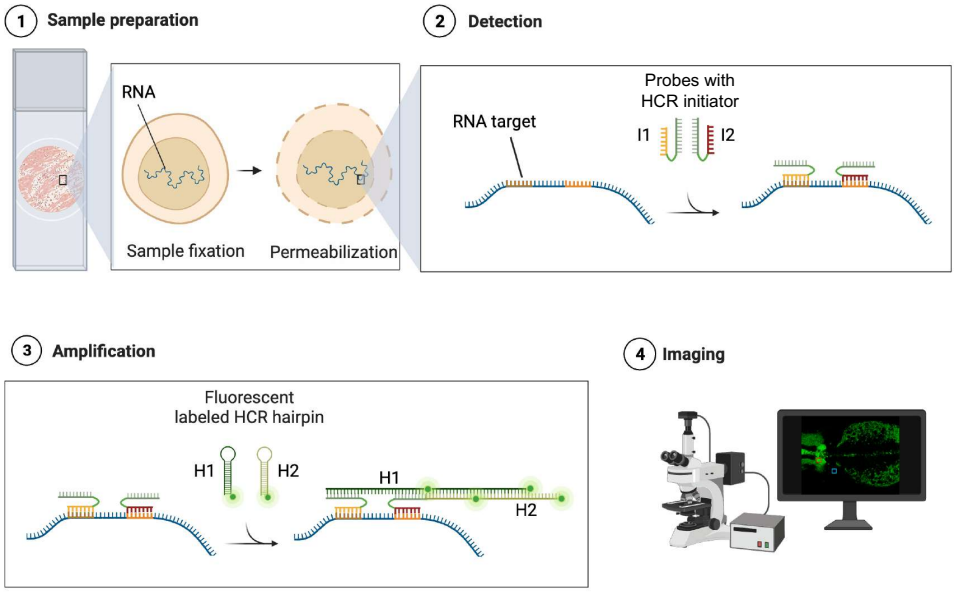

FIGURE 2.2: *In situ* HCR protocol. Sample preparation: The sample is fixed and permeabilised. Detection stage: custom probes with HCR initiator (i.e. I1 and I2) hybridise to RNA target. Amplification stage: fluorescently labelled HCR hairpins (H1 and H2) bind to custom probes, and self-assembly of a fluorescent amplification polymer is initiated. Imaging: targeted RNA of the sample is visualised using a microscope. Figure was created with BioRender.

Probe hybridisation

Before starting the procedure, all glassware and tubes were treated with RNase Zap to eliminate potential RNA contamination. A humidifying chamber was prepared using 50% formamide in 2× SSC, and 10 µg/mL proteinase K in DEPC-treated PBS was pre-warmed to 37°C. Solutions for rehydration, including a graded ethanol series (100%, 90%, 70%, and 50% ethanol in DEPC-PBS), DEPC water, and DEPC-PBS with 0.1% Tween-20, were freshly prepared.

Slides were first deparaffinised by incubating them twice in Histosol for 5 minutes each, followed by rehydration through successive incubations in 100% ethanol (2× 5 min), 90%, 70%, and 50% ethanol in DEPC-PBS (2 min each), and finally DEPC water and DEPC-PBS with 0.1% Tween-20 (2 min each). To improve probe penetration, sections were treated with 10 µg/mL proteinase K in DEPC-PBS at 37°C for

10 minutes. The reaction was stopped by rinsing the slides in DEPC water for 2 minutes.

Pre-hybridisation was performed by applying 2 mL of pre-warmed hybridisation buffer (HCR™ Probe hybridisation Buffer, Molecular Instruments) per slide, followed by incubation for 30 minutes in a humidifying chamber (2.6 L glass container, Pyrex™) at 37°C. During this step, probe sets were diluted by adding 0.8 µL of each 1 µM probe stock per 100 µL of hybridisation buffer and maintained at 37°C. After pre-hybridisation, the hybridisation buffer was drained, and 250 µL of probe-containing hybridisation buffer was applied to each slide except the negative control. Slides were then coverslipped with Parafilm and incubated overnight at 37°C in a humidifying chamber.

Signal Amplification

The following day, a humidifying chamber with DEPC water was prepared, and all required wash solutions were pre-warmed to 37°C. Hybridised slides were washed to remove unbound probes using a series of decreasing concentrations of HCR wash buffer and increasing concentrations of 5× SSCT (75%, 50%, 25%, and finally 100% 5× SSCT), with each wash performed for 15 minutes at 37°C. A final wash in 5× SSCT was performed at room temperature for 5 minutes.

For pre-amplification, 2.5 mL of amplification buffer (HCR™ Amplifier Buffer, Molecular Instruments) was applied per slide, and slides were incubated at room temperature for 30 minutes in a humidifying chamber. Fluorophore-labelled HCR hairpins (B2-647, HCR™ Amplifier, Molecular Instruments) were prepared by heating 8 µL of each hairpin at 95°C for 90 seconds, followed by cooling at room temperature in the dark for 30 minutes. Hairpins were then diluted in amplification buffer (200 µL per slide) and briefly vortexed. The pre-amplification buffer was removed from the slides, and the hairpin mixture was applied within 4 minutes to ensure proper integration. Slides were coverslipped with Parafilm and incubated overnight in a humidifying chamber at room temperature in the dark.

DAPI Staining and Mounting

DAPI stain (0.1 mg/mL) was prepared by diluting the DAPI stock solution (5 mg/mL, DAPI and Hoechst Nucleic Acid Stains, Invitrogen™) in 5× SSCT. The mounting medium was prepared by mixing 990 µL of Fluoromount-G with 10 µL of DAPI solution (0.1 mg/mL).

Slides were washed in the dark in 5× SSCT for 5 minutes, followed by two washes in 5× SSCT for 15 minutes, and one wash in 5× SSCT for 5 minutes. After washing, two dime-sized drops of Fluoromount-G with DAPI were placed on each slide—one near the centre and the other near the edge. A coverslip was gently laid down from one edge to prevent air bubbles, and excess mounting medium was removed if necessary. Slides were stored in the dark overnight to allow proper curing before imaging.

Samples were imaged with a Zeiss LSM microscope with an AxioCam HRm camera. The images were analysed using the image processing software ImageJ FIJI.

2.4 Results

Spatial Transcriptomics

Spatial transcriptomics analysis revealed distinct gene expression patterns of COLEC12 (jg39838) across different anatomical regions of *B. stephanieae*. Preliminary clustering of the spatial transcriptomics data identified several spatially distinct regions within the whole animal section, each corresponding to a unique transcriptional profile (Fig. 2.3A). Based on morphology, cluster 1, 2 and 3 are suggested to represent the digestive system, including the digestive gland and cluster 7, the cnidosacs at the distal end of the cerata.

The spatial distribution of COLEC12 exhibited a heterogeneous expression pattern throughout the whole animal section (Fig. 2.3B). Elevated expression levels were primarily detected in the digestive system, while the central body showed comparatively lower expression. A more detailed examination of the cerata revealed a pronounced enrichment of COLEC12 expression, particularly in the proximal regions where the digestive gland system is located (Fig. 2.3C). Notably, expression was much lower at the distal ends of the cerata, where the cnidosacs are found.

The cluster-specific regulation of COLEC12 was further confirmed by a quantitative analysis across clusters (Fig. 2.3D). Each violin represents the distribution of gene expression levels of COLEC12 within a specific cluster, with the width of the violins representing the density of data points at each expression level. The digestive system-associated cluster 1 and 2 display the highest median expression of COLEC12.

HCR

The negative control without any added probe showed no signal or background from the Alexa 647 amplifier in refed or starved slugs (see Fig. 2.4). The positive control, UNK10, showed a clear signal for both samples and was localised in the distal cerata within the cnidosac. For our designed COLEC12 probes, a signal was detected in both starved and refed slugs, specifically around the digestive gland, where photobiont sequestration is known to occur. The signal, however, appeared stronger in the refed slug (see Fig. 2.4A) compared to the starved slug (see Fig. 2.4B).

2.5 Discussion

The mechanisms by which *Berghia stephanieae* selectively incorporates the microalgae *Breviolum minutum* without digesting it remain largely unresolved. In cnidarians, photobionts are recognised through specific pattern recognition receptors (PRRs) that bind to microbial-associated molecular patterns (MAMPs) on the algal surface (Davy et al., 2012; Mansfield & Gilmore, 2019). It has been proposed that similar molecular pathways may operate in photosymbiotic cladobranchs (Goodheart et al., 2025; Melo Clavijo et al., 2022). Transcriptomic data from *B. stephanieae* revealed the upregulation of 14 transcripts identified as PRRs, including a C-type lectin classified as Collectin-12, which was strongly upregulated in both starved and refed individuals (Melo Clavijo et al., 2022). Collectin-12 belongs to the collectin family of C-type lectins and is well-established in innate immunity for its ability to bind carbohydrate structures on pathogens and facilitate phagocytosis (Zhang et al., 2020). Structurally,

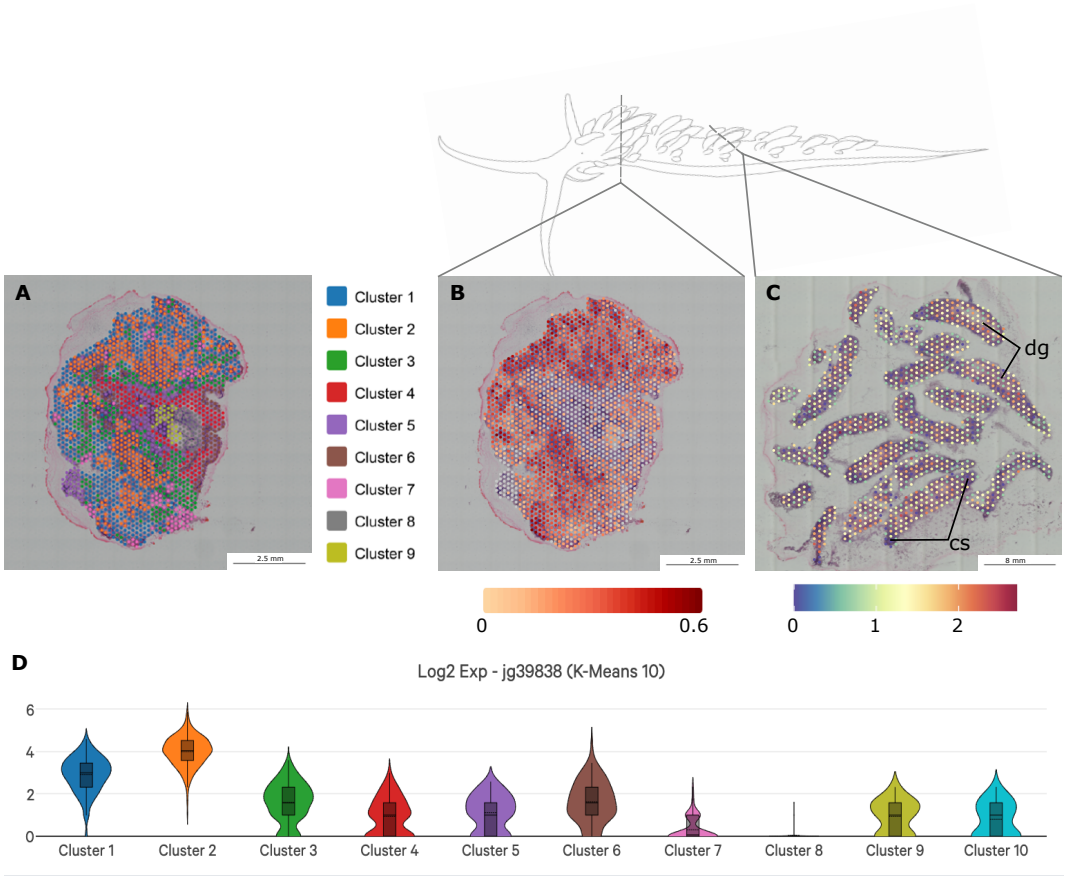

FIGURE 2.3: Preliminary spatial transcriptomic data for *B. stephanieae*. Image of a tissue section of a whole adult animal and the corresponding preliminary clusters (A). Tissue cluster analysis of COLEC12 in a whole animal section (B) and the cerata (C) inside a 10X target capture area. Spots represent regions where RNA was captured, and colours delimit clusters from the counts analysis. Violin plot showing expression of the COLEC12 (jg39838) gene across all clusters (D). Clusters 1, 2 and 3 are suggested to represent the digestive system and cluster 7 the cnidosac, based on morphology. cs = cnidosac, n = nematocysts, dg = digestive gland.

it contains a carbohydrate-recognition domain that enables binding to glycan motifs such as galactose and fucose on symbiont surfaces, similar to C-type lectins in corals such as Millectin, PdC-Lectin or AtTL-2 which bind to Symbiodiniaceae (Kuniya et al., 2015; Kvennefors et al., 2008, 2010; Veldhuizen et al., 2011; Zhou et al., 2018). Our study is the first to examine Collectin-12 in an endosymbiotic context and reveal its potential role in photobiont recognition.

Our spatial transcriptomic analysis results showed that Collectin-12 is mainly expressed in the digestive system and the proximal part of the cerata of *B. stephanieae*, where the photobionts are located. Additionally, our HCR analysis showed pronounced signals exclusively around the digestive gland. Notably, no expression of Collectin-12 was observed in the distal region of the cerata, including the cnidosac, in either condition. These results suggest that Collectin-12 does not seem to be involved in nematocyst recognition but could play a role in the recognition of *B. minutum*. Although Collectin-12 has not been associated with photobiont recognition, several members of the collectin family, including Collectin-10, -11, and -12, have been identified in the saccoglossan sea slugs *Elysia chlorotica*, *Elysia cornigera*, *Elysia timida*, *Elysia viridis* and *Elysia crispata* (Allard et al., 2025; C. X. Chan et al., 2018;

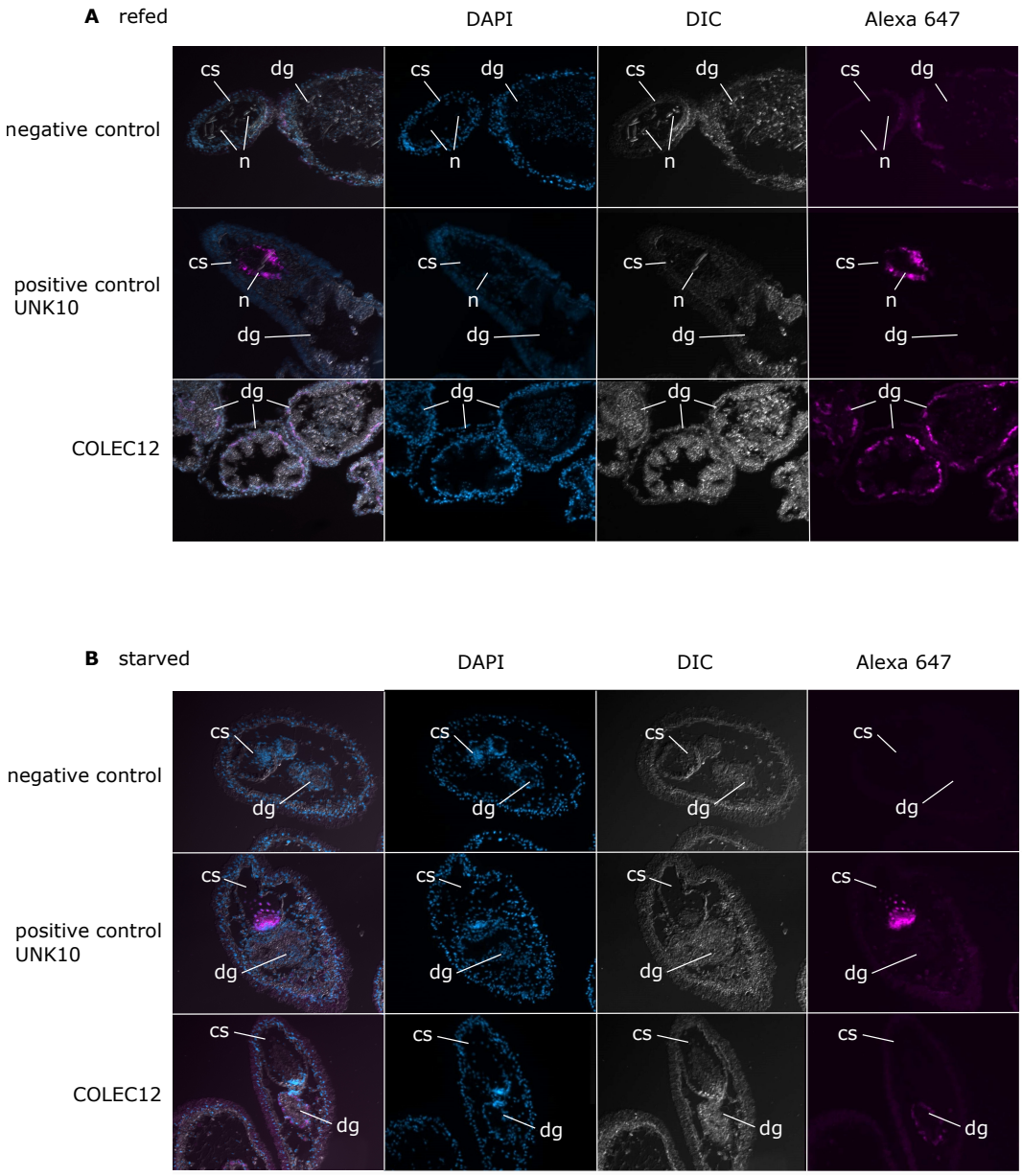

FIGURE 2.4: *In situ* HCR results in sections of *B. stephanieae* stained with DAPI and Alexa 647 are shown for the negative control (no probes added), UNK10 (Collagen alpha-1(VIII)), and COLEC12 (Collectin-12) in a refed slug (A) and a starved slug (B). cs = cnidosac, n = nematocysts, dg = digestive gland.

Melo Clavijo et al., 2020; Mendoza et al., 2023).

Interestingly, Collectin-12 expression was strongest in refed individuals and lower, but still detectable, in starved slugs, which contrasts with the transcriptomic data previously reported for *B. stephanieae* where starved slugs showed the highest TMM values (average of 1108) and refed slugs moderate TMM values (average of 570) (Melo Clavijo et al., 2022). Transcriptomic analyses reveal average RNA abundance from the sampled tissue, often pooling many cell types and may capture transient upregulation or changes that do not translate into robust protein (or localised mRNA) presence at the time of the HCR analysis (Trapnell, 2015; Z. Wang et al., 2009). In starved slugs, upregulation detected by transcriptomics could be widespread but moderate, while in refed slugs, gene expression could be more spatially focused or

intense in certain regions, resulting in a stronger local HCR signal in refed slugs even if the overall average is lower, as observed in our samples.

The observed HCR expression pattern in our samples could reflect a physiological response to the presence of microalgae in the digestive system. Studies in other species have demonstrated that pattern recognition receptors like collectins are dynamically regulated according to immune challenges and the physiological state of the host (Ma et al., 2015). For example, the saccoglossan sea slug *Elysia chlorotica* shows a significant upregulation of genes involved in the MAMP-PRR signalling cascade (including Collectin-11) upon initial exposure to its food algae. This pattern suggests that these genes may play a role in the initial recognition and intracellular uptake of symbionts and less in the maintenance of photosymbiosis in *E. chlorotica*, as these gene expression patterns gradually return to baseline (C. X. Chan et al., 2018).

As mentioned before, *B. stephanieae* is unable to establish a stable photosymbiosis with the microalga *B. minutum*. The algae are recognised and subsequently incorporated into the epithelial cells of the digestive gland system, as shown by microscopic analyses, potentially mediated by the C-type lectin Collectin-12 (Borgstein et al., 2024a; Rola et al., 2022). However, the algal cells are not retained within the host tissue and are excreted after a couple of days. This study represents an important first step toward identifying potential PRRs in a cladobranch sea slug and demonstrates that Collectin-12 expression is upregulated around the digestive gland in the proximal region of the cerata in response to the presence of photobionts. Further spatial transcriptomic and *in situ* HCR analyses in sea slugs with stable photosymbioses, such as *Phyllodesmium* or *Pteraeolidia*, would help to disentangle which PRRs are specifically involved in symbiont recognition and long-term maintenance.

2.6 Conclusion

Our results provide the first spatial results that the pattern recognition receptor Collectin-12 may be involved in the recognition of the microalgae *B. minutum* in *Berghia stephanieae*. The specific expression of Collectin-12 in the digestive gland and proximal cerata, combined with its absence in the cnidosac, suggests a targeted role in mediating algal recognition and uptake. These findings support the hypothesis that *B. stephanieae* uses conserved innate immune pathways, similar to those found in cnidarian hosts. This work represents an initial step toward uncovering the molecular mechanisms underlying photosymbiosis in Cladobranchia and contributes to a growing understanding of host-symbiont interactions in metazoans.

Acknowledgments

This work was supported by the Annette Kade Graduate Student Fellowship of the Richard Gilder Graduate School of the American Museum of Natural History (AMNH).

Author Contributions

CS, JG and SPS planned the experiments, and CS conducted the experiments. CS wrote the manuscript and revised it together with JG, RLA and SPS.

References

Allard, C. A., Thies, A. B., Mitra, R., Vaelli, P. M., Leto, O. D., Walsh, B. L., Laetz, E. M., Tresguerres, M., Lee, A. S., & Bellono, N. W. (2025). A host organelle integrates stolen chloroplasts for animal photosynthesis. *Cell*.

Borgstein, N. M., van der Meij, S. E., Christa, G., & Laetz, E. M. (2024a). Potential energetic and oxygenic benefits to unstable photosymbiosis in the cladobranch slug, *Berghia stephanieae* (nudibranchia, aeolidiidae). *Marine Biology Research*, *20*(1-2), 45–58.

Chan, C. X., Vaysberg, P., Price, D. C., Pelletreau, K. N., Rumpho, M. E., & Bhattacharya, D. (2018). Active host response to algal symbionts in the sea slug *Elysia chlorotica*. *Molecular biology and evolution*, *35*(7), 1706–1711.

Choi, H. M., Schwarzkopf, M., Fornace, M. E., Acharya, A., Artavanis, G., Stegmaier, J., Cunha, A., & Pierce, N. A. (2018). Third-generation *in situ* hybridization chain reaction: Multiplexed, quantitative, sensitive, versatile, robust. *Development*, *145*(12), dev165753.

Criswell, K. E., & Gillis, J. A. (2020). Resegmentation is an ancestral feature of the gnathostome vertebral skeleton. *Elife*, *9*, e51696.

Davy, S. K., Allemand, D., & Weis, V. M. (2012). Cell biology of cnidarian-dinoflagellate symbiosis. *Microbiology and Molecular Biology Reviews*, *76*, 229–261.

Emery, M. A., Beavers, K. M., Van Buren, E. W., Batiste, R., Dimos, B., Pellegrino, M. W., & Mydlarz, L. D. (2024). Trade-off between photosymbiosis and innate immunity influences cnidarian's response to pathogenic bacteria. *Proceedings of the Royal Society B*, *291*(2032), 20240428.

Gasteiger, E., Hoogland, C., Gattiker, A., Duvaud, S., Wilkins, M. R., Appel, R. D., & Bairoch, A. (2005). Protein identification and analysis tools on the ExPASy server. *The Proteomics Protocols Handbook*, 571–607.

Gayoso, A., Lopez, R., Xing, G., Boyeau, P., Valiollah Pour Amiri, V., Hong, J., Wu, K., Jayasuriya, M., Mehlman, E., Langevin, M., et al. (2022). A Python library for probabilistic analysis of single-cell omics data. *Nature Biotechnology*, *40*(2), 163–166.

Goodheart, J. A., Bleidißel, S., Schillo, D., Strong, E. E., Ayres, D. L., Preisfeld, A., Collins, A. G., Cummings, M. P., & Wägele, H. (2018). Comparative morphology and evolution of the cnidosac in Cladobranchia (Gastropoda: Heterobranchia: Nudibranchia). *Frontiers in Zoology*, *15*, 1–18.

Goodheart, J. A., Fiorenza, R., Rio, R., Lopez-Anido, R. N., Martin, N. J., Herrlinger, T. J., Tarvin, R. D., & Lyons, D. C. (2025). A subset of conserved phagocytic genes are likely used for the intracellular theft of cnidarian stinging organelles in nudibranch gastropods. *EvoDevo*.

Goodheart, J. A., Rio, R. A., Taraporevala, N. F., Fiorenza, R. A., Barnes, S. R., Morrill, K., Jacob, M. A. C., Whitesel, C., Masterson, P., Batzel, G. O., et al. (2024). A chromosome-level genome for the nudibranch gastropod *Berghia stephanieae* helps parse clade-specific gene expression in novel and conserved phenotypes. *BMC Biology*, *22*(1), 9.

Hamada, M., Schröder, K., Bathia, J., Kürn, U., Fraune, S., Khalturina, M., Khalturin, K., Shinzato, C., Satoh, N., & Bosch, T. C. (2018). Metabolic co-dependence drives the evolutionarily ancient *Hydra–Chlorella* symbiosis. *Elife*, *7*, e35122.

Jimbo, M., Koike, K., Sakai, R., Muramoto, K., & Kamiya, H. (2005). Cloning and characterization of a lectin from the octocoral *Sinularia lochmodes*. *Biochemical and Biophysical Research Communications*, *330*(1), 157–162.

Kuehn, E., Clausen, D. S., Null, R. W., Metzger, B. M., Willis, A. D., & Özpolat, B. D. (2022). Segment number threshold determines juvenile onset of germline cluster expansion in *Platynereis dumerilii*. *Journal of Experimental Zoology Part B: Molecular and Developmental Evolution*, *338*(4), 225–240.

Kuniya, N., Jimbo, M., Tanimoto, F., Yamashita, H., Koike, K., Harii, S., Nakano, Y., Iwao, K., Yasumoto, K., & Watabe, S. (2015). Possible involvement of Tachylectin-2-like lectin from *Acropora tenuis* in the process of *Symbiodinium* acquisition. *Fisheries Science*, *81*(3), 473–483.

Kvennefors, E. C. E., Leggat, W., Hoegh-Guldberg, O., Degnan, B. M., & Barnes, A. C. (2008). An ancient and variable mannose-binding lectin from the coral *Acropora millepora* binds both pathogens and symbionts. *Developmental & Comparative Immunology*, *32*(12), 1582–1592.

Kvennefors, E. C. E., Leggat, W., Kerr, C. C., Ainsworth, T. D., Hoegh-Guldberg, O., & Barnes, A. C. (2010). Analysis of evolutionarily conserved innate immune components in coral links immunity and symbiosis. *Developmental & Comparative Immunology*, *34*(11), 1219–1229.

Li, Q., Tintut, Y., Demer, L. L., Vazquez-Padron, R. I., Bendeck, M. P., & Hsu, J. J. (2024). Collagen VIII in Vascular Diseases. *Matrix Biology*.

Ma, Y. J., Hein, E., Munthe-Fog, L., Skjoedt, M.-O., Bayarri-Olmos, R., Romani, L., & Garred, P. (2015). Soluble collectin-12 (CL-12) is a pattern recognition molecule initiating complement activation via the alternative pathway. *The Journal of Immunology*, *195*(7), 3365–3373.

Malcolm, H., & April, H. (2012). The magnesium inhibition and arrested phagosome hypotheses: New perspectives on the evolution and ecology of *Symbiodinium* symbioses. *Biological Reviews*, *87*(4), 804–821.

Mansfield, K. M., & Gilmore, T. D. (2019). Innate immunity and cnidarian-Symbiodiniaceae mutualism. *Developmental & Comparative Immunology*, *90*, 199–209.

McFall-Ngai, M., Hadfield, M. G., Bosch, T. C., Carey, H. V., Domazet-Lošo, T., Douglas, A. E., Dubilier, N., Eberl, G., Fukami, T., Gilbert, S. F., et al. (2013). Animals in a bacterial world, a new imperative for the life sciences. *Proceedings of the National Academy of Sciences*, *110*(9), 3229–3236.

Melo Clavijo, J., Frankenbach, S., Fidalgo, C., Serôdio, J., Donath, A., Preisfeld, A., & Christa, G. (2020). Identification of scavenger receptors and thrombospondin-type-1 repeat proteins potentially relevant for plastid recognition in Sacoglossa. *Ecology and Evolution*, *10*(21), 12348–12363.

Melo Clavijo, J., Sickinger, C., Bleidißel, S., Gasparoni, G., Tierling, S., Preisfeld, A., & Christa, G. (2022). The nudibranch *Berghia stephanieae* (Valdés, 2005) is not able to initiate a functional symbiosome-like environment to maintain *Breviolum minutum* (JE Parkinson & LaJeunesse 2018). *Frontiers in Marine Science*.

Mendoza, M., Rocha, S., Troncoso, J., Posada, D., & Canchaya, C. (2023). Transcriptomic landscape of the kleptoplastic sea slug *Elysia viridis*. *Journal of Molluscan Studies*, *89*(1), eyad001.

Monteiro, E. A., Güth, A. Z., Banha, T. N., Sumida, P. Y., & Mies, M. (2019). Evidence against mutualism in an aeolid nudibranch associated with Symbiodiniaceae dinoflagellates. *Symbiosis*, *79*, 183–189.

Robinson, J. T., Thorvaldsdóttir, H., Winckler, W., Guttman, M., Lander, E. S., Getz, G., & Mesirov, J. P. (2011). Integrative genomics viewer. *Nature Biotechnology*, *29*(1), 24–26.

Rola, M., Frankenbach, S., Bleidissel, S., Sickinger, C., Donath, A., Frommlet, J. C., Greve, C., Serôdio, J., Preisfeld, A., Melo Clavijo, J., et al. (2022). Cladobranchia

(Gastropoda, Nudibranchia) as a promising model to understand the molecular evolution of photosymbiosis in animals. *Frontiers in Marine Science*, *8*, 745644.

Rosset, S. L., Oakley, C. A., Ferrier-Pagès, C., Suggett, D. J., Weis, V. M., & Davy, S. K. (2021). The molecular language of the cnidarian–dinoflagellate symbiosis. *Trends in Microbiology*, *29*(4), 320–333.

Shinzato, C., Shoguchi, E., Kawashima, T., Hamada, M., Hisata, K., Tanaka, M., Fujie, M., Fujiwara, M., Koyanagi, R., Ikuta, T., et al. (2011). Using the *Acropora digitifera* genome to understand coral responses to environmental change. *Nature*, *476*(7360), 320–323.

Tivey, T. R., Parkinson, J. E., Mandelare, P. E., Adpressa, D. A., Peng, W., Dong, X., Mechref, Y., Weis, V. M., & Loesgen, S. (2020). N-linked surface glycan biosynthesis, composition, inhibition, and function in cnidarian-dinoflagellate symbiosis. *Microbial Ecology*, *80*(1), 223–236.

Trapnell, C. (2015). Defining cell types and states with single-cell genomics. *Genome Research*, *25*(10), 1491–1498.

Veldhuizen, E. J., van Eijk, M., & Haagsman, H. P. (2011). The carbohydrate recognition domain of collectins. *The FEBS journal*, *278*(20), 3930–3941.

Wägele, H., Raupach, M. J., Burghardt, I., Grzymbowski, Y., & Händeler, K. (2010). Solar powered seaslugs (Opisthobranchia, Gastropoda, Mollusca): Incorporation of photosynthetic units: A key character enhancing radiation? *Evolution in action: Case studies in adaptive radiation, speciation and the origin of biodiversity*, 263–282.

Wang, Z., Gerstein, M., & Snyder, M. (2009). RNA-Seq: A revolutionary tool for transcriptomics. *Nature Reviews Genetics*, *10*(1), 57–63.

Weis, V. M., Davy, S. K., Hoegh-Guldberg, O., Rodriguez-Lanetty, M., & Pringle, J. R. (2008). Cell biology in model systems as the key to understanding corals. *Trends in Ecology & Evolution*, *23*(7), 369–376.

Wood-Charlson, E. M., & Weis, V. M. (2009). The diversity of C-type lectins in the genome of a basal metazoan, *Nematostella vectensis*. *Developmental & Comparative Immunology*, *33*(8), 881–889.

Zhang, J., Song, L., Pedersen, D. V., Li, A., Lambris, J. D., Andersen, G. R., Mollnes, T. E., Ma, Y. J., & Garred, P. (2020). Soluble collectin-12 mediates C3-independent docking of properdin that activates the alternative pathway of complement. *Elife*, *9*, e60908.

Zhou, Z., Zhao, S., Ni, J., Su, Y., Wang, L., & Xu, Y. (2018). Effects of environmental factors on c-type lectin recognition to zooxanthellae in the stony coral *Pocillopora damicornis*. *Fish & Shellfish Immunology*, *79*, 228–233.

Chapter 3

The Phototactic Behavior of the Kleptoplastic Sea Slug *Elysia viridis* (Montagu, 1804) is not Connected to the Photosynthetic Activity of Kleptoplasts

Corinna Sickinger[1], Elisa Weimann[2], Johannes Wenning[1] and Gregor Christa[2]

[1]*Institute for Zoology and Didactics of Biology, University of Wuppertal, Wuppertal, Germany*
[2]*Department of Evolution and Biodiversity, University of Wuppertal, Wuppertal, Germany*

Published: 18 November 2025, *Marine Biology Research* 21(8–10), 417–426
https://doi.org/10.1080/17451000.2025.2577445

3.1 Abstract

Sacoglossan sea slugs are particularly famous for the ability of some species to retain photosynthetic chloroplasts in their cells. While it is still uncertain how and to what degree the slugs might benefit from these alien organelles (kleptoplasts), some studies investigated whether a phototactic behavior could be related to increasing the kleptoplasts' photosynthetic activity. To address whether this behavior is connected to increasing photosynthetic activity, we investigated the plastid-bearing Sacoglossa *Elysia viridis*. Using a side-choice experiment, we analyzed the time the slugs spent in either white or red light compared to a shaded area. We also investigated the general mobility of the slugs and determined the number of changes between the two areas. We performed our experiments with freshly fed and several weeks-starved animals, and performed the same experiments with animals constantly exposed to a photosynthetic blocker. Most of the slugs spent approximately 80% of the time in the illuminated area, independent of the experimental set-up, suggesting that the photobehavior of *Elysia viridis* is not connected to increasing the photosynthetic activity of the kleptoplasts. Yet, tested under white light, the photosynthetic blocker induced a shift in behavior during the first two weeks of starvation, leading to a more balanced distribution between shaded and illuminated areas. This shift could be linked to higher stress levels, potentially resulting from greater kleptoplast damage.

Keywords *Elysia* · functional · kleptoplasty · photobehavior · photosymbiosis · Sacoglossa

3.2 Introduction

Sacoglossa are a clade of heterobranch sea slugs that are particularly known for the ability of some species to retain photosynthetic chloroplasts. Only non-shelled species selectively incorporate the algae's chloroplasts into cells of the digestive gland system, while the basal, shelled species extracellularly digest the chloroplasts (Christa et al., 2015; Händeler et al., 2009; Hirokane et al., 2022). The slugs obtain these chloroplasts by piercing the cell walls of their food algae with their radula teeth and subsequently suck out the cytosol (Gascoigne, 1977). Incorporating chloroplasts is known as kleptoplasty (Christa, 2023; Cruz & Cartaxana, 2022; Trench, 1969), but species differ significantly in the ability to maintain the chloroplasts photosynthetically active inside their cells. Most non-shelled Sacoglossa incorporate the kleptoplasts photosynthetically dysfunctional and digest them rapidly after incorporation (non-retention, NR) (Händeler et al., 2009; Laetz et al., 2017a). The ability to maintain the chloroplasts for a couple of weeks during starvation (short-term retention; StR) evolved twice independently within the Sacoglossa, and only five species are known to keep the chloroplasts for several months photosynthetically active (long-term retention; LtR) (Christa et al., 2015). This difference in the retention ability is not exclusively related to the exact food source because NR and LtR forms feed on the same algae (Christa et al., 2014a; Händeler et al., 2010), and it seems that a combination of slug intrinsic factors and robustness of the chloroplasts is needed de Vries et al., 2014. Independent of the retention ability, feeding slugs digest the kleptoplasts (Cartaxana et al., 2023; Frankenbach et al., 2023; Maeda et al., 2012), and even the LtR species intracellularly digest the kleptoplasts while starving, albeit with reduced digestion activity (de Vries et al., 2015; Laetz et al., 2017a).

This so-called functional kleptoplasty in Sacoglossa is an extraordinary symbiosis between an animal and a photoautotrophic organism. In most cases, the symbiont is an entire organism and provides nutrients, such as sugars, to the host, while the host supplies the symbiont with CO2 and nitrogen (Davy et al., 2012; Stanley Jr & Lipps, 2011). This nutrient exchange is essential for the stability of the symbioses, and disrupting this nutrient cycle leads to a symbiosis breakdown (Rädecker et al., 2021). The exact mechanisms of this nutrient exchange have not been fully elucidated and are primarily studied in corals. There is no evidence of a nutritional cycle in Sacoglossa, but in the LtR species *Elysia timida*, the kleptoplasts accumulate starch during starvation. This accumulation of assimilates questions an active export, and some studies suggest that the slugs can presumably acquire these resources by recycling the chloroplast and its contents via autophagy (Frankenbach et al., 2023; Laetz et al., 2017b). Nonetheless, some studies indicate that the slugs show a positive phototactic behavior to increase the photosynthetic activity, and consequently the synthesis of nutrients, of the kleptoplasts (Cartaxana et al., 2018; Miyamoto et al., 2015; Schmitt & Wägele, 2011). If true, such behavior would promote communication between the kleptoplasts and the slugs' cytosol. How this communication would be realized is unknown, but behavior to optimize the symbiont's photosynthesis is known from other animals such as the acoel *Symsagittifera roscoffensis* (Serôdio et al., 2011; Strumpen et al., 2022). Nonetheless, several studies in Sacoglossa have analyzed the phototactic behavior of different species (Cartaxana et al., 2018;

Miyamoto et al., 2015; Schmitt & Wägele, 2011; Weaver & Clark, 1981). Species bearing functional kleptoplasts preferred slightly higher light intensities than their original culturing conditions, while avoiding light intensities exceeding. It was further proposed that the kleptoplast's photoacclimation condition might induce a selective preference of the slugs for light (Cartaxana et al., 2018). Moreover, in *Elysia timida*, the opening of the parapodia was correlated with enhancing the light availability and, consequently, the kleptoplast's photosynthesis (Schmitt & Wägele, 2011). Further, some species preferred blue light and avoided red light, while others showed an opposite behavior unrelated to bearing functional kleptoplasts (Weaver & Clark, 1981). Although the slugs preferred lower light intensities than the algae's chloroplasts were acclimated to, most of the data were interpreted as reducing photodamage to the kleptoplasts and increasing their photosynthetic efficiency. Hence, the photobehavior can also be a photoprotection to reduce light-induced damage to the kleptoplasts that would otherwise damage the photosynthetic machinery (Cartaxana et al., 2019; Christa et al., 2018; Havurinne et al., 2021). However, more research is still needed to determine whether all reported behavioral tendencies are based on actively enhancing photosynthesis in kleptoplasts. A noteworthy finding was that some LtR species avoided red light, which is essential for photosynthesis, and that starving individuals preferred light over shade even when their kleptoplasts were no longer functional (Miyamoto et al., 2015). Even in the acoel *Symsagittifera roscoffensis* (Graff, 1891), the red light was equally avoided as complete darkness (Nissen et al., 2015), suggesting that the photobehavior of the worm is not exclusively linked to optimizing the photosynthesis of the algae and could be based on a diurnal cycle. To further understand the phototactic behavior of Sacoglossa, we tested *Elysia viridis* (Montagu, 1804) from the Baltic Sea under photosynthetic and photosynthesis blocked conditions and during starvation, which also eventually leads to non-photosynthetic conditions. We conducted a side-choice experiment using a white or red light on one side and a shaded area on the other. Our results suggest that the behavior of the slugs is not connected to optimizing the photosynthetic activity of the kleptoplasts.

3.3 Materials and Methods

Collection and culturing of slugs Specimens of *Elysia viridis* were collected from Bryopsis sp. in Bockholmwik (Germany, 54°49'51.8"N, 9°36'51.4"E) in August 2022. The slugs were transported to our laboratory and cultivated in groups of 20 individuals in 2 L plastic containers in artificial seawater (ASW) (ABReef Salt, Aqua Medic, Germany) with a salinity of 18 PSU matching the salinity at the collection site. We cultured the slugs under a 12 h light / 12 h dark day/night cycle, starting the illumination at 8 a.m. Slugs were cultured at 21 °C and under 25 µmol photons m-2 s-1 of white light (sunrise daylight, sera, Germany) and were fed with Bryopsis sp. three days a week with the container's water changes during the provision of new food. The algae were cultured under the same conditions as the slugs, except for enriching the ASW with F/2 (Guillard 1975) medium at a salinity of 30 PSU and providing constant aeration. We were not successful in culturing the algae at a salinity of 18 PSU, so we had to culture the algae at 30 PSU. To ensure that the algae's salinity transition did not interfere with the function of the kleptoplasts in the slugs, we fed the slugs for three months before the phototactic behavior experiments and measured the maximum quantum yield (Fv/Fm) of photosystem II of randomly chosen slugs on a weekly basis. For Fv/Fm measurements, the slugs were dark adapted for five

minutes and Fv/Fm was measured using a DIVING PAM (Pulse Amplitude Modulated fluorometer) (Walz, Germany) by placing the fiber optic approx. 2 mm above the pericard region and applying a saturation pulse (> 4.000 µmol photons m-2 s-1) to obtain the ground fluorescence F0 and the maximum fluorescence Fm, where Fv is the variable fluorescence calculated as Fm – F0. All measurements of freshly fed slugs exceeded a Fv/Fm of 0.7, which is well within the known range of *E. viridis* collected at different localities, indicating that the salinity switch did not affect the functionality of kleptoplasts.

Side-choice experiment

We randomly selected specimens with a size between 1 and 1.5 cm and isolated them into small plastic boxes containing 50 mL of fresh ASW (Normal) or 50 mL of fresh ASW supplemented with 2 µg Monolinuron / mL (Mono). Mono completely blocks the CO2-fixation of kleptoplast (Christa et al., 2014a; de Vries et al., 2015; Rauch et al., 2018) and thus serves as an alternative to DCMU often used in corals (Jinkerson et al., 2022), for instance. Both chemicals are herbicides, but because Mono is used for controlling algae blooms in aquaria, we consider Mono to be a less harmful herbicide with fewer effects on the physiology of the slugs than DCMU. Nonetheless, we do not exclude that the behavior of the slugs can be affected by the blocker. Previous experiments, however, showed that at least for the survival time of the slugs, Mono has no negative effects on *Elysia viridis* (Rauch et al. 2018). Both groups were starved for three weeks under identical conditions as described above. Immediately after separating the two groups and before starting the light-choice experiments, the Fv/Fm of kleptoplasts was measured as described above. The Fv/Fm was also measured before the water was supplemented with Mono for the Mono group. For the side-choice experiment, slugs were placed with a random orientation of the head in the middle of one of eight compartments (each 8 cm in length, 3 cm in width, and 4 cm in height) of a plastic container. Each slug was tested in the same compartment at each starvation time. Each compartment was filled with 50 mL of freshly prepared ASW, either with or without Monolinuron, according to the group tested. The container was illuminated with the same light source as under culturing conditions (White) or with 25 µmol photons m-2 s-1 red vision LED chips (Red) (sera, Germany, emission peak at 625 nm). Half of the container was shaded with a black cover, resulting in an area beneath the cover with a light intensity of < 3 µmol photons m-2 s-1 and 8 µmol photons m-2 s-1 at the border between the shaded and the illuminated area. Light intensities were always confirmed before the experiment run using the miniature light sensor of the DIVING-PAM (Walz, Germany). We then recorded the behavior of the slugs for one hour using an iPad 11 (Apple, USA) (Figure 1). We determined the time the slugs spent in the illuminated and shaded areas, respectively, and how often the slugs changed between both areas. A change was considered when at least half of the slugs' body was head first in the respective area. Our preliminary trials, in which we either let the slugs acclimate for 20 min or only started recording the slugs after each side was at least visited for one minute, did not reveal a difference in the time spent on each side. A potential exploration of the plastic container can thus be considered less relevant, as shown in other studies before (Miyamoto et al., 2015; Schmitt & Wägele, 2011). Hence, we did not include an acclimation phase before the start of the recording, similar to other studies (Cartaxana et al., 2018; Miyamoto et al., 2015; Schmitt & Wägele, 2011; Weaver & Clark, 1981). We conducted our experiments during the daytime (between 10 a.m. and 2 p.m.) and thoroughly cleaned the container with distilled water after each experimental run. This set-up resulted in four groups composed of White/Normal (n=12), White/Mono (n=12), Red/Normal

(n=24), and Red/Mono (n=24) that were observed freshly fed (Fed), after one (St_1), two (St_2), and three (St_3) weeks of starvation.

FIGURE 3.1: Scheme of the experimental setup. The behavior of the slugs was recorded for one hour, and the number of changes between the two areas and the time spent in each area were determined. Each slug was always tested in the same compartment during the starvation experiment. We either used the culturing light of the slugs, or red vision LED chips with an emission peak at 625 nm.

Statistical analyzes

We statistically analyzed whether there were differences in the time spent in light, the number of changes between the two areas, and differences between the groups during each observation time point. The statistical analyses were conducted using the SciPy module in Python 3.10.10 (Virtanen et al., 2020). The data were first tested for normality using the Shapiro-Wilk test and then analyzed using the independent t-test or the Mann-Whitney U test when comparing White and Red samples, or the Kruskal-Wallis test when comparing the additional effect of different observation points within White or Red. Data were visualized using the Seaborn and Matplotlib modules implemented in Python.

3.4 Results

The slugs prefer light, also under non-photosynthetic conditions We analyzed the behavior of the slugs using a side choice experiment with a white-light illuminated and a shaded area. Freshly fed animals in White/Normal (n=12) spent 82% $\pm$ 16% of their time in the illuminated area, and this general behavior pattern did not change during starvation (Figure 2A). Fed animals exposed to White/Mono (n=12) spent 92% $\pm$ 12% of the experimental time in the illuminated area (Fig. 2B), but significantly less when starved for one week (49% $\pm$ 30%, Independent t-test; p = 0.0002; Fig. 1B). After two and three weeks of starvation, White/Mono animals spent more time in the light compared to the first week of starvation (60% $\pm$ 36%, Mann-Whitney U test; p = 0.08 and 83% $\pm$ 12%, Mann-Whitney U test; p = 0.005, Figure 2B). We found a significant difference between the White/Normal and the White/Mono group for fed specimens (Mann-Whitney U test; p = 0.03), where the White/Normal group spent significantly more time in the white-illuminated area after one week of starvation (Mann-Whitney U test; p = 0.006).

Subsequently, we performed the same experiments but used a red light instead of a white light. Like under white light, freshly fed animals (Red/Normal; n=24) spent 87% $\pm$ 14% of their time in the red-illuminated area (Fig. 2C), which decreased gradually during the three weeks of starvation to 74% $\pm$ 30% but not significantly (Mann-Whitney U test; p > 0.3). When exposed to Mono, fed slugs (Red/Mono;

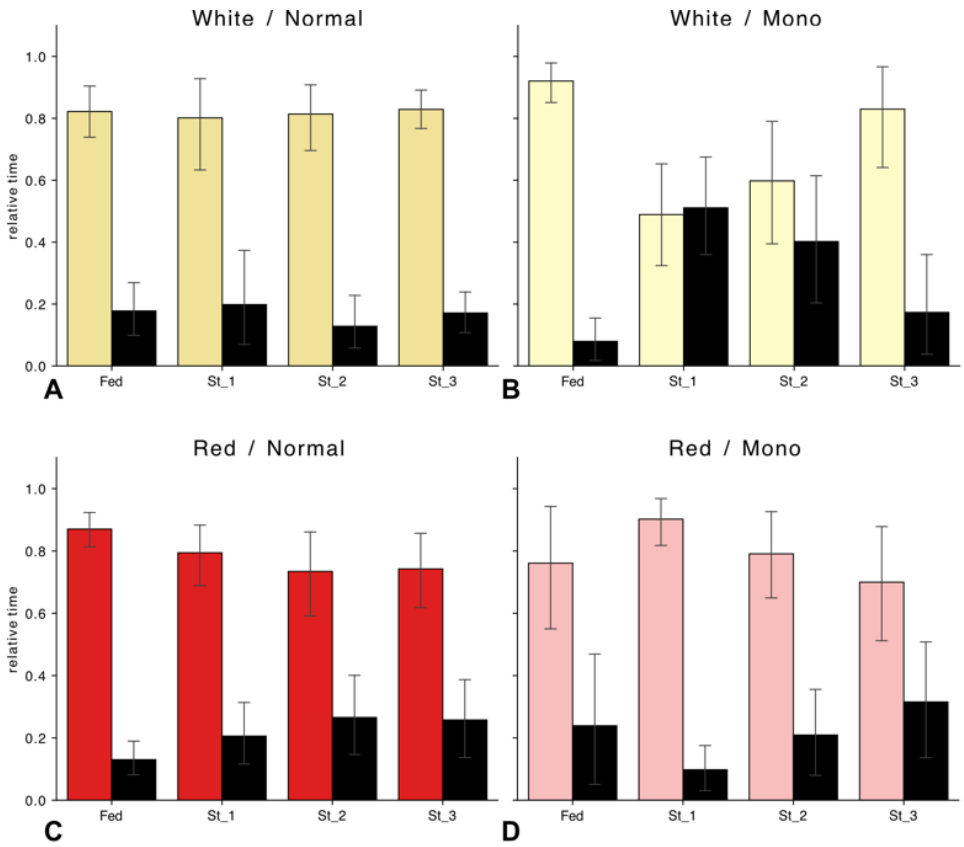

FIGURE 3.2: Relative time of individuals of *Elysia viridis* spent in the illuminated and shaded area of our side-choice experiment while freshly fed (Fed), or starved for one (St_1), two (St_2), or three (St_3) weeks. (A) Individuals cultured under regular conditions and tested with white light (White / Normal; n=12), (B) Individuals cultured in the presence of the photosynthesis blocker Monolinuron and tested with white light (White / Mono; n=12), (C) Individuals cultured under regular conditions, and tested with red light (Red / Normal; n=24), (D) Individuals cultured in the presence of the photosynthesis blocker Monolinuron and tested with red light (Red / Mono; n=24). Colored bars represent time spent in the illuminated area; black bars represent time spent in the shaded area. Error bars are the standard deviation.

n=12) spent 76% $\pm$ 37% of their time in the red-illuminated area, which is comparable to the Red/Normal group (Fig. 2C, D) and then decreased to 69% $\pm$ 31% after three weeks of starvation. We could not find significant differences between Red/Normal and Red/Mono starvation time points. When comparing the light source, only Red/Mono animals starved for one week spent significantly more time in the illuminated area than White/Mono animals (Mann-Whitney U test; p=0.002).

The activity of the slugs decreases under red light

Freshly fed White/Normal specimens showed high activity with 16 $\pm$ 12 changes during our one-hour experiment (Fig. 3A). The activity of the slugs decreased to 10 $\pm$ 5 changes after three weeks of starvation (St_3), but not statistically significant (Independent t-test > 0.05). Fed White/Mono specimens showed significantly lower activity with 4 $\pm$ 5 changes than animals fed under regular conditions (Independent t-test; p = 0.007). During starvation, the activity of White/Mono specimens increased significantly to 9 $\pm$ 8 changes (Independent t-test, p = 0.009) and subsequently decreased significantly to 6 $\pm$ 6 and 5 $\pm$ 6 (Independent t-test, p = 0.047 and

p = 0.009) after two and three weeks of starvation. White/Mono specimens starved for three weeks were also significantly less active than White/Normal specimens (Mann-Whitney U test, p = 0.013).

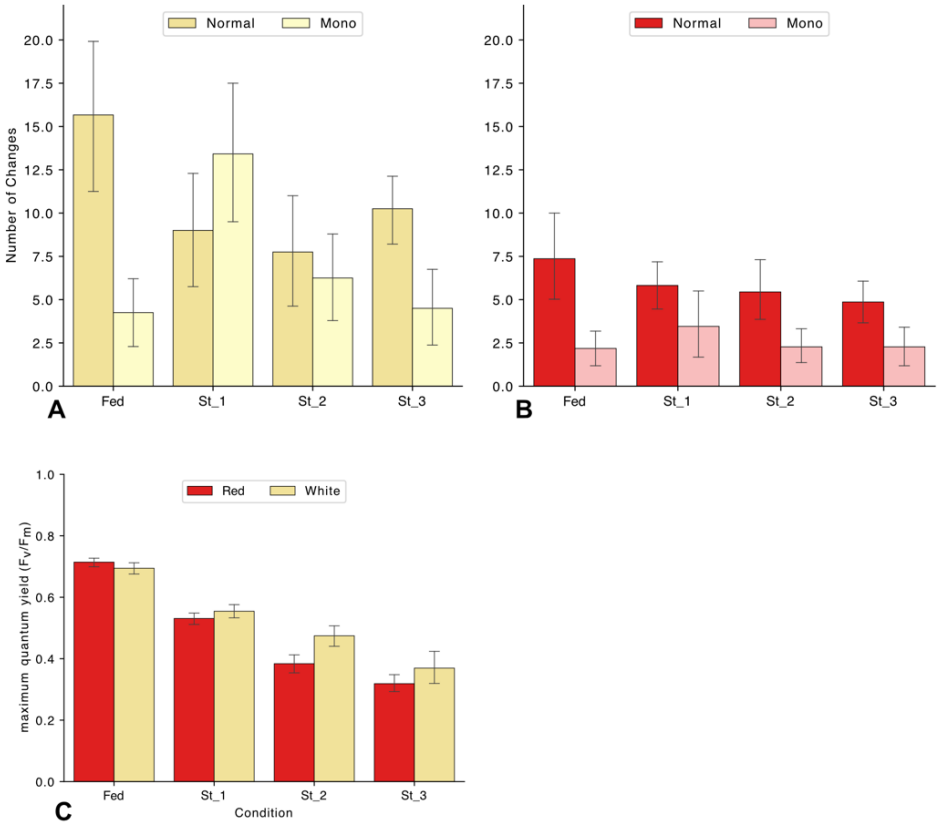

FIGURE 3.3: Number of changes of individuals of *Elysia viridis* between the illuminated and shaded area and the photosynthetic activity of kleptoplasts while freshly fed (Fed), or starved for one (St_1), two (St_2), or three (St_3) weeks. (A) Individuals cultured under regular conditions or in the presence of the blocker were tested with white light. (B) Individuals cultured under regular conditions or in the presence of the blocker were tested with red light. (C) Maximum quantum yield of individuals cultured under regular conditions, tested under white or red light. Error bars are the standard deviation. White/Normal (n=12), White/Mono (n=12), Red/Normal (n=24), and Red/Mono (n=24)

Generally, specimens exposed to red light were less active than those in white light (Figure 3B). Freshly fed Red/Normal animals changed the sites 7 $\pm$ 9 times, which was significantly less than under White/Normal (Mann-Whitney U test, p = 0.034). During starvation, the activity of Red/Normal slugs stayed at a low level but was only significantly lower compared to the White/Normal group after three weeks of starvation (5 $\pm$ 5, Mann-Whitney U test, p = 0.004). Fed Red/Mono slugs were significantly less active (2 $\pm$ 2) than fed Normal/Red slugs (Mann-Whitney U test, p = 0.028). The activity did not change substantially during starvation under Mono/Red but was significantly lower after one week of starvation than under Mono/White conditions (Mann-Whitney U test, p = 0.005).

The photosynthetic activity of kleptoplasts decreased during starvation

We monitored Fv/Fm during the experiments to ensure that the kleptoplast of all

animals were physiological intact and in the range of known measurements of previous studies. In both groups, White/Normal and Red/Normal, the Fv/Fm decreased significantly during starvation from 0.694 ± 0.047 and 0.741 ± 0.050, respectively to 0.369 ± 0.138 and 0.318 ± 0.099 after our three-week starvation experiment (Independent t-test, $p < 0.001$; Fig. 3C). Additionally, after the three weeks of starvation, there was a significantly lower Fv/Fm in Red/Normal starved animals than White/Normal (Independent t-test, $p = 0.015$). Still, these values fall well below õ.4 — a level at which PAM-derived fluorescence signals increasingly conflate with instrument noise or baseline shifts (Kalaji et al., 2014; Zhang et al., 2020) — suggesting that the differences are unlikely to reflect genuine physiological variation and may instead arise from measurement artefacts or sampling uncertainty.

3.5 Discussion

Our results show that *Elysia viridis* spent the most time in the illuminated area, independent of the light source, the starvation condition, and kleptoplast photophysiological state. This behavior of *E. viridis* is likely driven by searching for food, at least in a laboratory setting, because the slug species was reported to avoid food in darkness (Cartaxana et al., 2021). Other sacoglossans feed at night, such as the NR species *Oxynoe antillarum* Mörch, 1863 and the StR species *Elysia tuca* Ev. Marcus & Er. Marcus, 1967 (Weaver & Clark, 1981). These species preferred either low light conditions or darkness over light, which is probably based on their feeding behavior. Species known to feed during the late afternoon, such as the LtR species *Elysia crispata* Mörch, 1863 (Weaver & Clark, 1981) or during the day, such as the LtR species *Costasiella ocellifera* (Simroth, 1895), chose the light over darkness (Weaver & Clark, 1981). Furthermore, these previous and our experiments were performed at midday. Hence, the phototactic behavior we observed might simply be based on searching for food algae. This food-oriented photobehavior is common to other animal that are not harboring photosynthetic symbionts (Jékely, 2009) and suggests that the orientation towards light is a fundamental behavior of *Elysia viridis*. In addition, the nudibranchs were kept in the laboratory and acclimatized to unnatural conditions. Future experiments should therefore also be carried out with animals freshly collected in the field under natural light conditions. In this way, the natural behavior of nudibranchs could be better understood.

The positive phototactic behavior of different Sacoglossa does not necessarily have to be adaptive to increase the photosynthetic activity of the kleptoplasts, as suggested before for another species (Miyamoto et al., 2015). Such an adaptive behavior would be relevant if the slugs and the kleptoplasts would actively exchange nutrients, which is known, for instance, to occur in corals and giant clams (Armstrong et al., 2018; Matthews et al., 2017). In Sacoglossa, whether the slugs and kleptoplasts exchange nutrients is still unclear. During starvation, a constant accumulation of photosynthates in the kleptoplasts indicates a non-existing export of these assimilates (Laetz & Wägele, 2019; Laetz et al., 2017b). The distribution of photosynthates in the slug tissue during the day (Cruz et al., 2020) further favors the digestion of kleptoplasts, which was shown to occur while feeding (Cartaxana et al., 2023; Frankenbach et al., 2021; Maeda et al., 2012). During starvation, however, autophagy is the most likely option to obtain the assimilates (Frankenbach et al., 2023; Laetz et al., 2017a). Furthermore, because the Fv/Fm values significantly decreased in the starving slugs, as also reported in former studies (Evertsen & Johnsen, 2009;

Frankenbach et al., 2023; Laetz et al., 2017a; Rauch et al., 2018; Vieira et al., 2009; Yamamoto et al., 2013), the dependency on fresh kleptoplasts to ensure photosynthetic activity suggests that photosynthesis per se cannot be of significant influence for *E. viridis* and its photobehavior.

Additionally, there was no difference in the photobehavior between white and red light in *E. viridis*. This behavior is comparable to *Berthelinia caribbea* Edmunds, 1963, a non-kleptoplastic species, and the short-term-retention species *Elysia tuca* (Weaver & Clark, 1981). On the contrary, the non-kleptoplastic *Oxynoe antillarum* and the two long-term-retention species *Elysia crispata* and *Costasiella ocellifera* actively avoided red light (Weaver & Clark, 1981). This red-avoidance behavior resembles the acoel *Symsagittifera roscoffensis* (Nissen et al., 2015). Yet, avoiding red light would also inhibit photosynthesis. If these organisms behave to increase the photosynthetic activity of their photobionts, red light should be equally preferred as white or blue light. Yet, albeit *E. viridis* chose the red light, the slugs became less motile and entered some sort of resting phase. This decline in activity during starvation, which was also partially observed for individuals tested in white light, could also stem from a stress response and lower metabolic activity in general, as proposed in former studies (Frankenbach et al., 2023; Miyamoto et al., 2015). Why red light induces different behavior in the slugs remains to be tested, but the presence or absence of specific photoreceptors could be relevant, as shown for corals (Gornik et al., 2021).

We also found that Monolinuron induces a switch in the behavior during starvation. The reasons for this switch remain unknown, but starvation and blocked photosynthesis (and concomitant faster degradation of the chloroplasts) might trigger an increased generation of reactive oxygen species (ROS) that the slugs try to avoid. This would then be similar to reducing damage to the kleptoplasts by avoiding excessive light intensities (Miyamoto et al., 2015; Schmitt & Wägele, 2011) due to photoprotection mechanisms that cannot fully protect the photosystems from damage (Cartaxana et al., 2019; Christa et al., 2018; de Vries et al., 2013; Havurinne et al., 2021). In prolonged starvation periods, the kleptoplasts are likely entirely damaged, and the behavior is similar to the freshly fed state in which a constant replacement of kleptoplasts occurs (Frankenbach et al., 2021). Thus, although Monolinuron does not influence the life span of the animals in our experiments, it impacts the behavior of the slugs in the first two weeks of starvation. Further studies are needed to understand why this behavior occurs and whether other slugs behave similarly with and without functional kleptoplasts.

Previous results on *Elysia viridis* revealed that the slug preferred high light intensities when acclimated to these light conditions (Cartaxana et al., 2018). The results were interpreted that the kleptoplasts modulate the photobehavior of the slugs. Yet, the study missed experiments that included low light acclimated slugs feeding on high light acclimated algae, to understand whether the light history of the slug or the kleptoplast is indeed relevant for the phototactic behavior. Our results point towards a modulation of the photobehavior of the slugs based on the light history. If the kleptoplasts were to trigger a photobehavior, we would have expected that slugs in the photosynthesis blocker would crawl around more randomly to search for light conditions that enable photosynthesis, or spend more time in the dark, similar to some non-symbiotic animals that favor darkness over light conditions (Weaver & Clark, 1981). An algal photoacclimation-induced photobehavior was shown for the acoel *Symsagittifera roscoffensis* (Serôdio et al., 2011). Yet, in this system, the symbiont is a complete organism actively supporting the worm with nutrients. For Sacoglossa, it appears that a species-specific diurnal cycle is more relevant than optimizing the

photosynthetic activity of the kleptoplasts. Hence, the active search for light of *Elysia viridis* might simply be for searching food that inhabits the phototrophic zone.

3.6 Conclusion

The phototactic behavior of the sea slug *Elysia viridis* is likely based on a diurnal cycle rather than increasing the photosynthetic activity of the kleptoplasts. Whether this holds for other species, especially long-term retention species, has yet to be tested. However, the need to search for light might simply be based on searching for food. Chemically blocking the photosynthesis induces a behavior change under white light, possibly due to increased damage to the kleptoplasts. On the other hand, red light causes some sort of resting phase in the slugs. This induction of a resting phase also shows that the behavior is not connected to the photosynthetic activity of the kleptoplasts.

Author Contributions

GC and CS planned and designed the experiments. EW and JW performed the experiments. GC, CS, and EW analyzed and visualized the data. CS and GC wrote the initial manuscript. All authors contributed to the manuscript's text and read and approved the final version.

Funding

The study was conducted without financial support.

Conflict of interests

The authors declare no conflicts of interest.

Declarations

Ethical Approval

Not applicable

Availability of data and materials

All data of this study are available from the corresponding author on request.

References

Armstrong, E. J., Roa, J. N., Stillman, J. H., & Tresguerres, M. (2018). Symbiont photosynthesis in giant clams is promoted by V-type H^+-ATPase from host cells. *Journal of Experimental Biology*, *221:jeb177220*.

Cartaxana, P., Morelli, L., Cassin, E., Havurinne, V., Cabral, M., & Cruz, S. (2023). Prey species and abundance affect growth and photosynthetic performance of the polyphagous sea slug *Elysia crispata*. *Royal Society Open Science*, *10*, 230810.

Cartaxana, P., Morelli, L., Jesus, B., Calado, G., Calado, R., & Cruz, S. (2019). The photon menace: Kleptoplast protection in the photosynthetic sea slug *Elysia timida*. *Journal of Experimental Biology*, *222:jeb202580*.

Cartaxana, P., Rey, F., LeKieffre, C., Lopes, D., Hubas, C., Spangenberg, J. E., Escrig, S., Jesus, B., Calado, G., Domingues, R., Kühl, M., Calado, R., Meibom, A., & Cruz, S. (2021). Photosynthesis from stolen chloroplasts can support sea slug reproductive fitness. *Proceedings of the Royal Society B*, *288*.

Cartaxana, P., Morelli, L., Quintaneiro, C., Calado, G., Calado, R., & Cruz, S. (2018). Kleptoplast photoacclimation state modulates the photobehaviour of the solar-powered sea slug *Elysia viridis*. *Journal of Experimental Biology*, *221*(12).

Christa, G. (2023). Kleptoplasty. *Current Biology*, *33*, 465–467.

Christa, G., Händeler, K., Schäberle, T. F., König, G. M., & Wägele, H. (2014a). Identification of sequestered chloroplasts in photosynthetic and non-photosynthetic sacoglossan sea slugs (Mollusca, Gastropoda). *Frontiers in Zoology*, *11*, 15.

Christa, G., Pütz, L., Sickinger, C., Melo Clavijo, J., Laetz, E. M., Greve, C., & Serôdio, J. (2018). Photoprotective non-photochemical quenching does not prevent kleptoplasts from net photoinactivation. *Frontiers in Ecology and Evolution*, *6*, 121.

Christa, G., Händeler, K., Kück, P., Vleugels, M., Franken, J., Karmeinski, D., & Wägele, H. (2015). Phylogenetic evidence for multiple independent origins of functional kleptoplasty in Sacoglossa (Heterobranchia, Gastropoda). *Organisms Diversity & Evolution*, *15*(1), 23–36.

Cruz, S., & Cartaxana, P. (2022). Kleptoplasty: Getting away with stolen chloroplasts. *PLoS Biol*, *20*.

Cruz, S., LeKieffre, C., Cartaxana, P., Hubas, C., Thiney, N., Jakobsen, S., Escrig, S., Jesus, B., Kühl, M., Calado, R., et al. (2020). Functional kleptoplasts intermediate incorporation of carbon and nitrogen in cells of the Sacoglossa sea slug *Elysia viridis*. *Scientific Reports*, *10*(1), 10548.

Davy, S. K., Allemand, D., & Weis, V. M. (2012). Cell biology of cnidarian-dinoflagellate symbiosis. *Microbiology and Molecular Biology Reviews*, *76*, 229–261.

de Vries, J., Habicht, J., Woehle, C., Huang, C., Christa, G., Wägele, H., Nickelsen, J., Martin, W. F., & Gould, S. B. (2013). Is ftsH the key to plastid longevity in sacoglossan slugs? *Genome Biology and Evolution*, *5*, 2540–2548.

de Vries, J., Rauch, C., Christa, G., & Gould, S. B. (2014). A sea slug's guide to plastid symbiosis. *Acta Societatis Botanicorum Poloniae*, *83*, 415–421.

de Vries, J., Woehle, C., Christa, G., Wägele, H., Tielens, A. G. M., Jahns, P., & Gould, S. B. (2015). Comparison of sister species identifies factors underpinning plastid compatibility in green sea slugs. *Proceedings of the Royal Society B*, *282*.

Evertsen, J., & Johnsen, G. (2009). *In vivo* and *in vitro* differences in chloroplast functionality in the two north atlantic sacoglossans (Gastropoda, Opisthobranchia) *Placida dendritica* and *Elysia viridis*. *Marine Biology*, *156*, 847–859.

Frankenbach, S., Luppa, Q., Serôdio, J., Greve, C., Bleidissel, S., Melo Clavijo, J., Laetz, E. M., Preisfeld, A., & Christa, G. (2021). Kleptoplasts are continuously digested during feeding in the plastid-bearing sea slug *Elysia viridis*. *Journal of Molluscan Studies*, *87*(3), eyab022.

Frankenbach, S., Melo Clavijo, J., Brück, M., Bleidißel, S., Simon, M., Gasparoni, G., Lo Porto, C., Laetz, E. M., Greve, C., Donath, A., et al. (2023). Shedding light on starvation in darkness in the plastid-bearing sea slug *Elysia viridis* (Montagu, 1804). *Marine Biology*, *170*(7), 89.

Gascoigne, T. (1977). Sacoglossan teeth. *Malacologia*, *16*, 101–105.

Gornik, S. G., Bergheim, B. G., Morel, B., Stamatakis, A., Foulkes, N. S., & Guse, A. (2021). Photoreceptor diversification accompanies the evolution of anthozoa. *Molecular Biology and Evolution*, *38*, 1744–1760.

Händeler, K., Wägele, H., Wahrmund, U., Rüdinger, M., & Knoop, V. (2010). Slugs' last meals: Molecular identification of sequestered chloroplasts from different algal origins in Sacoglossa (Opisthobranchia, Gastropoda). *Molecular Ecology Resources*, *10*, 968–978.

Händeler, K., Grzymbowski, Y. P., Krug, P. J., & Wägele, H. (2009). Functional chloroplasts in metazoan cells-a unique evolutionary strategy in animal life. *Frontiers in Zoology*, *6*, 1–18.

Havurinne, V., Handrich, M., Antinluoma, M., Khorobrykh, S., Gould, S. B., & Tyystjärvi, E. (2021). Genetic autonomy and low singlet oxygen yield support kleptoplast functionality in photosynthetic sea slugs. *Journal of Experimental Botany*, *erab216*.

Hirokane, Y., Miyamoto, A., Kitaura, J., Nakano, R., Hirano, Y. M., Kawane, M., & Yusa, Y. (2022). Phylogeny and evolution of functional chloroplast retention in sacoglossan sea slugs (Gastropoda: Heterobranchia). *Organisms Diversity & Evolution*, *22*, 419–429.

Jékely, G. (2009). Evolution of phototaxis. *Philosophical Transactions of the Royal Society B: Biological Sciences*, *364*, 2795–2808.

Jinkerson, R. E., Russo, J. A., Newkirk, C. R., Kirk, A. L., Chi, R. J., Martindale, M. Q., Grossman, A. R., Hatta, M., & Xiang, T. (2022). Cnidarian-Symbiodiniaceae symbiosis establishment is independent of photosynthesis. *Current Biology*, *32*, 2402–2415.e4.

Kalaji, H. M., Schansker, G., Ladle, R. J., Goltsev, V., Bosa, K., Allakhverdiev, S. I., Brestic, M., Bussotti, F., Calatayud, A., Dąbrowski, P., et al. (2014). Frequently asked questions about *in vivo* chlorophyll fluorescence: Practical issues. *Photosynthesis Research*, *122*(2), 121–158.

Laetz, E. M., Moris, V. C., Moritz, L., Haubrich, A. N., & Wägele, H. (2017b). Photosynthate accumulation in solar-powered sea slugs-starving slugs survive due to accumulated starch reserves. *Frontiers in Zoology*, *14*, 1–9.

Laetz, E. M., Rühr, P. T., Bartolomaeus, T., Preisfeld, A., & Wägele, H. (2017a). Examining the retention of functional kleptoplasts and digestive activity in sacoglossan sea slugs. *Organisms Diversity & Evolution*, *17*, 87–99.

Laetz, E. M., & Wägele, H. (2019). Comparing amylose production in two solar-powered sea slugs: The sister taxa *Elysia timida* and *E. cornigera* (Heterobranchia: Sacoglossa). *Journal of Molluscan Studies*, *85*, 166–171.

Maeda, T., Hirose, E., Chikaraishi, Y., Kawato, M., Takishita, K., Yoshida, T., Verbruggen, H., Tanaka, J., Shimamura, S., Takaki, Y., Tsuchiya, M., Iwai, K., & Maruyama, T. (2012). Algivore or phototroph? *Plakobranchus ocellatus* (Gastropoda) continuously acquires kleptoplasts and nutrition from multiple algal species in nature. *PLoS ONE*, *7*, e42024.

Matthews, J. L., Crowder, C. M., Oakley, C. A., Lutz, A., Roessner, U., Meyer, E., Grossman, A. R., Weis, V. M., & Davy, S. K. (2017). Optimal nutrient exchange and immune responses operate in partner specificity in the cnidarian-dinoflagellate symbiosis. *Proceedings of the National Academy of Sciences*, *114*(50), 13194–13199.

Miyamoto, A., Sakai, A., Nakano, R., & Yusa, Y. (2015). Phototaxis of sacoglossan sea slugs with different photosynthetic abilities: A test of the 'crawling leaves' hypothesis. *Marine Biology*, *162*, 1343–1349.

Nissen, M., Shcherbakov, D., Heyer, A., Brümmer, F., & Schill, R. O. (2015). Behaviour of the plathelminth *Symsagittifera roscoffensis* under different light conditions and the consequences on the symbiotic algae *Tetraselmis convolutae*. *Journal of Experimental Biology*, *110429*.

Rädecker, N., Pogoreutz, C., Gegner, H. M., Cárdenas, A., Roth, F., Bougoure, J., Guagliardo, P., Wild, C., Pernice, M., Raina, J.-B., Meibom, A., & Voolstra, C. R. (2021). Heat stress destabilizes symbiotic nutrient cycling in corals. *Proceedings of the National Academy of Sciences*, *118*.

Rauch, C., Tielens, A. G., Serôdio, J., Gould, S. B., & Christa, G. (2018). The ability to incorporate functional plastids by the sea slug *Elysia viridis* is governed by its food source. *Marine Biology*, *165*(5), 82.

Schmitt, V., & Wägele, H. (2011). Behavioral adaptations in relation to long-term retention of endosymbiotic chloroplasts in the sea slug *Elysia timida* (Opisthobranchia, Sacoglossa). *Thalassas*, *27*(2), 225–238.

Serôdio, J., Silva, R., Ezequiel, J., & Calado, R. (2011). Photobiology of the symbiotic acoel flatworm *Symsagittifera roscoffensis*: Algal symbiont photoacclimation and host photobehaviour. *Journal of the Marine Biological Association of the United Kingdom*, *91*, 163–171.

Stanley Jr, G. D., & Lipps, J. H. (2011). Photosymbiosis: The driving force for reef success and failure. *The Paleontological Society Papers*, *17*, 33–59.

Strumpen, N. F., Rädecker, N., Pogoreutz, C., Meibom, A., & Voolstra, C. R. (2022). High light quantity suppresses locomotion in symbiotic *Aiptasia*. *Symbiosis*, *86*, 293–304.

Trench, R. K. (1969). Chloroplasts as functional endosymbionts in the mollusc *Tridachia crispata* (Bërgh), (Opisthobranchia, Sacoglossa). *Nature*, *222*(5198), 1071–1072.

Vieira, S., Calado, R., Coelho, H., & Serôdio, J. (2009). Effects of light exposure on the retention of kleptoplastic photosynthetic activity in the sacoglossan mollusc *Elysia viridis*. *Marine Biology*, *156*, 1007–1020.

Virtanen, P., Gommers, R., Oliphant, T. E., Haberland, M., Reddy, T., Cournapeau, D., Burovski, E., Peterson, P., Weckesser, W., Bright, J., van der Walt, S. J., Brett, M., Wilson, J., Millman, K. J., Mayorov, N., Arj, N., Jones, E., Kern, R., Larson, E., … van Mulbregt P. SciPy. (2020). Scipy 1.0: Fundamental algorithms for scientific computing in python. *Nature Methods*, *17*, 261–272.

Weaver, S., & Clark, K. (1981). Light intensity and color preferences of five ascoglossan (= sacoglossan) molluscs (Gastropoda: Opisthobranchia): A comparison of chloroplast-symbiotic and aposymbiotic species. *Marine & Freshwater Behaviour & Phy*, *7*(4), 297–306.

Yamamoto, S., Hirano, Y. M., Hirano, Y. J., Trowbridge, C. D., Akimoto, A., Sakai, A., & Yusa, Y. (2013). Effects of photosynthesis on the survival and weight retention of two kleptoplastic sacoglossan opisthobranchs. *Journal of the Marine Biological Association of the United Kingdom*, *93*, 209–215.

Zhang, J., Song, L., Pedersen, D. V., Li, A., Lambris, J. D., Andersen, G. R., Mollnes, T. E., Ma, Y. J., & Garred, P. (2020). Soluble collectin-12 mediates C3-independent docking of properdin that activates the alternative pathway of complement. *Elife*, *9*, e60908.

Chapter 4

Photosymbiosis Shapes the Microbiome of the Saccoglossan Sea Slug *Elysia viridis* (Montagu, 1804)

Corinna Sickinger[1], Katarina Kodzoman[1], Angelika Preisfeld[1] and Gregor Christa[2]

[1]*Institute for Zoology and Didactics of Biology, University of Wuppertal, Wuppertal, Germany*
[2]*Department of Evolution and Biodiversity, University of Wuppertal, Wuppertal, Germany*

4.1 Abstract

Kleptoplasty, the functional retention of photosynthetically active chloroplasts stolen from algae, is a unique form of photosymbiosis found in sacoglossan sea slugs such as *Elysia viridis*. While the question of whether sacoglossans benefit from kleptoplasty has been extensively studied, little is known about how the presence and functionality of kleptoplasts influence the host's associated microbial community. In this study, we analysed the microbiome of *E. viridis* under three different conditions: non-incorporation of kleptoplasts (slugs fed with *Cladophora* sp.), short-term retention with functional kleptoplasts (slugs fed with *Bryopsis* sp.), and short-term retention with chemically inhibited photosynthesis (slugs fed with *Bryopsis* sp. and kept in monolinuron). Despite identical food algae in two of the treatments, the microbial community structure and functional profiles differed significantly depending on the presence and activity of kleptoplasts. Photosynthesis inhibition led to a distinct microbiome composition characterised by increased sulfur metabolism pathways, such as sulfate reduction and sulfide oxidation, likely induced by oxidative stress from Monolinuron treatment and disrupted photosynthesis. In contrast, slugs, which were fed with *Bryopsis* sp. and retained functional chloroplasts, showed lower microbiome diversity and were dominated by Rhodobacteraceae and *Candidatus* Megaira sp., with moderate activity in sulfur metabolism and an upregulation of dehalogenation pathways. Interestingly, slugs fed with *Cladophora* sp. and lacking chloroplast retention harboured the most diverse microbiome and showed upregulation of pathways involved in xylan and aromatic hydrocarbon degradation. Our findings highlight the importance of considering the holobiont perspective in

kleptoplastic systems, where microbial partners may support or respond to photosymbiotic function.

Keywords Kleptoplasty · Photosymbiosis Status · Monolinuron · Core Microbiome

4.2 Introduction

Among Metazoans, different forms of photosymbiosis, a symbiotic relationship between a phototrophic symbiont and a host, can be found (Melo Clavijo et al., 2018). Within the Heterobranchia, two forms of photosymbiosis have evolved independently: the symbiosis with dinoflagellates of the family Symbiodiniaceae and the so-called functional kleptoplasty. The first one can be found in a group of Nudibranchs, the Cladobranchia, which show different modes of stability of this photosymbiosis (Rola et al., 2022). The latter has only evolved within the group of Sacoglossa. Sacoglossan sea slugs can "steal" the photosynthetically active chloroplasts from their food algae and incorporate them into their cytosol (Händeler et al., 2009). Species are distinguished by whether the stolen chloroplasts (kleptoplasts) remain photosynthetically active for up to two weeks (short-term retention: StR), for several months (long-term retention: LtR) or if they are not able to incorporate them at all (non-incorporation: NI; Händeler et al., 2009; Rauch et al., 2018.

The benefit of the photosymbiosis for Sacoglossa is still not well understood. Since the ingested kleptoplasts are sequestered intracellular by the slug, adapting both osmotically and metabolically to the new cellular environment many sacoglossan slugs resemble their food algae in colour, earning the nickname "crawling leaves" (Cruz et al., 2013; Jensen, 1997; Miyamoto et al., 2015; Rumpho et al., 2006). Sacoglossa may deter predators by using algae pigments for camouflage, known as nutritional homochromy (Marín & Ros, 2004). Additionally, the high survival rate of short-term and long-term retention species (StR and LtR) during starvation, lasting from two weeks up to a month, suggests that photosynthesis and the additional energy from photosynthetic assimilates play a key role for the slug (Cartaxana et al., 2017; Hinde & Smith, 1975; Mitoh & Yusa, 2021). Previous studies using radio-labelled carbon and nitrogen showed that sacoglossan slugs may use photosynthates, for example, in the reproductive system (Cruz et al., 2020; Trench et al., 1974). However, the active transfer of photosynthetic products from kleptoplasts to the slug's cells remains controversial. To enable nutrient exchange, a symbiosome membrane with transmembrane transporters surrounding the symbiont is crucial (Matthews et al., 2017; A. Mohamed et al., 2016). Just recently, phagosomes specialised for the maintenance of functional chloroplasts, so-called kleptosomes, were identified in the LtR species *Elysia crispata* (Mörch, 1863) (Allard et al., 2025). The study demonstrated that *E. crispata* relies on these kleptosomes to retain and sustain functional chloroplasts. However, when starvation persists for more than six weeks, the slugs shift from preserving the chloroplasts to breaking them down, tapping into them as a final energy reserve. Studies on *Elysia viridis* (Montagu, 1804) have shown that kleptoplasts function as storage units for starch produced during photosynthesis, holding the polysaccharides for a certain period until the slug digests the kleptoplasts to endure longer periods of starvation (Frankenbach et al., 2021, 2023; Laetz et al., 2017a, 2017b). In StR species, whether nutrient transporters exist in the membrane surrounding kleptoplasts or how they access photosynthetically derived assimilates is still unknown.

Photosymbiosis is a complex interaction that goes beyond the relationship between host and phototrophic organisms and also involves other microorganisms shaping the so-called holobiont. A holobiont refers to the close ecological unit consisting of a host and all its associated microbial organisms. This community includes bacteria, fungi, viruses and other microorganisms that live in or on the host. Holobionts form complex, interdependent relationships in which the microorganisms often fulfil essential functions for the host, such as aiding digestion, protecting against pathogens and regulating the immune system. The concept of the holobiont expands the understanding of an organism from a single species-based entity to an integrated ecosystem comprising many species that work together and contribute to the health and function of the overall system (Baedke et al., 2020; Bordenstein & Theis, 2008). Research on corals has demonstrated that their bacterial communities (microbiome) play a vital role in the host's physiology and are essential for maintaining stable photosymbiosis. These dynamic communities are thought to support photosymbiosis by providing the host with key elements such as carbon, nitrogen, and sulfur (E. Curtis et al., 2023; Meunier et al., 2021; K. B. Ritchie, 2011; Röthig et al., 2016; Voolstra & Ziegler, 2020). Beyond nutrient cycling, these bacteria may also enhance the host's defence mechanisms by producing antimicrobial compounds and outcompeting potential opportunistic pathogens (Bourne et al., 2016; Daniels et al., 2015; Rädecker et al., 2015; Silveira et al., 2017).

Aside from corals, little is known about the interaction between the microbiome and other photosymbiotic hosts. Only a few studies have examined the microbiomes of photosymbiotic sea slugs, and most have focused on describing the observed bacteria without conducting metabolic profiling. For example, *Elysia rufescens'* (Pease, 1871) microbiome was dominated by *Mycoplasma* spp. and *Vibrio* spp. and showed a high bacterial richness in its mucus (Davis et al., 2013). *Elysia chlorotica* A. Gould, 1870 harbours a diverse microbiome, mainly consisting of Actinobacteria, Bacilli, Flavobacteria, and Sphingobacteria with notable differences between wild-caught and laboratory-reared slugs (Devine et al., 2012). Mahadevan and Middlebrooks (2020) conducted a microbiome analysis of eight wild-caught *Elysia crispata* and identified significant variation in the metabolic pathways between individuals, suggesting that many of these microbiome relationships are opportunistic rather than obligate, with the microbiome primarily shaped by the food algae. However, a study on the photosymbiotic cladobranch *Berghia stephanieae* (Á. Valdés, 2005) found that its microbiome does not originate from its food source or the water column, suggesting a vertical transfer of symbiotic bacteria, which appear to be essential for nitrogen cycling (Sickinger et al., 2024).

We chose *Elysia viridis* for our microbiome and metabolic profiling analysis as it is classified as non-incorporation (NI), StR, or LtR depending on its food algae. Kleptoplasts from the algae *Codium tomentosum* can remain functional in *E. viridis* for several weeks (LtR), whereas kleptoplasts from *Bryopsis* sp. are of limited use in terms of photosynthetic capacity (StR). The plastids of *Cladophora* sp. cannot be taken up by the slug at all (NI; Rauch et al., 2018). This now enables us to understand functional kleptoplasty in a more detailed way. The object of the current study was to understand if the bacterial community of *E. viridis* shifts in the presence or absence of kleptoplasts by feeding the slug *Bryopsis* sp. or *Cladophora* sp.. Additionally, we treated *E. viridis* fed with *Bryopsis* sp. with the photosynthesis blocker Monolinuron, to assess whether a non-functioning kleptoplast and chemically inhibiting photosynthesis affects the slug's microbiome.

4.3 Methods

Culturing and sampling

Elysia viridis was collected in the Baltic Sea in the area of Bockholmwik, Germany (54°49'52.3"N 9°36'51.3"E) in August 2022 from either *Bryopsis* sp. or *Cladophora* sp. and subsequently cultivated in the laboratory of the University of Wuppertal, Germany. All organisms were cultured in artificial seawater (ASW) at a salinity of 18 ppt with a weekly water change and maintained at 21 ± 1 °C, with a light intensity of 25–30 µmol photons m^{-2} s^{-1} (provided by Daylight Sunrise 520, Sera), following a 12-hour day/night cycle. *Elysia viridis* were kept in groups of 10 individuals in 600 ml for two months and were provided with the food source they were collected from. After the acclimation phase, five randomly chosen slugs from each group were snap frozen in liquid nitrogen.

The third group was fed with *Bryopsis* sp. for five months and were kept as stated above. For the experiment, five slugs were randomly chosen and kept in ASW containing the photosynthesis blocker Monolinuron (JBL Algol®) of a concentration of 2µg/ml (M1-5) for three weeks. After these three weeks, all five slugs were snap-frozen in liquid nitrogen for further preparation.

RNA extraction

RNA extraction was performed using the my-Budget DNA/RNA Mini Kit (Bio-Budget Technologies GmbH, Germany) following the manufacturer's guidelines. RNA concentrations were quantified using a QubitTM 4 fluorometer (Invitrogen, USA) and cDNA templates generated with 50 ng of each RNA sample using the LunaScript® RT SuperMix Kit (NewEngland Biolabs, USA), following the manufacturer's protocol.

The cDNA was used as a PCR template to analyse the bacterial community of the slugs. We amplified the V1–V2 region of the 16S rRNA gene using primers that contained Illumina adapters (underlined): V1V2forward (5'-TCTTTCCCTACACGACG CTCTTCCGATCT AGAGTTTGATCCTGGCTCAG-3'), V1V2rev (5'-GTGACTGGAG TTCAGACGTGTGCTCTTCCGATCT TGCTGCCTCCCGTAGGAGT-3') (Weisburg et al., 1991). The adapter PCR was conducted in a total volume of 20 µL, comprising 5 µL of template cDNA, 10 µL DreamTaq Green PCR Master Mix (2X) (Thermo Fisher, USA), and 2 µL of 10 µM primer for each. The reaction volume was adjusted to 20 µL with distilled and sterilised water. PCR amplification included 30 cycles of denaturation at 94°C for 1 min, annealing at 54°C for 1 min, and extension at 72°C for 1 min, with initial denaturation at 95°C for 15 min and final elongation at 72°C for 10 min. PCR products were purified using the Monarch® PCR & DNA Cleanup Kit (NewEngland Biolabs, USA). Subsequently, an indexing PCR was performed using the purified adapter PCR products to attach Illumina sequencing adapters containing TrueSeq indices. Index PCR was executed in a 20 µL volume with 5 µL of the previously purified adapter PCR product, 10 µL Q5® High-Fidelity 2X Master Mix (NewEngland Biolabs, USA), 1 µL of 10 µM forward and reverse index primer each, and 3 µL distilled and autoclaved water. The index PCR products were purified with the Agencourt AMPure XP magnetic bead system (Beckman Coulter, USA). Final DNA concentrations were quantified using a QubitTM 4 Fluorometer before equimolar pooling of samples. The pooled samples were sequenced on an Illumina MiSeq platform, utilising a 2x250bp paired-end approach, targeting at least 30,000 reads per sample.

Sequencing data workflow and diversity analyses

Raw, demultiplexed MiSeq reads were joined in QIIME2 v2023.9 (Bolyen et al., 2019), and denoising was performed with the DADA2 plugin (Callahan et al., 2016), applying a maximum error rate of 2. Taxonomic assignments were executed in QIIME2 against a SILVA database (v132) (Quast et al., 2012). Any amplicon sequence variants (ASVs) identified as eukaryotes, mitochondria, or chloroplasts were subsequently filtered out. The relative abundance of bacterial families, along with alpha and beta diversity calculations, as well as statistical analyses, were conducted in QIIME2 v2023.9 (Bolyen et al., 2019) and R v4.0.3 (R Core Team, 2021), with significance set at p <0.05. The Shannon index (Shannon, 1948) was employed to describe and compare alpha diversity across samples. Differences in Shannon diversity between samples were assessed using one-way analysis of variance (ANOVA, Girden, 1992). Beta diversity differences were examined using Bray–Curtis dissimilarity matrices (Bray & Curtis, 1957) and tested via permutational multivariate analysis of variance (PERMANOVA, M. J. Anderson, 2001). A Principal Coordinate Analysis (PCoA) plot illustrating the variation in community composition among samples, paired with the Shannon index, was generated in R v4.0.3 using the packages devtools (Wickham et al., 2022), ggplot2 (Wickham, 2016), tidyverse (Wickham et al., 2019), and qiime2R (Bisanz, 2018). Differences in pathway abundance between groups were evaluated using ANOVA or, if the data deviated from normality and/or homogeneity of variance, by Kruskal-Wallis-Test (Kruskal & Wallis, 1952).

Core Microbiome

The core microbiome was analysed in QIIME2 v.2021.4. Using the command qiime feature-table core-features, a list of ASVs, present in at least 80% of the samples analysed was created for each sample group. Venn diagram, dot plot and pie charts were created in R v4.0.3 using the packages ggplot2 and RColorBrewer (Neuwirth, 2022).

Pathway Abundance

ASV IDs were removed and ASVs sharing the same taxonomic assignment were aggregated utilising the web server METAGENassist (Arndt et al., 2012). Furthermore, unassigned and unmapped reads were omitted and filtered based on the interquartile range (IQR; Hackstadt and Hess, 2009). The resultant dataset comprised 935 variables normalised across samples by sum and across taxa by Pareto scaling.

Subsequently, data analysis focused on the "metabolism" phenotype, employing the Spearman distance measure to cluster the most prevalent metabolic processes. Differences in pathway abundance among conditions were assessed using METAGENassist through one-way analysis of variance (ANOVA) and Tukey HSD post hoc comparison of means. Statistical significance was established at p <0.05.

A heatmap combined with agglomerative hierarchical clustering depicting putative functional disparities based on the bacterial community composition of each sample was generated using METAGENassist.

4.4 Results

DNA sequencing produced 8,403,136 reads across all samples (n = 15). After merging, denoising, and chimera filtering, 4,127,574 reads remained. After removing

contaminants, 2,808,468 ASVs were kept (Additional File 1: Table 1 and 2). Rarefaction curves for bacterial sequences plateaued in all samples, suggesting sufficient sequencing depth to capture bacterial species diversity (Additional File 2: Figure 1).

The core microbiome of *E. viridis* reflects the functionality of retained chloroplasts

E. viridis fed with *Cladophora* sp. (C) showed the highest alpha-diversity metric (Shannon indices), while one slug fed with *Bryopsis* sp. (B1) showed the lowest Shannon indices. A one-way ANOVA revealed a statistically significant difference in Alpha-diversity metrics (Shannon index) between at least two groups ($F_{(2,12)}$ = 15.96, p <0.001). Subsequent Tukey's HSD Test for multiple comparisons indicated that the groups C-M and B-C differed significantly (Additional File 1: Table 3). In contrast, slugs fed with *Bryopsis* sp. (B) and Mono+*Bryospis* sp. (M) did not differ significantly compared to each other (Additional File 1: Table 3). PCoA visualisation of beta-diversity using the Bray–Curtis dissimilarity index revealed a coherent grouping of group B, C, and M, respectively (Fig. 4.1A; Additional File 1: Table 4). PERMANOVA testing (999 permutations) indicated that bacterial community structure varied significantly depending on the feeding condition (pseudo-F_3 = 10.2782,p = 0.001). Pairwise comparisons between all conditions did yield significant differences between all groups (Additional File 1: Table 5).

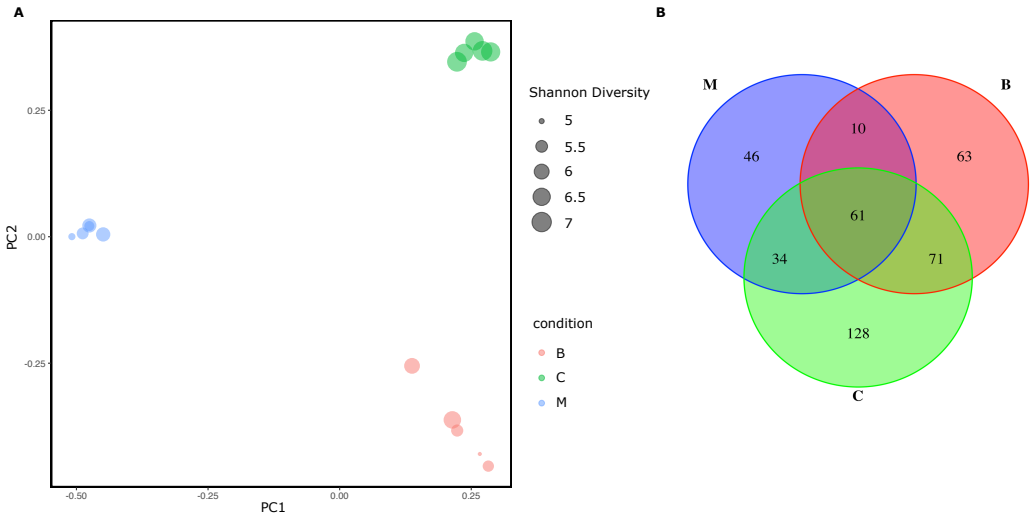

FIGURE 4.1: (A) Principal Coordinate Analysis (PCoA) plot of alpha- and beta-diversity based on Bray-Curtis dissimilarity. Size of circle indicates Shannon diversity index, and colour of circle represents the feeding condition (fed with *Bryopsis* sp. (B), *Cladophora* sp. (C), or with *Bryopsis* sp. and kept in Monolinuron (M). (B) Venn diagram comparing core microbiome composition of *E. viridis* under different feeding conditions. Numbers indicate the total abundance of either unique or shared ASVs.

On the species level, all slugs shared 61 ASVs of their core microbiome. Slugs of the group M and B shared only 10 ASVs, group C and M 34 ASVs, and group B and C 71 ASVs of their core microbiome. Slugs fed with *Cladophora* sp. (C) showed the highest number of unique ASVs with 128, followed by slugs fed with *Bryopsis* sp. (B, 63 ASVs) and slugs of group M (46 ASVs) (Fig. 4.1B, Additional File 3: Figure 1).

Almost all 61 shared ASVs were represented in very small numbers with a relative frequency lower than 4%. The uncultured bacterium of the family Rhodobacteraceae was the only bacterium with an abundance of over 4% shared between all

slugs. Group C and M further shared the bacterium *Marivita* sp., which also occurred in group B, but with under 1% much less abundant (Additional File 1: Table 6 and 7).

In slugs of group B, an uncultured bacterium of the family Rhodobacteraceae accounted for 32.3% of the core microbiome, *Alteromonas* sp. for 15.6%, an uncultured Gammaproteobacterium for 12.4%, and 11.4% was identified as a bacterium of the obligate symbiotic genus *Candidatus* Megaira. ASVs that were present less than 4% were clustered under "Others". The core microbiome of *E. viridis* fed with *Cladophora* sp. (C) consisted of 17.3% of an uncultured bacterium *Phaedactylibacter* sp., 14.2% of *Marivita* sp., 9.6% of an uncultured bacterium Rhodobacteraceae, 9% of *Tenacibaculum* sp. and 4.7% of the family Cyclobacteriaceae. In slugs of group M the core microbiome showed 16.5% classified as *Catenovulum* sp., 16.4% as *Marivita* sp., 10.7% as uncultured Rhodobacteraceae, 10.4% as *Donghicola* sp., 5.1% as an uncultured bacterium of the family Simkaniaceae, and 4.6% as *Owenweeksia* sp.. (Fig. 4.2).

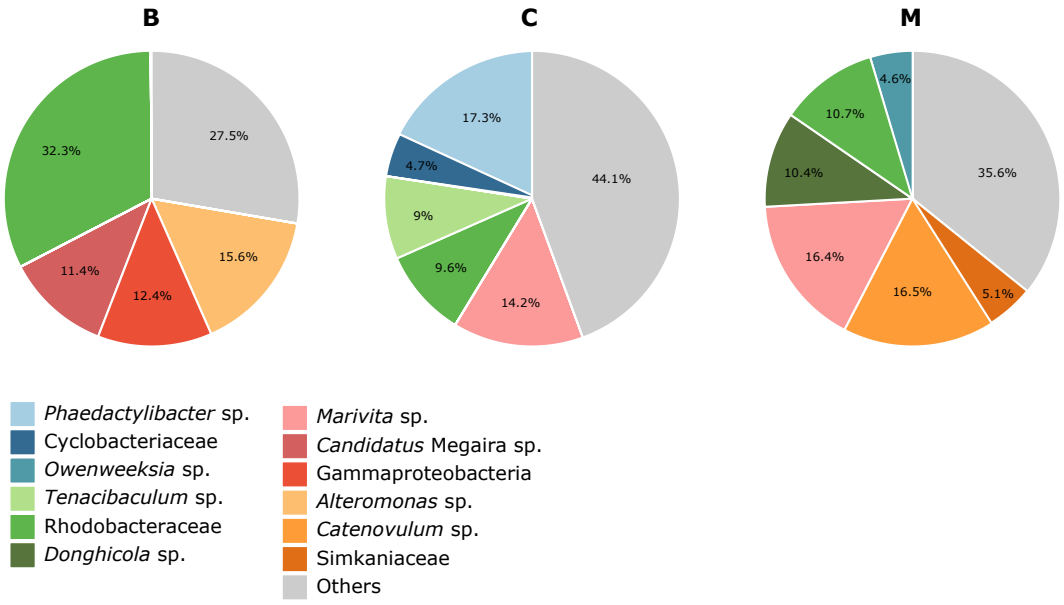

FIGURE 4.2: Core microbiome of *E. viridis* under different feeding conditions. All ASVs found in at least 80% of all samples of the corresponding condition were classified as "B core microbiome", "C core microbiome", or "M core microbiome". Each colour denotes a unique ASV represented by more than 4%; rare ASVs have been condensed in the group "Others" and are shown in grey.

The change in bacterial communities causes significant differences in the regulation of metabolic pathways

We further determined the metabolic pathway abundances of each sample and compared them regarding the condition (Additional File 1: Table 8).

E. viridis of group M and C clustered together, respectively, indicating homogeneity in the enrichment and depletion of metabolic pathways. Group B did not cluster together due to sample B3, which clustered closer to group C (Fig. 4.3).

Testing for differences (ANOVA or Kruskal-Wallis Test) and Post hoc testing (either Tukey's HSD or Dunn's test with Bonferroni correction; see Additional File 1: Table 9 for further information) revealed the most statistically significant differences in the regulation of the metabolic pathways between group M and C, with a total

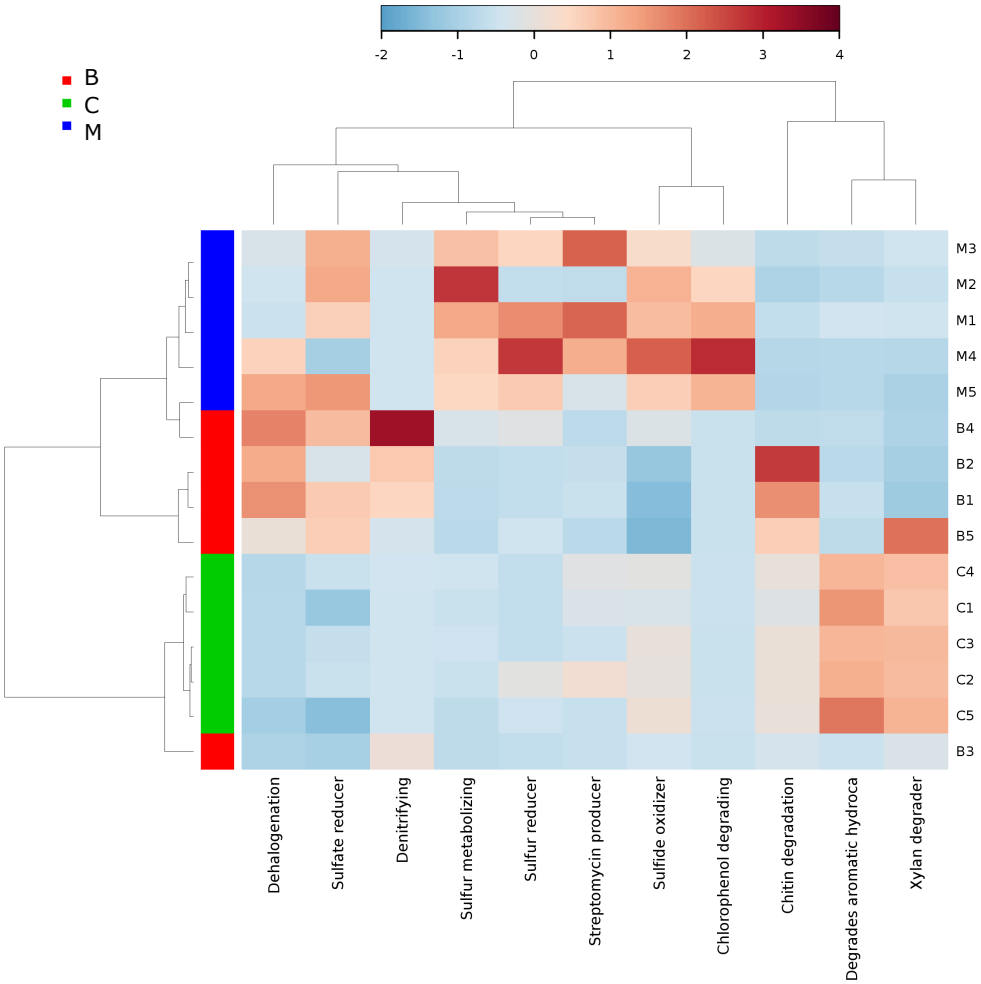

FIGURE 4.3: Taxonomy-based functional profiling of bacterial communities. Heatmap combined with agglomerative hierarchical clustering displaying changes in putative functional differences between the three groups B (fed with *Bryopsis* sp.), C (fed with *Cladophora* sp.), or M (fed with *Bryopsis* sp. + Mono) on a relative scale, with enrichment indicated in red and depletion in blue.

of 6 pathways out of 11. The pathways which differed were Sulfate reducer, Dehalogenation, Sulfide oxidiser, Chitin degradation, Xylan degrader and Degrades aromatic hydrocarbons, whereby the first four pathways were upregulated in group M and the last two pathways were upregulated in group C. Group M and B showed significant differences in 4 pathways: Sulfide oxidiser, Chlorophenol degrading, and Sulfur metabolising were the pathways upregulated in group M, whereas Denitrifying was downregulated in group M. Based on testing for differences, Groups B and C showed significant differences in 4 pathways. In group C, the pathways Sulfide oxidiser, Degrades aromatic hydrocarbons and Streptomycin producer were upregulated and the pathway Denitrifying downregulated.

4.5 Discussion

Depending on its food source, *E. viridis* can be classified as a non-, short-, or long-term photosymbiotic slug. In this study, we fed *E. viridis* with the alga *Cladophora* sp., whose chloroplasts are not retained by the slug, and *Bryopsis* sp., from which the slug

incorporates chloroplasts, making it a short-term retention form (Rauch et al., 2018). Additionally, we kept group M in artificial seawater (ASW) with Monolinuron, an algicide commonly used in photosynthesis studies with *Elysia* sp. to investigate the influence of a non-functioning chloroplast on the microbiome of the slug.

Slugs fed with *Cladophora* sp., which do not retain chloroplasts and lack active photosynthetic performance, exhibited the highest alpha diversity based on the Shannon index. In contrast, Groups B and M showed no significant differences in alpha diversity. However, beta diversity analysis using the Bray-Curtis index revealed clear clustering patterns, indicating that while Groups B and M had similar diversity and abundance, all three groups differed significantly in their overall bacterial community composition. The core microbiome analysis showed that only 61 out of 413 ASVs were shared across all three groups, albeit at very low abundances. The core microbiome refers to a group of microbial taxa, along with their genomic and functional traits, that are consistently associated with a specific host or environment (Risely, 2020; Turnbaugh et al., 2007). We applied an 80% occurrence threshold, meaning that any ASV present in at least 80% of samples was considered a core member, even if at low abundance, to account for rare taxa with potential ecological or functional relevance (Neu et al., 2021). Rhodobacteraceae was the most abundant ASV in the core microbiome of *E. viridis*, regardless of the feeding alga. This diverse family of gram-negative bacteria includes both chemoorganotrophic and phototheterotrophic species (Pujalte et al., 2014). Group M had the lowest number of unique ASVs (46), followed by Group B (63), while Group C exhibited the highest number of unique ASVs (128). This suggests that the absence of functional chloroplasts in Group C allows for greater microbiome diversification compared to the other groups.

Group B vs. Group M

Interestingly, groups B and M shared the fewest ASVs, with only 10 matches, although the slugs were fed with the same algae; one group was treated with Monolinuron. The cluster formation, as well as the few overlaps between group B and M, clearly show that Monolinuron affects the microbiome. The core microbiome of group B was dominated by Rhodobacteracea, followed by *Alteromonas* sp., Gammaproteobacteria and *Candidatus* Megaira sp.. *Candidatus* Megaira sp. is an obligate symbiont and can be found in a diversity of eukaryotic hosts such as protist (i.e. Paramecium spp.; Davison et al., 2023; Pasqualetti et al., 2020), green algae (i.e. *Bryopsis* sp., *Volvox carteri*; Hollants et al., 2013; Kawafune et al., 2015) and cnidarians (i.e. *Hydra* sp., *Montastraea faveolate*; Augustin et al., 2017; Sunagawa et al., 2009). We assume that *Candidatus* Megaira sp. is associated with the gut content of *E. viridis*, as it has previously been detected in the gut content of various other species, including ascidians, fish, and worms (Dishaw et al., 2014; Miyake et al., 2016; Murakami et al., 2017). Moreover, this bacterium was exclusively found in group B, and since *Candidatus* Megaira sp. has already been detected in *Bryopsis* sp., its presence in *E. viridis* seems plausible (Hollants et al., 2013). Group B was the only group that did not group together in the taxonomy-based functional profiling of bacterial communities, as sample B3 coincided with group C and showed downregulation in all indicated pathways. Slugs of group B overall showed low bacterial activity in the sulfur cycle, but an upregulation of sulfate reduction and dehalogenation. In contrast, in slugs treated with Monolinuron and fed with *Bryopsis* sp., there was a significant increase in the bacterial sulfur cycle, particularly in the pathways sulfur metabolising, sulfur

reducer and sulfide oxidiser. Monolinuron is a herbicide that disrupts photosynthesis in photosystem II (PSII) by binding to the plastoquinone binding site (QB) of the D1 protein in chloroplasts, thereby preventing the normal electron transport process (Gatidou et al., 2015). As a result, the excess light energy that cannot be utilised accumulates, leading to oxidative stress. This oxidative stress causes damage to lipids and other cellular components within the photosynthetic organism (Krieger-Liszkay, 2005). As a result, glutathione is formed, which reduces hydrogen peroxide and lipid peroxide (Lu, 2013). A key factor in glutathione synthesis is the availability of cysteine, a sulfur-containing amino acid. The γ-glutamyl cycle enables the continuous recycling of glutathione as a cysteine source. In this cycle, glutathione forms γ-glutamyl compounds with amino acids, which are then broken down, regenerating glutathione and releasing the amino acid inside the cell. Most cells efficiently absorb cysteine, which is primarily reincorporated into glutathione, while some is used for protein synthesis or converted to sulfate (Lu, 2013; Ripps and Shen, 2012; Turley et al., 1988; Additional file 4: Figure 1). This would explain the upregulation of the pathways Sulfate reducer, Sulfide oxidiser and Sulfur reducer as the extra Sulfate released by the cysteine degradation is metabolised by sulfate-reducing bacteria and sulfide-oxidising bacteria *Bradymonadales* sp. or *Paracoccus* sp., which were more present in group M. This highlights the effect of Monolinuron and the resulting oxidative stress in shaping the microbiome and differentiating it from Group B, despite both groups consuming the same algae. Further experiments, such as glutathione quantification and measurement of the superoxide dismutase enzymatic activity, would give more insights into the effect of Monolinuron on *E. viridis*.

Although slugs in Group M were fed for a longer period (five months) compared to Group B (two months), we do not consider feeding duration to be a major factor influencing microbiome composition. If time had a strong impact, we would expect Group B, having a shorter feeding period and thus a supposedly less stabilised microbiome, to show greater variability among samples. However, microbiome composition within Group B is remarkably consistent, suggesting that a stable community is already established after two months. Conversely, if prolonged feeding time alone shaped the microbiome, Groups B and M, both fed with *Bryopsis* sp., should exhibit similar microbial communities. Instead, we observe significant differences between them, indicating that even three weeks of Monolinuron treatment were sufficient to induce distinct shifts in the microbiome. This is further supported by the lower number of unique ASVs in Group M, pointing to a more selective and potentially stress-adapted microbial community shaped by Monolinuron exposure rather than by feeding duration.

Group B vs Group C

Group B and group C shared the highest number of ASVs, with 71 bacteria. Slugs that were fed *Cladophora* sp. and did not retain chloroplasts had a core microbiome primarily composed of *Phaedactylibacter* sp. and *Marivita* sp., followed by *Tenacibaculum* sp., Rhodobacteraceae, and Cyclobacteriaceae. The genus *Tenacibaculum*, part of the Flavobacteriaceae family, includes eight species known to be fish pathogens. These species are responsible for tenacibaculosis, a disease characterised by epidermal lesions, skin and fin erosion, and respiratory distress (Avendaño-Herrera et al., 2006; Frisch et al., 2018). In this study, *Tenacibaculum* sp. was detected not only in group C but also in groups M and B, though at lower abundances (<4%). However, it remains unclear whether the *Tenacibaculum* sp. found here has pathogenic potential. All slugs appeared healthy, showing no signs of distress and continuing

to feed normally throughout the experiment. Beyond its role as a pathogen, the ecological function of *Tenacibaculum* spp. is not yet fully understood. Many members of the Flavobacteriaceae family are capable of degrading polymers such as polysaccharides, chitin, agar, and cellulose, contributing significantly to carbon cycling in marine environments (Almeida et al., 2021; Romero et al., 2014). Specifically, environmental *Tenacibaculum* spp. are enriched in response to increased polysaccharide availability (Bunse et al., 2021; Taylor et al., 2014).

Interestingly, group C showed downregulation in all anaylsed pathways except for the pathways Degrades aromatic hydrocarbonates and Xylan degrader, which were significantly upregulated compared to group B and M. Polycyclic aromatic hydrocarbons are hydrophobic, planar aromatic molecules composed of two to six benzene rings arranged in linear, clustered, or angular configurations (Mojiri et al., 2019; Patel et al., 2020). Due to their hydrophobic nature, polycyclic aromatic hydrocarbons can diffuse across cell membranes and accumulate within cells (Gao et al., 2013). Once inside, these compounds can disrupt membrane function and interfere with embedded proteins, making them particularly harmful. *Cladophora vagabunda* (Linnaeus) Hoek, 1963, but also other algae species such as *Ulva lactuca* Linnaeus, 1753 are known to accumulate and to metabolise polycyclic aromatic hydrocarbons (González et al., 2021, 2022; Kirso & Irha, 1998; Othman et al., 2023). This would promote the occurrence of bacteria such as those known to metabolise PHAs in slugs which were fed with *Cladophora* sp. in our study.

Group C vs Group M

While Groups C and M differed in their overall microbiome composition, they shared more ASVs compared to Group B. Groups C and M shared a total of 34 ASVs, of which the bacterium *Marivita* sp. showed the highest abundance of the shared bacteria. The genus *Marivita* belongs to the family Rhodobacteraceae, and several species have been described to have aerobic anoxygenic photosynthesis genes (Budinoff et al., 2011; Hwang et al., 2009). Aerobic anoxygenic phototrophic bacteria are thought to play an important role in carbon cycling by relying on organic matter substrates and acting as sinks for dissolved organic carbon (A. E. Ritchie & Johnson, 2012). Her,e it seems that the absence of a functioning chloroplast promotes the abundance of *Marivita* sp..

4.6 Conclusion

This study is the first to investigate how the photosymbiotic status of *E. viridis*, ranging from non-retaining to short-term chloroplast retention with or without photosynthetic activity, influences its associated microbiome. We show that both the presence and functionality of kleptoplasts significantly shape the microbial community composition and predicted metabolic potential. Slugs with inactive or absent chloroplasts exhibited higher microbial diversity, while those with functional kleptoplasts harboured distinct communities with altered functional profiles. Inhibition of photosynthesis by Monolinuron led to pronounced shifts in sulfur metabolism, likely as a response to oxidative stress. These findings underscore the role of photosymbiosis in structuring the *E. viridis* holobiont and emphasise the importance of considering symbiotic function in microbiome studies.

Supplementary Materials

The supplementary material is included in the digital version of this thesis.

Additional File 1

— Table 1. ASV table. Number of ASVs organised by sample and treatment and after filtering and denoising. Biosample ID and Accession number are included for each sample. — Table 2. Absolute abundance of bacterial families across all samples. — Table 3. Results of ANOVA based on Shannon alpha diversity metric and pairwise t-tests between conditions. — Table 4. List of vectors PC1 and PC2 of PCoA plot and Shannon entropy for each sample. — Table 5. Results of PERMANOVA based on Bray-Curtis beta diversity metric and pairwise comparison of conditions. — Table 6. Absolute abundance of core bacteria species for all samples. — Table 7. Relative abundance of core bacteria species for all samples. — Table 8. List of absolute pathway abundance for all samples. — Table 9. Results of the statistical analysis of the metabolic pathways between the different conditions.

Additional File 2

— Figure 1. Rarefaction curves illustrate ASV richness as a function of sequencing depth for subsampled dataset. The three groups shown correspond to *E. viridis* fed with *Bryopsis* sp. (B), with *Cladophora* sp. (C), *Bryopsis* sp. + Monolinuron (M).

Additional File 3

— Figure 1. Dot plot showing absolute frequencies of the 61 shared ASVs of *E. viridis'* core microbiome under different feeding conditions. B (fed with *Bryopsis* sp.), C (fed with *Cladophora* sp.), or M (fed with Mono+*Bryopsis* sp.). Colour scale indicates relative frequency, circle size indicates absolute frequency.

Additional File 4

— Figure 1. Cysteine degradation to sulfate and the resulting sulfate degradation by bacterial metabolic pathways.

Declarations

Author's contributions

CS and GC planned and conducted the experiments. CS processed the data, performed data analyses and wrote the manuscript. CS, AP, and GC discussed, interpreted the results, and revised the final version of the manuscript.

Funding

This work was supported by the DFG Research Infrastructure NGS_CC (project 407495230) as part of the Next Generation Sequencing Competence Network (project 423957469). NGS analyses were conducted at the Competence Centre for Genomic Analysis (Kiel).

References

Allard, C. A., Thies, A. B., Mitra, R., Vaelli, P. M., Leto, O. D., Walsh, B. L., Laetz, E. M., Tresguerres, M., Lee, A. S., & Bellono, N. W. (2025). A host organelle integrates stolen chloroplasts for animal photosynthesis. *Cell*.

Almeida, D. B., Magalhães, C., Sousa, Z., Borges, M. T., Silva, E., Blanquet, I., & Mucha, A. P. (2021). Microbial community dynamics in a hatchery recirculating aquaculture system (RAS) of sole (*Solea senegalensis*). *Aquaculture*, *539*, 736592.

Anderson, M. J. (2001). A new method for non-parametric multivariate analysis of variance. *Austral Ecology*, *26*(1), 32–46.

Arndt, D., Xia, J., Liu, Y., Zhou, Y., Guo, A. C., Cruz, J. A., Sinelnikov, I., Budwill, K., Nesbø, C. L., & Wishart, D. S. (2012). METAGENassist: A comprehensive web server for comparative metagenomics. *Nucleic Acids Research*, *40*(W1), W88–W95.

Augustin, R., Schröder, K., Murillo Rincón, A. P., Fraune, S., Anton-Erxleben, F., Herbst, E.-M., Wittlieb, J., Schwentner, M., Grötzinger, J., Wassenaar, T. M., et al. (2017). A secreted antibacterial neuropeptide shapes the microbiome of *Hydra*. *Nature communications*, *8*(1), 698.

Avendaño-Herrera, R., Toranzo, A. E., & Magariños, B. (2006). Tenacibaculosis infection in marine fish caused by *Tenacibaculum maritimum*: A review. *Diseases of Aquatic Organisms*, *71*(3), 255–266.

Baedke, J., Fábregas-Tejeda, A., & Nieves Delgado, A. (2020). The holobiont concept before Margulis. *Journal of Experimental Zoology Part B: Molecular and Developmental Evolution*, *334*(3), 149–155.

Bisanz, J. E. (2018). *qiime2R: Importing QIIME2 artifacts and associated data into R sessions* [v0.99].

Bolyen, E., Rideout, J. R., Dillon, M. R., Bokulich, N. A., Abnet, C. C., Al-Ghalith, G. A., Alexander, H., Alm, E. J., Arumugam, M., Asnicar, F., et al. (2019). Reproducible, interactive, scalable and extensible microbiome data science using QIIME 2. *Nature Biotechnology*, *37*(8), 852–857.

Bordenstein, S., & Theis, K. (2008). Host biology in light of the microbiome: Ten principles of holobionts and hologenomes. *PLoS Biology*, *13*(8), 1–23.

Bourne, D. G., Morrow, K. M., & Webster, N. S. (2016). Insights into the coral microbiome: Underpinning the health and resilience of reef ecosystems. *Annual Review of Microbiology*.

Bray, J. R., & Curtis, J. T. (1957). An ordination of the upland forest communities of southern Wisconsin. *Ecological Monographs*, *27*(4), 326–349.

Budinoff, C. R., Dunlap, J. R., Hadden, M., & Buchan, A. (2011). *Marivita roseacus* sp. nov., of the family Rhodobacteraceae, isolated from a temperate estuary and an emended description of the genus *Marivita*. *The Journal of General and Applied Microbiology*, *57*(5), 259–267.

Bunse, C., Koch, H., Breider, S., Simon, M., & Wietz, M. (2021). Sweet spheres: Succession and CAZyme expression of marine bacterial communities colonizing a mix of alginate and pectin particles. *Environmental Microbiology*, *23*(6), 3130–3148.

Callahan, B. J., McMurdie, P. J., Rosen, M. J., Han, A. W., Johnson, A. J. A., & Holmes, S. P. (2016). DADA2: High-resolution sample inference from Illumina amplicon data. *Nature Methods*, *13*(7), 581–583.

Cartaxana, P., Trampe, E., Kühl, M., & Cruz, S. (2017). Kleptoplast photosynthesis is nutritionally relevant in the sea slug *Elysia viridis*. *Scientific Reports*, *7*(1), 7714.

Cruz, S., Calado, R., Serôdio, J., & Cartaxana, P. (2013). Crawling leaves: Photosynthesis in sacoglossan sea slugs. *Journal of Experimental Botany*, *64*(13), 3999–4009.

Cruz, S., LeKieffre, C., Cartaxana, P., Hubas, C., Thiney, N., Jakobsen, S., Escrig, S., Jesus, B., Kühl, M., Calado, R., et al. (2020). Functional kleptoplasts intermediate incorporation of carbon and nitrogen in cells of the Sacoglossa sea slug *Elysia viridis*. *Scientific Reports*, *10*(1), 10548.

Curtis, E., Moseley, J., Racicot, R., & Wright, R. M. (2023). Bacterial microbiome variation across symbiotic states and clonal lines in a cnidarian model. *Frontiers in Marine Science*.

Daniels, C. A., Baumgarten, S., Yum, L. K., Michell, C. T., Bayer, T., Arif, C., Roder, C., Weil, E., & Voolstra, C. R. (2015). Metatranscriptome analysis of the reef-building coral *Orbicella faveolata* indicates holobiont response to coral disease. *Frontiers in Marine Science*, *2*, 62.

Davis, J., Fricke, W. F., Hamann, M. T., Esquenazi, E., Dorrestein, P. C., & Hill, R. T. (2013). Characterization of the bacterial community of the chemically defended Hawaiian sacoglossan *Elysia rufescens*. *Applied and Environmental Microbiology*, *79*(22), 7073–7081.

Davison, H. R., Hurst, G. D., & Siozios, S. (2023). *'Candidatus* Megaira 'are diverse symbionts of algae and ciliates with the potential for defensive symbiosis. *Microbial Genomics*, *9*(3), 000950.

Devine, S. P., Pelletreau, K. N., & Rumpho, M. E. (2012). 16S rDNA-based metagenomic analysis of bacterial diversity associated with two populations of the kleptoplastic sea slug *Elysia chlorotica* and its algal prey *Vaucheria litorea*. *The Biological Bulletin*, *223*(1), 138–154.

Dishaw, L. J., Flores-Torres, J., Lax, S., Gemayel, K., Leigh, B., Melillo, D., Mueller, M. G., Natale, L., Zucchetti, I., De Santis, R., et al. (2014). The gut of geographically disparate *Ciona intestinalis* harbors a core microbiota. *PLoS One*, *9*(4), e93386.

Frankenbach, S., Luppa, Q., Serôdio, J., Greve, C., Bleidissel, S., Melo Clavijo, J., Laetz, E. M., Preisfeld, A., & Christa, G. (2021). Kleptoplasts are continuously digested during feeding in the plastid-bearing sea slug *Elysia viridis*. *Journal of Molluscan Studies*, *87*(3), eyab022.

Frankenbach, S., Melo Clavijo, J., Brück, M., Bleidißel, S., Simon, M., Gasparoni, G., Lo Porto, C., Laetz, E. M., Greve, C., Donath, A., et al. (2023). Shedding light on starvation in darkness in the plastid-bearing sea slug *Elysia viridis* (Montagu, 1804). *Marine Biology*, *170*(7), 89.

Frisch, K., Småge, S. B., Brevik, Ø. J., Duesund, H., & Nylund, A. (2018). Genotyping of *Tenacibaculum maritimum* isolates from farmed Atlantic salmon in Western Canada. *Journal of Fish Diseases*, *41*(1), 131–137.

Gao, Y., Zhang, Y., Liu, J., & Kong, H. (2013). Metabolism and subcellular distribution of anthracene in tall fescue (*Festuca arundinacea* Schreb.) *Plant and Soil*, *365*, 171–182.

Gatidou, G., Stasinakis, A. S., & Iatrou, E. I. (2015). Assessing single and joint toxicity of three phenylurea herbicides using *Lemna minor* and *Vibrio fischeri* bioassays. *Chemosphere*, *119*, S69–S74.

Girden, E. R. (1992). *ANOVA: Repeated measures*. Sage.

González, A., Osorio, H., Romero, S., Méndez, P., Sepúlveda, M., Laporte, D., Gutierrez-Cutiño, M., Santander, R., Castro-Nallar, E., & Moenne, A. (2022). Transcriptomic analyses reveal increased expression of dioxygenases, monooxygenases, and other metabolizing enzymes involved in anthracene degradation in the marine alga *Ulva lactuca*. *Frontiers in Plant Science*, *13*, 955601.

González, A., Vidal, C., Espinoza, D., & Moenne, A. (2021). Anthracene induces oxidative stress and activation of antioxidant and detoxification enzymes in *Ulva lactuca* (Chlorophyta). *Scientific Reports*, *11*(1), 7748.

Hackstadt, A. J., & Hess, A. M. (2009). Filtering for increased power for microarray data analysis. *BMC Bioinformatics*, *10*, 1–12.

Händeler, K., Grzymbowski, Y. P., Krug, P. J., & Wägele, H. (2009). Functional chloroplasts in metazoan cells-a unique evolutionary strategy in animal life. *Frontiers in Zoology*, *6*, 1–18.

Hinde, R., & Smith, D. (1975). The role of photosynthesis in the nutrition of the mollusc *Elysia viridis*. *Biological Journal of the Linnean Society*, *7*(2), 161–171.

Hollants, J., Leliaert, F., Verbruggen, H., De Clerck, O., & Willems, A. (2013). Host specificity and coevolution of Flavobacteriaceae endosymbionts within the siphonous green seaweed *Bryopsis*. *Molecular Phylogenetics and Evolution*, *67*(3), 608–614.

Hwang, C. Y., Bae, G. D., Yih, W., & Cho, B. C. (2009). *Marivita cryptomonadis* gen. nov., sp. nov. and *Marivita litorea* sp. nov., of the family Rhodobacteraceae, isolated from marine habitats. *International Journal of Systematic and Evolutionary Microbiology*, *59*(7), 1568–1575.

Jensen, K. R. (1997). Evolution of the Sacoglossa (Mollusca, Opisthobranchia) and the ecological associations with their food plants. *Evolutionary Ecology*, *11*(3), 301–335.

Kawafune, K., Hongoh, Y., Hamaji, T., Sakamoto, T., Kurata, T., Hirooka, S., Miyagishima, S.-y., & Nozaki, H. (2015). Two different rickettsial bacteria invading *Volvox carteri*. *PLoS One*, *10*(2), e0116192.

Kirso, U., & Irha, N. (1998). Role of algae in fate of carcinogenic polycyclic aromatic hydrocarbons in the aquatic environment. *Ecotoxicology and Environmental Safety*, *41*(1), 83–89.

Krieger-Liszkay, A. (2005). Singlet oxygen production in photosynthesis. *Journal of Experimental Botany*, *56*(411), 337–346.

Kruskal, W. H., & Wallis, W. A. (1952). Use of ranks in one-criterion variance analysis. *Journal of the American Statistical Association*, *47*(260), 583–621.

Laetz, E. M., Moris, V. C., Moritz, L., Haubrich, A. N., & Wägele, H. (2017b). Photosynthate accumulation in solar-powered sea slugs-starving slugs survive due to accumulated starch reserves. *Frontiers in Zoology*, *14*, 1–9.

Laetz, E. M., Rühr, P. T., Bartolomaeus, T., Preisfeld, A., & Wägele, H. (2017a). Examining the retention of functional kleptoplasts and digestive activity in sacoglossan sea slugs. *Organisms Diversity & Evolution*, *17*, 87–99.

Lu, S. C. (2013). Glutathione synthesis. *Biochimica et Biophysica Acta (BBA)-General Subjects*, *1830*(5), 3143–3153.

Mahadevan, P., & Middlebrooks, M. L. (2020). Bacterial diversity in the *clarki* ecotype of the photosynthetic sacoglossan, *Elysia crispata*. *MicrobiologyOpen*, *9*(9), e1098.

Marín, A., & Ros, J. (2004). Chemical defenses in Sacoglossan Opisthobranchs: Taxonomic trends and evolutionary implications. *Scientia Marina*, *68*(S1), 227–241.

Matthews, J. L., Crowder, C. M., Oakley, C. A., Lutz, A., Roessner, U., Meyer, E., Grossman, A. R., Weis, V. M., & Davy, S. K. (2017). Optimal nutrient exchange and immune responses operate in partner specificity in the cnidarian-dinoflagellate symbiosis. *Proceedings of the National Academy of Sciences*, *114*(50), 13194–13199.

Melo Clavijo, J., Donath, A., Serôdio, J., & Christa, G. (2018). Polymorphic adaptations in metazoans to establish and maintain photosymbioses. *Biological Reviews*, *93*(4), 2006–2020.

Meunier, V., Geissler, L., Bonnet, S., Rädecker, N., Perna, G., Grosso, O., Lambert, C., Rodolfo-Metalpa, R., Voolstra, C. R., & Houlbrèque, F. (2021). Microbes support enhanced nitrogen requirements of coral holobionts in a high CO2 environment. *Molecular Ecology*, *30*(22), 5888–5899.

Mitoh, S., & Yusa, Y. (2021). Extreme autotomy and whole-body regeneration in photosynthetic sea slugs. *Current Biology*, *31*(5), R233–R234.

Miyake, S., Ngugi, D. K., & Stingl, U. (2016). Phylogenetic diversity, distribution, and cophylogeny of giant bacteria (*Epulopiscium*) with their surgeonfish hosts in the Red Sea. *Frontiers in Microbiology*, *7*, 285.

Miyamoto, A., Sakai, A., Nakano, R., & Yusa, Y. (2015). Phototaxis of sacoglossan sea slugs with different photosynthetic abilities: A test of the 'crawling leaves' hypothesis. *Marine Biology*, *162*, 1343–1349.

Mohamed, A., Cumbo, V., Harii, S., Shinzato, C., Chan, C., Ragan, M., Bourne, D., Willis, B., Ball, E., Satoh, N., et al. (2016). The transcriptomic response of the coral *Acropora digitifera* to a competent *Symbiodinium* strain: The symbiosome as an arrested early phagosome. *Molecular Ecology*, *25*(13), 3127–3141.

Mojiri, A., Zhou, J. L., Ohashi, A., Ozaki, N., & Kindaichi, T. (2019). Comprehensive review of polycyclic aromatic hydrocarbons in water sources, their effects and treatments. *Science of the Total Environment*, *696*, 133971.

Murakami, T., Segawa, T., Dial, R., Takeuchi, N., Kohshima, S., & Hongoh, Y. (2017). Bacterial microbiota associated with the glacier ice worm is dominated by both worm-specific and glacier-derived facultative lineages. *Microbes and Environments*, *32*(1), 32–39.

Neu, A. T., Allen, E. E., & Roy, K. (2021). Defining and quantifying the core microbiome: Challenges and prospects. *Proceedings of the National Academy of Sciences*, *118*(51), e2104429118.

Neuwirth, E. (2022). *RColorBrewer: ColorBrewer Palettes* [R package version 1.1-3].

Othman, H. B., Pick, F. R., Hlaili, A. S., & Leboulanger, C. (2023). Effects of polycyclic aromatic hydrocarbons on marine and freshwater microalgae–A review. *Journal of Hazardous Materials*, *441*, 129869.

Pasqualetti, C., Szokoli, F., Rindi, L., Petroni, G., & Schrallhammer, M. (2020). The obligate symbiont "*Candidatus Megaira polyxenophila*" has variable effects on the growth of different host species. *Frontiers in Microbiology*, *11*, 1425.

Patel, A. B., Shaikh, S., Jain, K. R., Desai, C., & Madamwar, D. (2020). Polycyclic aromatic hydrocarbons: Sources, toxicity, and remediation approaches. *Frontiers in Microbiology*, *11*, 562813.

Pujalte, M. J., Lucena, T., Ruvira, M. A., Arahal, D. R., & Macián, M. C. (2014). The family rhodobacteraceae. In *The Prokaryotes*. Springer.

Quast, C., Pruesse, E., Yilmaz, P., Gerken, J., Schweer, T., Yarza, P., Peplies, J., & Glöckner, F. O. (2012). The SILVA ribosomal RNA gene database project: Improved data processing and web-based tools. *Nucleic Acids Research*, *41*(D1), D590–D596.

R Core Team. (2021). *R: A Language and Environment for Statistical Computing*. R Foundation for Statistical Computing. Vienna, Austria.

Rädecker, N., Pogoreutz, C., Voolstra, C. R., Wiedenmann, J., & Wild, C. (2015). Nitrogen cycling in corals: The key to understanding holobiont functioning? *Trends in Microbiology*, *23*(8), 490–497.

Rauch, C., Tielens, A. G., Serôdio, J., Gould, S. B., & Christa, G. (2018). The ability to incorporate functional plastids by the sea slug *Elysia viridis* is governed by its food source. *Marine Biology*, *165*(5), 82.

Ripps, H., & Shen, W. (2012). Taurine: A "very essential" amino acid. *Molecular Vision*, *18*, 2673.

Risely, A. (2020). Applying the core microbiome to understand host–microbe systems. *Journal of Animal Ecology*, *89*(7), 1549–1558.

Ritchie, A. E., & Johnson, Z. I. (2012). Abundance and genetic diversity of aerobic anoxygenic phototrophic bacteria of coastal regions of the Pacific Ocean. *Applied and Environmental Microbiology*, *78*(8), 2858–2866.

Ritchie, K. B. (2011). Bacterial symbionts of corals and *Symbiodinium*. *Beneficial Microorganisms in Multicellular Life Forms*, 139–150.

Rola, M., Frankenbach, S., Bleidissel, S., Sickinger, C., Donath, A., Frommlet, J. C., Greve, C., Serôdio, J., Preisfeld, A., Melo Clavijo, J., et al. (2022). Cladobranchia (Gastropoda, Nudibranchia) as a promising model to understand the molecular evolution of photosymbiosis in animals. *Frontiers in Marine Science*, *8*, 745644.

Romero, M., Muras, A., Mayer, C., Buján, N., Magariños, B., & Otero, A. (2014). In vitro quenching of fish pathogen *Edwardsiella tarda* AHL production using marine bacterium *Tenacibaculum* sp. strain 20J cell extracts. *Diseases of Aquatic Organisms*, *108*(3), 217–225.

Röthig, T., Costa, R. M., Simona, F., Baumgarten, S., Torres, A. F., Radhakrishnan, A., Aranda, M., & Voolstra, C. R. (2016). Distinct bacterial communities associated with the coral model *Aiptasia* in aposymbiotic and symbiotic states with *Symbiodinium*. *Frontiers in Marine Science*, *3*, 234.

Rumpho, M. E., Dastoor, F. P., Manhart, J. R., & Lee, J. (2006). The Kleptoplast. *The Structure and Function of Plastids*, 451–473.

Shannon, C. E. (1948). A mathematical theory of communication. *The Bell System Technical Journal*, *27*(3), 379–423.

Sickinger, C., Brackwehr, S. M., Melo Clavijo, J., Gasperoni, G., Tierling, S., Preisfeld, A., & Christa, G. (2024). Microbiome origin and stress-related changes in bacterial abundance of the photosymbiotic sea slug *Berghia stephanieae* (Á. valdés, 2005). *Symbiosis*, 1–16.

Silveira, C. B., Cavalcanti, G. S., Walter, J. M., Silva-Lima, A. W., Dinsdale, E. A., Bourne, D. G., Thompson, C. C., & Thompson, F. L. (2017). Microbial processes driving coral reef organic carbon flow. *FEMS Microbiology Reviews*, *41*(4), 575–595.

Sunagawa, S., DeSantis, T. Z., Piceno, Y. M., Brodie, E. L., DeSalvo, M. K., Voolstra, C. R., Weil, E., Andersen, G. L., & Medina, M. (2009). Bacterial diversity and white plague disease-associated community changes in the caribbean coral *Montastraea faveolata*. *The ISME Journal*, *3*(5), 512–521.

Taylor, J. D., Cottingham, S. D., Billinge, J., & Cunliffe, M. (2014). Seasonal microbial community dynamics correlate with phytoplankton-derived polysaccharides in surface coastal waters. *The ISME Journal*, *8*(1), 245–248.

Trench, R., Boyle, J. E., & Smith, D. (1974). The association between chloroplasts of *Codium fragile* and the mollusc *Elysia viridis*-III. Movement of photosynthetically fixed 14C in tissues of intact living *E. viridis* and in *Tridachia crispata*. *Proceedings of the Royal Society of London. Series B. Biological Sciences*, *185*(1081), 453–464.

Turley, S., Dietschy, J., Arias, I., et al. (1988). The liver: Biology and pathobiology. *Arias, IM, Jakoby, WB, Popper, H., Schachter, D., Shafritz, DS, Eds*, 617–641.

Turnbaugh, P. J., Ley, R. E., Hamady, M., Fraser-Liggett, C. M., Knight, R., & Gordon, J. I. (2007). The human microbiome project. *Nature*, *449*(7164), 804–810.

Voolstra, C. R., & Ziegler, M. (2020). Adapting with microbial help: Microbiome flexibility facilitates rapid responses to environmental change. *BioEssays*, *42*(7), 2000004.

Weisburg, W. G., Barns, S. M., Pelletier, D. A., & Lane, D. J. (1991). 16S ribosomal DNA amplification for phylogenetic study. *Journal of Bacteriology*, *173*(2), 697–703.

Wickham, H. (2016). *ggplot2: Elegant Graphics for Data Analysis*. Springer-Verlag New York.

Wickham, H., Averick, M., Bryan, J., Chang, W., McGowan, L. D., François, R., Grolemund, G., Hayes, A., Henry, L., Hester, J., Kuhn, M., Pedersen, T. L., Miller, E., Bache, S. M., Müller, K., Ooms, J., Robinson, D., Seidel, D. P., Spinu, V., … Yutani, H. (2019). Welcome to the tidyverse. *Journal of Open Source Software*, *4*(43), 1686.

Wickham, H., Hester, J., Chang, W., & Bryan, J. (2022). *devtools: Tools to Make Developing R Packages Easier* [R package version 2.4.5].

Chapter 5

Microbiome Origin and Stress-Related Changes in Bacterial Abundance of the Photosymbiotic Sea Slug *Berghia stephanieae* (Á. Valdés, 2005)

Corinna Sickinger[1], Sofie Marie Brackwehr[2], Jenny Melo Clavijo[1], Gilles Gasparoni[3], Sascha Tierling[3], Angelika Preisfeld[1] and Gregor Christa[1]

[1]*Institute for Zoology and Didactics of Biology, University of Wuppertal, Wuppertal, Germany*
[2]*Food Chemistry, University of Wuppertal, Wuppertal, Germany*
[3]*Department of Genetics, Saarland University, Saarbrücken, Germany*

Published: 14 June 2024, *Symbiosis* 93, 177–192 (2024)
https://doi.org/10.1007/s13199-024-00995-3

5.1 Abstract

The precise mechanisms that allow animals and phototrophic organisms to form a stable photosymbiotic relationship are still unknown. While previous studies focused on genomic adaptations of the animal host, more recent research looked into the role of bacteria in photosymbiosis. Here, we analyzed the core microbiome of the sea slug *Berghia stephanieae* and its food source *Exaiptasia diaphana* to understand if the microbiome and the linked bacterial metabolic pathways differ between unstable and stable photosymbiosis. This sea slug feeds solely on the model cnidarian *E. diaphana* and steals their photobionts which the slug can only maintain for a week. We additionally examined the influence of light and starvation stress on the slug's bacterial composition, which are common experimental set-ups to elucidate the photosymbiotic relationship in the slugs. Our results show that the core microbiome of *B. stephanieae* and *E. diaphana* differed significantly suggesting that the slug's microbiome is not obtained from its food source or the water column and indicates a vertical transmission. Further, differences in metabolic pathways imply that the microbiome of *B. stephanieae* does not support a stable photosymbiosis due to an insufficient nitrogen cycle on part of the photobiont. Starving the slugs induced a shift towards an increased abundance of potential pathogens and led to a downregulation in the sulphur cycle. Yet, starvation in darkness resulted in the depletion

of most bacteria and induced a metabolic switch toward bacterial nitrogen fixation. This emphasizes that different holobiont members contribute to essential nutrient cycles, and it is important to look beyond the photobiont to understand the sea slug holobiont.

Keywords *Exaiptasia diaphana* · Nudibranchia · Photosymbiosis · Core microbiome · Starvation · Light stress

5.2 Introduction

Photosymbiosis is a symbiotic relationship between a heterotrophic and a phototrophic organism (Cowen, 1988). While this symbiosis is best known for corals that harbour Symbiodiniaceae Fensome, Taylor, Norris, Sarjeant, Wharton & Williams, 1993 (Muscatine & Porter, 1977) photosymbiosis is quite prevalent among metazoans (Melo Clavijo et al., 2018). Porifera, for instance, can establish symbiotic relationships with photoautotrophic cyanobacteria, chlorophyte algae, or Symbiodiniaceae (Diaz et al., 2007; Hill et al., 2011; Reisser, 1984). Tropical colonial ascidians establish photosymbiosis with cyanobacteria of the genus *Prochloron* (Hirose, 2015) or *Synechocystis trididemni* (Hirose et al., 2009) and even several molluscs, including bivalves and heterobranch sea slugs, are photosymbiotic. While bivalves are in symbiosis with Symbiodiniaceae, in Heterobranchia Burmeister, 1837 two types of photosymbiosis can be distinguished. Sacoglossa Bergh, 1867 can incorporate photosynthetically active chloroplasts in their cytosol from their food algae (Händeler et al., 2009; Rauch et al., 2018), a phenomenon known as functional kleptoplasty (Händeler et al., 2009). Among Nudibranchia Cuvier, 1817 members of the suborder Cladobranchia are known to incorporate symbionts of the family Symbiodiniaceae. These slugs must acquire new symbionts (photobionts) in each generation by feeding on photosymbiotic cnidarians and, in a special case, by filtering water (Burghardt & Wägele, 2014). The photobionts are then incorporated into epithelial cells of the digestive gland system and remain photosynthetic (Burghardt, Stemmer, & Wägele, 2008; Burghardt et al., 2005; Rola et al., 2022).

Photosymbiosis is considered to be highly advantageous for the animal host. Yet, aside from corals, the photobionts' contribution to the hosts' physiology is poorly understood. Previous studies used starvation experiments under photosynthetic and non-photosynthetic conditions to investigate the stability and benefits of the photosymbiosis between Heterobranchia sea slugs and their photobionts (Kempf, 1991; Melo Clavijo et al., 2018; Monteiro et al., 2019; Silva et al., 2021; Teugels et al., 2008). When starved in the light, the slugs lost weight less rapidly compared to those starved in the dark (Hawes & Cobb, 1980; Hinde & Smith, 1975; Hinde & Smith, 1972). This indicates a beneficial effect of light on the slugs probably due to the nutritional support by the photobionts. Further, degraded cells of Symbiodiniaceae in the feces of starving photosymbiotic sea slug species, suggest that slugs can also obtain nutrients by digesting the algae (Kempf, 1984). Aside from starvation, light stress is also often used that leads to the photodynamic production of reactive oxygen species (ROS) by the photobiont, causing additional stress for the host (Halliwell & Gutteridge, 1985). This formation of ROS has also been observed for Symbiodiniaceae which have been kept in the dark (Tolleter et al., 2013). Melo Clavijo et al. (2022) showed that starvation stress before feeding enhances ROS quenching in the sea slug *Berghia stephanieae*, notably inducing glutathione peroxidase (Melo Clavijo et al., 2022). These studies, however, neglect that the slugs not only harbour

algal symbionts but also host a variety of bacteria phyla. Consequently, light and starvation stress may also affect these symbiotic bacteria, which could have consequences for the entire holobiont. Such a holobiont is a biological system composed of a eukaryotic host organism and cohabiting species from different phyla that perform diverse metabolic, immune, and environmental adaptation-related tasks (Baedke et al., 2020; Bordenstein & Theis, 2008). For example, the composition of the hosts' symbiotic bacteria is important for the host and the photobiont, leading towards an increased photochemical performance if certain bacteria are present (Matthews et al., 2023). Hence, it is crucial to identify all organisms involved in this system to better understand the physiology of the holobiont and its photosymbiosis.

The concept of holobiont has already been implemented in coral research, but it's only been in the past ten years that the microbiome's importance for corals has become apparent(Hernandez-Agreda et al., 2017; A. R. Mohamed et al., 2023; K. B. Ritchie, 2011; Rosenberg et al., 2007). The bacterial communities appear to be highly dynamic and seem to contribute significantly to photosymbiosis, providing the host with carbon, nitrogen, and sulphur (Meunier et al., 2021; K. B. Ritchie, 2011; Rohwer et al., 2002; Röthig et al., 2016; Voolstra & Ziegler, 2020). Despite the importance of the microbiome for the coral holobiont and its photosymbiosis, only a few studies investigated the bacterial communities of other photosymbiotic animals (Britstein et al., 2020; Luter et al., 2020; Mahadevan & Middlebrooks, 2020; Ng et al., 2022; Posadas et al., 2022; Prazeres et al., 2017; Röthig et al., 2021).

Sea slugs and their symbiotic bacteria received increased attention in past years due to antitumor and antibiotic potential of specific heterobranch-associated bacteria (Abdelrahman et al., 2021; Böhringer et al., 2017; Džunková et al., 2023; Elfeky et al., 2023; Gerwick & Fenner, 2013; Kristiana et al., 2019). The detection of typical bacterial fatty acids, as well as ultrastructural analyses, revealed a high abundance of bacteria, especially in the notum, indicating the involvement of bacteria in nutrition and defence against predators (Doepke et al., 2012; Leal et al., 2012; Martinez-Pita et al., 2005; Zhukova & Eliseikina, 2012). Heterobranchs probably obtain some of their symbiotic bacteria horizontally from their food source (Davis et al., 2013; Mahadevan & Middlebrooks, 2020; Schuett & Doepke, 2013), yet, the diversity of symbiotic bacteria, as well as their contribution to the slug holobiont and photosymbiosis, are still not well understood.

Here, we used *Berghia stephanieae* (Á. Valdés, 2005) to shed light on the origin, abundance, and impact of stressors on the microbiome of photosymbiotic cladobranchs. *B. stephanieae* feeds exclusively on the sea anemone *Exaiptasia diaphana* (Rapp, 1892), and incorporates the photobionts of its food source into cells of its digestive gland system where they remain active for up to a week before being digested or excreted (Rola et al., 2022). Both species are well-studied model organisms in the realm of mollusc-dinoflagellate ecology (Monteiro et al., 2019; Rola et al., 2022; Silva et al., 2023; Weis et al., 2008). *E. diaphana* has already been studied intensively regarding its microbiome. Various studies showed strong overlaps in the bacterial phyla and core microbiome (the microbial taxa shared by two or more samples from the same host or environment) of different clonal lines of *E. diaphana*. These results favoured a horizontally obtained microbiome in the anemones (Hartman et al., 2020; Herrera Sarrias et al., 2017; Maire et al., 2021). Contrarily, Curtis et al. (2023) could not replicate these findings and were unable to identify a shared core microbiome for different clonal lines of *E. diaphana* kept under identical rearing conditions. Hence, the microbiome in the anemones seems to be genetically shaped (vertical transmission) (E. Curtis et al., 2023). Furthermore, aposymbiotic and symbiotic *E. diaphana*

show different bacterial microbiomes and core microbiomes, which seem to significantly impact the cnidarian holobiont and indicates a horizontal microbiome acquisition. These ramifications support the hypothesis that the entire holobiont adapts to the symbiotic state and that the microbiome likely plays a significant part in photosymbiosis (E. Curtis et al., 2023; Röthig et al., 2016; Xiang et al., 2022).

In our present study, we investigated the bacterial community of the sea slug *Berghia stephanieae* (Á. Valdés, 2005) and its food source *Exaiptasia diaphana* (Rapp, 1829) as well as the aquarium water to determine the origin of the slug's microbiome, hypothesizing that the slug's bacterial composition may originate from its food source, similar to its photobiont. Concurrently, we explored how starvation-induced stress, combined with different light conditions (regular, high, and darkness), may impact the microbiome over a week-long period. By analyzing bacterial abundance and metabolic pathways, we aim to understand the impact of applied light and starvation stress on symbiotic bacteria in *B. stephanieae* and their association with the photobiont. While previous studies have examined photosymbiosis under stress, none have delved into the symbiotic bacteria possibly shaping the photosymbiosis. We anticipate stress to influence bacterial composition and pathways, potentially leading to a reduction in bacterial abundance during starvation and a shift in composition under light stress. This investigation sheds light on the intricate interplay between the slug and its symbiotic bacteria within the context of photosymbiosis.

5.3 Methods

Exaiptasia diaphana culture

Several specimens of *E. diaphana* were purchased from a local provider (Seepferdchen24 Meeresaquaristik GmbH, Germany) in January 2022 and maintained in a 55 L tank (60 cm x 30 cm x 30 cm) filled with circulating artificial seawater (ASW) (AB Reef Salt, Aqua Medic, Germany) at a light intensity of 30 µmol photons m^{-2} s^{-1} (Daylight Sunrise 520, Sera), on a 12h light/ 12h dark cycle. The salinity was kept at 33 Practical Salinity Unit (PSU), the temperature at 21 °C, and two BactoBalls (Fauna Marin GmbH, Germany) were added and replaced every two weeks. Further, *Artemia nauplii* were cultivated using the Artemio® Set (JBL, Germany) and 16 g of Ready-to-use Artemia (brine shrimp) mixture (JBL, Germany). Anemones were fed with freshly hatched *Artemia nauplii* two times per week.

Berghia stephanieae culture

Six breeding pairs of *B. stephanieae* were purchased from a local provider (Seepferdchen24 Meeresaquaristik GmbH, Germany) in February 2019. Each pair was kept in a 75 mm diameter plastic container with a lid (FAUST, Germany) in 35 ml ASW at 21°C, a light intensity of 30 µmol photons m^{-2} s^{-1} (Daylight Sunrise 520, Sera), and a day/night cycle of 12 h / 12 h. Water was changed three times per week, using freshly prepared ASW with a salinity of 33 PSU, a pH of 8.0, and a temperature of 21 °C. Slugs were fed with small *E. diaphana* anemones (7 mm foot and 4 mm oral disk or 4 mm foot and 3 mm oral disk) three times per week. Once the breeding pairs spawned, the egg masses were collected and placed individually in 55 mm diameter plastic containers with lids (FAUST, Germany) in 20 ml ASW and maintained as stated above. The larvae were observed and fed with tentacles of *E. diaphana* three

times a week immediately after hatching. When the juvenile stage was reached, the slugs were fed with small anemones three times a week.

Sampling and sample processing

Twenty adult cladobranchs were randomly selected from the culture and separated into four groups (n=5). Each group was placed in one 75 mm diameter container with 35 ml ASW, and water was changed three times a week. The first group was kept under standard husbandry conditions as described above (Fed; BS 1-5) and were sampled directly after feeding. The second group was starved under regular light conditions of 30 µmol photons m^{-2} s^{-1} (Starved L; BS 11-15). The third group was starved under high light with a light intensity of 90 µmol photons m^{-2} s^{-1} (Starved HL; BS 16-20), and the last group was starved under complete darkness (Starved D; BS 21-25). After a starvation period of seven days, all slugs were snap-frozen at -80 °C until further preparation. Five whole *E. diaphana* specimens were sampled directly from the tank after feeding and snap-frozen at -80 °C until further preparation. Water samples (W1-W5) were sampled from the aquarium and directly processed.

Following the manufacturer's instructions, RNA from each sample was extracted using the TRItidy GTM (PanReac AppliChem, Spain) to get an understanding of the functional microbiome. RNA concentrations of samples were quantified on a QubitTM 4 Fluorometer (Invitrogen, USA). To generate a cDNA template, 50 ng of each RNA sample or 1 µL of aquarium water was used with the LunaScript® RT SuperMix Kit (NewEngland Biolabs, UK) following the manufacturer's instructions. For DNA sequencing, bacterial DNA was amplified by PCR using primers with Illumina adapters (underlined) targeting the V1–V2 regions of the 16S rRNA gene: V1V2forward (5'-TCTTTCCCTACACGACGCTCTTCCGATCT AGAGTTTGATCCT GGCTCAG-3'), V1V2rev (5'-GTGACTGGAGTTCAGACGTGTGCTCTTCCGATCT T GCTGCCTCCCGTAGGAGT-3') (Weisburg et al., 1991). Adapter PCR was performed in a total volume of 20 µL: 5 µL template cDNA, 10 µL DreamTaq Green PCR Master Mix (2X) (Thermo Fisher, USA), and 2 µL of 10 µM of each primer. Each sample was adjusted to 20 µL with distilled and sterilised water. The PCR amplification was performed with 30 cycles of denaturation at 94°C for 1 min, annealing at 54°C for 1 min, and extension at 72°C for 1 min. The initial denaturation and final elongation were 95°C for 15 min and 72°C for 10 min, respectively. The PCR product for each sample was cleaned with the Agencourt AMPure XP magnetic bead system (Beckman Coulter, USA). Subsequently, an indexing PCR was performed to add Illumina sequencing adapters containing TrueSeq indices. Index PCR was conducted in 20 µL volume using 5 µL of the previous purified adapter PCR product, 10 µL Q5® High-Fidelity 2X Master Mix (NewEngland Biolabs, UK), 1 µL of 10 µM of the respective forward and reverse index primer, and 3 µL distilled and autoclaved water. The PCR amplification was performed following the manufacturer's instructions. Indexed PCR products were cleaned using the Agencourt AMPure XP magnetic bead system. Final DNA concentrations of samples were quantified on a QubitTM 4 Fluorometer and samples were then pooled in equimolarly and sent to the University of Saarbrucken for sequencing on an Illumina MiSeq platform. Sequencing was conducted with a 2x250bp paired-end approach according to the manufacturer´s instructions aiming at 30,000 reads per sample.

Sequencing data workflow and diversity analyses

Raw, demultiplexed MiSeq reads were joined in QIIME2 v.2021.4 (Bolyen et al., 2019), and denoised using the DADA2 plugin (Callahan et al., 2016) with a maximum error rate of 2. Taxonomy was assigned in QIIME2 against a SILVA database (v132) (Bolyen et al., 2019) and amplicon sequence variants (ASVs) identified as eukaryotes, mitochondria, or chloroplasts were removed (Additional File 1; Table 1). Relative abundance of bacterial families, alpha and beta diversity calculations, as well as statistical analyses, were performed in QIIME2 v2023.9 (Bolyen et al., 2019) and R v4.0.3 (R Core Team, 2021) with differences considered significant at p <0.05. Shannon index (Shannon, 1948) was used to describe and compare alpha diversity across samples. Differences in Shannon diversity between samples were evaluated by one-way analysis of variance (ANOVA, Girden, 1992. Differences in beta diversity were analysed using Bray–Curtis dissimilarity matrices and tested via permutational multivariate analysis of variance (PERMANOVA, (M. J. Anderson, 2001). Principal Coordinate Analysis (PCoA) plot showing the variation in community composition among samples paired with the Shannon index was compiled in R v4.0.3 using the packages devtools (Wickham et al., 2022), ggplot2 (Wickham, 2016), tidyverse (Wickham et al., 2019) and qiime2R (Bisanz, 2018). Differences in pathway abundance between groups were evaluated by ANOVA or if data deviated from normality and/or homogeneity of variance by Kruskal-Wallis-Test (Kruskal & Wallis, 1952).

Core Microbiome

The core microbiome was analysed in QIIME2 v.2021.4. Using the command qiime feature-table core-features, a list of ASVs, present in at least 80% of the samples analysed, was created for each sample group. Venn diagrams and Pie charts were created in R v4.0.3 using the packages ggplot2 and RColorBrewer (Neuwirth, 2022). ASVs that were present less than 1% were clustered under "Others".

Pathway Abundance

ASV IDs were stripped and ASVs with the same taxonomic assignment were combined using the web server METAGENassist (Arndt et al., 2012). Further, unassigned and unmapped reads were excluded, and 7 taxa were filtered out based on interquartile range (IQR) (Hackstadt & Hess, 2009). The remaining 146 taxa were normalized across samples by sum and across taxa by Pareto scaling. Data were analysed by phenotype “metabolism” using the Spearman distance measure to cluster the most abundant metabolic processes. Differences in pathway abundance between the conditions were evaluated using METAGENassist by one-way analysis of variance (ANOVA) and Tukey HSD post hoc comparison of means. Statistical analyses were considered significant when p <0.05. A Heatmap displaying putative functional differences based on the bacterial community composition of each sample was created in METAGENasisst.

5.4 Results

DNA sequencing produced 646,391 reads across anemone samples (n = 5) and slug samples (n = 20). After merging, denoising, and chimera filtering, 372,783 reads remained. After removing contaminants, 346,225 ASVs were kept. Rarefaction curves

for bacterial sequences plateaued in all samples, suggesting sufficient sequencing depth to capture bacterial species diversity (Additional File 2: Figure 1).

B. stephanieae's distinct bacterial composition shifts during starvation

Sequence identification at the family level revealed noticeable differences between the most abundant bacterial communities associated with *E. diaphana* and *B. stephanieae* (Fig. 1; Additional file 1: Table 2). For instance, Endozoicomonadaceae, Clostridiaceae, Pleomorphomonadaceae, and Rhodocyclaceae, were the most common bacterial families in *E. diaphana*, accounting for more than 50% of all identified bacteria (Fig. 1). In the slugs, Mycoplasmataceae, Pseudoalteromonadaceae, and Rhodobacteraceae were the most dominant and accounted for more than 50% of all bacteria, irrespective of the experimental condition. Mycoplasmataceae were absent in anemones, but Comamonadaceae (clustering under others for *B. stephanieae* fed, Fig. 5.1), Flavobacteriaceae, Propionibacteriaceae, and Beijerinckiaceae (all clustering under others for *E. diaphana*, Fig. 5.1) were present in almost all anemones and slugs, albeit on a low abundance.

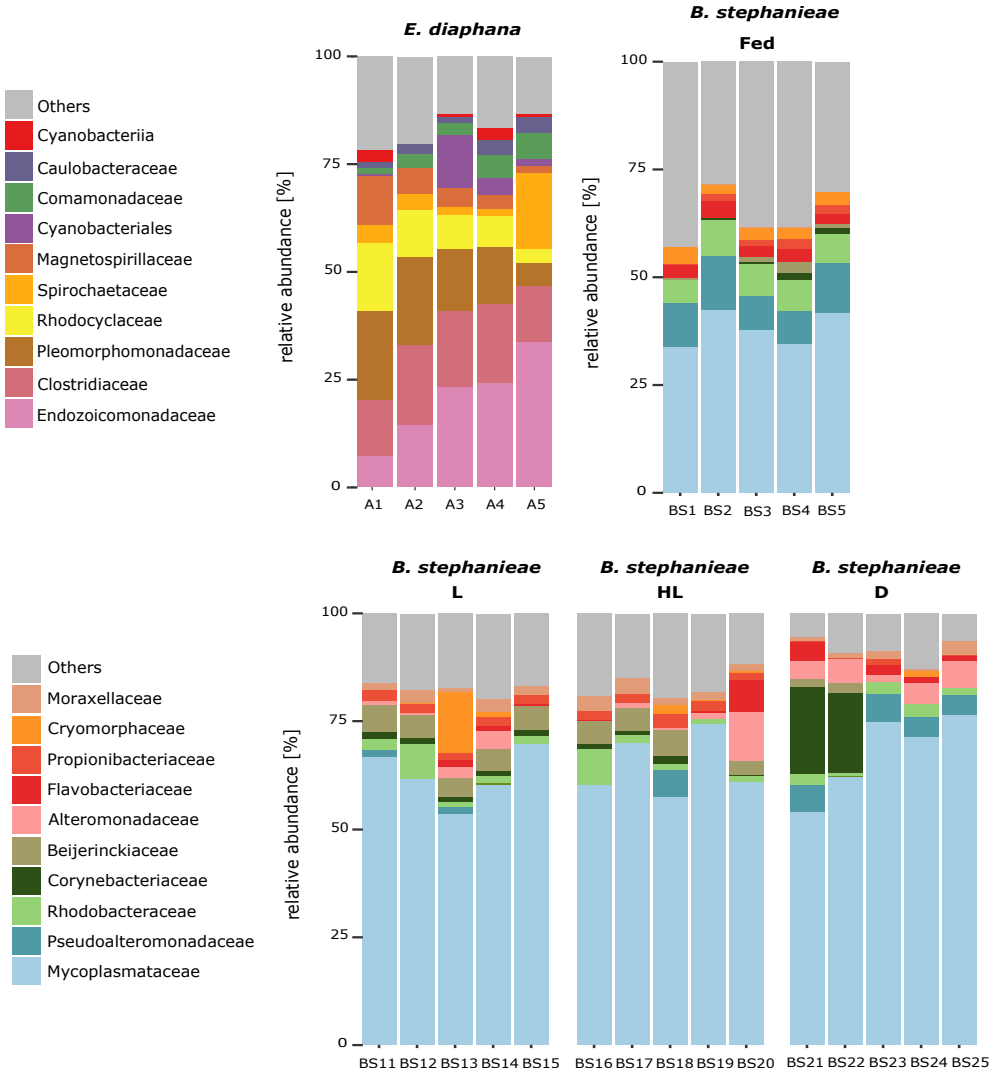

FIGURE 5.1: Relative frequency of the most abundant bacterial families. The ten most abundant bacterial families across all anemone and all slug samples are represented by a different colour. Less abundant families are grouped under "Others"

To further identify patterns of differential abundance of ASVs, we determined the core microbiome for each condition group (all ASVs present in at least 80% of all samples of the respective condition; Additional File 1: Table 3 and 4). The core microbiome of the anemones contained 41 ASVs, with 40 ASVs exclusive to the anemones (Fig. 3 and 4A). On the ASV level of the core microbiome, several bacteria were highly abundant in the anemones, including *Clostridium* sensu stricto 11 sp. 2 (25.51 %), *Rhizobiales* sp. (18.42 %), *Azirospira* sp. (11.11 %), and *Endozoicomonas* sp. (9.83 %) that in combination account for approximately 65 % of total reads of the anemones' core microbiome. The fed slugs' core microbiome contained 28 ASVs, with *Mycoplasma* sp. as the most abundant bacteria, accounting for 43.39 %. Besides *Mycoplasma* sp., an unclassified *Rhodobacteraceae* (7.36 %), *Cytophaga* sp. (6.98 %), and *Kordiimonas* sp. (5.9 %) dominated the core microbiome of fed slugs (Fig. 3). Only *Endozoicomonas* sp. was present in both the anemones' and the fed slugs' core microbiome (Fig. 3 and 4A).

From the 216 ASV detected in the water samples, 9 were shared with the slugs and 4 with the anemones. None of these ASV could be taxonomically assigned differently than "uncultured bacteria"(see Additional file 1: Table 5 and Additional File 2A).

In the slugs, starvation resulted in a microbiome composition shift, including an increase in Mycoplasmataceae. For example, in the fed sample BS2 (*B. stephanieae* fed), Mycoplasmataceae represented approximately 42% of the total, whereas in the dark-starved sample BS 25 (*B. stephanieae* starved in darkness), Mycoplasmataceae represented 76% of the total (Fig. 1). Starvation further induced the depletion of Pseudoalteromonadaceae and Cryomorphaceae in most samples and an increase in Moraxellaceae. Moreover, Alteromonadaceae were found only in starved slugs.

On the ASV level, starvation led to a depletion of 17 bacterial species identified in the core microbiome of fed slugs. Fed and starved slugs shared only two bacterial species, *Mycoplasma* sp. and *Cutibacterium* sp. in their core microbiome (Fig. 5.3B). In starved L slugs, *Mycoplasma* sp. accounted for 93.19 % of all 27 identified ASVs, *Cutibacterium* sp. for 2.59 %, and the remaining 25 ASVs accounted for 4.22% (Fig. 5.2). Only in starved L slugs, *Enhydrobacter* sp. (0.9 %, included in "Others") could be identified (Fig 4B). The core microbiome of starved HL slugs contained 43 ASVs, out of which 80.96 % of the reads were *Mycoplasma* sp., 3.49 % *Methylobacterium* sp., 2.58 % *Cutibacterium* sp., and the remaining ASVs with an abundance lower than 2 % (Fig. 5.2). Among the starved slugs, HL slugs showed the highest number of unique ASVs (17; Fig. 5.3B) and shared the most ASVs with a total of 15 bacterial phyla with slugs starved in regular light (L; Fig. 5.3B). *Lawsonella* sp. was only present in the core microbiome of starved L and HL slugs. In starved D slugs, the core microbiome contained 94.70 % *Mycoplasma* sp., 2.84 % *Alteromonas* sp., and 14 ASVs that accounted for 2.46 % in total (Fig. 5.2). *Paracoccus marinus*, *Coxiella* sp., and unclassified Terasakiellaceae were exclusive to the core microbiome of starved D slugs (Fig. 5.3B).

The diversity of the microbiome declines during starvation

Anemones showed the highest alpha-diversity metric (Shannon indices), while one starved L slug (BS14) showed the lowest Shannon indices. A one-way ANOVA revealed a statistically significant difference in Alpha-diversity metrics (Shannon index) between at least two groups $F_{(4,20)} = 20.93$, $p < 0.001$; Fig. 5.4). Subsequent Tukey's HSD Test for multiple comparisons indicated that the starved groups (L, HL, and D) did not differ significantly from each other (Additional File 1:Table 4). In

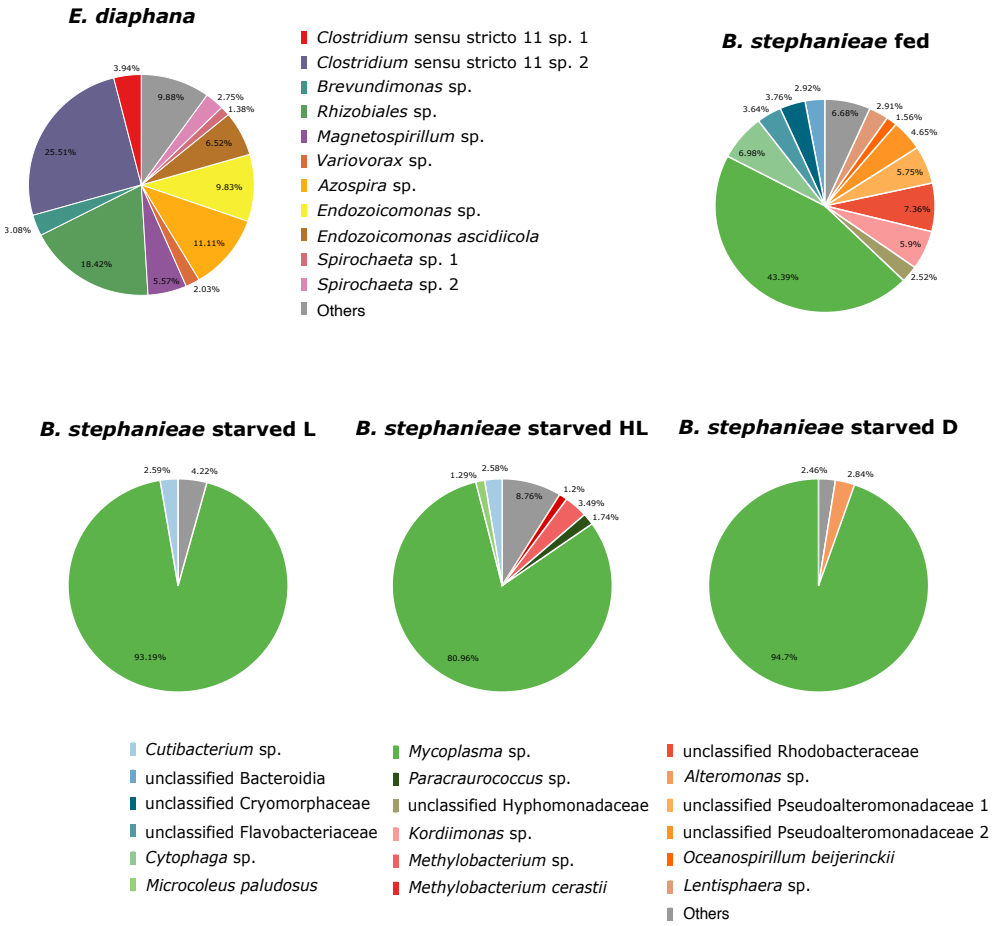

FIGURE 5.2: Core microbiome of anemone and slugs kept under different husbandry conditions. All ASVs found in at least 80% of all samples of the corresponding condition were classified as "*E. diaphana* core microbiome", "*B. stephanieae* fed core microbiome", "*B. stephanieae* starved L core microbiome", "*B. stephanieae* starved HL core microbiome", and "*B. stephanieae* starved D core microbiome". Each colour denotes a unique ASV represented by more than 1%; rare ASVs have been condensed in the group "Others" and are shown in grey.

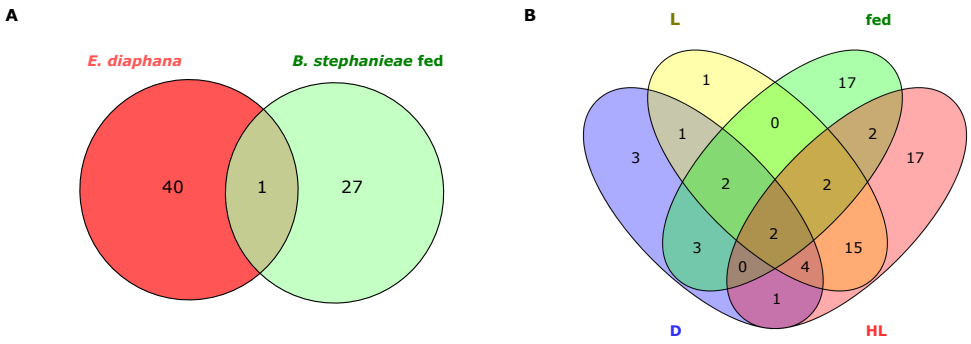

FIGURE 5.3: Venn diagrams comparing core microbiome composition of anemone and slug. Shared ASVs of the core microbiome of *E. diaphana* and fed *B. stephanieae* (A) and all *B. stephanieae* samples (fed, starved in light (L), high light (HL) and darkness (D)) (B). Numbers indicate total abundance of either unique or shared ASVs.

contrast, fed slugs and the anemones differed significantly compared to all starved groups but not to each other (Additional File 1: Table 6). PCoA visualization of beta-diversity using the Bray–Curtis dissimilarity index revealed a coherent grouping of anemones, fed slugs, and starved slugs, respectively (Fig. 5.4; Additional File 1: Table 7). PERMANOVA testing (999 permutations) indicated that bacterial community structure varied significantly depending on the husbandry condition (pseudo-F_4 = 24.01,p = 0.001). Pairwise comparisons between all conditions did yield significant differences between all groups except between Starved L and HL (Additional File 1: Table 8). Analysis of the water samples revealed significant differences in alpha and beta diversity between water samples and fed slugs (statistical results and see Additional Material File 1: Table 9).

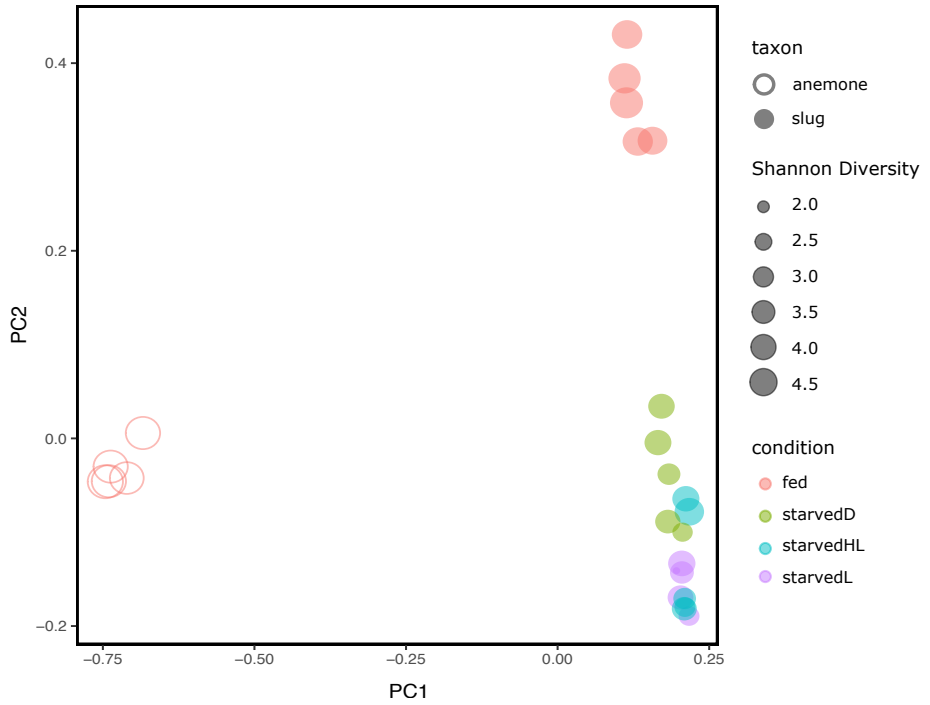

FIGURE 5.4: Principal Coordinate Analysis (PCoA) plot of alpha- and beta-diversity. PCoA plot based on Bray-Curtis dissimilarity. Shape of circle represents taxon (anemone or slug), size of circle indicates Shannon diversity index, colour of circle represents husbandry condition (fed, starved in darkness (starvedD), high light (starvedHL), or regular light(starvedL)

The change in bacterial communities causes significant differences in the regulation of metabolic pathways

The observed differences in the relative abundance of bacterial taxa in *E. diaphana* and *B. stephanieae* could indicate a functional change in the bacterial composition. Therefore, we determined the metabolic pathway abundances of each sample and compared them regarding the condition (Additional File 1: Table 10). Anemones and fed *B. stephanieae* clustered together, indicating homogeneity in the enrichment and depletion of metabolic pathways. However, starved L, HL, and D slugs did not cluster and differed in the enrichment and depletion of metabolic pathways (Fig. 5.5).

Regarding the regulation of metabolic pathways, “Dehalogenation” and “Ammonia oxidizer” were enriched for all anemones and *B. stephanieae* fed samples, while “Nitrogen fixation” was upregulated only in starved *B. stephanieae* samples. “Chitin degradation”, “Sulfur metabolizing” and “Xylan degrader” were only enriched in anemone samples (Fig. 5.5). Testing for differences (ANOVA or Kruskal-Wallis Test; see Additional File 1: Table 11 for further information) revealed a statistically significant difference in the regulation of the metabolic pathways between at least two groups for all pathways except "Sulfate reducer" (p <0.05). Post hoc testing was conducted using either Tukey’s HSD or Dunn’s test with Bonferroni correction (Additional File 1: Table 11 and Additional File 4: Figure 1). These revealed significant differences in the regulation of 4 metabolic pathways between *E. diaphana* and *B. stephanieae* fed “Chitin degradation”, “Xylan degradation”, “Sulfur metabolizing”, and “Nitrite reducer”) with the first 3 being depleted in the slug and the last one in the anemone. Between fed slugs and all starved slugs, significant differences in the regulation of 1 metabolic pathway was detected (“Nitrogen fixation”) being the only pathway significantly enriched in starved slugs. Compared to fed slugs, in HL starved slugs, an additional 5 bacterial metabolic pathways were enriched (“Xylan degrader”, “Degrades aromatic hydrocarbon”, “Atrazine metabolism”, “Sulfur oxidizer”, and “Carbon fixation”), and in LL starved slugs 4 ("Ammonia oxidizer", Dehalogenation", "Sulfide oxidizer" and "Atrazine metabolism"). Furthermore, in HL slugs, the pathway "Chlorophenol degrading" was significantly enriched compared to dark-starved slugs. LL starved slugs showed no significant changes in metabolic pathways compared to the other starved slugs.

5.5 Discussion

The slug microbiome differs from the anemone

The horizontal acquisition of the microbiome is usual for marine organisms, and we anticipated that the slugs obtain at least part of their bacteria simultaneously with their photobionts from the anemones. The slugs are maintained in plastic containers devoid of any substrates (i.e. stones) capable of transmitting microbes through physical contact, thereby minimizing potential microbial transmission. The anemones provided for the slugs’ feeding represent the sole organisms introduced to the container harbouring potential symbiotic microbes. Moreover, the slugs not only consume these anemones but also manoeuvre in their proximity, facilitating physical contact and, consequently, exposure to the microbes inhabiting the anemone’s surface. Thus, alongside the bacteria hypothesized to inhabit the slug’s gut owing to dietary intake, an anticipated microbial overlap between the anemones and the slugs due to physical interaction was expected. Nonetheless, such overlap was not evident in our investigation. Additionally, we analysed the bacterial composition of the water housing both the slugs and the anemones to ascertain whether the slugs acquire symbiotic bacteria from this source. Our slugs exhibited an overlap of 9 out of 28 bacteria species in their core microbiome with the water. Nevertheless, all corresponding bacteria elude species-level identification and are classified as uncultured. Analysis of alpha and beta diversity further unveiled significant disparities between the water and slug samples. According to our data, *B. stephanieae* receives the majority of its microbiome vertically, not by feeding on its food anemone *E. diaphana* or the water column. Vertical transmission from parent to offspring is essential in ensuring the accuracy of the microbiome for the next generation (Rosenberg & Zilber-Rosenberg, 2021). For instance, Porifera are known for their “sponge-specific”

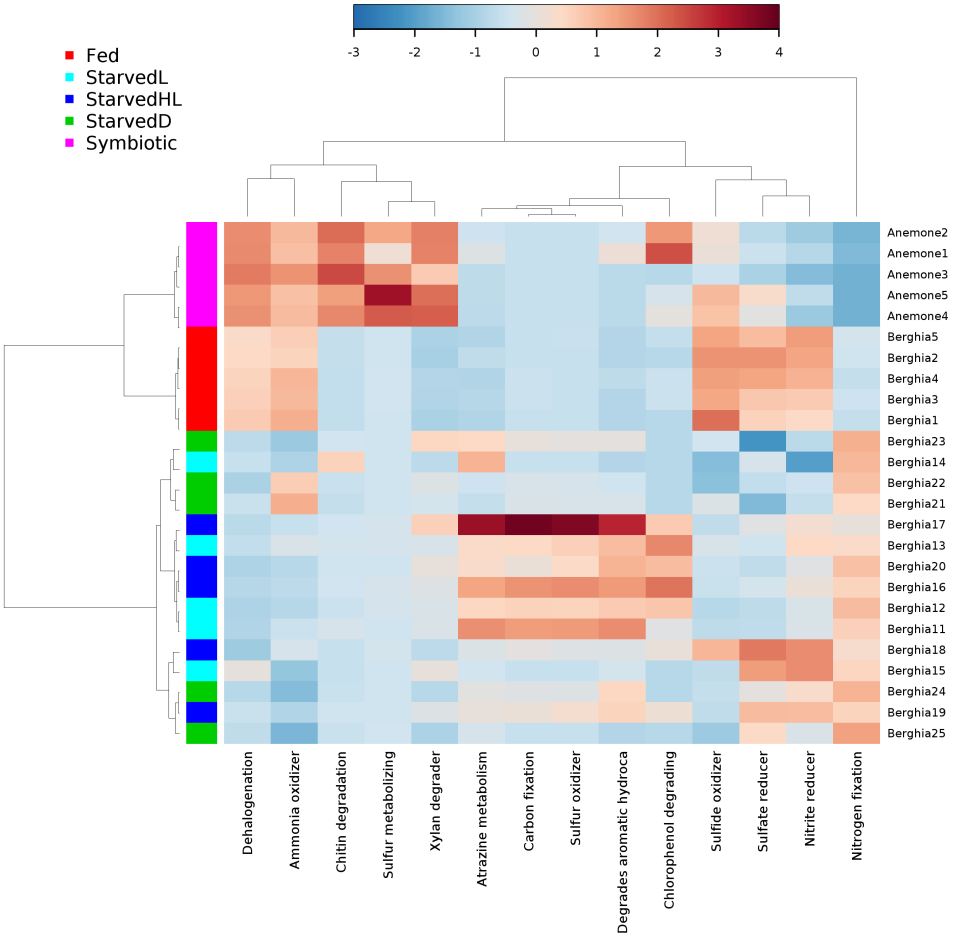

FIGURE 5.5: Taxonomy-based functional profiling of bacterial communities. Heatmap displaying changes in putative functional differences between the five groups (*E. diaphana*(anemone), *B. stephanieae* fed and starved in light (StarvedL), high light (StarvedHL), and darkness (StarvedD) on a relative scale, with enrichment indicated in red and depletion in blue.

microbiome, inherited from the parental lineage (de Oliveira et al., 2020; Funkhouser & Bordenstein, 2013). In sea slugs, little is known about the microbiome and its origin. While the microbiome has been studied in a handful of different sea slugs, its origin has not been explored (Abdelrahman et al., 2021; Davis et al., 2013; Mahadevan & Middlebrooks, 2020; Ng et al., 2022). Further microbiome studies in sea slugs will enhance our understanding of their biology and also will shed light on their adaptations to changing environments and their potential roles in marine ecosystem health and resilience.

The use of RNA and subsequently cDNA for microbiome analyses comes with a few biases as well as challenges related to transcript abundance leading to an overrepresentation of certain taxa compared to others, differential expression, and temporal dynamics. However, we have decided to use RNA for our analysis because we prioritize gaining functional insights into microbial communities, understanding metabolic activities, and tracking responses to environmental stimuli. Despite potential issues such as temporal bias and RNA stability concerns, RNA sequencing allows us to identify active microbial taxa and differentiate functionally redundant species. Thus, we can delve deeper into microbial community dynamics and

uncover their functional roles, ultimately enhancing our understanding of complex ecosystems (A. L. Brown et al., 2022; Giroux et al., 2022; Laroche et al., 2017; Stewart, 2013).

In *E. diaphana*, *Clostridium* sensu stricto 11 sp. 2 and *Rhizobiales* sp. were the most abundant bacteria of the core microbiome. *Clostridium* are ambient pathogens, especially in soils and as normal flora in the intestines of higher organisms (Wiegel et al., 2006). *Rhizobiales* are diazotrophs belonging to the Alphaproteobacteria and reside in the tissue, skeleton, and mucus of several coral species (Herrera Sarrias et al., 2017; Lesser et al., 2007; Rohwer et al., 2002; Shashar et al., 1994). In addition to the photobiont, they are known to be involved in the production of bacterial dimethylsulfopropionate (DMSP) (Curson et al., 2017; Kuek et al., 2022). DMSP is a stable and soluble sulfate source and an important molecule in the marine sulfur cycle involved in several cellular processes, such as antioxidant, osmolytic functions, or cryptoprotection (Kiene et al., 2000). In our *E. diaphana*, the microbiome was up-regulated in "Sulfur metabolizing" by bacteria metabolizing sulfur to DMSP, while "Sulfate reducer" was mostly down-regulated. One possibility might be that the absorbed sulfate gets transformed into DMSP by *Rhizobiales* in the anemones providing excessive sulfate to other bacterial groups as substrate. Further, we identified two species of *Endozoicomonas*, a genus that is generally the highest abundant bacterial group in the coral microbiome (Bayer et al., 2013; Hernandez-Agreda et al., 2017; J. L. Meyer et al., 2014). According to Neave et al. (2016), the main functions of *Endozoicomonas* for the coral holobiont are nutrient metabolism, microbiome structuring, and antimicrobial activity (Neave et al., 2016).

In the slugs, *Mycoplasma* sp. is the most abundant bacterial genus, followed by *Methylobacterium cerastii* and *Cytophaga* sp.. Mycoplasmas are obligate parasitic, intracellular, and extracellular bacteria that can be the cause of numerous diseases in humans and vertebrates. They live on and in epithelial cells from which they obtain essential growth factors such as cholesterol, nucleotides, amino acids, and fatty acids (Johansson & Pettersson, 2002; Razin et al., 1998). Still, they seem to be a key phylum of the microbiome of many marine animals such as fish but also sea slugs (Abdelrahman et al., 2021; Davis et al., 2013; Mahadevan & Middlebrooks, 2020; Ng et al., 2022; Rasmussen et al., 2021, 2023). Moreover, in *B. stephanieae* "Sulfate metabolizing" is down-regulated, while "Sulfate reducer" is up-regulated, the opposite to its food anemone.

Nitrogen fixation, meaning the conversion of elemental dinitrogen into ammonia, is a fundamental process for corals to increase the input of fixed nitrogen into the reef ecosystem (Rädecker et al., 2015). Here, the pathway "Nitrogen fixation" is down-regulated in both *E. diaphana* and *B. stephanieae* and thus not performed by specific bacteria. Nitrogen is a limiting nutrient in the coral holobiont, and the density of algal symbionts is controlled by nitrogen availability (Falkowski et al., 1993). Thus, in anemones, the photobiont is the primary nitrogen metaboliser, and the abundance of nitrogen-cycling bacteria in corals may be dependent on the presence of a photobiont (Röthig et al., 2016). The first essential step of nitrification is ammonia oxidation, the conversion of ammonia to nitrite and further to nitrate (Lehtovirta-Morley, 2018). Although nitrification ("Ammonia oxidizer") is up-regulated in *E. diaphana*, resulting in nitrite, denitrifying pathways are down-regulated or not present. The photobiont prefers dissolved inorganic nitrogen in the form of ammonium (D'elia et al., 1983; Taguchi & Kinzie Iii, 2001). Nitrification may eventually limit the amount of nitrogen available for the photobiont's growth (Rädecker et al., 2015). Further, denitrification is an energy-consuming process. Xiang et al. (2022) proposed that denitrifying bacteria may be regulated by the holobiont's nutritional status and thus

contribute to the maintenance of a nitrogen-limited state (Xiang et al., 2022). In *B. stephanieae* “Nitrogen fixation” is down-regulated, while “Ammonia oxidizer”, as well as “Nitrite reducer”, are up-regulated. This suggests that the photobiont is still the primary nitrogen fixator, with bacteria converting the resulting ammonia to nitrite. In contrast to *E. diaphana*, the formed nitrite is then probably further reduced by bacteria (Additional File 5: Figure 2 A and B).

Thus, there are distinct differences between the anemone and the slug regarding their roles as holobionts in nitrogen cycling. In *E. diaphana*, the photobiont is the primary nitrogen fixator, and its growth is regulated through controlled nitrogen limitation. In *B. stephanieae*, the photobiont seems to be involved in nitrogen fixation but does not contribute to the nitrogen cycle any further and is not controlled by nitrification and/or denitrification regulation.

The bacterial metabolic pathway abundance of *B. stephanieae* is similar in function to aposymbiotic *E. diaphana*. Aposymbiotic *E. diaphana* show downregulation in "Sulfur metabolizing" and "Sulfur oxidizer", whereas "Sulfide oxidizer", "Sulfate reducer" and "Nitrite reducer" are upregulated (Röthig et al., 2016). Unlike symbiotic *E. diaphana*, aposymbiotic anemones are unable to produce DMSP (Van Alstyne et al., 2009) and are restricted in their sulfur cycling. Further, aposymbiotic *E. diaphana* show an increased abundance in denitrifying bacteria as more nitrogen is available due to the missing photobiont. We observed a similar pathway abundance pattern for *B. stephanieae* in the presence of its photobiont *Breviolum*. This indicates that the core microbiome of this sea slug is not adapted for a photobiont and could help to explain why *B. stephanieae* is not suited for stable photosymbiosis and lacks core molecular adaptations (Melo Clavijo et al., 2018). Microbiome analyses of Cladobranchia with a stable photosymbiosis like *Phyllodesmium briareum* would give valuable insights into the relevance and interplay of bacteria with the photobionts and animal host.

Furthermore, we see differences in the metabolic pathways "Chitin degradation" and "Xylan degrader", which can be explained because *E. diaphana* has a different mode of life than *B. stephanieae*. Both pathways are up-regulated in the anemones, which is consistent with the results of other studies (Herrera Sarrias et al., 2017; Röthig et al., 2016). The anemones in our study were fed with *Artemia nauplii* which contain chitin, thus, it is plausible that bacteria that utilize chitin are also more abundant in anemones than in slugs. Xylan is a common carbohydrate component of plant cell walls that is required for vascular tissue development and appropriate cell wall construction (Curry et al., 2023)."Xylan degrader" is up-regulated in the anemones indicating an involvement of xylan-degrading bacteria, such as *Clostridium* in the carbon cycling related functions (Zverlov et al., 2005).

Influence of starvation

Starvation is a great stressor for an organism triggering a cascade of reactions and greatly impacting the microbiome in the slugs. Particularly, there was a strong decline in the diversity and abundance of bacterial groups. However, the most striking was the increase in *Mycoplasma* sp., which accounts for over 80% of the total core microbiome of starved slugs. Because Mycoplasmatales were also found in high abundance in other sea slugs like *Chormodoris quadricolor*, *Pteraeolidia semperi*, *Elysia rufescens*, and *Elysia crispata*, *Mycoplasma* sp. seems to be a significant part of the core microbiome of *B. stephanieae* (Abdelrahman et al., 2021; Davis et al., 2013; Mahadevan & Middlebrooks, 2020; Ng et al., 2022) but could nevertheless increase the

stress of the host during starvation. The exact role of these bacteria in the heterobranch holobiont is not yet clarified. Here, reducing the microbiome composition due to starvation seems to give the *Mycoplasma* enough space to spread and possibly become pathological, reducing the slug's fitness.

Starvation caused a decrease in the diversity and abundance of bacterial phyla, which was followed by severe changes in the slug's metabolic pathways. Thus, the pathways "Dehalogenation", "Sulphide oxidizer", and Ammonia oxidizer" showed significant differences between fed slugs and slugs starved in light. Whereas the pathways "Xylan degrader", "Degrades aromatic hydrocarbonates", "Sulfur oxidizer" and "Carbon fixation" were significantly different between fed and starved in high light slugs. Worthy to note is that out of the analysed pathways, "Nitrogen fixation" was the only pathway that was significantly up-regulated in all starved slugs regardless of the light condition. *B. stephanieae* has an unstable symbiosis with its photobiont, which means that, unlike other Cladobranchia, the slug cannot rely solely on its photobiont for nutrition. Further, the symbionts remain photosynthetically active for up to five days before they get digested or expelled (Melo Clavijo et al., 2022; Monteiro et al., 2019). If the slug is not provided with any prey containing Symbiodiniaceae, the slug loses its photobiont turning into an aposymbiotic state. Here, we starved *B. stephanieae* for one week, meaning that after this week, the slug lost almost all its photobionts that provide a range of functions, including nitrogen fixation, as shown in this study. Nitrogen is considered to be the limiting factor for the photobiont. As a result, excessive available nitrogen caused by the loss of the photobiont may encourage the growth of diazotrophic bacteria, which then take over nitrogen fixation in the slug. Further, nitrifying as well as denitrifying pathways are down-regulated, indicating an insufficient nitrogen cycle in starved slugs (Additional File 5: Figure 2C).

Light and darkness

Slugs starved in high light showed the highest number of total and unique bacterial phyla compared to the other starved groups and showed the most significant differences in metabolic pathways compared to fed slugs. Additionally, *B. stephanieae* starved L and HL shared the most common bacterial phyla such as the cyanobacteria *Microcoleus* sp., *Nostoc* sp., and *Arthrospira* sp.. This is contrary to slugs starved in darkness which showed the lowest number of total bacterial phyla and a significant difference in beta-diversity to L and HL slugs. Studies that looked at the influence of light on the microbiome of photosymbiotic sponges observed similar results. The heterotrophic species *Stylissa flabelliformis* and *Ianthella basta* remained unaffected by light stress, while the phototrophic species *Cliona orientalis* and *Carteriospongia foliascens* underwent a significant change in microbiome composition and discoloured after a few days in the darkness caused by loss of Cyanobacteria (Curdt et al., 2022; Pineda et al., 2016). This alteration in the microbiome could imply an attempt at symbiont shuffling to a community that can operate better under low light conditions which has been observed for *Rhopaloeides odorabile* (Webster et al., 2011). However, we assume that the shift in the microbiome of slugs starved in darkness can be attributed to the lack of light. Due to the deprivation of light, the slug loses its symbiont *Breviolum* and phototrophic bacteria such as cyanobacteria, which gives more space to non-light-dependent bacteria such as Mycoplasmatales. Further, "Chlorophenol degrading" was the only pathway that differed significantly between HL and D and was upregulated in HL slugs. Chlorophenols are aromatic ring structures that have one or more hydroxyl and chlorine atoms attached to benzene rings

and are highly toxic due to their carcinogenic, mutagenic, and cytotoxic properties. Bacteria that can use Chlorophenol as a source of carbon and energy through aerobic degradation include several species of the genus *Pseudomonas*, which were found to be abundant in HL slugs (Arora & Bae, 2014). The significant differences in beta-diversity between slugs starved in the dark (D) and slugs starved in the light (L and HL) indicate that darkness as a stress factor has a greater impact on the microbiome composition than high light stress however with little effect on metabolic pathway abundance.

5.6 Conclusion

In coral research, the microbiome's importance and the holobiont's idea have already found wide acceptance. In terms of photosymbiotic molluscs, the cladobranch *B. stephanieae* is a well-studied model organism. Our results indicate a vertical transmission of the slug's microbiome since *B. stephanieae* and its food source *E. diaphana* differed significantly in their alpha and beta diversity, as well as in their core microbiome. The microbiome of *Berghia stephanieae* is not accommodated to support photobionts which can explain why *B. stephanieae* cannot maintain its photobionts in the long term. In addition, our data show that light and starvation experiments, which are commonly used in photosymbiosis research, induce a shift in the slug's microbiome towards an increased abundance of potential pathogens, with serious consequences for metabolic pathways such as sulphur and nitrogen cycling. These results emphasize that *B. stephanieae* is more than just a host to its photobiont, and it is time to apply the concept of the holobiont to other photosymbiotic animals like molluscs.

Acknowledgment

We thank Christina Lo Porto and Jasmin Kirch for excellent technical assistance when conducting local deep sequencing.

Author's contributions

CS, SMB, and GC planned and conducted the experiments. CS, SMB, GG, and ST processed the data and performed data analyses. CS, SMB, JMC, AP, and GC discussed, interpreted the results, wrote, and revised the final version of the manuscript.

Funding

Open access publication was made possible by the DEAL-Springer Nature contract.

Availability of data and materials

The data have been deposited with links to BioProject accession number PRJNA988282 in the NCBI BioProject database https://www.ncbi.nlm.nih.gov/bioproject/988282 with SRA accession numbers listed in Additional File 1: Table 1.

Supplementary Materials

The supplementary material is included in the digital version of this paper.

Additional File 1

— Table 1. ASV table. Number of ASVs organised by sample and treatment, as well as after filtering and denoising. Biosample ID and Accession number are included for each sample. — Table 2. Absolute abundance of bacterial families cross all samples. — Table 3. Absolute abundance of core bacteria species for all samples. — Table 4. Relative abundance of core bacteria species for all samples. — Table 5. ASVs shared with water samples. — Table 6. Results of ANOVA based on Shannon alpha diversity metric and pairwise t-tests between conditions. — Table 7. List of vectors PC1 and PC2 of PCoA plot and Shannon entropy for each sample. — Table 8. Results of PERMANOVA based on Bray-Curtis beta diversity metric and pairwise comparison of conditions. — Table 9. Shannon alpha diversity and Bray-Curtis beta-diversity between water samples and all groups. — Table 10. List of absolute pathway abundance for all samples.— Table 11. Results of the statistical analysis of the metabolic pathways between the different conditions.

Additional File 2

— Figure 2. Rarefaction curves illustrate ASV richness as a function of sequencing depth for subsampled dataset. The five groups shown correspond to *E. diaphana* (Symbiotic), *B. stephanieae* fed and starved in light (StarvedL), high light (StarvedHL), and darkness (StarvedD).

Additional File 3

— Figure 3 A - B. Venn diagrams comparing core microbiome composition of anemone, fed slugs and water. Numbers indicate total abundance of either unique or shared ASVs (A). Principal Coordinate Analysis (PCoA) plot of alpha- and beta-diversity. PCoA plot based on Bray-Curtis dissimilarity. Shape of circle represents taxon (anemone, slug or water), size of circle indicates Shannon diversity index, colour of circle represents husbandry condition fed, starved in darkness (starvedD), high light (starvedHL), regular light(starvedL), anemone or water.

Additional File 4

— Figure 4 A - M. Boxplots of post-hoc Tukey's HSD pair- wise test between conditions for each metabolic pathway with original and normalised abundance. The five groups are indicated by different colours: *E. diaphana* in pink, *B. stephanieae* fed in red, starved in light (StarvedL) in light blue, starved in high light (StarvedHL) in dark blue and starved in darkness (StarvedD) in green. Additional

Additional File 5

— Figure 5 A - C. Differences in nitrogen cycle of *E. diaphana* (A), *B. stephanieae* fed (B) and *B. stephanieae* starved (C). Created with BioRender.com.

References

Abdelrahman, S. M., Patin, N. V., Hanora, A., Aboseidah, A., Desoky, S., Desoky, S. G., Stewart, F. J., & Lopanik, N. B. (2021). The natural product biosynthetic potential of Red Sea nudibranch microbiomes. *PeerJ*, *9*, e10525.

Anderson, M. J. (2001). A new method for non-parametric multivariate analysis of variance. *Austral Ecology*, *26*(1), 32–46.

Arndt, D., Xia, J., Liu, Y., Zhou, Y., Guo, A. C., Cruz, J. A., Sinelnikov, I., Budwill, K., Nesbø, C. L., & Wishart, D. S. (2012). METAGENassist: A comprehensive web server for comparative metagenomics. *Nucleic Acids Research*, *40*(W1), W88–W95.

Arora, P. K., & Bae, H. (2014). Bacterial degradation of chlorophenols and their derivatives. *Microbial Cell Factories*, *13*, 1–17.

Baedke, J., Fábregas-Tejeda, A., & Nieves Delgado, A. (2020). The holobiont concept before Margulis. *Journal of Experimental Zoology Part B: Molecular and Developmental Evolution*, *334*(3), 149–155.

Bayer, T., Neave, M. J., Alsheikh-Hussain, A., Aranda, M., Yum, L. K., Mincer, T., Hughen, K., Apprill, A., & Voolstra, C. R. (2013). The microbiome of the Red Sea coral *Stylophora pistillata* is dominated by tissue-associated *Endozoicomonas* bacteria. *Applied and Environmental Microbiology*, *79*(15), 4759–4762.

Bisanz, J. E. (2018). *qiime2R: Importing QIIME2 artifacts and associated data into R sessions* [v0.99].

Böhringer, N., Fisch, K. M., Schillo, D., Bara, R., Hertzer, C., Grein, F., Eisenbarth, J.-H., Kaligis, F., Schneider, T., Wägele, H., et al. (2017). Antimicrobial potential of bacteria associated with marine sea slugs from North Sulawesi, Indonesia. *Frontiers in Microbiology*, *8*, 1092.

Bolyen, E., Rideout, J. R., Dillon, M. R., Bokulich, N. A., Abnet, C. C., Al-Ghalith, G. A., Alexander, H., Alm, E. J., Arumugam, M., Asnicar, F., et al. (2019). Reproducible, interactive, scalable and extensible microbiome data science using QIIME 2. *Nature Biotechnology*, *37*(8), 852–857.

Bordenstein, S., & Theis, K. (2008). Host biology in light of the microbiome: Ten principles of holobionts and hologenomes. *PLoS Biology*, *13*(8), 1–23.

Britstein, M., Cerrano, C., Burgsdorf, I., Zoccarato, L., Kenny, N. J., Riesgo, A., Lalzar, M., & Steindler, L. (2020). Sponge microbiome stability during environmental acquisition of highly specific photosymbionts. *Environmental Microbiology*, *22*(8), 3593–3607.

Brown, A. L., Sharp, K., & Apprill, A. (2022). Reshuffling of the coral microbiome during dormancy. *Applied and Environmental Microbiology*, *88*(23), e01391–22.

Burghardt, I., Evertsen, J., Johnsen, G., & Wägele, H. (2005). Solar powered seaslugs - Mutualistic symbiosis of aeolid nudibranchia (Mollusca, Gastropoda, Opisthobranchia) with *Symbiodinium*. *Symbiosis*.

Burghardt, I., Stemmer, K., & Wägele, H. (2008). Symbiosis between *Symbiodinium* (Dinophyceae) and various taxa of Nudibranchia (Mollusca: Gastropoda), with analyses of long-term retention. *Organisms Diversity & Evolution*, *8*(1), 66–76.

Burghardt, I., & Wägele, H. (2014). The symbiosis between the 'solar-powered'nudibranch *Melibe engeli* Risbec, 1937 (Dendronotoidea) and *Symbiodinium* sp. (Dinophyceae). *Journal of Molluscan Studies*, *80*(5), 508–517.

Callahan, B. J., McMurdie, P. J., Rosen, M. J., Han, A. W., Johnson, A. J. A., & Holmes, S. P. (2016). DADA2: High-resolution sample inference from Illumina amplicon data. *Nature Methods*, *13*(7), 581–583.

Cowen, R. (1988). The role of algal symbiosis in reefs through time. *Palaios*, 221–227.

Curdt, F., Schupp, P. J., & Rohde, S. (2022). Light availability affects the symbiosis of sponge specific cyanobacteria and the common blue aquarium sponge (*Lendenfeldia chondrodes*). *Animals*, *12*(10), 1283.

Curry, T. M., Peña, M. J., & Urbanowicz, B. R. (2023). An update on xylan structure, biosynthesis, and potential commercial applications. *The Cell Surface*, 100101.

Curson, A. R., Liu, J., Bermejo Martínez, A., Green, R. T., Chan, Y., Carrión, O., Williams, B. T., Zhang, S.-H., Yang, G.-P., Bulman Page, P. C., et al. (2017). Dimethylsulfoniopropionate biosynthesis in marine bacteria and identification of the key gene in this process. *Nature Microbiology*, *2*(5), 1–9.

Curtis, E., Moseley, J., Racicot, R., & Wright, R. M. (2023). Bacterial microbiome variation across symbiotic states and clonal lines in a cnidarian model. *Frontiers in Marine Science*.

Davis, J., Fricke, W. F., Hamann, M. T., Esquenazi, E., Dorrestein, P. C., & Hill, R. T. (2013). Characterization of the bacterial community of the chemically defended Hawaiian sacoglossan *Elysia rufescens*. *Applied and Environmental Microbiology*, *79*(22), 7073–7081.

de Oliveira, B. F. R., Freitas-Silva, J., Sánchez-Robinet, C., & Laport, M. S. (2020). Transmission of the sponge microbiome: Moving towards a unified model. *Environmental Microbiology Reports*, *12*(6), 619–638.

D'elia, C., Domotor, S., & Webb, K. (1983). Nutrient uptake kinetics of freshly isolated zooxanthellae. *Marine Biology*, *75*, 157–167.

Diaz, M. C., Thacker, R. W., Rützler, K., & Piantoni Dietrich, C. (2007). Two new haplosclerid sponges from Caribbean Panama with symbiotic filamentous cyanobacteria, and an overview of sponge-cyanobacteria associations. *Porifera research: Biodiversity, innovation and sustainability*.

Doepke, H., Herrmann, K., & Schuett, C. (2012). Endobacteria in the tentacles of selected cnidarian species and in the cerata of their nudibranch predators. *Helgoland Marine Research*, *66*(1), 43–50.

Džunková, M., La Clair, J. J., Tyml, T., Doud, D., Schulz, F., Piquer-Esteban, S., Porcel Sanchis, D., Osborn, A., Robinson, D., Louie, K. B., Bowen, B. P., Bowers, R. M., Lee, J., Arnau, V., Díaz-Villanueva, W., Stepanauskas, R., Gosliner, T., Date, S. V., Northen, T. R., … Woyke, T. (2023). Synthase-selected sorting approach identifies a beta-lactone synthase in a nudibranch symbiotic bacterium. *Microbiome*, *11*(130).

Elfeky, H. H., Hanora, A., & Solyman, S. M. (2023). Bioactivity of bacteria associated with Red Sea nudibranchs and whole genome sequence of *Nocardiopsis dassonvillei* RACA-4. *Marine Genomics*, *67*, 101004.

Falkowski, P. G., Dubinsky, Z., Muscatine, L., & McCloskey, L. (1993). Population control in symbiotic corals. *Bioscience*, *43*(9), 606–611.

Funkhouser, L. J., & Bordenstein, S. R. (2013). Mom knows best: The universality of maternal microbial transmission. *PLoS Biology*, *11*(8), e1001631.

Gerwick, W. H., & Fenner, A. M. (2013). Drug Discovery from Marine Microbes. *Microbial Ecology*, *65*, 800–806.

Girden, E. R. (1992). *ANOVA: Repeated measures*. Sage.

Giroux, M. S., Reichman, J. R., Langknecht, T., Burgess, R. M., & Ho, K. T. (2022). Environmental RNA as a tool for marine community biodiversity assessments. *Scientific Reports*, *12*(1), 17782.

Hackstadt, A. J., & Hess, A. M. (2009). Filtering for increased power for microarray data analysis. *BMC Bioinformatics*, *10*, 1–12.

Halliwell, B., & Gutteridge, J. M. (1985). Free radicals in biology and medicine.

Händeler, K., Grzymbowski, Y. P., Krug, P. J., & Wägele, H. (2009). Functional chloroplasts in metazoan cells-a unique evolutionary strategy in animal life. *Frontiers in Zoology*, *6*, 1–18.

Hartman, L. M., van Oppen, M. J. H., & Blackall, L. L. (2020). Microbiota characterization of *Exaiptasia diaphana* from the Great Barrier Reef. *Animal Microbiome*, *2*(1), 1–14.

Hawes, C., & Cobb, A. (1980). The effects of starvation on the symbiotic chloroplasts in *Elysia viridis*: A fine structural study. *New Phytologist*, 375–379.

Hernandez-Agreda, A., Gates, R. D., & Ainsworth, T. D. (2017). Defining the core microbiome in corals' microbial soup. *Trends in Microbiology*, *25*(2), 125–140.

Herrera Sarrias, M., Ziegler, M., Voolstra, C. R., & Aranda, M. (2017). Laboratory-Cultured Strains of the Sea Anemone *Exaiptasia* Reveal Distinct Bacterial Communities. *Frontiers in Marine Science*.

Hill, M., Allenby, A., Ramsby, B., Schönberg, C., & Hill, A. (2011). *Symbiodinium* diversity among host clionaid sponges from caribbean and pacific reefs: evidence of heteroplasmy and putative host-specific symbiont lineages. *Molecular Phylogenetics and Evolution*, *59*(1), 81–88.

Hinde, R., & Smith, D. (1975). The role of photosynthesis in the nutrition of the mollusc *Elysia viridis*. *Biological Journal of the Linnean Society*, *7*(2), 161–171.

Hinde, R., & Smith, D. (1972). Persistence of functional chloroplasts in *Elysia viridis* (Opisthobranchia, Sacoglossa). *Nature New Biology*, *239*(88), 30–31.

Hirose, E. (2015). Ascidian photosymbiosis: Diversity of cyanobacterial transmission during embryogenesis. *Genesis*, *53*(1), 121–131.

Hirose, E., Neilan, B. A., Schmidt, E. W., Murakami, A., Gault, P., et al. (2009). Enigmatic life and evolution of *Prochloron* and related cyanobacteria inhabiting colonial ascidians. *Handbook on Cyanobacteria*, 161–189.

Johansson, K.-E., & Pettersson, B. (2002). Taxonomy of Mollicutes. *Molecular biology and pathogenicity of Mycoplasmas*, 1–29.

Kempf, S. C. (1984). Symbiosis between the zooxanthella *Symbiodinium* (= *Gymnodinium*) *microadriaticum* (Freudenthal) and four species of nudibranchs. *The Biological Bulletin*, *166*(1), 110–126.

Kempf, S. C. (1991). A 'primitive'symbiosis between the aeolid nudibranch *Berghia verrucicornis* (A. Costa, 1867) and a zooxanthella. *Journal of Molluscan Studies*, *57*(Supplement_Part_4), 75–85.

Kiene, R. P., Linn, L. J., & Bruton, J. A. (2000). New and important roles for DMSP in marine microbial communities. *Journal of Sea Research*, *43*(3-4), 209–224.

Kristiana, R., Sibero, M. T., Farisa, M. Y., Ayuningrum, D., Dirgantara, D., Hanafi, M., Radjasa, O. K., Sabdono, A., & Trianto, A. (2019). Antibacterial potential of nudibranch-associated bacteria from Saparua and Nusa Laut Islands, Indonesia. *Biodiversitas Journal of Biological Diversity*, *20*(7).

Kruskal, W. H., & Wallis, W. A. (1952). Use of ranks in one-criterion variance analysis. *Journal of the American Statistical Association*, *47*(260), 583–621.

Kuek, F. W., Motti, C. A., Zhang, J., Cooke, I. R., Todd, J. D., Miller, D. J., Bourne, D. G., & Raina, J.-B. (2022). DMSP production by coral-associated bacteria. *Frontiers in Marine Science*, *9*.

Laroche, O., Wood, S. A., Tremblay, L. A., Lear, G., Ellis, J. I., & Pochon, X. (2017). Metabarcoding monitoring analysis: The pros and cons of using co-extracted environmental DNA and RNA data to assess offshore oil production impacts on benthic communities. *PeerJ*, *5*, e3347.

Leal, M. C., Nunes, C., Alexandre, D., Da Silva, T. L., Reis, A., Dinis, M. T., & Calado, R. (2012). Parental diets determine the embryonic fatty acid profile of the tropical nudibranch *Aeolidiella stephanieae*: The effect of eating bleached anemones. *Marine Biology*, *159*, 1745–1751.

Lehtovirta-Morley, L. E. (2018). Ammonia oxidation: Ecology, physiology, biochemistry and why they must all come together. *FEMS microbiology letters*, *365*(9), fny058.

Lesser, M., Falcón, L. I., Rodríguez-Román, A., Enríquez, S., Hoegh-Guldberg, O., & Iglesias-Prieto, R. (2007). Nitrogen fixation by symbiotic cyanobacteria provides a source of nitrogen for the scleractinian coral *Montastraea cavernosa*. *Marine Ecology Progress Series*, *346*, 143–152.

Luter, H. M., Andersen, M., Versteegen, E., Laffy, P., Uthicke, S., Bell, J. J., & Webster, N. S. (2020). Cross-generational effects of climate change on the microbiome of a photosynthetic sponge. *Environmental Microbiology*, *22*(11), 4732–4744.

Mahadevan, P., & Middlebrooks, M. L. (2020). Bacterial diversity in the *clarki* ecotype of the photosynthetic sacoglossan, *Elysia crispata*. *MicrobiologyOpen*, *9*(9), e1098.

Maire, J., Blackall, L. L., & van Oppen, M. J. (2021). Microbiome characterization of defensive tissues in the model anemone *Exaiptasia diaphana*. *BMC Microbiology*, *21*(1), 152.

Martinez-Pita, I., Garcia, F., & Pita, M.-L. (2005). Fatty acid composition and utilization in developing eggs of some marine nudibranchs (Mollusca: Gastropoda: Opistobranchia) from southwest Spain. *Journal of Shellfish Research*, *24*(4), 1209–1216.

Matthews, J. L., Hoch, L., Raina, J.-B., Pablo, M., Hughes, D. J., Camp, E. F., Seymour, J. R., Ralph, P. J., Suggett, D. J., & Herdean, A. (2023). Symbiodiniaceae photophysiology and stress resilience is enhanced by microbial associations. *Scientific Reports*, *13*(1), 20724.

Melo Clavijo, J., Donath, A., Serôdio, J., & Christa, G. (2018). Polymorphic adaptations in metazoans to establish and maintain photosymbioses. *Biological Reviews*, *93*(4), 2006–2020.

Melo Clavijo, J., Sickinger, C., Bleidißel, S., Gasparoni, G., Tierling, S., Preisfeld, A., & Christa, G. (2022). The nudibranch *Berghia stephanieae* (Valdés, 2005) is not able to initiate a functional symbiosome-like environment to maintain *Breviolum minutum* (JE Parkinson & LaJeunesse 2018). *Frontiers in Marine Science*.

Meunier, V., Geissler, L., Bonnet, S., Rädecker, N., Perna, G., Grosso, O., Lambert, C., Rodolfo-Metalpa, R., Voolstra, C. R., & Houlbrèque, F. (2021). Microbes support enhanced nitrogen requirements of coral holobionts in a high CO2 environment. *Molecular Ecology*, *30*(22), 5888–5899.

Meyer, J. L., Paul, V. J., & Teplitski, M. (2014). Community shifts in the surface microbiomes of the coral *Porites astreoides* with unusual lesions. *PLoS One*, *9*(6), e100316.

Mohamed, A. R., Ochsenkühn, M. A., Kazlak, A. M., Moustafa, A., & Amin, S. A. (2023). The coral microbiome: Towards an understanding of the molecular mechanisms of coral–microbiota interactions. *FEMS Microbiology Reviews*, *47*(2), fuad005.

Monteiro, E. A., Güth, A. Z., Banha, T. N., Sumida, P. Y., & Mies, M. (2019). Evidence against mutualism in an aeolid nudibranch associated with Symbiodiniaceae dinoflagellates. *Symbiosis*, *79*, 183–189.

Muscatine, L., & Porter, J. W. (1977). Reef corals: Mutualistic symbioses adapted to nutrient-poor environments. *Bioscience*, *27*(7), 454–460.

Neave, M. J., Apprill, A., Ferrier-Pagès, C., & Voolstra, C. R. (2016). Diversity and function of prevalent symbiotic marine bacteria in the genus *Endozoicomonas*. *Applied Microbiology and Biotechnology*, *100*, 8315–8324.

Neuwirth, E. (2022). *RColorBrewer: ColorBrewer Palettes* [R package version 1.1-3].

Ng, M. S., Soon, N., Chang, Y., & Wainwright, B. J. (2022). Bacterial and fungal co-occurrence in the nudibranch, *Pteraeolidia semperi*. *Life*, *12*(12), 1988.

Pineda, M. C., Strehlow, B., Duckworth, A., Doyle, J., Jones, R., & Webster, N. S. (2016). Effects of light attenuation on the sponge holobiont-implications for dredging management. *Scientific Reports*, *6*(1), 39038.

Posadas, N., Baquiran, J. I. P., Nada, M. A. L., Kelly, M., & Conaco, C. (2022). Microbiome diversity and host immune functions influence survivorship of sponge holobionts under future ocean conditions. *The ISME Journal*, *16*(1), 58–67.

Prazeres, M., Ainsworth, T., Roberts, T. E., Pandolfi, J. M., & Leggat, W. (2017). Symbiosis and microbiome flexibility in calcifying benthic foraminifera of the Great Barrier Reef. *Microbiome*, *5*(1), 1–11.

R Core Team. (2021). *R: A Language and Environment for Statistical Computing*. R Foundation for Statistical Computing. Vienna, Austria.

Rädecker, N., Pogoreutz, C., Voolstra, C. R., Wiedenmann, J., & Wild, C. (2015). Nitrogen cycling in corals: The key to understanding holobiont functioning? *Trends in Microbiology*, *23*(8), 490–497.

Rasmussen, J. A., Kiilerich, P., Madhun, A. S., Waagbø, R., Lock, E.-J. R., Madsen, L., Gilbert, M. T. P., Kristiansen, K., & Limborg, M. T. (2023). Co-diversification of an intestinal *Mycoplasma* and its salmonid host. *The ISME journal*, *17*(5), 682–692.

Rasmussen, J. A., Villumsen, K. R., Duchêne, D. A., Puetz, L. C., Delmont, T. O., Sveier, H., Jørgensen, L. v. G., Præbel, K., Martin, M. D., Bojesen, A. M., et al. (2021). Genome-resolved metagenomics suggests a mutualistic relationship between *Mycoplasma* and salmonid hosts. *Communications Biology*, *4*(1), 579.

Rauch, C., Tielens, A. G., Serôdio, J., Gould, S. B., & Christa, G. (2018). The ability to incorporate functional plastids by the sea slug *Elysia viridis* is governed by its food source. *Marine Biology*, *165*(5), 82.

Razin, S., Yogev, D., & Naot, Y. (1998). Molecular biology and pathogenicity of *Mycoplasmas*. *Microbiology and Molecular Biology Reviews*, *62*(4), 1094–1156.

Reisser, W. (1984). The taxonomy of green algae endosymbiotic in ciliates and a sponge. *British Phycological Journal*, *19*(4), 309–318.

Ritchie, K. B. (2011). Bacterial symbionts of corals and *Symbiodinium*. *Beneficial Microorganisms in Multicellular Life Forms*, 139–150.

Rohwer, F., Seguritan, V., Azam, F., & Knowlton, N. (2002). Diversity and distribution of coral-associated bacteria. *Marine Ecology Progress Series*, *243*, 1–10.

Rola, M., Frankenbach, S., Bleidissel, S., Sickinger, C., Donath, A., Frommlet, J. C., Greve, C., Serôdio, J., Preisfeld, A., Melo Clavijo, J., et al. (2022). Cladobranchia (Gastropoda, Nudibranchia) as a promising model to understand the molecular evolution of photosymbiosis in animals. *Frontiers in Marine Science*, *8*, 745644.

Rosenberg, E., Koren, O., Reshef, L., Efrony, R., & Zilber-Rosenberg, I. (2007). The role of microorganisms in coral health, disease and evolution. *Nature Reviews Microbiology*, *5*(5), 355–362.

Rosenberg, E., & Zilber-Rosenberg, I. (2021). Reconstitution and transmission of gut microbiomes and their genes between generations. *Microorganisms*, *10*(1), 70.

Röthig, T., Costa, R. M., Simona, F., Baumgarten, S., Torres, A. F., Radhakrishnan, A., Aranda, M., & Voolstra, C. R. (2016). Distinct bacterial communities associated with the coral model *Aiptasia* in aposymbiotic and symbiotic states with *Symbiodinium*. *Frontiers in Marine Science*, *3*, 234.

Röthig, T., Puntin, G., Wong, J. C., Burian, A., McLeod, W., & Baker, D. M. (2021). Holobiont nitrogen control and its potential for eutrophication resistance in an obligate photosymbiotic jellyfish. *Microbiome*, *9*(1), 127.

Schuett, C., & Doepke, H. (2013). Endobacterial morphotypes in nudibranch cerata tips: A SEM analysis. *Helgoland Marine Research*, *67*, 219–227.

Shannon, C. E. (1948). A mathematical theory of communication. *The Bell System Technical Journal*, *27*(3), 379–423.

Shashar, N., Cohen, Y., Loya, Y., & Sar, N. (1994). Nitrogen fixation (acetylene reduction) in stony corals: Evidence for coral-bacteria interactions. *Marine Ecology Progress Series*, 259–264.

Silva, R. X., Cartaxana, P., & Calado, R. (2021). Prevalence and photobiology of photosynthetic dinoflagellate endosymbionts in the nudibranch *Berghia stephanieae*. *Animals*, *11*(8), 2200.

Silva, R. X., Madeira, D., Cartaxana, P., & Calado, R. (2023). Assessing the trophic impact of bleaching: The model pair *Berghia stephanieae/Exaiptasia diaphana*. *Animals*, *13*(2), 291.

Stewart, F. J. (2013). Preparation of microbial community cDNA for metatranscriptomic analysis in marine plankton. In *Methods in Enzymology* (pp. 187–218, Vol. 531). Elsevier.

Taguchi, S., & Kinzie Iii, R. (2001). Growth of zooxanthellae in culture with two nitrogen sources. *Marine Biology*, *138*, 149–155.

Teugels, B., Bouillon, S., Veuger, B., Middelburg, J., & Koedam, N. (2008). Kleptoplasts mediate nitrogen acquisition in the sea slug *Elysia viridis*. *Aquatic Biology*, *4*(1), 15–21.

Tolleter, D., Seneca, F. O., DeNofrio, J. C., Krediet, C. J., Palumbi, S. R., Pringle, J. R., & Grossman, A. R. (2013). Coral bleaching independent of photosynthetic activity. *Current Biology*, *23*(18), 1782–1786.

Van Alstyne, K., Dominique, V., & Muller-Parker, G. (2009). Is dimethylsulfoniopropionate (DMSP) produced by the symbionts or the host in an anemone–zooxanthella symbiosis? *Coral Reefs*, *28*, 167–176.

Voolstra, C. R., & Ziegler, M. (2020). Adapting with microbial help: Microbiome flexibility facilitates rapid responses to environmental change. *BioEssays*, *42*(7), 2000004.

Webster, N. S., Cobb, R. E., Soo, R., Anthony, S. L., Battershill, C. N., Whalan, S., & Evans-Illidge, E. (2011). Bacterial community dynamics in the marine sponge *Rhopaloeides odorabile* under *in situ* and *ex situ* cultivation. *Marine Biotechnology*, *13*, 296–304.

Weis, V. M., Davy, S. K., Hoegh-Guldberg, O., Rodriguez-Lanetty, M., & Pringle, J. R. (2008). Cell biology in model systems as the key to understanding corals. *Trends in Ecology & Evolution*, *23*(7), 369–376.

Weisburg, W. G., Barns, S. M., Pelletier, D. A., & Lane, D. J. (1991). 16S ribosomal DNA amplification for phylogenetic study. *Journal of Bacteriology*, *173*(2), 697–703.

Wickham, H. (2016). *ggplot2: Elegant Graphics for Data Analysis*. Springer-Verlag New York.

Wickham, H., Averick, M., Bryan, J., Chang, W., McGowan, L. D., François, R., Grolemund, G., Hayes, A., Henry, L., Hester, J., Kuhn, M., Pedersen, T. L., Miller, E., Bache, S. M., Müller, K., Ooms, J., Robinson, D., Seidel, D. P., Spinu, V., … Yutani, H. (2019). Welcome to the tidyverse. *Journal of Open Source Software*, *4*(43), 1686.

Wickham, H., Hester, J., Chang, W., & Bryan, J. (2022). *devtools: Tools to Make Developing R Packages Easier* [R package version 2.4.5].

Wiegel, J., Tanner, R., Rainey, F. A., et al. (2006). An introduction to the family Clostridiaceae. *The Prokaryotes*, *4*, 654–678.

Xiang, N., Rädecker, N., Pogoreutz, C., Cárdenas, A., Meibom, A., Wild, C., Gärdes, A., & Voolstra, C. R. (2022). Presence of algal symbionts affects denitrifying bacterial communities in the sea anemone *Aiptasia* coral model. *ISME Communications*, *2*(1), 105.

Zhukova, N. V., & Eliseikina, M. G. (2012). Symbiotic bacteria in the nudibranch mollusk *Dendrodoris nigra*: Fatty acid composition and ultrastructure analysis. *Marine Biology*, *159*, 1783–1794.

Zverlov, V. V., Kellermann, J., & Schwarz, W. H. (2005). Functional subgenomics of *Clostridium thermocellum* cellulosomal genes: Identification of the major catalytic components in the extracellular complex and detection of three new enzymes. *Proteomics*, *5*(14), 3646–3653.

Chapter 6

Nickel and Cobalt Disrupt the Microbiome and Metabolic Function of the Photosymbiotic Sea Slug *Berghia stephanieae* (Á. Valdés, 2005)

Corinna Sickinger[1], Jana Kosky[1], Andriy Tkach[2], Alicia Thiel [2], Julia Bornhorst [2], Gregor Christa[3] and Angelika Preisfeld[1]

[1]*Institute for Zoology and Didactics of Biology, University of Wuppertal, Wuppertal, Germany*
[2]*Food Chemistry with focus on Toxicology, University of Wuppertal, Wuppertal, Germany*
[3]*Department of Evolution and Biodiversity, University of Wuppertal, Wuppertal, Germany*

Published: 17 January 2026, *Marine Environmental Research* 216, 107845 (2026)
https://doi.org/10.1016/j.marenvres.2026.107845

6.1 Abstract

The rapid global expansion of electromobility has increased demand for nickel and cobalt, which are key components in lithium-ion batteries. As a result, mining activities are intensifying, yet their ecological impact on marine ecosystems remains poorly understood. In this study, we examine the effects of nickel and cobalt on the microbiome composition and bacterial metabolic pathways of the marine photosymbiotic gastropod *Berghia stephanieae*. Preliminary toxicity tests showed concentration-dependent metal uptake, with behavioural stress responses such as lethargy, cessation of feeding, and shedding of cerata occurring at high concentrations (around 18 mg/L for nickel and cobalt). Microbiome analysis across three concentrations (1, 3, and 17 mg/L for nickel and cobalt) revealed significant changes in community composition and function. At 1 mg/L, the observed effects were concentration-dependent rather than metal-specific, as indicated by a decline in alpha diversity and a shift in community composition, characterised by a reduction in *Mycoplasma* sp. and an increase in Pseudofulvibacter and *Endozoicomonas* sp.. At 3 mg/L, *Shewanella* spp. abundance increased and metal-specific effects emerged, with a strong downregulation of the metabolic pathways denitrification and lignin degradation for cobalt and an upregulation of sulfur oxidation for nickel. At 17 mg/L, many functional pathways were downregulated, aligning with observed host stress and

pointing to a possible loss of functional redundancy. Overall, nickel and cobalt exposure led to distinct microbiome alterations, with intermediate levels eliciting the strongest metabolic response.

Keywords core microbiome · holobiont · bacterial metabolic pathways · core microbiome · metal pollution · ICP-OES

6.2 Introduction

In recent years, a shift away from reliance on fossil fuels toward sustainable energy sources, including renewable energy and electric mobility, has commenced. Cobalt and nickel significantly benefit from the electric vehicle revolution as they are integral components of lithium-ion batteries (International Energy Agency, 2021). Nickel concentrations in open ocean waters typically range between 0.2–0.7 µg/L (Apte et al., 2006; Donat & Bruland, 1988). However, in areas impacted by mining, concentrations are significantly elevated. Environmental contamination by nickel has been reported in regions such as Australia, Canada, Cuba, Russia, and South Africa, with levels ranging from 100 to 2000 µg/L (Wood et al., 2012). The most severe nickel pollution has been observed in Sudbury, Ontario (Canada), a major nickel mining hub, where contamination has extended across both terrestrial and aquatic environments (Arnott et al., 2001; Pyle & Couture, 2011). This Canadian site is also one of the most cobalt-contaminated areas globally, with surface water concentrations reaching up to 2028 µg/L (Environment and Climate Change Canada, 2017). In the United States, cobalt concentrations in surface waters near mining areas have been reported between 0.1–1000 µg/L (Mebane et al., 2015), far exceeding natural seawater levels, which are typically in the range of 0.002–0.02 µg/L (Donat & Bruland, 1988; Schrauzer, 1991).

Despite these alarming values, determining the exact concentrations of nickel and cobalt in mining-affected marine ecosystems remains difficult, particularly in countries like Indonesia and New Caledonia, where mining is expanding rapidly and operations are often located close to rivers or coastlines. In New Caledonia, sediment samples from coastal areas have revealed extreme nickel enrichment, with concentrations up to 7700 mg/kg (Fernandez et al., 2006; Merrot et al., 2019; Noël et al., 2015), but comparable marine water measurements are largely missing. Similarly, for Indonesia, a country now ranking among the top global producers of both nickel and cobalt, detailed and consistent data on metal concentrations and their ecological consequences remain scarce (Naryono, 2023).

To date, most studies on the effects of nickel and cobalt have focused primarily on classical toxicity endpoints in temperate marine organisms. In contrast, sublethal effects, such as disruptions to physiological functions or shifts in host-associated microbial communities, have received little attention (Gissi et al., 2016; A. Reichelt-Brushett, 2012; Van Dam et al., 2008). Yet, microbiome analyses represent a powerful tool to assess precisely such hidden effects, as they offer insights into how environmental pollutants influence symbiotic relationships, developmental processes, and host resilience (Brocco French, 2024; J. Li et al., 2023). Microbial communities associated with marine invertebrates can adapt to chemical stress through shifts in taxonomic composition or transposon-mediated genetic plasticity (Xu et al., 2025). Moreover, host-associated microbiomes often harbour bacterial taxa capable of degrading complex compounds such as hydrocarbons or even metals (Ansari et al., 2021; Bayat et al., 2015; Diner et al., 2024; Fragoso ados Santos et al., 2015). This

functional plasticity can be highly beneficial for the host, enhancing its ability to cope with environmental stressors and supporting detoxification processes under metal exposure.

Metals such as nickel or cobalt are often accumulated in host tissues, impairing ion transport, disrupting metabolic and developmental processes, and triggering oxidative stress (Gissi et al., 2018; Kimbrough, 2008; Nechev et al., 2006; Ravera, 2001; Sun et al., 2020). Although cobalt is an essential trace element and a component of vitamin B12, its biological role is limited, and only minimal amounts are required for normal cellular function (Eitinger et al., 2005). Excessive cobalt levels can trigger the production of reactive oxygen species (ROS), particularly within lysosomes, leading to oxidative DNA damage and mitochondria-mediated apoptosis (Zeeshan et al., 2017). Similarly, nickel exposure has been shown to induce oxidative stress, impairing key biomolecules such as DNA, proteins, and lipids. One proposed mechanism is that nickel may substitute essential metals in metalloproteins or interfere with enzymatic activity through allosteric inhibition, either by binding directly to catalytic residues or outside the active site. These disruptions can compromise cellular homeostasis and ultimately impair organism health (Macomber & Hausinger, 2011). For example, individuals of the tunicate *Botryllus schlosseri* collected from the coast of Connecticut contained a high amount of nickel (up to 9 mg/L) and cobalt (up to 1 mg/L), which were at substantially higher concentrations compared with the surrounding seawater. In *B. schlosseri*, nickel was negatively correlated with several unannotated metabolites and with bacteria from the order Pirellulales, suggesting sensitivity of these compounds and microbes to elevated nickel levels. Cobalt showed strong negative correlations with known metabolites such as thalassospiramide D and talaroconvolutin D, indicating potential chelating interactions that may affect cobalt availability and metabolic processes (Guillén Matus et al., 2024). On the other hand, the hard coral *Acropora muricata* showed no changes in its microbiome composition when exposed to nickel concentrations of 45, 90, 470, 900, and 9050 µg Ni/L, although bleaching was already observed at a concentration of 470 µg/L (Gissi et al., 2019).

In this study, we conducted the first preliminary toxicity test on nickel and cobalt, the metal bioavailability, and the effects of nickel and cobalt on the microbiome of the photosymbiotic sea slug *Berghia stephanieae* (Á. Valdés, 2005). *B. stephanieae* belongs to the gastropod clade Cladobranchia and feeds exclusively on the sea anemone *Exaiptasia diaphana* (Rapp, 1829). *B. stephanieae* is known for its unstable photosymbiosis with the symbiotic unicellular algae of the family Symbiodiniaceae from its food source. These unicellular algae are incorporated into cells of the digestive gland system of the slug and kept photosynthetically active for a couple of days before they are expelled (Rola et al., 2022). *B. stephanieae* is a mollusc model organism and has been studied extensively regarding its genome (Goodheart et al., 2024), transcriptome (Clavijo et al., 2022), and microbiome (Sickinger et al., 2024). This study represents the first comprehensive investigation of how nickel and cobalt exposure affect the microbial community structure and the predicted bacterial metabolic pathways of a marine gastropod. While previous research on metal stress in marine invertebrates has largely focused on corals and sponges, our approach combines taxonomic profiling with functional pathway analysis, offering unprecedented insight into how nickel and cobalt may reshape the microbiome and its potential metabolic contributions in *Berghia stephanieae*. We hypothesise that nickel and cobalt exposure destabilise the microbiome of the nudibranch *B. stephanieae* by reshaping community composition and microbial metabolic functions. Such disruptions are expected to be

concentration-dependent and may have downstream consequences for nutrient cycling processes.

6.3 Materials and Methods

Berghia stephanieae culture

Adult individuals of *B. stephanieae* were obtained in January 2023 from a local supplier (Seepferdchen24 Meeresaquaristik GmbH, Germany). Breeding pairs were kept separately in plastic containers (75 mm diameter, 35 mL artificial seawater, ASW) at 21 °C under a 12 h light/dark rhythm (light intensity approximately 30 µmol photons m^{-2} s^{-1}, Daylight Sunrise 520, Sera). The ASW (33 PSU, pH 8.0) was replaced three times per week. Animals were provided with small polyps of *Exaiptasia diaphana* (7 mm foot and 4 mm oral disk or 4 mm foot and 3 mm oral disk). Following spawning, egg masses were transferred into 55 mm containers (25 mL ASW) and reared under identical conditions. Juveniles were supplied with tentacles of the anemone until reaching maturity.

Exaiptasia diaphana culture

Specimens of *Exaiptasia diaphana* were obtained from a commercial supplier (Seepferdchen24 Meeresaquaristik GmbH, Germany) in January 2022 and maintained in a 55 L aquarium (60 × 30 × 30 cm) containing recirculating artificial seawater (AB Reef Salt, Aqua Medic, Germany). Animals were kept under a 12 h light / 12 h dark cycle at an irradiance of 30 µmol photons m^{-2} s^{-1} (Daylight Sunrise 520, Sera). Salinity and temperature were held at 33 PSU and 21 °C, respectively. To support water quality, two BactoBalls (Fauna Marin GmbH, Germany) were added and replaced every two weeks. *Artemia nauplii* were reared using the Artemio® Set (JBL, Germany) with 16 g of ready-to-use brine shrimp mixture (JBL, Germany). Anemones were fed freshly hatched *Artemia* twice per week.

Preliminary toxicity range-finding

To assess tolerance thresholds and metal uptake, preliminary range-finding assays were conducted for nickel and cobalt. Stock solutions (150 mg/L) were prepared in ASW from nickel(II) chloride hexahydrate (99.9%, Aldrich) and cobalt(II) chloride hexahydrate (99.998%, Puratronic, Alfa Aesar). From these, test solutions at five concentrations plus a seawater control were generated (cobalt: 3–32 mg/L; nickel: 3–37 mg/L; see Table 6.1). Five slugs per concentration were randomly selected and incubated individually in 75 mm containers for 96 h, with mortality checked at defined intervals (0, 1, 6, 12, 18, and 24 h, and every 24 h thereafter). The 96-h exposure period was selected to align with standard acute toxicity testing protocols and to facilitate comparison with previous metal-toxicity studies in marine invertebrates (**USA2002methods**). Death was defined as cessation of pericard contraction. Surviving and deceased animals were snap-frozen at –80 °C.

Metal quantification

Bioavailability of cobalt and nickel was determined by inductively coupled plasma-optical emission spectrometry (ICP–OES, Amaya et al., 2023). Each slug was homogenised in 2 mL isolation buffer (pH 8.0, containing Tricin, $MgCl_2$, and NaCl) on

TABLE 6.1: Concentration of cobalt and nickel used for the toxicity range finding test and ICP OES analysis. Concentrations correspond to elemental cobalt measured with ICP OES. For each group n = 5.

group name	c(Co) [mg/L]	group name	c(Ni) [mg/L]
Co_A	3.7	Ni_A	3.7
Co_B	11.12	Ni_B	14.82
Co_C	18.53	Ni_C	18.53
Co_D	24.7	Ni_D	32.11
Co_E	32.11	Ni_E	37.05

ice, followed by centrifugation (20,817 rcf, 4 °C, 15 min). Supernatants and pellets were separated and stored at –20 °C until analysis. Pellets were digested overnight with a mixture of hydrogen peroxide (30%) and nitric acid (65%) at 90 °C. Samples were spiked with 100 µg/L Yttrium as internal standard and analysed with an Avio 220 Max ICP–OES (PerkinElmer). Metal concentrations were normalised to protein content determined by Bradford assay. Certified reference materials BCR-274 and SRM 1643f served as quality controls.

Exposure experiment

Based on preliminary results, three concentrations were selected for subsequent microbiome analyses (Table 6.2): 1 mg/L, representing levels common in contaminated habitats; 3 mg/L, corresponding to first detectable uptake; and 17 mg/L, where initial behavioural stress symptoms (lethargy, loss of feeding, cerata shedding) were recorded. For each concentration and the seawater control, five slugs were randomly selected and exposed in individual containers for 96 h.

TABLE 6.2: Concentration of cobalt and nickel used for microbiome analysis. Concentrations correspond to elemental cobalt measured with ICP OES.

group name	c(Co) [mg/L]	group name	c(Ni) [mg/L]
Co1	1	Ni1	1
Co2	3.22	Ni2	3.21
Co3	17.3	Ni3	17.2

Nucleic acid extraction and sequencing

The microbiome analysis in this study was based on 16S rRNA gene amplicon sequencing. Total RNA was isolated from each sample using the my-Budget DNA/RNA Mini Kit (Bio-Budget Technologies GmbH, Germany). RNA quantity was assessed with a Qubit™ 4 Fluorometer (Invitrogen, USA). cDNA was synthesised from 50 ng RNA using the LunaScript® RT SuperMix Kit (New England Biolabs, USA) following the manufacturer's instructions. The V1–V2 region of the 16S rRNA gene was amplified by PCR with primers containing Illumina adapters: V1V2forward (5'-TCTTTCCCTACACGACGCTCTTCCGATCT AGAGTTTGATCCTGGCTCAG-3'), V1 V2rev (5'-GTGACTGGAGTTCAGACGTGTGCTCTTCCGATCT TGCTGCCTCCCGT AGGAGT-3') (Sickinger et al., 2024; Weisburg et al., 1991). Adapter PCR was performed in a total volume of 20 µL: 5 µL template cDNA, 10 µL DreamTaq Green

PCR Master Mix (2X) (Thermo Fisher, USA), and 2 µL of 10 µM primers. Each sample was diluted to 20 µL using distilled and sterilised water. The PCR amplification was carried out in 30 cycles: denaturation at 94°C for 1 minute, annealing at 54°C for 1 minute, and extension at 72°C for 1 minute. The initial denaturation and final elongation temperatures were 95°C for 15 minutes and 72°C for 10 minutes, respectively. The Agencourt AMPure XP magnetic bead system (Beckman Coulter, USA) was used to clean the PCR product of each sample. To add Illumina sequencing adapters with TrueSeq indices, an indexing PCR was performed. Following the manufacturer's instructions, 5 µL of the previously purified adapter PCR product, 10 µL Q5® High-Fidelity 2X Master Mix (NewEngland Biolabs, UK), 1 µL of 10 µM of the corresponding forward and reverse index primer, and 3 µL of distilled and sterilised water were used to perform index PCR in a 20 µL volume. Subsequently, index-based PCR products were cleaned with Agencourt AMPure XP magnetic bead technique, and samples were pooled in equimolar amounts after their final DNA concentrations were measured using a QubitTM 4 Fluorometer. Sequencing was performed on an Illumina MiSeq platform with 2 × 250 bp chemistry, yielding approximately 30,000 reads per sample at the Competence Centre for Genomic Analysis (Kiel).

Bioinformatic processing and diversity analysis

Demultiplexed reads were processed with QIIME2 (v2021.4) (Bolyen et al., 2019). Using DADA2 with a maximum error rate of 2, sequencing errors were modelled and corrected, and noisy, chimeric reads, as well as singletons, were removed. Prior to paired-end merging, forward and reverse reads were quality filtered and truncated at 230 bp and 100 bp, respectively, based on inspection of quality score profiles. The denoised paired-end reads were then merged and dereplicated to generate high-resolution amplicon sequence variants (ASVs). Taxonomic assignment was performed against the SILVA v132 reference database. Non-bacterial reads (eukaryotic, mitochondrial, chloroplast) were excluded. Alpha diversity (Shannon index) and beta diversity (Bray–Curtis distances) were calculated in R (v4.0.3). Alpha diversity (Shannon index) was compared among treatment groups using a one-way ANOVA and Tukey's Honestly Significant Difference (HSD) post hoc test. Differences in beta diversity were assessed using Bray–Curtis distance matrices and Aitchison distances, and evaluated with a PERMANOVA. Differences were considered significant at $p < 0.05$. Principal Coordinate Analyses (PCoA) were visualised in R (v4.0.3) using the devtools, ggplot2, tidyverse, and qiime2R packages.

Core microbiome

Amplicon sequence variants (ASVs) present in at least 80% of replicates within each treatment were defined as core members. Venn diagrams and pie charts were produced in R using ggplot2 and RColorBrewer. Taxa below 2% relative abundance were pooled under the category "Others".

Functional profiling

Functional predictions were carried out using METAGENassist (Arndt et al., 2012). Taxonomic profiles were aggregated at genus level, normalised by sample sum and

Pareto scaling, and subjected to comparative analyses. Predicted metabolic pathways were analysed using both z-score–based enrichment and $\log_2$ fold-change calculations to quantify functional differences between treatment groups. Z-scores were computed relative to the control group to identify significantly enriched or depleted pathways. Log_2 fold-changes were calculated for each treatment comparison, and pathway abundances were statistically evaluated using group-wise ANOVA or Kruskal–Wallis tests (depending on data distribution), followed by adjusted post-hoc comparisons. This approach allowed for quantitative assessment of functional shifts despite the predictive nature of amplicon-based pathway inference. Heatmaps were created to visualise z-transformed data and $\log_2$ fold changes relative to controls. Enrichment is shown in red, depletion in blue. All tests and visualisations were conducted in R (v4.0.3).

6.4 Results

Lethal responses of *B. stephanieae* to cobalt and nickel

Throughout the 96-hour preliminary toxicity range-finding test (cobalt: 3 mg/L - 32 mg/L; nickel: 3 mg/L - 37 mg/L), all slugs in the control group remained healthy, and feeding and movement were observed within 96 hours. For cobalt and nickel, lethargic behaviour (no feeding, no movement, cerata autotomy) was noticed at a concentration of around 18 mg/L for nickel and cobalt.

Since the protein concentrations obtained from the dead slugs were too low, normalisation to the sample protein amount was only possible for the slugs that survived the toxicity range-finding test (Additional file 1: Table 1). The ICP-OES analysis revealed that with increasing cobalt and nickel concentrations, the metal bioavailability increased (Kruskal Wallis test: cobalt: H = 18.234, p = 0.002657 **, df = 5; nickel: H = 20.192, p = 0.00115 **, df = 5; Additional file 1: Table 2-5). First significant differences to the control were already observed in group Co_A (3 mg/L) with an average of 9 pg Co/µg protein (Dunn's test with Bonferroni correction: p = 0.04167 *). With an average of 24 pg Co/µg protein, the cobalt concentration in the group Co_C (18 mg/L) differed significantly from the control group (Dunn's test with Bonferroni correction: p = 0.0009 **). Also, the group Co_E (32 mg/L) differed significantly from the control group with an average cobalt concentration of 33 pg Co/µg protein (Dunn's test with Bonferroni correction: p = 0.0024 **; Additional Fig. 1A). Interestingly, the nickel content of the control group already showed a relatively high concentration with an average of 5 pg Ni/µg protein (Additional file 1: Tables 6 and 7). All groups differed significantly in their averaged nickel concentration to the control group, reaching a concentration of 45 pg Ni/µg protein in group Ni_E (37 mg/L) (Dunn's test with Bonferroni correction: Ni_A (3 mg/L): p = 0.0325 *, Ni_B (14 mg/L): p = 0.0016 **, Ni_C (18 mg/L): p = 0.0117 *, Ni_D (32 mg/L): p = 0.0186 *, Ni_E (37 mg/L): p = 0.0042 **; Supplementary Material 1: Table 6 and 7). Further post hoc testing revealed that the groups Ni_B (14 mg/L) and Ni_E (37 mg/L) differed significantly from group Ni_A (3 mg/L) (Dunn's test with Bonferroni correction: Ni_B (14 mg/L): p = 0.047 *, Ni_E (37 mg/L): p = 0.0336*; Additional Fig. 1B).

Microbiome diversity metrics

Sequencing generated a total of 1,079,009 raw reads from all 36 samples. Following quality processing (merging, denoising, and chimera removal), 400,104 reads were retained, corresponding to an average of 11,114 sequences per sample. Rarefaction

analyses reached saturation for all datasets, indicating that bacterial diversity was adequately captured.

The control samples exhibited the highest alpha diversity, with slightly lower values observed in slugs exposed to 1 mg/L nickel or cobalt (N1 and C1; Fig. 1A). In contrast, the lowest diversity was recorded in one replicate of the 17 mg/L cobalt treatment (C3), which reached a Shannon index of 2.1 (Additional file 2: Table 3). One-way ANOVA showed significant variation in Shannon indices among the groups ($F_{(6,29)}$ = 8.047, $p < 0.001$; Additional file 2: Table 4). Post hoc Tukey's HSD tests revealed that all cobalt treatments (1, 3, and 17 mg/L) differed significantly from the control. For nickel, only the lowest (N1, 1 mg/L) and highest (N3, 17 mg/L) concentrations showed significant differences from the control group. A direct comparison between treatments indicated one additional significant contrast, namely between the 3 mg/L nickel group (N2) and the 17 mg/L cobalt group (C3).

Principal coordinate analysis (PCoA) based on Bray–Curtis dissimilarities showed distinct clustering patterns. Along the first two axes (PC1 and PC2), samples grouped consistently by treatment: controls clustered together with the highest exposure groups (N3 and C3), the lowest exposure groups (C1 and N1) formed another cluster, and the intermediate groups (N2 and C2) clustered separately (Fig. 1B). When visualised along PC2 and PC3, however, the control samples separated clearly from all metal-exposed groups, indicating that exposure strongly altered community composition (Fig. 1C). These patterns were supported by PERMANOVA analysis (999 permutations), which confirmed that beta diversity differed significantly among treatments (pseudo-F_7 = 7.142927, p = 0.001). Pairwise post hoc tests detected significant contrasts between nearly all treatment combinations, with the sole exception of N1 (1 mg/L nickel) and C1 (1 mg/L cobalt), which did not differ significantly (Additional file 2: Tables 5 and 6; Additional Fig. 3). To account for compositional effects, beta diversity was additionally assessed using Aitchison distances calculated from centered log-ratio (CLR)–transformed relative abundances. PCoA based on Aitchison distances showed clustering patterns consistent with the Bray–Curtis results. PERMANOVA on Aitchison distances confirmed a significant treatment effect for both metal groups (metal C: pseudo-F_3 = 5.41, R^2 = 0.49, p = 0.001; metal N: pseudo-F_3 = 5.05, R^2 = 0.49, p = 0.001), indicating that the observed beta diversity patterns were robust to the choice of distance metric.

Core microbiome

The core microbiome of the control group comprised 40 ASVs. Among these, *Mycoplasma* spp. accounted for 35.2% of the total reads, followed by members of the Rhodobacteraceae (19.3%) and uncultured bacteria affiliated with the NS10 marine group (5.2%) (Fig. 6.2).

Within the cobalt-treated group, the C1 (1 mg/L) group harboured the highest number of unique ASVs (18) and shared the greatest number of ASVs with N1, encompassing taxa from 12 different bacterial phyla (Additional file 2: Tables 7 and 8). In C1, *Mycoplasma* sp. remained dominant (45%), followed by *Pseudofulvibacter* (24%). The core microbiome of C2 (3 mg/L) consisted of 12 ASVs, with *Shewanella* sp. (33%), *Mycoplasma* sp. (25%), *Alteromonas* sp. (21%), and Rhodobacteraceae (8.9%) being the most abundant taxa. In contrast, C3 (17 mg/L) exhibited the lowest ASV richness (11 ASVs), with *Mycoplasma* sp. reaching a relative abundance of 52%, followed by *Arcticibacterium luteifluviistationis* (14.4%), *Alteromonas* sp. (11.6%), and *Roseivirga* sp. (10.3%). Among all cobalt-treated groups, C1 shared the most ASVs

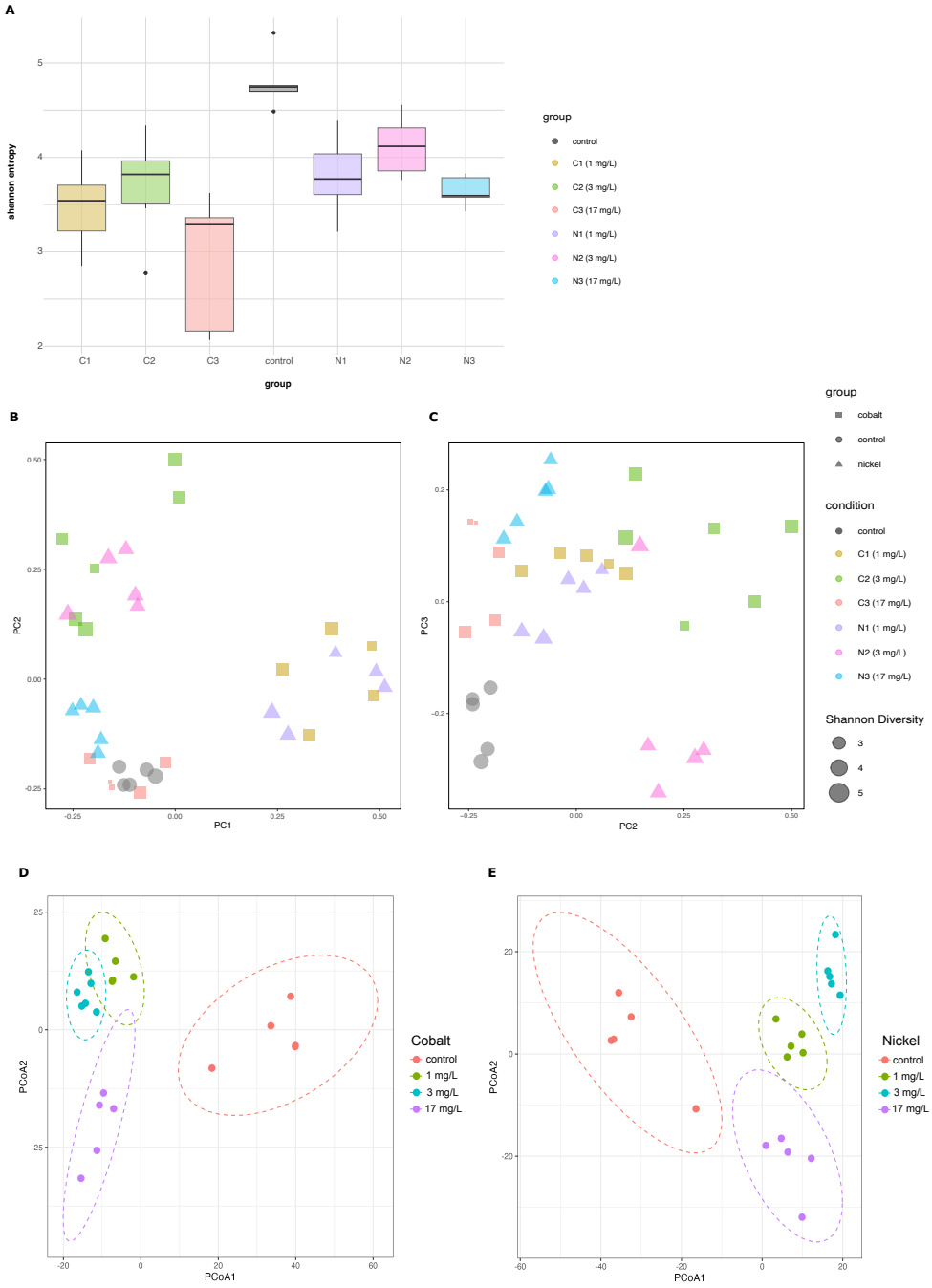

FIGURE 6.1: Box plots displaying alpha-diversity based on Shannon entropy of the different groups (A). Colours indicate exposure dose (control, Cobalt groups: C1 = 1 mg/L; C2 = 3 mg/L; C3 = 17 mg/L. Nickel groups: N1 = 1 mg/L; N2 = 3 mg/L; N3 = 17 mg/L). Principal coordinate analysis (PCoA) illustrating patterns of alpha- and beta-diversity. Plots show sample distribution along PC1 vs. PC2 (B) and PC2 vs. PC3 (C) based on Bray–Curtis distances. Circles denote treatment groups (control, cobalt, nickel); colours indicate exposure condition (control, Cobalt groups: C1 = 1 mg/L; C2 = 3 mg/L; C3 = 17 mg/L. Nickel groups: N1 = 1 mg/L; N2 = 3 mg/L; N3 = 17 mg/L); circle size reflects the Shannon index. Principal coordinate analysis (PCoA) illustrating patterns of beta-diversity based on Aitchison distances for cobalt (D) and nickel (E). Colours represent different exposure condition (control, Cobalt groups: C1 = 1 mg/L; C2 = 3 mg/L; C3 = 17 mg/L. Nickel groups: N1 = 1 mg/L; N2 = 3 mg/L; N3 = 17 mg/L).

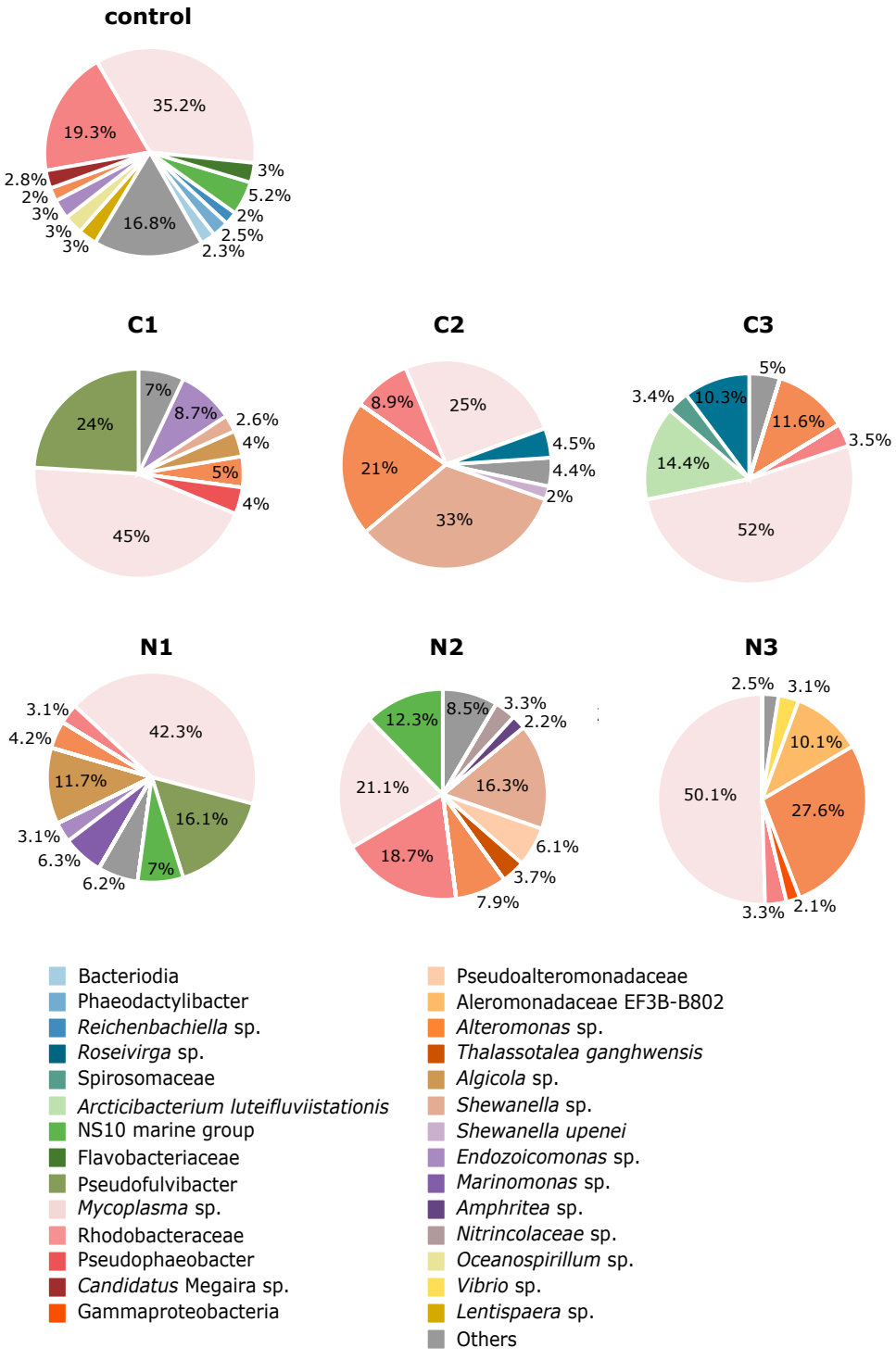

FIGURE 6.2: Core microbiome of *B. stephanieae* treated with different Co or Ni concentrations. All ASVs found in at least 80% of all samples of the corresponding condition were classified as core microbiome. Each colour denotes a unique ASV represented by more than 2%; rare ASVs have been condensed in the group "Others" and are shown in grey. Cobalt groups: C1 = 1 mg/L; C2 = 3 mg/L; C3 = 17 mg/L. Nickel groups: N1 = 1 mg/L; N2 = 3 mg/L; N3 = 17 mg/L.

with the control (11 shared ASVs), followed by C1 and C2, which had 8 ASVs in common (Fig. 6.3A).

In the nickel-treated group, N1 (1 mg/L) harboured 21 ASVs, with *Mycoplasma*

sp. again being the most dominant (42.3%), followed by *Pseudofulvibacter* (16.1%) and *Algicola* sp. (11.7%) (Additional File 4: Tables 9 and 10). The N2 (3 mg/L) group shared 13 ASVs with N1, out of a total of 21 ASVs (Fig. 6.3B). Dominant taxa in N2 included *Mycoplasma* sp. (21.1%), Rhodobacteraceae (18.7%), *Shewanella* sp. (16.3%), and uncultured bacteria from the NS10 marine group (12.3%). N3 (17 mg/L) displayed the lowest ASV richness among the nickel-treated groups (12 ASVs), with *Mycoplasma* sp. reaching 50.1% relative abundance. Other major taxa included *Alteromonas* sp. (27.6%) and Alteromonadaceae EF3B-B802 (10.1%).

Across all treatments, five ASVs were consistently present in the core microbiome: *Mycoplasma* sp., Rhodobacteraceae, *Alteromonas*, *Vibrio*, and an unclassified member of Gammaproteobacteria, suggesting a shared core community independent of metal exposure.

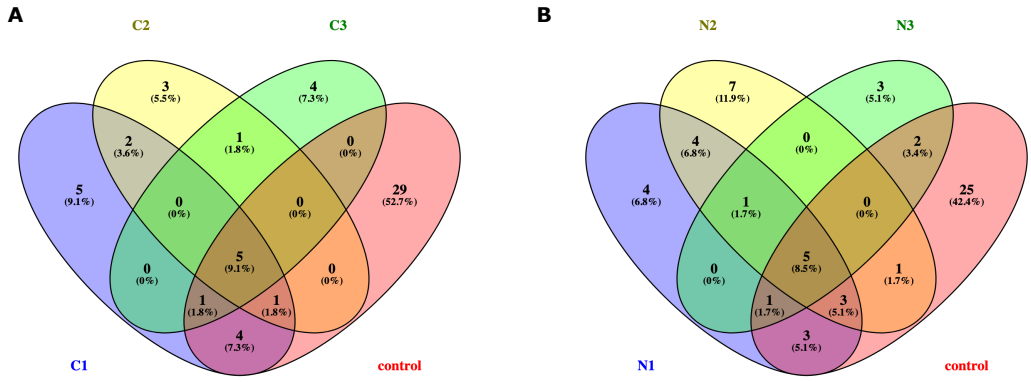

FIGURE 6.3: Comparison of core microbiomes of B. stephanieae across metal treatments using Venn diagrams. Shared and unique ASVs are indicated for the control versus cobalt groups (A) and for the control versus nickel groups (B). Numbers represent the counts of ASVs in each category. Cobalt groups: C1 = 1 mg/L; C2 = 3 mg/L; C3 = 17 mg/L. Nickel groups: N1 = 1 mg/L; N2 = 3 mg/L; N3 = 17 mg/L.

Pathway abundance

We further analysed the absolute abundances of metabolic pathways in each sample and compared them across treatment groups (Additional file 2: Table 11; Additional Fig. 4). Clustering based on z-transformed data revealed distinct groupings of the samples (Fig. 4A; Additional file 2: Table 12). Samples from groups N2 and C2 (both 3 mg/L) formed a tight cluster, along with one N3 sample (17 mg/L; N4), indicating strong similarity in metabolic activity within this subset. Another clearly defined cluster comprised a mix of C1 and N1 samples (both 1 mg/L), suggesting comparable pathway profiles between these groups. The remaining samples, including most of C3, N3, and the controls, grouped together in a broader cluster, with the exception of one C1 sample (C15), which deviated from its group and associated with this set.

Clustering based on log2 fold changes in pathway abundance relative to the control revealed distinct treatment group patterns (Fig. 4B; Additional file 2: Table 13). Groups C3 and N3 (both 17 mg/L) clustered closely together, largely driven by a pronounced downregulation of the "Denitrifying" pathway and a general trend of mild downregulation across most pathways, with "Atrazine metabolism" slightly upregulated in N3. Group C2 (3 mg/L) grouped near C3/N3, reflecting a similarly

strong reduction in "Denitrifying." Across all four groups — C1 and N1 (both 1 mg/L), N2, and C2 (both 3 mg/L) — the pathway "Stores polyhydroxybutyrate" was consistently downregulated, while "Atrazine metabolism" showed a modest upregulation. N2, however, clustered with C1 and N1, likely due to upregulation of pathways such as "Lignin degrader," "Denitrifying," and "Sulfur oxidizer," which distinguished it from C2. Overall, C1 and N1 displayed highly similar profiles, though C1 showed a stronger downregulation of the "Xylan degrader" pathway.

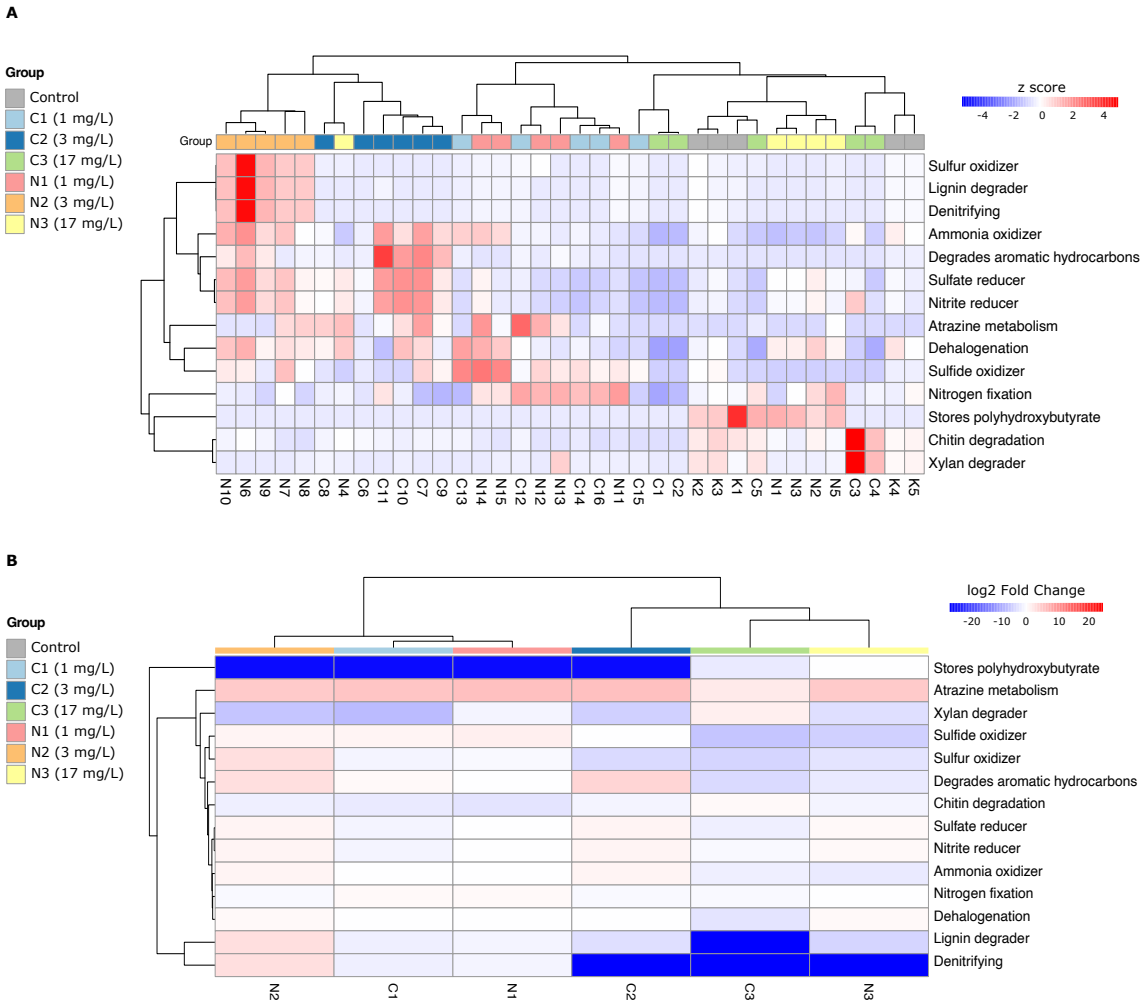

FIGURE 6.4: Taxonomy-based functional profiling of bacterial communities. Heatmaps illustrate predicted functional shifts across the seven treatment groups (control, C1–C3, N1–N3). Pathway abundances are shown on a z-transformed scale (A), and log2 fold changes relative to the control are displayed (B). Enrichment is indicated in red, depletion in blue, with treatment groups distinguished by colour. Cobalt groups: C1 = 1 mg/L; C2 = 3 mg/L; C3 = 17 mg/L. Nickel groups: N1 = 1 mg/L; N2 = 3 mg/L; N3 = 17 mg/L.

Statistical analyses using either ANOVA or Kruskal-Wallis tests revealed significant differences in the regulation of all 14 predicted metabolic pathways across at least two treatment groups. To identify which groups differed, appropriate post hoc tests were applied: Tukey's HSD, Games-Howell, or Dunn's test with Bonferroni correction, depending on the underlying data distribution (Additional file 2: Table 14 for details). Significant differences between control and cobalt-treated slugs were observed in three metabolic pathways: "Chitin degradation" (C1), "Atrazine

metabolism" (C2), and "Denitrifying" (C2). For the nickel-treated groups, two pathways differed significantly from the control: "Chitin degradation" (N1) and "Xylan degrader" (N2). In addition, six pathways showed significant differences between cobalt- and nickel-treated slugs. Notably, group C3 (17 mg/L) differed from all nickel-treated groups in the pathway "Dehalogenation". Furthermore, groups N2 (3 mg/L) and C3 showed significant differences in three pathways: "Ammonia oxidizer", "Sulfate reducer", and "Nitrite reducer". Group N3 (17 mg/L) also differed from C3 in "Ammonia oxidizer" and "Degrades aromatic hydrocarbons", while N2 differed from C1 (1 mg/L) in the pathways "Sulfate reducer" and "Nitrite reducer". Apart from the pathway "Dehalogenation" (N3–C3), no significant differences were observed between groups treated with the same metal concentration. Within the cobalt-treated groups, five metabolic pathways differed significantly. Group C2 (3 mg/L) showed elevated "Sulfate reducer" and "Nitrite reducer" activity compared to C1 and C3. In addition, C2 differed significantly from C3 in three further pathways: "Ammonia oxidizer", "Degrades aromatic hydrocarbons", and "Atrazine metabolism". Among the nickel-treated groups, seven metabolic pathways were significantly different. Group N1 (1 mg/L) differed from N2 in "Nitrogen fixation" and "Denitrifying", and from N3 in "Stores polyhydroxybutyrate" and "Sulfide oxidizer". Group N2 also differed from N3 in five metabolic pathways: "Degrades aromatic hydrocarbons", "Stores polyhydroxybutyrate", "Denitrifying", "Lignin degrader", and "Sulfur oxidizer". All were upregulated in N2, except "Stores polyhydroxybutyrate".

6.5 Discussion

In preliminary toxicity tests, we investigated the effects of nickel and cobalt exposure on *B. stephanieae*. Metal uptake increased with rising concentrations, and the first signs of strong lethargic behaviour (little movement, no feeding, shedding of the cerata) were observed at a relatively high concentration of around 18 mg/L for nickel and cobalt. In cnidarians, the photobionts play a central role in the regulation of internal metal concentrations. The photobionts accumulate significantly more metal than their coral host, and under stress conditions, e.g. increased metal exposure, the symbiosis can break down, leading to expulsion of the photobiont, a reaction commonly referred to as bleaching (Douglas, 2003). This loss is thought to act as a detoxification strategy, allowing the host to reduce the intracellular metal load by removing the symbionts that have accumulated these metals (Bastidas & Garcia, 2004; Hardefeldt & Reichelt-Brushett, 2015; Meehan & Ostrander, 1997; Peters et al., 1997; A. J. Reichelt-Brushett & McOrist, 2003). In our study, individuals of *B. stephanieae* exposed to a concentration of around 18 mg/L of nickel or cobalt began to actively shed their cerata, a behaviour not observed at lower concentrations. Since the photobionts are stored intracellularly in the epithelial cells of the digestive gland system located within the cerata, this autotomy behaviour may serve as a detoxification strategy, allowing the slug to discard tissue compartments in which metal-accumulating symbionts reside (J. W. Brown et al., 2024). Similar to bleaching in corals, the loss of cerata could therefore represent a stress-induced mechanism to mitigate intracellular metal burden by eliminating the symbiont-bearing structures.

Interestingly, individuals from the control group already exhibited relatively high baseline levels of nickel. One possible explanation for this observation is the presence of the metalloenzyme urease, which contains two nickel ions at its active site. Urease plays a key role in nitrogen metabolism by catalysing the hydrolysis of urea

into ammonia and carbon dioxide. In the photosymbiotic giant clam *Tridacna squamosa*, for example, urease enables the host to supply nitrogen to its algal symbionts in the form of urea, which the symbionts then utilise for their own metabolism (Ip et al., 2020). A similar mechanism may exist in *B. stephanieae*, in which the slug provides nitrogen to the intracellularly retained Symbiodiniaceae. However, further experimental evidence is needed to confirm this hypothesis, such as the quantification of urease gene expression.

The metal concentrations used for the microbiome analysis in this study were selected based on both environmentally measurements and results from our preliminary toxicity tests. A concentration of 1 mg/L (group C1/N1) reflects values already exceeded in mining-impacted coastal waters such as those in Canada and New Caledonia, and lies within the range of estimated EC10 values reported for some marine molluscs such as *Mytilus galloprovincialis* and *Crassostrea gigas* (Environment and Climate Change Canada, 2017; Fernandez et al., 2006; Merrot et al., 2019; Noël et al., 2015; Saili et al., 2021). Our intermediate concentration of 3 mg/L (group C2/N2) was chosen based on our pre-tests showing the first significant uptake of cobalt in *B. stephanieae*. The highest test concentration, 17 mg/L (group C3/N3), was selected because it induced the first clear behavioural stress responses in the slugs during our initial preliminary toxicity range finding tests.

Our results demonstrate that both nickel and cobalt exposure cause concentration-dependent shifts in the bacterial microbiome of *B. stephanieae*, with changes detectable already at 1 mg/L. This contrasts with findings from coral studies, such as *Acropora muricata*, where similar nickel concentrations did not elicit microbiome shifts (Gissi et al., 2019). In tropical marine invertebrates, chronic nickel toxicity studies report effects primarily on survival, growth and reproduction across taxa such as copepods, echinoderms and gastropods, with chronic effect concentrations ranging from approximately 1 – 3.7 mg Ni/L (Gissi et al., 2020). This highlights that the microbiome of *B. stephanieae* may represent a particularly sensitive and early-responding compartment compared to classical ecotoxicological endpoints in other invertebrate models. At our lowest concentration, alpha diversity declined significantly, and beta diversity analyses revealed marked shifts in bacterial composition, regardless of whether nickel or cobalt was applied. This suggests that the microbiome responds primarily to metal concentration at low exposure levels, rather than to the specific metal itself. For example, both C1 and N1 (1 mg/L) were dominated by *Mycoplasma* sp., but *Pseudofulvibacter* sp. and *Endozoicomonas* sp. also increased compared to the control. *Pseudofulvibacter* are widespread in marine environments, having been found in hydrothermal fluid sediments, oil-polluted coastal areas, and microbial mats (Acosta-González et al., 2013; R. E. Anderson et al., 2013; Bai et al., 2009; Goudriaan et al., 2024; Schauer et al., 2010). *Endozoicomonas* sp. are known as parasites and pathogens in fish and clams but are also the most common and most frequently found bacterial genus in photosymbiotic Cnidarians worldwide (Epstein et al., 2025; Hochart et al., 2023; Katharios et al., 2015; McCauley et al., 2023). They are involved in various metabolic pathways such as carbon and nitrogen cycling, as well as sulphur (DMSP) and phosphorus degradation (Maire et al., 2023; Neave et al., 2017; Pogoreutz et al., 2022; Tandon et al., 2020). Therefore, *Endozoicomonas* are considered an important mutualist for photosymbiosis in corals and have also been detected in other marine slugs such as *Elysia crispata* (Keller-Costa et al., 2021; Mahadevan & Middlebrooks, 2020; McDevitt-Irwin et al., 2017). In this context, the relative increase of *Endozoicomonas* at 1 mg/L metal exposure suggests that taxa typically associated with coral health and stress mediation may also contribute to functional buffering under metal stress in non-cnidarian hosts, analogous to proposed roles in

coral probiotic or microbiome-transplant frameworks (Doering et al., 2021). At 3 mg/L, metal-specific effects began to emerge: while bacterial richness remained stable, community composition changed drastically, leading to strong upregulation of functional pathways. *Mycoplasma* sp. declined further, while *Shewanella* sp., a genus known for its broad metal reduction capabilities (Dikow, 2011), increased notably in both cobalt (C2) and nickel (N2) treatments. Although *Shewanella* is not known to reduce Co(II) or Ni(II), its metabolic versatility and potential for metal binding or sequestration may offer a competitive advantage under metal stress (Cerbino et al., 2023; Heidelberg et al., 2002). Similar patterns of metal-induced physiological and metabolic responses, including oxidative stress and shifts in microbial associations, have been reported in marine bivalves such as *Mytilus* spp. exposed to nickel, where altered biomarker profiles point to community-level adaptation rather than uniform collapse under chronic exposure (Correia et al., 2025). At this concentration, several functional pathways were slightly upregulted in N2, such as "Lignin degrader", "Denitrifying" and "Sulfur oxidizer", clustering with group N1 and C1. In C2 "Denitrifying" was strongly downregulted, similar to the groups C3 and N3. It therefore appears that C2 and N2 represent a transitional concentration regarding bacterial pathway shifts as the groups cluster either with N1/C1 or N3/C3 in terms of their log2 fold change. This non-linear response is consistent with observations from multi-stressor metal studies on marine invertebrates, where intermediate contamination levels often coincide with pronounced metabolic and transcriptomic reprogramming, while very low or very high levels show weaker relative change (Bonaventura et al., 2022; Brooks et al., 2023; Poynton et al., 2014) Interestingly, many of these functional changes were downregulated again at 17 mg/L (C3 and N3), which manifests itself in lethargic behaviour of *B. stephanieae* as observed in our preliminary tests. This suggests a potential tipping point at which functional redundancy is lost, or key microbial contributors are no longer present. The overall pattern indicates that intermediate concentrations (3 mg/L) elicit the strongest metabolic responses, likely driven by a shift toward stress-tolerant or opportunistic taxa that can temporarily compensate for lost functions before overall microbial resilience declines under high metal exposure. In contrast to corals, where microbiome structure often remains comparatively stable across a range of metal exposures and most documented effects manifest in host physiology and calcification, *B. stephanieae* shows that the microbiome itself is a primary and sensitive target of nickel and cobalt stress (Gissi et al., 2019; A. R. Mohamed et al., 2023; Ruiz-Toquica et al., 2025). A major strength of the present study is the integrative approach combining metal bioavailability, host stress responses, microbiome composition, and predicted microbial metabolic functions. Moreover, this is the first study to investigate nickel- and cobalt-induced microbiome shifts in a photosymbiotic marine gastropod, thereby extending metal ecotoxicology beyond traditional coral models. This study is directly relevant to the United Nations Sustainable Development Goals (SDG), particularly SDG 14 (Life Below Water), as it improves our understanding of how metal pollution affects marine host–microbiome systems (United Nations, Department of Economic and Social Affairs, 2015b). Furthermore, our findings contribute to SDG 12 (Responsible Consumption and Production) by highlighting potential ecological trade-offs associated with the growing demand for nickel and cobalt in renewable energy technologies (United Nations, Department of Economic and Social Affairs, 2015a). Future studies should focus on long-term exposures to assess chronic effects of metal contamination on host–microbiome stability. Integrating metatranscriptomic or metabolomic approaches would allow direct validation of predicted functional shifts. Moreover, extending this framework to field-based studies and

other photosymbiotic marine invertebrates will be essential to evaluate the broader ecological relevance of microbiome-mediated stress responses.

6.6 Conclusion

This study is a first step towards how nickel and cobalt affect the microbiome and microbial metabolic pathways in a marine gastropod, *B. stephanieae*. Our results demonstrate that even low metal concentrations (1 mg/L), already reported in mining-impacted coastal regions, are sufficient to trigger significant shifts in bacterial diversity and community structure. These early changes appear to be primarily concentration-driven rather than metal-specific. At intermediate concentrations (3 mg/L), metal-specific effects emerged, with distinct alterations in microbiome composition and a strong downregulation of functional pathways related to nitrogen and sulfur cycling as well as lignin degradation for cobalt-treated samples. Interestingly, these effects were attenuated at the highest concentration (17 mg/L), suggesting a potential threshold beyond which the microbiome loses functional redundancy, possibly due to toxicity-induced loss of key bacterial taxa. These findings highlight the potential of microbiome analyses as an early-warning indicator for host stress due to metal pollution, underscoring the relevance for coastal conservation and environmental monitoring efforts.

CRediT authorship contribution statement

Corinna Sickinger: Conceptualization, Project administration, Data curation, Writing – original draft, Writing – review and editing; Alicia Thiel: Methodology, Data curation, Writing – review and editing; Julia Bornhorst: Funding acquisition, Methodology, Writing – review and editing; Gregor Christa: Supervision, Writing – original draft, Writing – review and editing; Angelika Preisfeld: Supervision, Writing – review and editing

Funding

This work was supported by the initiative "Metal-based compounds (MeBaCo)", supported by the University of Wuppertal and the Faculty of Mathematics and Natural Sciences. This work was supported by the DFG Research Infrastructure NGS_CC (project 407495230) as part of the Next Generation Sequencing Competence Network (project 423957469). NGS analyses were carried out at the Competence Centre for Genomic Analysis (Kiel).

Conflicts of Interest

The authors declare that the research was conducted without any commercial or financial relationships that could be construed as a potential conflict of interest.

Data Availability

Data have been deposited with links to BioProject accession number PRJNA1298235 in the NCBI BioProject database https://www.ncbi.nlm.nih.gov/sra/PRJNA1298235 with SRA accession numbers listed in Additional File 4: Table 1.

Supplementary Materials

The supplementary material is included in the digital version of this paper.

Additional File 1

Results of the ICP OES analysis: — Table 1. Protein quantification via Bradford. — Table 2. ICP OES results for Co. — Table 3. Co normalisation to the protein content of sample. — Table 4. ICP OES results for Ni. — Table 5. Ni normalisation to the protein content of sample. — Table 6. Statistical analysis of Co concentration between groups. — Table 7. Statistical analysis of Ni concentration between groups.

Additional File 2

— Cellular content of cobalt [pg Co/µg protein] (A) and nickel [pg Ni/µg protein] (B) by element analysis by ICP-OES for *B. stephanieae* exposed to different metal concentrations for 96 hours.

Additional File 3

— Rarefaction curves illustrate ASV richness as a function of sequencing depth for the subsampled dataset.

Additional File 4

Results of the microbiome analysis: — Table 1. Sequencing stats. — Table 2. ASV abundance: Microbiome families. — Table 3. Shannon index. — Table 4. Statistic Shannon. — Table 5. Bray-Curtis distance matrix. — Table 6. Bray-Curtis statistics. — Table 7. Core microbiome Co: absolute frequency — Table 8. Core microbiome Co: relative frequency — Table 9. Core microbiome Ni: absolute frequency — Table 10. Core microbiome Ni: relative frequency. — Table 11. Pathway abundance: absolute frequency. — Table 12. Pathway abundance: z-transformed values. — Table 13. Pathway abundance: log2 Fold Change values. — Table 14. Pathway abundance: statistic.

Additional File 5

— Interactive 3D Principal Coordinate Analysis (PCoA) plot of alpha- and beta-diversity based on PC1, PC2 and PC3. PCoA plot based on Bray-Curtis dissimilarity. Shape of circle represents group (control, Co or Ni), colour of circle represents condition (control, C1, C2, C3, N1, N2 or N3), size of circle indicates Shannon diversity indexs.

6.6.1 Additional File 6

— Correlation analyses between specific microbial taxa and metabolic changes based on Spearman correlation for each condition (control, C1 = 1 mg/L; C2 = 3 mg/L; C3 = 17 mg/L; N1 = 1 mg/L; N2 = 3 mg/L; N3 = 17 mg/L).

References

Acosta-González, A., Rosselló-Móra, R., & Marqués, S. (2013). Characterization of the anaerobic microbial community in oil-polluted subtidal sediments: Aromatic biodegradation potential after the Prestige oil spill. *Environmental Microbiology*, *15*(1), 77–92.

Amaya, D. L. G., Thiel, A., Möller, M., Gasparoni, G., Pirritano, M., Drews, F., Bornhorst, J., & Simon, M. (2023). Microbial impact to environmental toxicants Ni (II) and Co (II): Joint toxicity and cellular response in *Paramecium*. *Chemosphere*, *345*, 140434.

Anderson, R. E., Beltrán, M. T., Hallam, S. J., & Baross, J. A. (2013). Microbial community structure across fluid gradients in the Juan de Fuca Ridge hydrothermal system. *FEMS Microbiology Ecology*, *83*(2), 324–339.

Ansari, N., Rokhbakhsh-Zamin, F., Hassanshahian, M., & Hesni, M. A. (2021). Biodegradation of crude oil using symbiont crude-oil degrading bacteria isolated from corals collected at the Persian Gulf. *Journal of Chemical Technology & Biotechnology*, *96*(7), 1882–1892.

Apte, S., Andersen, L., Andrewartha, J., Angel, B., Shearer, D., Simpson, S., Stauber, J., & Vicente-Beckett, V. (2006). Contaminant pathways in Port Curtis: Final report. *Cooperative Research Centre for Coastal Zone, Estuary and Waterway Management (Coastal CRC), Indooroopilly, Australia*, *143*.

Arndt, D., Xia, J., Liu, Y., Zhou, Y., Guo, A. C., Cruz, J. A., Sinelnikov, I., Budwill, K., Nesbø, C. L., & Wishart, D. S. (2012). METAGENassist: A comprehensive web server for comparative metagenomics. *Nucleic Acids Research*, *40*(W1), W88–W95.

Arnott, S. E., Yan, N., Keller, W., & Nicholls, K. (2001). The influence of drought-induced acidification on the recovery of plankton in Swan Lake (Canada). *Ecological Applications*, *11*(3), 747–763.

Bai, J., Li, H., & Zhao, Y. (2009). Bacterial distribution at different stations in the Northern Yellow Sea. *Acta Microbiologica Sinica*, *49*(3), 343–350.

Bastidas, C., & Garcia, E. (2004). Sublethal effects of mercury and its distribution in the coral *Porites astreoides*. *Marine Ecology Progress Series*, *267*, 133–143.

Bayat, Z., Hassanshahian, M., & Hesni, M. A. (2015). Enrichment and isolation of crude oil degrading bacteria from some mussels collected from the Persian Gulf. *Marine Pollution Bulletin*, *101*(1), 85–91.

Bolyen, E., Rideout, J. R., Dillon, M. R., Bokulich, N. A., Abnet, C. C., Al-Ghalith, G. A., Alexander, H., Alm, E. J., Arumugam, M., Asnicar, F., et al. (2019). Reproducible, interactive, scalable and extensible microbiome data science using QIIME 2. *Nature Biotechnology*, *37*(8), 852–857.

Bonaventura, R., Costa, C., Deidda, I., Zito, F., & Russo, R. (2022). Gene expression analysis of the stress response to lithium, nickel, and zinc in paracentrotus lividus embryos. *Toxics*, *10*(6), 325.

Brocco French, K. I. (2024). With a little help from their friends: Marine Invertebrate Microbiomes in the Face of Global Change. *Diss. University of California, Irvine*.

Brooks, P. R., Browne, M. A., Benedetti-Cecchi, L., Lyons, D. A., & Crowe, T. P. (2023). A response-surface approach into the interactive effects of multiple stressors reveals new insights into complex responses. *Frontiers in Marine Science*, *10*, 1169677.

Brown, J. W., Berg, O. H., Boutko, A., Stoerck, C., Boersma, M. A., & Frost, W. N. (2024). Division of labor for defensive retaliation and preemption by the peripheral and central nervous systems in the nudibranch *Berghia*. *Current Biology*, *34*(10), 2175–2185.

Cerbino, G. N., Traglia, G. M., Ayala Nuñez, T., Parmeciano Di Noto, G., Ramírez, M. S., Centrón, D., Iriarte, A., & Quiroga, C. (2023). Comparative genome analysis of the genus *Shewanella* unravels the association of key genetic traits with known and potential pathogenic lineages. *Frontiers in Microbiology*, *14*, 1124225.

Clavijo, J. M., Sickinger, C., Bleidißel, S., Gasparoni, G., Tierling, S., Preisfeld, A., & Christa, G. (2022). The nudibranch *Berghia stephanieae* (Valdés, 2005) is not able to initiate a functional symbiosome-like environment to maintain *Breviolum minutum* (JE Parkinson & LaJeunesse 2018). *Frontiers in Marine Science*, *9*, 934307.

Correia, A. T., Motta, E., Daniel, D., Nunes, B., & Neves, J. (2025). Ecotoxicological effects of environmentally relevant concentrations of nickel nanoparticles on aquatic organisms from three trophic levels: Insights from oxidative stress biomarkers. *Journal of Xenobiotics*, *15*(4), 112.

Dikow, R. B. (2011). Genome-level homology and phylogeny of *Shewanella* (Gammaproteobacteria: Iteromonadales: Shewanellaceae). *BMC Genomics*, *12*, 1–14.

Diner, R. E., Allard, S. M., & Gilbert, J. A. (2024). Host-associated microbes mitigate the negative impacts of aquatic pollution. *Msystems*, *9*(10), e00868–24.

Doering, T., Wall, M., Putchim, L., Rattanawongwan, T., Schroeder, R., Hentschel, U., & Roik, A. (2021). Towards enhancing coral heat tolerance: A "microbiome transplantation" treatment using inoculations of homogenized coral tissues. *Microbiome*, *9*(1), 102.

Donat, J. R., & Bruland, K. W. (1988). Direct determination of dissolved cobalt and nickel in seawater by differential pulse cathodic stripping voltammetry preceded by adsorptive collection of cyclohexane-1, 2-dione dioxime complexes. *Analytical Chemistry*, *60*(3), 240–244.

Douglas, A. (2003). Coral bleaching–How and why? *Marine Pollution Bulletin*, *46*(4), 385–392.

Eitinger, T., Suhr, J., Moore, L., & Smith, J. A. C. (2005). Secondary transporters for nickel and cobalt ions: Theme and variations. *Biometals*, *18*, 399–405.

Environment and Climate Change Canada. (2017). Screening assessment Cobalt and Cobalt-Containing substances [Accessed: 2024-12-04].

Epstein, H. E., Brown, T., Akinrinade, A. O., McMinds, R., Pollock, F. J., Sonett, D., Smith, S., Bourne, D. G., Carpenter, C. S., Knight, R., et al. (2025). Evidence for microbially-mediated tradeoffs between growth and defense throughout coral evolution. *Animal Microbiome*, *7*(1), 1.

Fernandez, J.-M., Ouillon, S., Chevillon, C., Douillet, P., Fichez, R., & Le Gendre, R. (2006). A combined modelling and geochemical study of the fate of terrigenous inputs from mixed natural and mining sources in a coral reef lagoon (New Caledonia). *Marine Pollution Bulletin*, *52*(3), 320–331.

Fragoso ados Santos, H., Duarte, G. A. S., Rachid, C. T. d. C., Chaloub, R. M., Calderon, E. N., Marangoni, L. F. d. B., Bianchini, A., Nudi, A. H., Do Carmo, F. L., Van Elsas, J. D., et al. (2015). Impact of oil spills on coral reefs can be reduced by bioremediation using probiotic microbiota. *Scientific Reports*, *5*(1), 18268.

Gissi, F., Reichelt-Brushett, A. J., Chariton, A. A., Stauber, J. L., Greenfield, P., Humphrey, C., Salmon, M., Stephenson, S. A., Cresswell, T., & Jolley, D. F. (2019). The effect of dissolved nickel and copper on the adult coral *Acropora muricata* and its microbiome. *Environmental Pollution*, *250*, 792–806.

Gissi, F., Stauber, J. L., Binet, M. T., Golding, L. A., Adams, M. S., Schlekat, C. E., Garman, E. R., & Jolley, D. F. (2016). A review of nickel toxicity to marine and estuarine tropical biota with particular reference to the South East Asian and Melanesian region. *Environmental Pollution*, *218*, 1308–1323.

Gissi, F., Stauber, J. L., Binet, M. T., Trenfield, M. A., Van Dam, J. W., & Jolley, D. F. (2018). Assessing the chronic toxicity of nickel to a tropical marine gastropod and two crustaceans. *Ecotoxicology and Environmental Safety*, *159*, 284–292.

Gissi, F., Wang, Z., Batley, G. E., Leung, K. M., Schlekat, C. E., Garman, E. R., & Stauber, J. L. (2020). Deriving a chronic guideline value for nickel in tropical and temperate marine waters. *Environmental Toxicology and Chemistry*, *39*(12), 2540–2551.

Goodheart, J. A., Rio, R. A., Taraporevala, N. F., Fiorenza, R. A., Barnes, S. R., Morrill, K., Jacob, M. A. C., Whitesel, C., Masterson, P., Batzel, G. O., et al. (2024). A chromosome-level genome for the nudibranch gastropod *Berghia stephanieae* helps parse clade-specific gene expression in novel and conserved phenotypes. *BMC Biology*, *22*(1), 9.

Goudriaan, M., Zeghal, E., Witte, H., Vaksmaa, A., & Niemann, H. (2024). Differentiation of bacterial communities on five common plastics after six days of exposure to Caribbean coastal waters. *Environmental Advances*, *16*, 100518.

Guillén Matus, D. G., Donaghy, C. M., Vijayan, N., Lane, Z. T., Howell, M., Glavin, G. G., Angeles-Boza, A. M., Nyholm, S. V., & Balunas, M. J. (2024). Multiomics analysis reveals important role for microbial-derived metabolites from *Botryllus schlosseri* in metal interactions. *ASM Journals*, 2024–11.

Hardefeldt, J. M., & Reichelt-Brushett, A. J. (2015). Unravelling the role of zooxanthellae in the uptake and depuration of an essential metal in *Exaiptasia pallida*; an experiment using a model cnidarian. *Marine Pollution Bulletin*, *96*(1-2), 294–303.

Heidelberg, J. F., Paulsen, I. T., Nelson, K. E., Gaidos, E. J., Nelson, W. C., Read, T. D., Eisen, J. A., Seshadri, R., Ward, N., Methe, B., et al. (2002). Genome sequence of the dissimilatory metal ion–reducing bacterium *Shewanella oneidensis*. *Nature Biotechnology*, *20*(11), 1118–1123.

Hochart, C., Paoli, L., Ruscheweyh, H.-J., Salazar, G., Boissin, E., Romac, S., Poulain, J., Bourdin, G., Iwankow, G., Moulin, C., et al. (2023). Ecology of Endozoicomonadaceae in three coral genera across the Pacific Ocean. *Nature Communications*, *14*(1), 3037.

International Energy Agency. (2021). The Role of Critical World Energy Outlook Special Report Minerals in Clean Energy Transitions. World Energy Outlook Special Report [Accessed: 2024-12-04].

Ip, Y. K., Teng, G. C. Y., Boo, M. V., Poo, J. S. T., Hiong, K. C., Kim, H., Wong, W. P., & Chew, S. F. (2020). Symbiodiniaceae dinoflagellates express urease in three subcellular compartments and upregulate its expression levels *in situ* in three organs of a giant clam (*Tridacna squamosa*) during illumination. *Journal of Phycology*, *56*(6), 1696–1711.

Katharios, P., Seth-Smith, H. M., Fehr, A., Mateos, J. M., Qi, W., Richter, D., Nufer, L., Ruetten, M., Guevara Soto, M., Ziegler, U., et al. (2015). Environmental marine pathogen isolation using mesocosm culture of sharpsnout seabream:

Striking genomic and morphological features of novel *Endozoicomonas* sp. *Scientific Reports*, *5*(1), 17609.

Keller-Costa, T., Lago-Lestón, A., Saraiva, J., Toscan, R., Silva, S., Gonçalves, J., Cox, C. J., Kyrpides, N., Nunes da Rocha, U., & Costa, R. (2021). Metagenomic insights into the taxonomy, function, and dysbiosis of prokaryotic communities in octocorals. *Microbiome*, *9*, 1–21.

Kimbrough, K. L. (2008). An assessment of two decades of contaminant monitoring in the nation's coastal zone.

Li, J., Zhang, Y., Sun, J., Thompson, F., & Zhang, Y. (2023). Interaction between marine invertebrates and symbiotic microbes in a changing environment: Community structure and ecological functions.

Macomber, L., & Hausinger, R. P. (2011). Mechanisms of nickel toxicity in microorganisms. *Metallomics*, *3*(11), 1153–1162.

Mahadevan, P., & Middlebrooks, M. L. (2020). Bacterial diversity in the *clarki* ecotype of the photosynthetic sacoglossan, *Elysia crispata*. *MicrobiologyOpen*, *9*(9), e1098.

Maire, J., Tandon, K., Collingro, A., van de Meene, A., Damjanovic, K., Gotze, C. R., Stephenson, S., Philip, G. K., Horn, M., Cantin, N. E., et al. (2023). Colocalization and potential interactions of *Endozoicomonas* and Chlamydiae in microbial aggregates of the coral *Pocillopora acuta*. *Science Advances*, *9*(20), eadg0773.

McCauley, M., Goulet, T., Jackson, C., & Loesgen, S. (2023). Systematic review of cnidarian microbiomes reveals insights into the structure, specificity, and fidelity of marine associations. *Nature Communications*, *14*(1), 4899.

McDevitt-Irwin, J. M., Baum, J. K., Garren, M., & Vega Thurber, R. L. (2017). Responses of coral-associated bacterial communities to local and global stressors. *Frontiers in Marine Science*, *4*, 262.

Mebane, C. A., Eakins, R. J., Fraser, B. G., & Adams, W. J. (2015). Recovery of a mining-damaged stream ecosystem. *Elementa*, *3*.

Meehan, W. J., & Ostrander, G. K. (1997). Coral bleaching: A potential biomarker of environmental stress. *Journal of Toxicology and Environmental Health, Part A Current Issues*, *50*(6), 529–552.

Merrot, P., Juillot, F., Noël, V., Lefebvre, P., Brest, J., Menguy, N., Guigner, J.-M., Blondeau, M., Viollier, E., Fernandez, J.-M., et al. (2019). Nickel and iron partitioning between clay minerals, Fe-oxides and Fe-sulfides in lagoon sediments from New Caledonia. *Science of the Total Environment*, *689*, 1212–1227.

Mohamed, A. R., Ochsenkühn, M. A., Kazlak, A. M., Moustafa, A., & Amin, S. A. (2023). The coral microbiome: Towards an understanding of the molecular mechanisms of coral–microbiota interactions. *FEMS Microbiology Reviews*, *47*(2), fuad005.

Naryono, E. (2023). Nickel mine exploitation in Indonesia, between a blessing and a disaster of environmental damage. *Center for Open Science*, 1–22.

Neave, M. J., Michell, C. T., Apprill, A., & Voolstra, C. R. (2017). *Endozoicomonas* genomes reveal functional adaptation and plasticity in bacterial strains symbiotically associated with diverse marine hosts. *Scientific Reports*, *7*(1), 40579.

Nechev, J., Stefanov, K., & Popov, S. (2006). Effect of cobalt ions on lipid and sterol metabolism in the marine invertebrates *Mytilus galloprovincialis* and *Actinia equina*. *Comparative Biochemistry and Physiology Part A: Molecular & Integrative Physiology*, *144*(1), 112–118.

Noël, V., Morin, G., Juillot, F., Marchand, C., Brest, J., Bargar, J. R., Muñoz, M., Marakovic, G., Ardo, S., & Brown Jr, G. E. (2015). Ni cycling in mangrove sediments from New Caledonia. *Geochimica et Cosmochimica Acta*, *169*, 82–98.

Peters, E. C., Gassman, N. J., Firman, J. C., Richmond, R. H., & Power, E. A. (1997). Ecotoxicology of tropical marine ecosystems. *Environmental Toxicology and Chemistry*, *16*(1), 12–40.

Pogoreutz, C., Oakley, C. A., Rädecker, N., Cárdenas, A., Perna, G., Xiang, N., Peng, L., Davy, S. K., Ngugi, D. K., & Voolstra, C. R. (2022). Coral holobiont cues prime *Endozoicomonas* for a symbiotic lifestyle. *The ISME Journal*, *16*(8), 1883–1895.

Poynton, H. C., Robinson, W. E., Blalock, B. J., & Hannigan, R. E. (2014). Correlation of transcriptomic responses and metal bioaccumulation in mytilus edulis l. reveals early indicators of stress. *Aquatic Toxicology*, *155*, 129–141.

Pyle, G., & Couture, P. (2011). Nickel. In *Homeostasis and Toxicology of Essential Metals* (pp. 253–289, Vol. 31A). Elsevier.

Ravera, O. (2001). Monitoring of the aquatic environment by species accumulator of pollutants: A review. *Journal of Limnology*, *60*(1s), 63–78.

Reichelt-Brushett, A. (2012). Risk assessment and ecotoxicology: Limitations and recommendations for ocean disposal of mine waste in the coral triangle. *Oceanography*, *25*(4), 40–51.

Reichelt-Brushett, A. J., & McOrist, G. (2003). Trace metals in the living and nonliving components of scleractinian corals. *Marine Pollution Bulletin*, *46*(12), 1573–1582.

Rola, M., Frankenbach, S., Bleidissel, S., Sickinger, C., Donath, A., Frommlet, J. C., Greve, C., Serôdio, J., Preisfeld, A., Melo Clavijo, J., et al. (2022). Cladobranchia (Gastropoda, Nudibranchia) as a promising model to understand the molecular evolution of photosymbiosis in animals. *Frontiers in Marine Science*, *8*, 745644.

Ruiz-Toquica, J., Herrera, A. F., & Medina, M. (2025). Endozoicomonas dominance and vibrionaceae stability underpin resilience in urban coral madracis auretenra. *PeerJ*, *13*, e19226.

Saili, K. S., Cardwell, A. S., & Stubblefield, W. A. (2021). Chronic toxicity of cobalt to marine organisms: Application of a species sensitivity distribution approach to develop international water quality standards. *Environmental Toxicology and Chemistry*, *40*(5), 1405–1418.

Schauer, R., Bienhold, C., Ramette, A., & Harder, J. (2010). Bacterial diversity and biogeography in deep-sea surface sediments of the South Atlantic Ocean. *The ISME Journal*, *4*(2), 159–170.

Schrauzer, G. (1991). Cobalt in Metals and their compounds, in the environment occurrence, analysis and biological relevance. *Editor Merian EL Editorial VCH Verlagsgesellschaft Weinheim Alemania*, *879*.

Sickinger, C., Brackwehr, S. M., Melo Clavijo, J., Gasperoni, G., Tierling, S., Preisfeld, A., & Christa, G. (2024). Microbiome origin and stress-related changes in bacterial abundance of the photosymbiotic sea slug *Berghia stephanieae* (Á. valdés, 2005). *Symbiosis*, 1–16.

Sun, Z., Gong, C., Ren, J., Zhang, X., Wang, G., Liu, Y., Ren, Y., Zhao, Y., Yu, Q., Wang, Y., et al. (2020). Toxicity of nickel and cobalt in Japanese flounder. *Environmental Pollution*, *263*, 114516.

Tandon, K., Lu, C.-Y., Chiang, P.-W., Wada, N., Yang, S.-H., Chan, Y.-F., Chen, P.-Y., Chang, H.-Y., Chiou, Y.-J., Chou, M.-S., et al. (2020). Comparative genomics:

Dominant coral-bacterium *Endozoicomonas acroporae* metabolizes dimethylsulfoniopropionate (DMSP). *The ISME Journal*, *14*(5), 1290–1303.

United Nations, Department of Economic and Social Affairs. (2015a). Sustainable development goals (sdgs): Goal 12 - responsible consumption and production [Accessed: 2026-01-06].

United Nations, Department of Economic and Social Affairs. (2015b). Sustainable development goals (sdgs): Goal 14 - life below water [Accessed: 2026-01-06].

Van Dam, R., Harford, A., Houston, M., Hogan, A., & Negri, A. (2008). Tropical marine toxicity testing in Australia: A review and recommendations. *Australasian Journal of Ecotoxicology*, *14*(2/3), 55–88.

Weisburg, W. G., Barns, S. M., Pelletier, D. A., & Lane, D. J. (1991). 16S ribosomal DNA amplification for phylogenetic study. *Journal of Bacteriology*, *173*(2), 697–703.

Wood, C. M., Farrell, A. P., & Brauner, C. J. (2012). *Homeostasis and toxicology of essential metals* (Vol. 1). Academic Press.

Xu, L.-L., McIlroy, S. E., Ni, Y., Guibert, I., Chen, J., Rocha, U., Baker, D. M., & Panagiotou, G. (2025). Chemical pollution drives taxonomic and functional shifts in marine sediment microbiome, influencing benthic metazoans. *ISME Communications*, ycae141.

Zeeshan, M., Murugadas, A., Ghaskadbi, S., Ramaswamy, B. R., & Akbarsha, M. A. (2017). Ecotoxicological assessment of cobalt using *Hydra* model: ROS, oxidative stress, DNA damage, cell cycle arrest, and apoptosis as mechanisms of toxicity. *Environmental Pollution*, *224*, 54–69.

Chapter 7

Cobalt and Nickel Inhibit the Ontogenesis of the Cladobranch Sea Slug *Berghia stephanieae* (Á. Valdés, 2005)

Corinna Sickinger[1], Jana Kosky[1], Alicia Thiel[2], Julia Bornhorst[2], Gregor Christa[3] and Angelika Preisfeld[1]

[1]*Institute for Zoology and Didactics of Biology, University of Wuppertal, Wuppertal, Germany*
[2]*Food Chemistry, University of Wuppertal, Wuppertal, Germany*
[3]*Department of Evolution and Biodiversity, University of Wuppertal, Wuppertal, Germany*

7.1 Abstract

Nickel and cobalt are increasingly released into marine ecosystems due to the global rise in battery metal mining, especially in tropical coastal regions. While the toxicity of these metals is well-documented for some marine organisms, their effects on the early development of less-studied invertebrates remain largely unknown. In this study, we investigated the impact of nickel and cobalt on embryonic and larval development in the photosymbiotic sea slug *Berghia stephanieae*. Both metals delayed development and induced morphological abnormalities, with cobalt showing a stronger effect on egg survival than nickel. Our findings reveal the vulnerability of early developmental stages in marine gastropods to metal exposure and highlight the need to include such taxa in future ecotoxicological assessments.

Keywords Cobalt · Nickel · ontogenesis · veliger larvae

7.2 Introduction

As global industries expand and the demand for critical raw materials continues to rise, environmental contamination by heavy metals has emerged as a pressing concern (International Energy Agency, 2021). Nickel (Ni) and cobalt (Co), in particular, have gained increasing attention due to their widespread use in technologies such as lithium-ion batteries, pigments, and metal alloys. Their release into aquatic

environments, primarily through mining operations, industrial discharge, and improper waste management, has led to measurable increases in their concentrations in both coastal and open-water systems (Arnott et al., 2001; Mebane et al., 2015; Pyle & Couture, 2011; Wood et al., 2012). Once introduced into the marine environment, these metals can persist, accumulate in sediments, and bioaccumulate in organisms across trophic levels, ultimately posing risks to ecosystem health and biodiversity (De Schamphelaere et al., 2008; Foroutan et al., 2019; Pyle & Couture, 2011; Raju et al., 2022).

While the toxicological effects of metals on human health and some well-studied marine species are relatively well understood, little is known about their impact on non-commercial invertebrates such as sea slugs, particularly during early developmental stages (Jaishankar et al., 2014; Jomova et al., 2025; Santhosh et al., 2024; Y. Wang et al., 2022). Yet, these organisms play an essential role in coral reef ecosystems by contributing to the breakdown of plant and animal material. Many sea slugs are grazers or predators that feed on algae, sponges, hydroids, bryozoans, and even other sea slugs, helping to regulate populations and facilitate nutrient cycling within the reef environment (H. Y. Chan et al., 2022; Fritts-Penniman et al., 2020). Among marine gastropods, species in the clade Cladobranchia are of particular interest due to their unique biological traits, such as the evolution of photosymbiosis (harbouring photosynthetic symbionts), diverse strategies for prey acquisition and their use as model organisms in studies of evolutionary biology, symbiosis, and marine biodiversity (Rola et al., 2022). However, data on the effects of metal pollution on their early developmental stages remain scarce.

The sea slug *Berghia stephanieae* (Á. Valdés, 2005) is a member of Cladobranchia and has been used as a model organism in various studies due to its ease of laboratory culture and relatively short life cycle (Monteiro et al., 2019; Silva et al., 2021, 2023). Early life stages are typically considered the most sensitive phases in marine invertebrates' life cycles, as they involve rapid morphogenesis, organogenesis, and high metabolic demand (Chiarelli & Roccheri, 2014; Lange & Marshall, 2017; Pineda et al., 2012). Stressors like metal exposure can therefore have disproportionate effects, altering developmental trajectories and potentially impairing survival and reproductive fitness (Campbell et al., 2014; McDougall et al., 2022). These disruptions during early development can act as bottlenecks for population persistence and may have long-term consequences for reproductive success and species survival (Byrne, 2012; Leal et al., 2022)

In this study, we investigate how exposure to nickel and cobalt affects the embryonic and larval development of *B. stephanieae*, focusing on developmental timing and morphological progression under controlled laboratory conditions. By examining these early life stages, we provide valuable insight into how metal pollution may influence the ontogeny of marine gastropods. Our findings offer a first step toward better understanding the sensitivity of coral reef–associated invertebrates to environmental contamination during their most vulnerable developmental phases.

7.3 Materials and Methods

Berghia stephanieae culture

In January 2022, six breeding pairs of *B. stephanieae* were purchased from a local provider (aquaPro2000 GmbH, Germany). Each pair was kept in a 75 mm diameter plastic container with a lid (FAUST Lab Science) in 35 ml artificial seawater (ASW) at 21°C, 30 µmol photons m^{-2} s^{-1} light intensity (Daylight Sunrise 520, Sera), and a

day/night cycle of 12h / 12h. Freshly prepared ASW with a salinity of 33 PSU, pH of 8.0, and a temperature of 21°C was changed three times per week, and slugs were fed small *E. diaphana* anemones (7-mm foot and 4-mm oral disc or 4-mm foot and 3-mm oral disc). Once the breeding pairs spawned, the egg masses were collected and placed in 55 mm diameter plastic container with a lid (FAUST Lab Science) in 25 ml ASW. The egg masses were maintained as stated above, monitored and fed with anemone tentacles as soon as the larvae hatched.

Toxicity tests eggs

Stock solutions (100 mg/L) of nickel and cobalt were prepared using nickel(II) chloride hexahydrate (99.9%, Aldrich) and cobalt(II) chloride hexahydrate (99.998%, Puratronic, Alfa Aesar) in ASW. All test solutions were freshly prepared using stock solution and ASW at test beginning and for each 48-h renewal treatment. Five concentrations and a seawater control were used for both metals (see Table 7.1). For each metal concentration, five egg masses were randomly selected, individually placed in a 55 mm diameter plastic container with a lid, and maintained as stated above. Every 48-h embryological development was checked under a microscope (SteREO Discovery.V8, Zeiss) and noted. As soon as the slugs hatched, they were fed with anemone tentacles. The embryological development of the slugs was categorised into the following stages: 1. Multicell, 2. Early veliger larvae, 3. Veliger larvae, 4. Hatching (Kristof & Klussmann-Kolb, 2010). As embryos and larvae can develop at different rates within one egg mass, the developmental stage at which the majority of embryos or larvae were found was recorded. The embryos or larvae were considered dead if they showed signs of dissolution and no rotation, or if there was no detectable rotation of the embryos or larvae in the egg capsules for at least two consecutive days of observation. When the embryos or larvae were not distinguishable from the inner membrane of the egg, it was considered dissolved. In contrast to the developmental stages, the egg mass was only classified as dead when the above criteria applied to all embryos or larvae and not just the majority. All statistical analyses were conducted in R (Version 2023.09.1+494; R Core Team, 2021).

TABLE 7.1: Concentration of Co and Ni used for the egg toxicity test and the regarding group names. Concentrations correspond to elemental Co or Ni measured with ICP OES. For each group n = 5.

group name	c(Co) µg/L	group name	c(Ni) µg/L
Co_a	420.5	Ni_a	1678.4
Co_b	350.5	Ni_b	978.9
Co_c	280.3	Ni_c	839.5
Co_d	210.2	Ni_d	559.5
Co_e	140.1	Ni_e	419.6

7.4 Results

Regardless of the cobalt concentration, all embryos developed to the early veliger stage (Fig.7.2A). The average time to reach this stage was four days for the control group, nine days for the Co_a group, and 4.8 days for the Co_c group. None of the embryos reached the veliger stage when exposed to a concentration of 771 µg/L Co, and were classified as dead after no movement was noted, and the eggs started

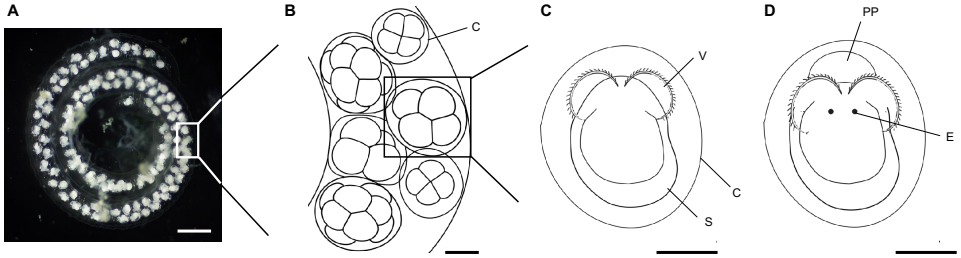

FIGURE 7.1: Egg mass of B. stephanieae (A). Close-up of egg mass with eggs in the multicell stage (B). C = capsule, scale bar represents 100 µm. Early veliger stage larva with a shell and a ciliated velum (C). S = shell, V = velum, scale bar represents 100 µm. Veliger stage larva with eyes and elaborated propodium (D). E = eyes, PP = propodium, scale bar represents 100 µm.

dissolving. All embryos reached the veliger stage in the remaining lower concentrations. However, the embryos took an average of nine to twelve days to develop to the veliger stage, which is longer than the control group's average of 8.4 days. The addition of cobalt notably inhibited embryo development up to hatching. The time from multicell stage to hatching averaged 19 days for group Co_c and 20 days for group Co_e, while the control group needed only 11.75 days (see Supplementary Material 1: Table 1). A Kruskal Wallis test showed that there was a statistically significant difference between at least two groups in the time to reach each development stage (early veliger stage: Chi square = 18.117, p = 0.002804 **, df = 5; veliger stage: Chi square = 91.383, p = 0.02751 *, df = 3; hatching: Chi square = 20.637, p = 0.02282*, df = 2; see Supplementary Material 1, Table 2). Post hoc Dunn's test with Bonferroni correction found that the mean value of days was significantly different between group Co_a and all other groups, except group Co_b to reach the early veliger stage (control: p = 0.001 **, Co_c: p = 0.0359 *, Co_d: p = 0.0221 *, Co_e: p = 0.0221 *; see Figure (Fig.7.2B). For the veliger stage, only the control and Co_d group differed significantly from each other (p = 0.0216 *), and the group Co_e took significantly longer to hatch than the control group (Co_e p = 0.0106 *).

For nickel, all embryos developed to the early veliger stage (Fig.7.3A). The embryos of group Ni_a needed an average of seven days to reach the early veliger stage, and was the only group that was considered dead before reaching the second state, the veliger stage. All lower concentrations developed up to the veliger stage, needing more than 10 days, which differed notably from the control group (8.4 days). Even though two groups, Ni_d and Ni_e, made it to hatching, they took longer compared to the control group with 14 and 19.5 days (see Supplementary Material 1: Table 3). A Kruskal Wallis test or one-way ANOVA was performed to compare the effect of nickel on the time of development till each stage which revealed a significant difference between at least two of the groups for all developing stages (early veliger: Chi square = 14.368, p = 0.01343 *, df = 5; veliger: F(4,11) = 10.13, p = 0.00109 **; hatching: F(2, 4) = 14.25, p = 0.0151 *; see Supplementary Material 1, Table 4). Post hoc Dunn's test with Bonferroni correction showed that there was no significant difference in days between the groups for the early veliger stage except between the control and group Ni_a (p = 0.0227 *) as well as control and Ni_c (p = 0.0273 *; Fig.7.3B). However, for the veliger stage significant differences were indicated between the control group and the groups Ni_b, Ni_c and Ni_e (Tukey's HSD: Ni_b p = 0.001068981 **, 95% C.I. = 2.7560958, 10.04390422; Ni_c p = 0.016689955 *, 95% C.I. = 0.7560958, 8.04390422; Ni_e p = 0.013398532 *, 95% C.I. = 0.7283769, 6.57162310; see)

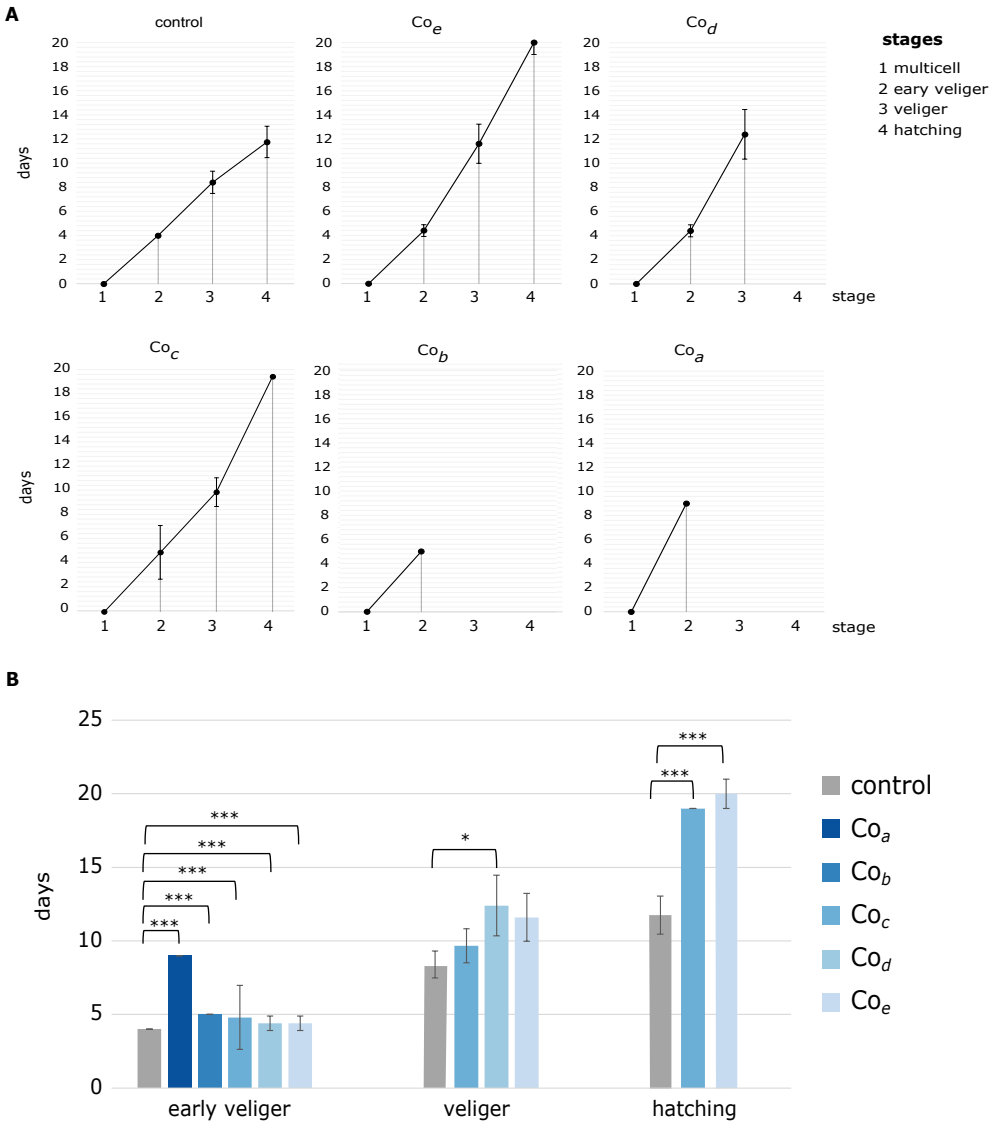

FIGURE 7.2: Egg development under Co exposure. The average duration in days to reach each developmental stage (multicell, early veliger, veliger and hatching) is shown for the control, Co_a, Co_b, Co_c, Co_d, Co_e (A) and the statistical differences in the duration of egg development under Co (B). Colours represent the control and metal-treated groups. Significant differences are depicted as follows: p <0.0005 '***', p <0.005 '**', p <0.05 '*'.

as well as between Ni_b and Ni_d (Tukey's HSD: p = 0.048422163, 95% C.I. = -7.9758255, -0.02417454). Further, only group Ni_d differed significantly from the control group regarding their time to reach the hatching stage (Tukey's HSD: p = 0.0129873 *, 95% C.I. = 2.573774, 12.926226).

In addition, we employed Fisher's Exact Test to explore the relationship between exposure to nickel or cobalt and mortality. The analysis was conducted using a contingency table that cross-tabulated group membership (including five different groups and one control group) against mortality status (alive or dead). The resulting p-value from Fisher's Exact Test was 0.0001153 for cobalt and 0.01636 for nickel, indicating a significant association between metal exposure and mortality.

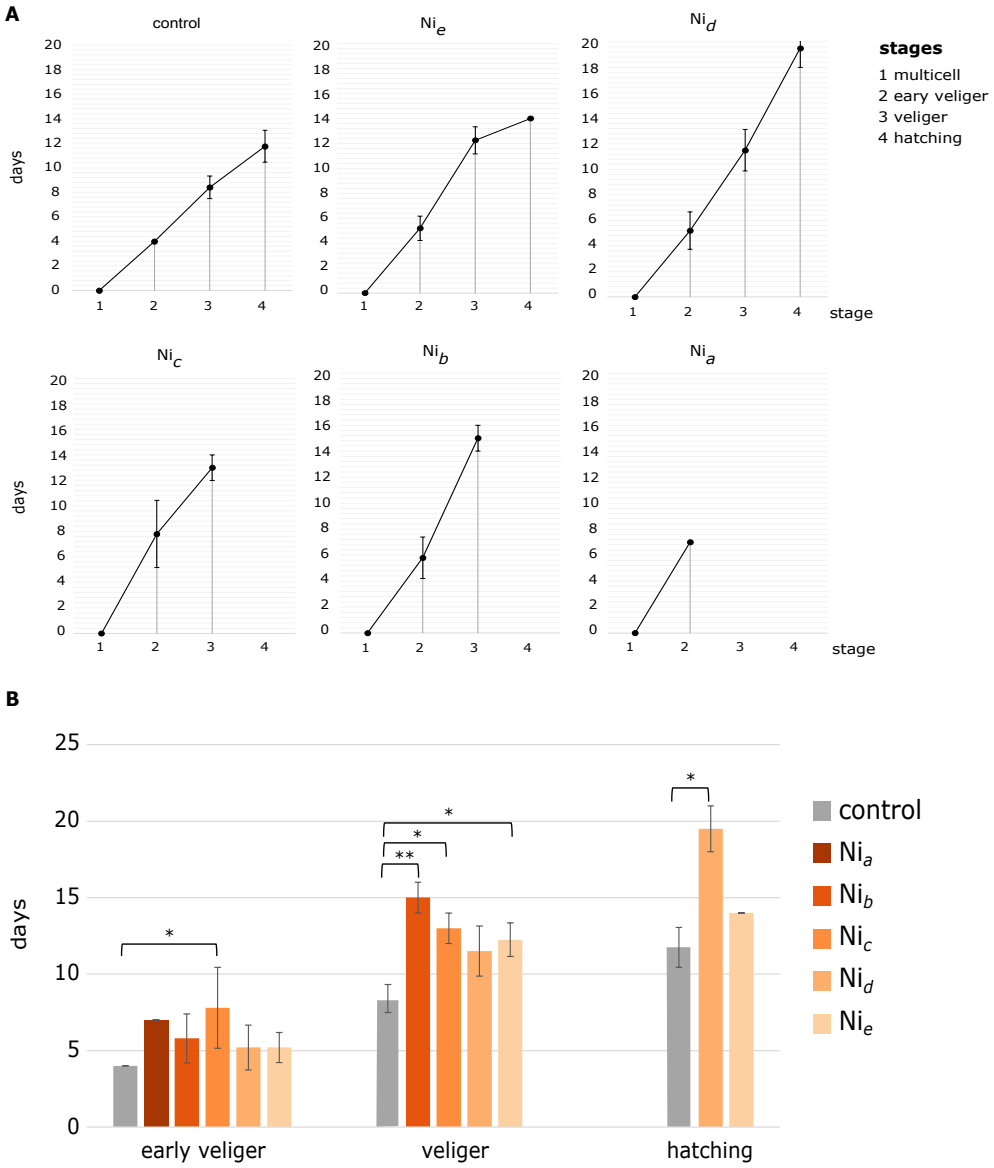

FIGURE 7.3: Egg development under Ni exposure. The average duration in days to reach each developmental stage (multicell, early veliger, veliger and hatching) is shown for the control, Ni_a, Ni_b, Ni_c, Ni_d, Ni_e (A) and the statistical differences in the duration of egg development under Ni (B). Colours represent the control and metal-treated groups. Significant differences are depicted as follows: p <0.0005 '***', p <0.005 '**', p <0.05 '*'.

7.5 Discussion

Both nickel and cobalt significantly affected the ontogeny of *Berghia stephanieae*, with developmental delays observed already at the lowest concentrations tested. Incomplete larval development was first observed at 1852 µg/L for Ni and 463 µg/L for Co, indicating that cobalt exerted stronger developmental toxicity at lower concentrations. Interestingly, all embryos developed normally through the multicellular stages, and developmental disruptions only became apparent from the early veliger stage onward. This stage, characterised by larval rotation within the egg capsule and the onset of ciliary movement, appears particularly sensitive to metal stress.

Comparative studies with other marine and freshwater species show a wide

range of sensitivities to both metals. For example, sea urchin (*Diadema africanum* Rodríguez, Hernández, Clemente & Coppard, 2013) larvae failed to progress beyond the blastula/gastrula stages at just 101 µg/L Ni, demonstrating a markedly higher sensitivity to nickel than what we observed in *B. stephanieae* (Bielmyer et al., 2005). Similarly, in zebrafish (*Danio rerio* (Hamilton, 1822)), nickel inhibited hatching at 40 µg/L, while cobalt only had comparable effects at much higher concentrations (3840 µg/L) (Dave & Xiu, 1991). In our study, the highest cobalt concentration tested (926 µg/L) resulted in high egg mortality, while the same concentration of nickel did not significantly impair survival, underlining cobalt's greater toxicity to *B. stephanieae* embryos.

Sensitivity also varies across molluscan taxa and between marine and freshwater species. Six species of Australian freshwater mussels showed similar LC50 values for both metals, ranging from 1826.83 to 3005 µg/L, indicating comparable sensitivity to nickel and cobalt (Markich, 2017). In contrast, larvae of the tropical marine gastropod *Nassarius dorsatus* (Röding, 1798) showed 50% inhibition of growth and metamorphosis only at 458 µg/L Ni, and *Haliotis rufescens* Swainson, 1822 (red abalone) had an EC50 for 48-hour development at 145.5 µg/L Ni (Gissi et al., 2018; Hunt et al., 2002). These comparisons illustrate the importance of species-specific assessments, particularly when evaluating the ecological risks of metal pollution during early life stages. More importantly, our findings, in line with previous studies, clearly show that early life stages, such as eggs and larvae, are considerably more susceptible to metal exposure than adult individuals. While adult *B. stephanieae* tolerate higher concentrations of nickel and cobalt without visible impairments; embryonic and larval development were already compromised at significantly lower concentrations (Sickinger et al., 2026). This differential sensitivity between life stages has important implications for natural populations. Even if adult invertebrates or molluscs are relatively resilient to elevated metal levels, successful reproduction and recruitment may still be compromised, ultimately threatening long-term population stability in polluted environments.

7.6 Conclusion

This study shows that early developmental stages of *Berghia stephanieae* are highly sensitive to nickel and cobalt, with cobalt exerting stronger toxic effects at lower concentrations. Developmental impairments became apparent from the early veliger stage onward, highlighting this phase as particularly vulnerable to metal stress. While adults tolerate higher concentrations, our results confirm that embryonic and larval stages represent a critical bottleneck for population persistence in polluted environments. These findings underscore the importance of species- and stage-specific assessments when evaluating the ecological risks of metal pollution. As demand for critical raw materials increases, understanding the impacts of heavy metals on early life stages of marine invertebrates is essential for predicting consequences for biodiversity and supporting effective conservation strategies.

Author Contributions

CS planned the experiments. CS, and JK conducted the experiments, processed the data, and performed data analyses. CS, JK, AP, and GC discussed, interpreted the results. CS wrote the manuscript.

Funding

This work was supported by the initiative "Metal-based compounds (MeBaCo)" supported by the University of Wuppertal and the Faculty of Mathematics and Natural Sciences.

Supplementary Materials

The supplementary material is included in the digital version of this thesis.

Additional File 1

Results of the egg development experiments: — Table 1. Duration of development for each egg mass under cobalt exposure. — Table 2. Statistical analysis of egg development under cobalt exposure. — Table 3. Duration of development for each egg mass under nickel exposure. — Table 4. Statistical analysis of egg development under nickel exposure.

References

Arnott, S. E., Yan, N., Keller, W., & Nicholls, K. (2001). The influence of drought-induced acidification on the recovery of plankton in Swan Lake (Canada). *Ecological Applications*, *11*(3), 747–763.

Bielmyer, G., Brix, K., Capo, T., & Grosell, M. (2005). The effects of metals on embryo-larval and adult life stages of the sea urchin, *Diadema antillarum*. *Aquatic Toxicology*, *74*(3), 254–263.

Byrne, M. (2012). Global change ecotoxicology: Identification of early life history bottlenecks in marine invertebrates, variable species responses and variable experimental approaches. *Marine Environmental Research*, *76*, 3–15.

Campbell, A. L., Mangan, S., Ellis, R. P., & Lewis, C. (2014). Ocean acidification increases copper toxicity to the early life history stages of the polychaete *Arenicola marina* in artificial seawater. *Environmental Science & Technology*, *48*(16), 9745–9753.

Chan, H. Y., Chang, Y.-W., Chen, L.-S., Nishida, K., & Shao, Y. T. (2022). The effect of environmental factors on spatial-temporal variation of heterobranch sea slug community in northern Taiwan. *Frontiers in Marine Science*, *9*, 1042961.

Chiarelli, R., & Roccheri, M. C. (2014). Marine invertebrates as bioindicators of heavy metal pollution.

Dave, G., & Xiu, R. (1991). Toxicity of mercury, copper, nickel, lead, and cobalt to embryos and larvae of zebrafish, *Brachydanio rerio*. *Archives of Environmental Contamination and Toxicology*, *21*, 126–134.

De Schamphelaere, K. A., Koene, J. M., Heijerick, D. G., & Janssen, C. R. (2008). Reduction of growth and haemolymph Ca levels in the freshwater snail *Lymnaea stagnalis* chronically exposed to cobalt. *Ecotoxicology and Environmental Safety*, *71*(1), 65–70.

Foroutan, R., Oujifard, A., Papari, F., & Esmaeili, H. (2019). Calcined *Umbonium vestiarium* snail shell as an efficient adsorbent for treatment of wastewater containing Co (II). *3 Biotech*, *9*(3), 78.

Fritts-Penniman, A. L., Gosliner, T. M., Mahardika, G. N., & Barber, P. H. (2020). Cryptic ecological and geographic diversification in coral-associated nudibranchs. *Molecular Phylogenetics and Evolution*, *144*, 106698.

Gissi, F., Stauber, J. L., Binet, M. T., Trenfield, M. A., Van Dam, J. W., & Jolley, D. F. (2018). Assessing the chronic toxicity of nickel to a tropical marine gastropod and two crustaceans. *Ecotoxicology and Environmental Safety*, *159*, 284–292.

Hunt, J. W., Anderson, B. S., Phillips, B. M., Tjeerdema, R. S., Puckett, H. M., Stephenson, M., Tucker, D. W., & Watson, D. (2002). Acute and chronic toxicity of nickel to marine organisms: Implications for water quality criteria. *Environmental Toxicology and Chemistry: An International Journal*, *21*(11), 2423–2430.

International Energy Agency. (2021). The Role of Critical World Energy Outlook Special Report Minerals in Clean Energy Transitions. World Energy Outlook Special Report [Accessed: 2024-12-04].

Jaishankar, M., Tseten, T., Anbalagan, N., Mathew, B. B., & Beeregowda, K. N. (2014). Toxicity, mechanism and health effects of some heavy metals. *Interdisciplinary Toxicology*, *7*(2), 60.

Jomova, K., Alomar, S. Y., Nepovimova, E., Kuca, K., & Valko, M. (2025). Heavy metals: Toxicity and human health effects. *Archives of Toxicology*, *99*(1), 153–209.

Kristof, A., & Klussmann-Kolb, A. (2010). Neuromuscular development of *Aeolidiella stephanieae* Valdéz, 2005 (mollusca, gastropoda, nudibranchia). *Frontiers in Zoology*, *7*(1), 5.

Lange, R., & Marshall, D. (2017). Ecologically relevant levels of multiple, common marine stressors suggest antagonistic effects. *Scientific Reports*, *7*(1), 6281.

Leal, M. C., Rey, F., Ferreira, G. D., Domingues, M. R., & Calado, R. (2022). Inter-individual variability of early life stages of a model marine invertebrate with a bi-phasic life cycle is shaped by contrasting oceanographic conditions. *Frontiers in Marine Science*, *9*, 984569.

Markich, S. J. (2017). Sensitivity of the glochidia (larvae) of freshwater mussels (Bivalvia: Unionida: Hyriidae) to cadmium, cobalt, copper, lead, nickel and zinc: Differences between metals, species and exposure time. *Science of the Total Environment*, *601*, 1427–1436.

McDougall, D. R., Toone, T. A., & Jeffs, A. G. (2022). Natural heavy metal concentrations in seawater as a possible cause of low survival of larval mussels. *Journal of Trace Elements in Medicine and Biology*, *74*, 127071.

Mebane, C. A., Eakins, R. J., Fraser, B. G., & Adams, W. J. (2015). Recovery of a mining-damaged stream ecosystem. *Elementa*, *3*.

Monteiro, E. A., Güth, A. Z., Banha, T. N., Sumida, P. Y., & Mies, M. (2019). Evidence against mutualism in an aeolid nudibranch associated with Symbiodiniaceae dinoflagellates. *Symbiosis*, *79*, 183–189.

Pineda, M. C., McQuaid, C. D., Turon, X., Lopez-Legentil, S., Ordonez, V., & Rius, M. (2012). Tough adults, frail babies: An analysis of stress sensitivity across early life-history stages of widely introduced marine invertebrates. *PlosOne*.

Pyle, G., & Couture, P. (2011). Nickel. In *Homeostasis and Toxicology of Essential Metals* (pp. 253–289, Vol. 31A). Elsevier.

R Core Team. (2021). *R: A Language and Environment for Statistical Computing*. R Foundation for Statistical Computing. Vienna, Austria.

Raju, N. V., Prasanth, P., Harsha, T., Naravula, J., Srikanth, K., & Nutalapati, V. (2022). Evaluation of oxidative stress biomarkers in Pila virens exposed to spinel Co_3O_4 nanoparticles. *Materials Science and Engineering: B*, *282*, 115757.

Rola, M., Frankenbach, S., Bleidissel, S., Sickinger, C., Donath, A., Frommlet, J. C., Greve, C., Serôdio, J., Preisfeld, A., Melo Clavijo, J., et al. (2022). Cladobranchia (Gastropoda, Nudibranchia) as a promising model to understand the molecular evolution of photosymbiosis in animals. *Frontiers in Marine Science*, *8*, 745644.

Santhosh, K., Kamala, K., Ramasamy, P., Musthafa, M. S., Almujri, S. S., Asdaq, S. M. B., & Sivaperumal, P. (2024). Unveiling the silent threat: Heavy metal toxicity devastating impact on aquatic organisms and DNA damage. *Marine Pollution Bulletin*, *200*, 116139.

Sickinger, C., Thiel, A., Bornhorst, J., Christa, G., & Preisfeld, A. (2026). Nickel and cobalt disrupt the microbiome and metabolic function of the photosymbiotic sea slug berghia stephanieae (á. valdés, 2005). *Marine Environmental Research*, 107845.

Silva, R. X., Cartaxana, P., & Calado, R. (2021). Prevalence and photobiology of photosynthetic dinoflagellate endosymbionts in the nudibranch *Berghia stephanieae*. *Animals*, *11*(8), 2200.

Silva, R. X., Madeira, D., Cartaxana, P., & Calado, R. (2023). Assessing the trophic impact of bleaching: The model pair *Berghia stephanieae/Exaiptasia diaphana*. *Animals*, *13*(2), 291.

Wang, Y., Li, Q., Yun, X., Zhou, J., & Wang, J. (2022). A review on the ecotoxicological effects of heavy metals on aquatic organisms. *Journal of Earth Sciences & Environmental Studies*, *6*(2), 148–161.

Wood, C. M., Farrell, A. P., & Brauner, C. J. (2012). *Homeostasis and toxicology of essential metals* (Vol. 1). Academic Press.

Discussion

Photosymbiotic Sea Slugs as Model Organisms to Understand Photosymbiosis

Photosymbiotic sea slugs are powerful model organisms for dissecting the interplay between host biology and photosynthetic symbionts at multiple levels. In Heterobranchia, photosymbiosis has evolved independently twice: kleptoplasty in Sacoglossa, where functional algal plastids are sequestered and maintained for varying periods, and whole-cell photosymbiosis in Cladobranchia, where intact Symbiodiniaceae cells are hosted intracellularly (Händeler et al., 2009; Rola et al., 2022). These associations enable direct investigation of the molecular mechanisms of symbiont recognition and immune modulation, the ecological determinants of symbiosis stability across habitats, and the behavioural adaptations, such as phototaxis, that can influence light acquisition and, in turn, the performance and persistence of the symbionts. Cladobranch sea slugs form a diverse, functionally versatile group of marine heterobranchs that have independently evolved the ability to host photosynthetic dinoflagellates from Symbiodiniaceae (Rola et al., 2022). These associations range from short-term retention, lasting only days, to months-long maintenance that can sustain growth and reproduction in the absence of heterotrophic feeding (Burghardt, Schrödl, & Wägele, 2008; Rudman, 1981, 1991).

Our study shows, for the first time, that in Cladobranchia, a correlation exists between the Symbiodiniaceae genera and the stability of the symbiosis in cladobranch slugs, and their occurrence appears to depend on both host species and environmental conditions (Sickinger et al., 2025a). For example, *Berghia stephanieae* exhibits an unstable photosymbiosis: without continuous feeding on photosymbiotic cnidarians, the dinoflagellates are lost within days, and there is little evidence for a long-term mutualistic relationship (Monteiro et al., 2019). Interestingly, this species consistently harbours *Breviolum minutum*, a genus also common in coral hosts and known for broad ecological tolerance (Monteiro et al., 2019; Silva et al., 2021, 2023). In our study, species with no or unstable photosymbiosis typically hosted *Breviolum* or *Symbiodinium* as dominant symbionts. In contrast, cladobranchs with stable photosymbiosis, such as *Phyllodesmium magnum* Rudman, 1991, which can retain photobionts for weeks to months and survive under light without heterotrophic input, almost exclusively harboured *Cladocopium* clades (Burghardt, Schrödl, & Wägele, 2008; Wägele et al., 2010).

This raises the question of whether symbiosis stability is determined primarily by the photobiont, as Symbiodiniaceae clades differ in their adaptations to factors such as thermal stress or light intensity (Lesser, 2019). Gorman et al. (2025) analysed the regulation of symbiont populations in *Exaiptasia diaphana* and showed that stability varies depending on the Symbiodiniaceae partner, with *Durusdinium* exhibiting lower host regulatory control and reduced long-term stability compared to *Breviolum* (Gorman et al., 2025). *Breviolum* species vary widely in their responses to environmental stress, particularly heat, a key factor in coral bleaching. Strains such

as *B. minutum* are highly heat-sensitive, whereas others are more tolerant (Dang et al., 2019). Heat or light stress can trigger phototrophic organisms to adjust photosynthetic pathways, including the use of alternative electron transport mechanisms, to reduce photo-damage and oxidative stress (Oakley et al., 2023). However, the prevalence and efficiency of these adaptations differ among *Breviolum* strains, influencing symbiotic performance. Ecologically, *Breviolum* is a key symbiont for a broad range of cnidarians, including corals, sea anemones, hydrozoans, and occasionally jellyfish (Dall'Olio et al., 2022).

Symbiodinium exhibits a wide range of stress adaptations, allowing survival in diverse and sometimes extreme marine environments. Compared to *Breviolum*, many *Symbiodinium* strains cope better with reactive oxygen species and protect their photosynthetic machinery under light stress by dissociating their antenna complexes from the reaction centres of photosystem II under strong light conditions, thereby increasing their capacity for cyclic electron flow and avoiding bleaching (Aihara et al., 2016; Reynolds et al., 2008). While both genera include heat-tolerant and heat-sensitive strains, *Symbiodinium* often displays broader photoprotective diversity and, in some cases, "stress memory," enabling faster responses to repeated stress (Dang et al., 2019; Levin et al., 2016; Oakley et al., 2023). Adaptation in *Symbiodinium* tends to involve rapid activation of protective and metabolic pathways, whereas *Breviolum* often excels in trophic and metabolic flexibility under nutrient-rich conditions (Kirk et al., 2020). Some corals experience reduced health when hosting *Symbiodinium*, likely due to lower nutrient contributions from this symbiont (Rouzé et al., 2016; Stat et al., 2008). In contrast, the upside-down jellyfish *Cassiopea* sp. can rely entirely on *Symbiodinium*, maintaining a stable photosymbiosis without any decline in health (Lampert, 2016). In our study, species hosting *Symbiodinium* showed no signs of compromised health, indicating that any potential parasitic effects are likely host-specific rather than a general feature of the genus (Goulet et al., 2019). Nonetheless, apart from a small proportion found in *Pteraeolidia ianthina* (Angas, 1864), this photobiont genus was detected only in species exhibiting absent or unstable photosymbiosis.

Cladocopium differs from *Breviolum* and *Symbiodinium* in both ecological role and stress response. Uptake by coral cells is generally slower and less efficient compared to other Symbiodiniaceae genera, and initial infection rates are lower, suggesting different adaptation mechanisms or more specific host preferences (de Souza et al., 2022; Ng et al., 2024; Sikorskaya et al., 2024). While *Cladocopium* can exhibit thermal tolerance comparable to or exceeding that of some *Breviolum* strains, the mechanisms are highly strain-dependent (Ng et al., 2024; Sikorskaya et al., 2024). Unlike *Symbiodinium*, it is less associated with strong cyclic electron transport in photosystem II, but it thrives in a broad range of coral hosts, especially in warm, shallow reefs, where it contributes to long-term symbiotic stability (de Souza et al., 2022). Globally, *Cladocopium* is among the most widespread Symbiodiniaceae genera in coral reefs, associating with many coral species across diverse regions (J. Li et al., 2025). Interestingly, in corals such as *Acropora tenuis* (Dana, 1846) or *Acropora humilis* (Dana, 1846), *Symbiodinium*, *Breviolum*, and *Durusdinium* are often acquired first and dominant during larval stages, with *Cladocopium* becoming more dominant in adulthood, likely reflecting changing environmental and physiological needs (Ng et al., 2024). In cladobranch sea slugs, we were able to show that *Cladocopium* correlates with long-term, stable symbiosis (maintenance of the photobiont for more than two weeks), whereas *Symbiodinium* and *Breviolum* are more often linked to transient or unstable associations (photobiont is immediately digested or maintained for some days).

Our data also show a correlation between the stability of photosymbiosis and food source, meaning that cladobranch species with a stable symbiosis mainly feed

on Octocorallia and species with no or an unstable symbiosis feed on Actinaria. However, no single Symbiodiniaceae genus appears to be exclusive to either Octocorallia or Actiniaria and both cnidarian clades host overlapping Symbiodiniaceae genera, including *Cladocopium*, *Durusdinium*, and *Breviolum*. For example, the octocorals *Briareum* and *Erythropodium*, both consumed by Cladobranchia species with stable photosymbiosis, host symbionts from the genus *Breviolum* and *Cladocopium* at the same time (Goulet & Coffroth, 2004; Goulet et al., 2008). In the sea slugs feeding on these corals, however, only *Cladocopium* is present. Future studies should also focus on sampling and analysing the cnidarian prey of the slugs to determine whether the abundance and diversity of symbionts in cladobranchs are maintained after they feed on their food source. This could provide initial answers to the question of whether cladobranchs actively select their symbionts. Could species such as *Phyllodesmium* have the ability to specifically select certain symbionts, while *Coryphella* or *Berghia* lack this ability? For answering this question, however, the molecular basis of photobiont recognition and maintenance is also important.

In cnidarian–dinoflagellate systems, symbiont acquisition is known to depend on highly specific molecular recognition processes. The host has to recognise and ingest the specific photobiont, a foreign organism, which comes with considerable risks, as it requires a modification of the immune system and, in the case of false recognition, carries the risk of introducing pathogens into the host's cells (Emery et al., 2024; McFall-Ngai et al., 2013). In cnidarians, a well-studied way to distinguish specific symbionts from pathogens and to regulate the immune system accordingly is the interaction between specific surface molecules of the photobiont called microbe-associated molecular patterns (MAMPs) and pattern recognition receptors (PRRs) of the host (Davy et al., 2012; Mansfield & Gilmore, 2019; Rosset et al., 2021). Here, MAMPs of the phototrophic microorganism are recognised by PRRs located on the host's cell membrane. If the host cell recognises the microbe as a suitable symbiont, phagocytosis is initiated, a signalling cascade regulating the immune system is triggered, and specific activator proteins, which induce the early phagosome formation by the recruitment of Rab5 are produced (Fig. 7.4). As a result, the symbiont is phagocytised into the host cell. The resulting phagosome, referred to as a symbiosome, surrounds the photobiont intracellularly and is crucial for the nutrient exchange between host and photobiont (Malcolm & April, 2012). In a stable photosymbiosis, as observed for corals, the phagosomal maturation is inhibited, and a functional symbiosome is established (Chen et al., 2003, 2004).

It is both possible and likely that different Symbiodiniaceae genera, such as *Breviolum*, *Symbiodinium*, and *Cladocopium*, exhibit distinct MAMPs. This stems from the considerable genomic and physiological divergence within the family Symbiodiniaceae, which is marked by deep evolutionary splits between its genera (Liu et al., 2018; Lo et al., 2022). Comparative genomic analyses have revealed significant differences in genome content and the expansion of specific gene families, including those involved in the biosynthesis and modification of cell surface structures, which are directly linked to MAMP composition and presentation (Aranda et al., 2016; Levin et al., 2016). Importantly, such molecular divergence has ecological implications. Differences in MAMPs are likely to contribute to the degree of host compatibility, the specificity of the symbiotic relationship, and the resilience of the coral-algal partnership under environmental stress. Instances in which corals alter or "shuffle" their symbiont communities during thermal stress events may partly reflect the need to establish immune-compatible partnerships based on MAMP recognition (Baker, 2004; Cunning et al., 2015; Voolstra et al., 2024). Variation in MAMPs is

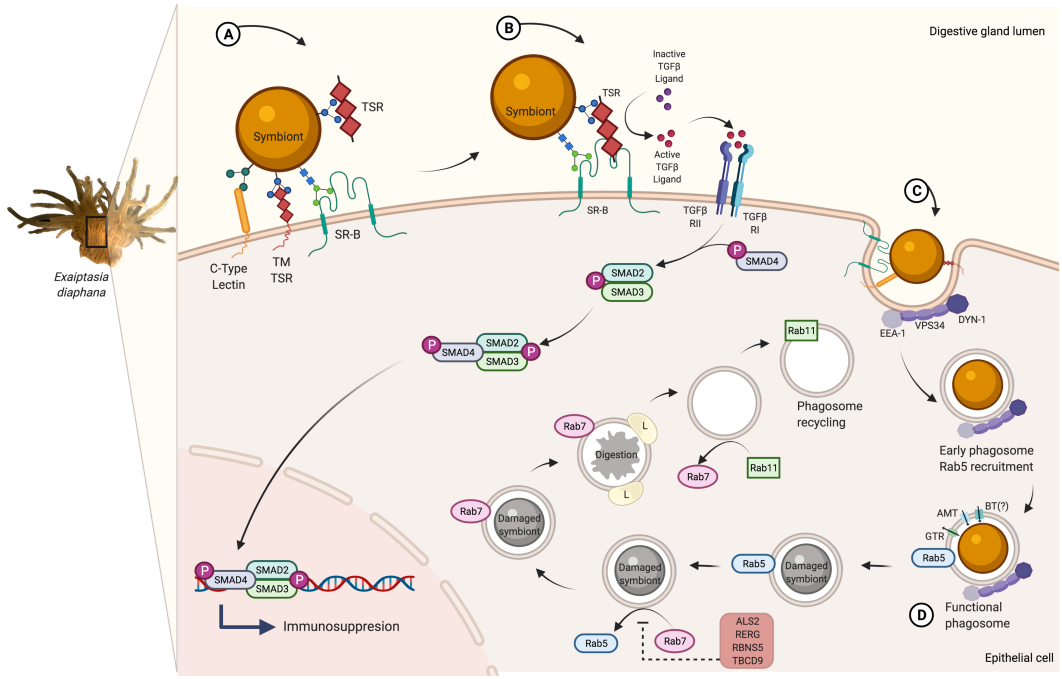

FIGURE 7.4: Symbiont recognition and maintenance in the sea anemone *Exaiptasia diaphana*. Symbiont is recognised by host PRRs (A), followed by activation of the TGF-β pathway and immune suppression (B). Symbionts are then phagocytosed (C). In successful symbiosis, phagosomal maturation is halted and a stable symbiosome forms, enabling nutrient exchange through bicarbonate, glucose, and ammonium transporters (D). Figure by Melo Clavijo et al., 2022.

also supported by host recognition and symbiosis specificity studies. Coral cell culture experiments have shown that coral host immune responses vary depending on the symbiont genus. Coral cells tend to more readily engulf symbionts from *Symbiodinium* and *Breviolum* than those from *Cladocopium*, suggesting that the host immune system perceives these genera differently, likely due to differences in their surface-exposed molecular patterns (Davy et al., 2012; Neubauer et al., 2016). Such specificity implies that specific PRRs on the host's side interact with distinct molecular configurations on the algal cell surface. This also means that compatibility is likely determined on the photobiont's side as well, depending on whether the MAMPs expressed by the photobiont match the PRRs expressed by the host. In cnidarians, promising PRR categories include scavenger receptor class B (SR-B) and class E (SR-E), thrombospondin type-1 repeat domain-containing proteins (TSRs), and C-type lectins (Chen et al., 2004; Davy et al., 2012; A. Mohamed et al., 2016; Neubauer et al., 2016). *Berghia stephanieae* maintains an unstable photosymbiosis with its photobiont *Breviolum minutum*, acquired from its food source *Exaiptasia diaphana* (Rapp, 1829). Unlike in cnidarians, Melo Clavijo et al., 2022 could show that in the slug, immune responses to the photobiont are not suppressed, nor is phagosome maturation inhibited. Consequently, a functional, stable symbiosome, essential for nutrient exchange, cannot form. Still, the question remains as to the mechanism by which the slugs initially recognise the symbionts and temporarily takes them up into its epithelial cells.

Our transcriptome analysis shows that in the presence of the symbiont *B. minutum*, *B. stephanieae* upregulates 14 transcripts classified as PRRs (Melo Clavijo et al., 2022). One C-type lectin identified as Collectin-12, was significantly upregulated and thus considered a first promising receptor for symbiont recognition. Spatial transcriptomics and *in situ* hybridisation chain reaction (HCR) localisation revealed strong Collectin-12 expression in epithelial cells surrounding the digestive gland in the proximal cerata, the main site of the photobionts (see Chapter 2). Collectins, a subgroup of C-type lectins, possess carbohydrate-recognition domains linked to collagen-like regions, allowing them to bind specific glycans on microbial surfaces (Zhang et al., 2020). The targeted expression of Collectin-12 in symbiont-rich tissues of the host indicates a potential role in photobiont recognition and selective uptake by the slug cell, mirroring lectin-mediated mechanisms described in cnidarian–Symbiodiniaceae systems (Kvennefors et al., 2008). Interestingly, transcriptomic studies in different scoglossan species have identified several PRRs that are potentially relevant for the recognition of kleptoplasts, among these Collectin-12, Collectin-11 and Collectin-10 (Allard et al., 2025; C. X. Chan et al., 2018; Melo Clavijo et al., 2020; Mendoza et al., 2023). Although their functional role has yet to be experimentally validated, the presence of these collectin transcripts suggests that lectin-like proteins seem to play a role in symbiont recognition in heterobranch sea slugs, even in kleptoplasts. These results indicate that photosymbiosis depends on multiple factors, including the compatibility between photobiont-derived MAMPs and host PRRs, as well as immune system adaptations of the slug host. Such principles likely apply not only to photosymbiosis in Cladobranchia but also to kleptoplasty in Sacoglossa.

Some studies even suggest that sacoglossan slugs such as the LtR species *Plakobranchus ocellatus* van Hasselt, 1824 exhibit positive phototactic behaviour in the course of successful symbiont recognition and maintenance in order to increase kleptoplast photosynthesis and thus nutrient production (Cartaxana et al., 2018; Miyamoto et al., 2015; Schmitt & Wägele, 2011; Weaver & Clark, 1981). *Elysia viridis* offers a particularly compelling case for such experiments, as its retention capacity spans the full range from non-retention to long-term retention depending on the food algae, enabling direct tests of whether and how host behaviour is modulated by the quality and persistence of its kleptoplasts (Händeler et al., 2009; Rauch et al., 2015). Our results demonstrate that *E. viridis* consistently exhibited positive phototaxis, spending the majority of time in the illuminated area regardless of light source, starvation condition, or kleptoplast photophysiological state. This indicates that light-seeking behaviour in this species is constitutive rather than context-dependent, and is not modulated by short-term changes in nutritional status or plastid performance (Sickinger et al., 2025c). Interestingly, other LtR species, such as *E. crispata*, were reported in an earlier study to actively avoid red light (Weaver & Clark, 1981), whereas *E. viridis* showed a light preference towards red light. However, a more recent investigation by Burgués Palau et al., 2024 showed that *E. crispata* did not exhibit consistent light-avoidance behaviour. Instead, this LtR species relies on effective photoprotective strategies: it can contract its parapodia to shade the kleptoplast-bearing tissues and reduce incident light by about 50%, and it maintains dense kleptoplast aggregations that provide self-shading and mitigate oxidative stress. In contrast, two short-term retention (StR) species, *Elysia velutinus* Pruvot-Fol, 1947 and *Elysia ornata* (Swainson, 1840), displayed strong negative phototaxis and consistently crawled away from high light intensities. *E. velutinus* depends mainly on hiding within its food algae and by that reduces potential photodamage and consequently oxidative activity,

while *E. ornata* did not hide or show any photoprotective mechanisms, resulting in high oxidative activity, explaining the quick turn over rate of kleptoplasts (3 days). *E. viridis* inhabits shallow, flat environments where it is regularly exposed to the full solar spectrum, including substantial red light (Baumgartner & Toth, 2014; Hayward & Ryland, 2017) but does not have photoprotection mechanisms that can fully protect the photosystems from damage. However, similar to *E. crispata*, *E. viridis* adjusts its parapodial folds in response to light intensity; under high irradiance, the parapodia close, shielding the kleptoplasts from excess light and thereby reducing photo-induced damage (Cartaxana et al., 2019; Cartaxana et al., 2018; Christa et al., 2018; de Vries et al., 2013; Havurinne et al., 2021). In Cladobranchia, phototactic experiments remain scarce. Field observations indicate that species with stable photosymbioses, such as *Melibe engeli* and *Phyllodesmium briareum* (Bergh, 1896), often engage in "sun-bathing" behaviour, consistent with positive phototaxis (Burghardt & Wägele, 2014; Rudman, 1991). By contrast, *Phidiana lynceus* Bergh, 1867 exhibits strong light avoidance in both field and laboratory settings (Borgstein et al., 2024b). Although this species is capable of retaining algal symbionts, it is primarily nocturnal and actively avoids light, thereby limiting photosynthesis and the potential nutritional benefits it could provide. Thus, phototactic behaviour in photsymbiotic sea slugs, for example, the sacoglossan species *E. viridis* is likely based on individual daily periodic activity of the species and, thus, if behavioural or molecular photoprotective adaptations are present, rather than actively increasing the photosynthetic activity of their kleptoplasts.

Photosymbiotic Sea Slugs in the Holobiont Framework

Photosymbiosis in heterobranch sea slugs is commonly investigated through experimental manipulations such as starvation, chemical inhibition of photosynthesis, or maintaining in darkness. These approaches aim to determine whether, and to what extent, photobionts or kleptoplasts contribute to host metabolism. In sacoglossan sea slugs such as *E. viridis*, individuals starved in darkness shrank and lost weight more rapidly than those starved in the light, indicating that kleptoplasts might provide an advantage under starvation (Cartaxana et al., 2017; Casalduero & Muniain, 2008; Maeda et al., 2021; Shiroyama et al., 2020). To avoid confounding effects of darkness, some studies have instead applied photosynthesis inhibitors such as monolinuron, which yielded starvation tolerances comparable to those observed under photosynthetically active conditions, suggesting that *E. viridis* rather slowly digests the kleptoplasts than using them for active photosynthesis (Christa et al., 2014b; de Vries et al., 2015; Laetz et al., 2017b). Within photosymbiotic Cladobranchia, the aeolid *B. stephanieae* has become a well-established model. Here, starvation experiments or comparison experiments between symbiotic and aposymbiotic (symbiont-free) specimens showed that *B. stephanieae* has an unstable symbiosis with its photobionts and seems to represent a transition form towards stable photosymbiosis as observed, for example, in *Phyllodesmium briareum* (Melo Clavijo et al., 2022; Monteiro et al., 2019; Silva et al., 2021). Light stress has frequently been applied as an experimental tool to evaluate the photobiont retention within the slug, since high light induces the photodynamic production of reactive oxygen species (ROS) and thereby increasing host stress (Halliwell & Gutteridge, 1985). More recently, Melo Clavijo et al. (2022) demonstrated that in *B. stephanieae* starvation stress prior to feeding enhances the ability of the slug to quench ROS, partly through the induction of glutathione peroxidase.

However, these studies have largely focused on the role of algal symbionts and have often overlooked the presence of bacterial partners. Sea slugs maintain diverse microbial communities, which can also be affected by experimental stressors such as light, starvation, or chemical inhibition. As a result, the outcomes of these manipulations are not limited to the algal symbionts but can impact the functioning of the entire holobiont. The holobiont, defined as the host together with its associated microbial communities, constitutes an integrated system in which microbes contribute to metabolism, immunity, and adaptation to environmental stress. While these experiments provide valuable insights into photobiont persistence, they overlook that host-associated microbiomes can undergo profound shifts in response to stress (Gatidou et al., 2015; Hinde & Smith, 1975; Teugels et al., 2008). Coral research has already demonstrated the central role of bacterial symbionts in supporting photosymbiosis, for example, through nitrogen, carbon, and sulfur cycling, as well as defence against pathogens (Meunier et al., 2021; K. B. Ritchie, 2011; Röthig et al., 2016; Voolstra & Ziegler, 2020). In corals, the microbiome is widely recognised as a key health indicator, and the holobiont framework is increasingly incorporated into reef restoration strategies. By contrast, photosymbiotic heterobranchs remain comparatively understudied. Existing research on sea slug microbiomes has primarily catalogued bacterial taxa, with only limited efforts to elucidate their functional contributions (Davis et al., 2013; Devine et al., 2012; Mahadevan & Middlebrooks, 2020; Ng et al., 2022; Zhukova & Eliseikina, 2012; Zhukova et al., 2022).

In our study, we focused on the sacoglossan species *E. viridis*, fed with *Cladophora* sp. (NR) and *Bryopsis* sp. (LtR), as well as individuals fed with *Bryopsis* sp. but kept in the photosynthesis blocker monolinuron and analysed not only the abundance of the bacteria but also their potential involvement in metabolic pathways. We were able to show that monolinuron has strong effects on the microbiome and that there is a significant shift in the bacterial community towards Sulfate reducer, Sulfide oxidiser and Sulfur reducer, such as *Bradymonadales* sp. and *Paracoccus* sp.. Monolinuron is a herbicide that interferes with photosynthesis by binding to the plastoquinone binding site (QB) of the D1 protein in the PSII, thereby blocking electron transport in the chloroplast (Gatidou et al., 2015). As a consequence, absorbed light energy can no longer be efficiently used, leading to its accumulation and the onset of oxidative stress. This stress damages lipids and other cellular components of the photosynthetic organism (Krieger-Liszkay, 2005). In response, glutathione is produced to neutralise reactive molecules such as hydrogen peroxide and lipid peroxides (Lu, 2013). The synthesis of glutathione depends strongly on cysteine, a sulfur-containing amino acid. Through the γ-glutamyl cycle, glutathione can be continuously recycled, both regenerating itself and providing cysteine. In this process, glutathione forms γ-glutamyl derivatives with amino acids, which are subsequently broken down to release the amino acid into the cell and restore glutathione. Most cells readily take up cysteine, which is primarily channelled back into glutathione production, though it can also be incorporated into proteins or oxidised to sulfate (Lu, 2013; Ripps & Shen, 2012; Turley et al., 1988). Thus, the extra sulfate released by the cysteine degradation can be metabolised by sulfate-reducing bacteria and sulfide-oxidising bacteria in *E. viridis* (Fig. 7.5).

In *B. stephanieae* blocking photosynthesis by keeping slugs in the dark induced a significant shift and reduction in microbiome diversity compared to slugs kept in the normal light or high-light indicate that darkness as a stress factor has a greater impact on the microbiome composition than high-light stress (Sickinger et al., 2024).

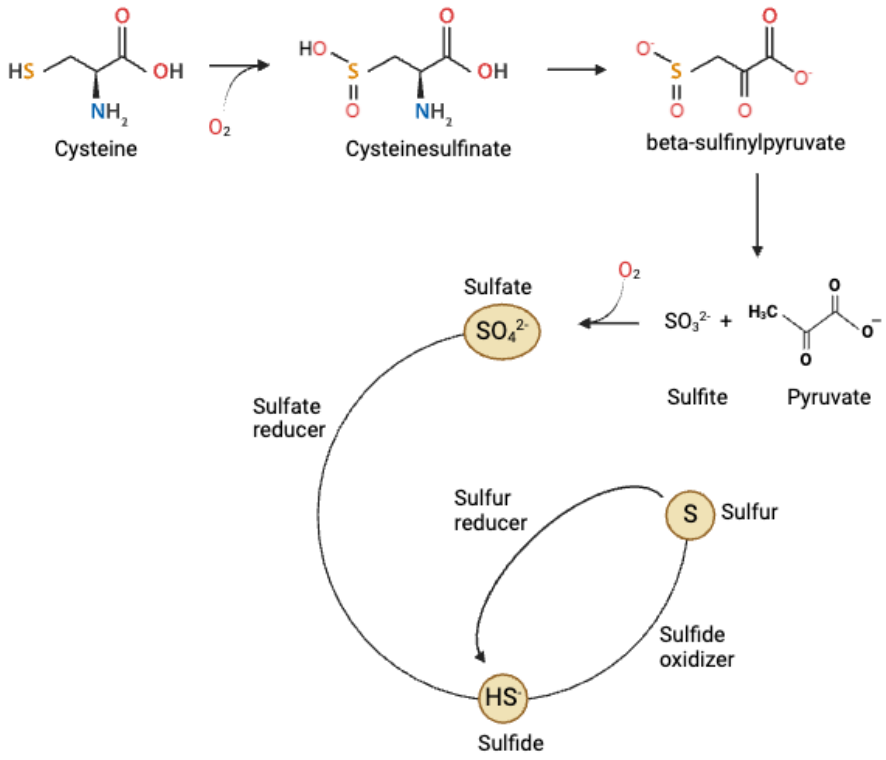

FIGURE 7.5: Potential bacterial sulfate reduction in *E. viridis* treated with Monolinuron.

However, with little effect on metabolic pathway abundance. Interestingly, starvation induced an increase in nitrogen-fixing bacteria and a reduction of both nitrifying and denitrifying bacteria, indicating an alteration in the nitrogen cycle in starving slugs compared to the control group, regardless of the light condition (Fig. 7.6). In contrast to other Cladobranchia, *B. stephanieae* cannot rely solely on its photobiont for nutrition due to its unstable photosymbiosis; the symbionts are photosynthetically active for up to five days before being digested or expelled (Melo Clavijo et al., 2022; Monteiro et al., 2019). If the slug is not given any Symbiodiniaceae-containing prey, it loses its photobiont and turns aposymbiotic. In this study, we starved *B. stephanieae* for one week. As a result, the slug lost nearly all of its photobionts, which are included in a variety of metabolic pathways, such as nitrogen fixation (Pupier et al., 2021). Alongside phosphate, nitrogen is a critical limiting nutrient for photobionts in corals, as both elements play key roles in controlling symbiont growth and metabolic performance (Buckingham et al., 2022; Morris et al., 2019; Rädecker et al., 2015). In photosymbiotic slugs, it remains unclear whether the host regulates its photobionts through nitrogen limitation; however, our results suggest that in the absence of photobionts, nitrogen availability increases, as indicated by the significant rise in diazotrophic bacteria.

Cladobranchia have to acquire their photobionts horizontally anew in each generation via their food source (Melo Clavijo et al., 2018; Rola et al., 2022; Sickinger et al., 2025a). In contrast, the bacterial communities in *B. stephanieae* do not appear to be acquired horizontally through food nor the environment, as we found little to no overlap between the microbiome of the food anemone *Exaiptasia diaphana* or the surrounding water and that of the slugs, strongly suggesting vertical transmission,

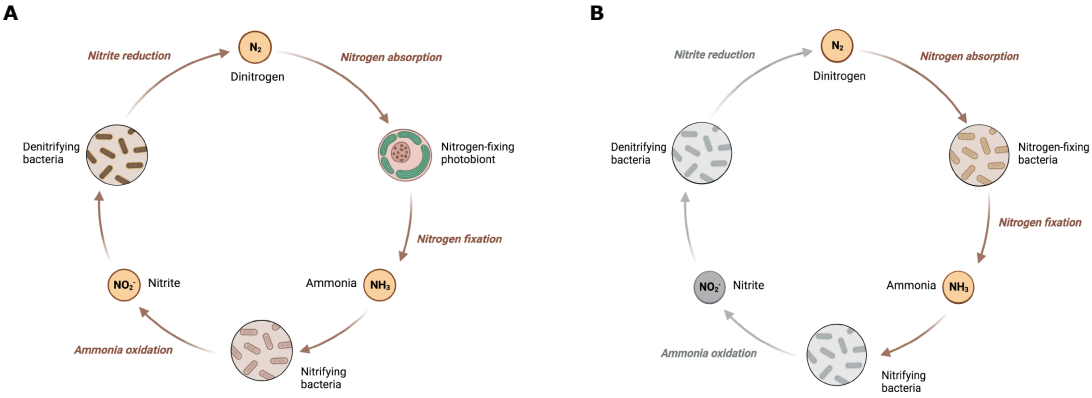

FIGURE 7.6: Potential role of photobiont and bacteria in the nitrogen cycle in fed (A) and starved (B) *B. stephanieaea*. Grey background indicates downregulated bacterial pathways.

meaning an inherited microbiome. A well-known example of vertically transmitted microbiome are Porifera, which maintain a characteristic "sponge-specific" microbiome that is passed down through the parental lineage to ensure the accuracy of the microbiome for the next generation (de Oliveira et al., 2020; Funkhouser & Bordenstein, 2013; Rosenberg & Zilber-Rosenberg, 2021). The core microbiome of *B. stephanieae* was dominated by *Mycoplasma* sp., which increased significantly in abundance in slugs starved in light, high light or darkness. Mycoplasmatales were also found in high abundance in other sea slugs like *Chromodoris quadricolor* (Rüppell & Leuckart, 1830), *Pteraeolidia semperi* (Bergh, 1870), *Elysia rufescens* (Pease, 1871), and *Elysia crispata* Mörch, 1863 (Abdelrahman et al., 2021; Davis et al., 2013; Mahadevan & Middlebrooks, 2020; Ng et al., 2022). The exact role of these bacteria in the heterobranch holobiont is not yet clarified. Although Mycoplasmatales have been described in other *Elysia* species, this bacterial taxon was not present in our samples of *E. viridis* and a dominant taxa was not observed in the core microbiome of *E. viridis*. Interestingly, in *E. viridis* the microbiome composition and the resulting metabolic pathways differed significantly depending on whether functional kleptoplasts were present.

An important limitation to our study on the microbiome of *E. viridis* is that we were not able to include the microbiome analysis of the algal food sources themselves, which limits our ability to distinguish between host-specific bacteria and those introduced with the diet. It therefore remains possible that part of the *E. viridis* microbiome is acquired horizontally through ingestion of algal-associated bacteria, which would be in contrast to our findings in *B. stephanieae* (Sickinger et al., 2024). Mahadevan and Middlebrooks, 2020 proposed that sacoglossan microbiomes are largely opportunistic and shaped by the bacterial communities of their algal food sources, although they were also unable to analyse the microbiome of the food algae directly.

Metal Toxicity and Holobiont Response of *B. stephanieae*

Metal pollution has emerged as an increasing concern in marine ecosystems as industrial mining and coastal runoff introduce elevated concentrations of elements such as nickel (Ni) and cobalt (Co) into the ocean (Arnott et al., 2001; Fernandez et al., 2006; International Energy Agency, 2021; Merrot et al., 2019; Noël et al., 2015;

Pyle & Couture, 2011; Wood et al., 2012). These metals are widely used in modern technologies such as electric cars, and their accumulation in coastal waters poses potential risks to sensitive organisms (Naryono, 2023). In coral reef systems, studies have shown that exposure to trace metals can disrupt symbiotic stability, impair calcification, and induce oxidative stress, thereby threatening both coral health and reef resilience (Biscéré et al., 2018; de Barros Marangoni et al., 2017; Iglic, 2011; T. Li et al., 2020; Montalbetti et al., 2021; Rodriguez et al., 2016). Such findings highlight the need to better understand how metal contamination affects other photosymbiotic marine invertebrates beyond corals, including gastropod holobionts.

In our study, we investigated the effects of nickel and cobalt on the marine gastropod *B. stephanieae* (Sickinger et al., 2026). In order to establish suitable experimental concentrations for Ni and Co, we first conducted preliminary range-finding tests. These range-finding assays show that adults tolerate a window between 3 mg/L - 32 mg/L for Co and 3 mg/L - 37 mg/L for Ni, and ICP-OES analyses verified that the nominal concentrations increased with increasing metal concentrations. Elevated concentrations around 18 mg/L of Ni and Co lead to visible signs of stress, such as no movement, no feeding and shedding of the cerata. Ni exposure is known to generate oxidative stress, which in turn damages critical biomolecules such as DNA, proteins, and lipids. Nickel can displace essential metals in metalloproteins or disrupt enzymatic activity through allosteric effects, either by binding directly to catalytic residues or to adjacent sites, thereby altering protein function (Cammack, 1988; Macomber & Hausinger, 2011). Such disruptions interfere with cellular homeostasis and can ultimately compromise organismal health (Macomber & Hausinger, 2011). Cobalt, by contrast, is an essential trace element as a component of vitamin B12, but its biological role is limited, and only very small quantities are required for normal cellular processes (Eitinger et al., 2005). In *Hydra magnipapillata*, elevated Co concentrations triggered the formation of reactive oxygen species (ROS), also within lysosomes, which suppressed the expression of antioxidant and stress-sensitive genes. This led to DNA damage and apoptosis mediated through mitochondrial pathways (Zeeshan et al., 2017). Marine molluscs show varying levels of tolerance to nickel and cobalt, with marked differences in sensitivity between species and exposure conditions. Most marine molluscs begin to show signs of physiological stress at concentrations significantly lower than susceptible fish or some other invertebrates, but a few species can endure rather high concentrations before lethal or sublethal effects appear (Lehel et al., 2023; Potet et al., 2018; Saili et al., 2021). Bivalves, for example *Mytilus galloprovincialis* Lamarck, 1819 and *Chamelea gallina* (Linnaeus, 1758) have been found to accumulate high nickel content without apparent lethality, with some recorded tissue concentrations up to 92 mg/kg (Lehel et al., 2023). For cobalt, Saili et al. (2021) conducted chronic toxicity tests, including *Mytilus galloprovincialis* and *Magallana gigas* (Thunberg, 1793). However, the cobalt concentrations tested (1660 µg/L Co for *M. galloprovincialis* and 2760 µg/L Co for *M. gigas*) were too low to detect a significant effect on these molluscs (Saili et al., 2021).

Our results indicate that *B. stephanieae* has relatively high tolerance against elevated Ni and Co exposure. However, when shifting the focus from adult *B. stephanieae* to early developmental stages, our results revealed that eggs and embryos are a lot more sensitive towards Ni and Co exposure. When exposed to increasing metal concentrations (Co: 140 – 420 µg/L; Ni: 419 – 1678 µg/L), we demonstrated that embryos displayed clear, dose-dependent responses to both metals, with elevated concentrations leading to prolonged developmental time period and reduced hatching success. The critical developmental stage was the early veliger stage, as the

multicell stage was reached by all eggs regardless of the metal and the concentration. The early veliger stage in molluscs, particularly in nudibranchs, is a critical developmental period characterised by the initial formation of the larval shell and the onset of rotational movement (Khan et al., 2020; Tyler-Walters & Williams, 2023). This stage is highly sensitive to environmental conditions and is considered a vulnerability point for the organism regarding exposure to contaminants. The rotation, along with the movement of the velar cilia, amplifies contact with environmental contaminants, especially those dissolved or suspended in the water column (Carriker, 2001; Hayashi & Nakano, 2024). Inactive larvae and abnormal developmental outcomes have been documented, for example, in oysters at higher contaminant concentrations, indicating sensitivity peaks during early veliger motility (Khan et al., 2020). Interestingly, eggs seemed to endure Ni better than Co, as the highest concentration tested for Co (420 µg/L) induced only slight changes in the developmental time frame for Ni samples. Co's structural similarity to other critical ions (e.g., magnesium and calcium) could lead to it substituting in biomolecules and interfering with vital processes more readily than Ni, thus, higher concentrations of Ni might be endured (Bida et al., 2025). Interestingly, the control group of our preliminary range finding test with adult *B. stephanieae* displayed relatively high baseline concentrations of Ni. A plausible explanation for this finding is the activity of the metalloenzyme urease, which requires two Ni ions at its catalytic centre. Urease is essential in nitrogen metabolism, as it hydrolyses urea into ammonia and carbon dioxide. In the photosymbiotic giant clam *Tridacna squamosa* Lamarck, 1819, for instance, urease enables the host to deliver nitrogen to its algal symbionts in the form of urea, which the algae then assimilate into their own metabolic processes (Ip et al., 2020). A comparable process may also take place in *B. stephanieae*, where the host could facilitate nitrogen supply to the intracellularly retained Symbiodiniaceae, thus Ni would be an important trace element for adult *B. stephanieae*. Nevertheless, this hypothesis requires further validation, for example, through the quantification of urease gene expression.

Based on the results of our preliminary range finding test of adult *B. stephanieae*, we selected a gradient of concentrations that encompassed low, sublethal levels as well as higher doses that were expected to induce measurable changes in holobiont physiology and conducted a microbiome and bacterial metabolic pathway analysis under exposure to Ni and Co. Although visible signs of stress (no movement, no feeding and shedding of the cerata) were only observed at a concentration around 18 mg/L for both metals, our microbiome analyses revealed significant changes in bacterial composition already at a concentration of 1 mg/L for Ni and Co (group N1 and C1). Interestingly, at this concentration, no significant difference was observed between the two metals, indicating a dose-dependent shift in the microbiome regardless of the metal itself. Both groups, N1 and C1, were dominated by *Mycoplasma* sp. (seemingly a key taxa as already observed in our microbiome analyses with *B. stephanieae* exposed to light stress and starvation (Sickinger et al., 2024) and increasing abundance of *Pseudofulvibacter* sp. and *Endozoicomonas* sp.. From 3 mg/L Ni and Co (group Ni2 and Co2), clear differences between the two groups emerged. Group N2 showed more similarities to C1 and N1 in terms of metabolic pathways, while C2 clustered with N3 and C3. This indicates that at 3mg/L a shift in microbiome composition occurs, resulting in significant changes in bacterial pathways. The highest concentration tested (17 mg/L, N3 and C3) showed a downregulation of almost all 14 observed metabolic pathways clustering with the control group. Still, C3 and N3 showed significant differences in microbiome composition compared to the control

group, thus indicating a potential tipping point at which functional redundancy is lost, or key microbial contributors are no longer present and potential pathogens such as *Mycoplasma* sp. increase rapidly.

Our findings show that exposure to nickel and cobalt led to clear, concentration-dependent alterations in the bacterial microbiome of *B. stephanieae*, with detectable changes already occurring at concentrations as low as 1 mg/L. This sensitivity contrasts with results from corals, for example, in *Acropora muricata* (Linnaeus, 1758), where comparable nickel levels did not induce noticeable shifts in microbial community composition (Gissi et al., 2019). The highest concentration tested, 9050 ug/L Ni, caused coral bleaching; however, no changes in the composition of their microbiome communities were observed. In cnidarians, the photobionts are key players in controlling internal metal levels. Compared to their coral hosts, these symbionts accumulate much higher amounts of metals, especially Ni, and when exposed to elevated concentrations, the coral can expel its photobionts and which eventually results in bleaching (Douglas, 2003). This response is thought to function as a detoxification mechanism, enabling the host to lower its intracellular metal burden by eliminating the symbionts that have accumulated the excess metals (Bastidas & Garcia, 2004; Hardefeldt & Reichelt-Brushett, 2015; Meehan & Ostrander, 1997; Peters et al., 1997; A. J. Reichelt-Brushett & McOrist, 2003). While corals are able to emit their symbionts and the accumulated metal, thus, probably stabilising their microbiome, *B. stephanieae* is not able to expel its symbionts that easily. In *B. stephanieae* the symbionts are stored within epithelial cells of the digestive gland system, which spreads into the cerata. Several nudibranchs, including *B. stephanieae* are able to shed their cerata as a defence mechanism. This self-amputation is typically triggered by predator attacks and plays an important role in survival, though it comes with energetic costs and functional trade-offs (Bickell-Page, 1989; Edmunds, 1966; Miller & Byrne, 2000; Piel, 1991). In our experiments, *B. stephanieae* individuals exposed to approximately 18 mg/L of Ni or Co displayed active shedding of their cerata, a response not observed at lower concentrations. This cerata autotomy could be a detoxification strategy, enabling the slug to eliminate tissue regions that contain metal-accumulating symbionts (J. W. Brown et al., 2024). However, regenerating lost cerata is energetically costly and temporarily reduces the nudibranch's respiratory, digestive, and defensive capabilities, leaving them more vulnerable to predators and less competitive until full regeneration, which may require several weeks (Marin et al., 1991; Miller & Byrne, 2000). Therefore, it seems likely that in *B. stephanieae*, cerata shedding represents a last-resort strategy to eliminate accumulated metals, occurring only at relatively high concentrations. Unlike corals, which can expel their symbionts to probably stabilising their microbiome, this mechanism is not available at lower concentrations, and thus the microbiome of *B. stephanieae* becomes destabilised even at 1 mg/L.

Our experiments clearly show that although adult *B. stephanieaea* seem to be quite tolerant to Ni and Co exposure; it is important to look at the early life stages in particular, as these are usually much more sensitive to pollution, and successful reproduction and recruitment may still be compromised, ultimately threatening long-term population stability in polluted environments. Further, the first signs of stress, such as reduced mobility, no feeding, and eventually cerata shedding, were only observed at comparatively high concentrations of around 18 mg/L, suggesting that adults can withstand short-term exposure without acute mortality. However, our microbiome analyses revealed that significant changes in bacterial community structure occurred at much lower concentrations, as early as 1 mg/L, well before any

behavioural or morphological symptoms became apparent. Such microbial restructuring could therefore be considered a sensitive early warning signal of holobiont health, offering a valuable tool for detecting sublethal impacts of pollution.

Outlook

Although this dissertation advances our understanding of photosymbiotic sea slugs as holobiont model systems, it also highlights several unresolved questions that warrant future investigation. A central question is how molecular and cellular mechanisms shape the difference between stable and unstable symbioses in Sacoglossa and Cladobranchia, which are still only partly understood. Some key questions that remain are: Are there differences in MAMPs among the various Symbiodiniaceae genera? Which PRRs are expressed by the host slug, and do these differ between cladobranch species with stable versus unstable photosymbioses? In sacoglossans, do species classified as short-term retainers (StR) also form a kleptosome, or is this feature restricted to long-term retainers (LtR) and thus responsible for the duration and stability of kleptoplasty? Finally, do kleptoplasts display MAMPs similar to those of Symbiodiniaceae, and which PRRs are involved in their recognition by sacoglossan hosts?

The role of the microbiome in shaping holobiont physiology also remains an open field. While this thesis demonstrated shifts in microbial communities depending on symbiotic state and environmental stress, it remains to be shown whether these changes are cause or consequence of altered host physiology. Furthermore, the origin of the microbiome remains an open question. In *B. stephanieae*, evidence points to vertical inheritance, whereas in *E. viridis* it is widely assumed to be acquired horizontally. It is possible that the source of the microbiome differs between Cladobranchia and Sacoglossa, reflecting distinct strategies to adapt to changing environmental conditions.

Finally, an important challenge is to place photosymbiotic sea slugs into the context of global change. Rising sea surface temperatures, ocean acidification, and increasing pollution will likely act in concert, creating complex stress scenarios for marine holobionts. Future studies should therefore adopt multilevel experimental designs that look at the whole organism as a holobiont, in which host and symbiotic partners interact and influence one another rather than examining them individually. This would allow us to gain insights early on, before the host exhibits pronounced signs of stress, and could thus serve as a valuable early warning system.

In summary, the dissertation underscores the promise of photosymbiotic sea slugs as tractable models for exploring the evolution, function, and vulnerability of animal–algal symbioses. By combining molecular, microbial, behavioural, and ecotoxicological approaches, future research can resolve long-standing questions about the mechanisms of symbiosis and provide urgently needed insights into how these delicate associations will fare in an era of accelerating environmental change.

Bibliography

Abdelrahman, S. M., Patin, N. V., Hanora, A., Aboseidah, A., Desoky, S., Desoky, S. G., Stewart, F. J., & Lopanik, N. B. (2021). The natural product biosynthetic potential of Red Sea nudibranch microbiomes. *PeerJ*, *9*, e10525.

Abrego, D., Ulstrup, K. E., Willis, B. L., & van Oppen, M. J. (2008). Species–specific interactions between algal endosymbionts and coral hosts define their bleaching response to heat and light stress. *Proceedings of the Royal Society B: Biological Sciences*, *275*(1648), 2273–2282.

Abrego, D., Van Oppen, M. J., & Willis, B. L. (2009). Onset of algal endosymbiont specificity varies among closely related species of *Acropora* corals during early ontogeny. *Molecular Ecology*, *18*(16), 3532–3543.

Acosta-González, A., Rosselló-Móra, R., & Marqués, S. (2013). Characterization of the anaerobic microbial community in oil-polluted subtidal sediments: Aromatic biodegradation potential after the Prestige oil spill. *Environmental Microbiology*, *15*(1), 77–92.

Aihara, Y., Takahashi, S., & Minagawa, J. (2016). Heat induction of cyclic electron flow around photosystem I in the symbiotic dinoflagellate *Symbiodinium*. *Plant Physiology*, *171*(1), 522–529.

Ajala, L. O., Wilson, J. E., Jiru, M., & Iwunze, M. O. (2025). Perspective on health and ecological risk assessments of potentially toxic metal (loid) s using aquatic biodiversity as biomonitoring indicators. *Toxicology Reports*, 102086.

Allard, C. A., Thies, A. B., Mitra, R., Vaelli, P. M., Leto, O. D., Walsh, B. L., Laetz, E. M., Tresguerres, M., Lee, A. S., & Bellono, N. W. (2025). A host organelle integrates stolen chloroplasts for animal photosynthesis. *Cell*.

Almeida, D. B., Magalhães, C., Sousa, Z., Borges, M. T., Silva, E., Blanquet, I., & Mucha, A. P. (2021). Microbial community dynamics in a hatchery recirculating aquaculture system (RAS) of sole (*Solea senegalensis*). *Aquaculture*, *539*, 736592.

Amaya, D. L. G., Thiel, A., Möller, M., Gasparoni, G., Pirritano, M., Drews, F., Bornhorst, J., & Simon, M. (2023). Microbial impact to environmental toxicants Ni (II) and Co (II): Joint toxicity and cellular response in *Paramecium*. *Chemosphere*, *345*, 140434.

Anderson, M. J. (2001). A new method for non-parametric multivariate analysis of variance. *Austral Ecology*, *26*(1), 32–46.

Anderson, M. J. (2014). Permutational multivariate analysis of variance (PERMANOVA). *Wiley Statsref: Statistics Reference Online*, 1–15.

Anderson, R. E., Beltrán, M. T., Hallam, S. J., & Baross, J. A. (2013). Microbial community structure across fluid gradients in the Juan de Fuca Ridge hydrothermal system. *FEMS Microbiology Ecology*, *83*(2), 324–339.

Ansari, N., Rokhbakhsh-Zamin, F., Hassanshahian, M., & Hesni, M. A. (2021). Biodegradation of crude oil using symbiont crude-oil degrading bacteria isolated from corals collected at the Persian Gulf. *Journal of Chemical Technology & Biotechnology*, *96*(7), 1882–1892.

Apprill, A. M., & Gates, R. D. (2007). Recognizing diversity in coral symbiotic dinoflagellate communities. *Molecular Ecology*, *16*(6), 1127–1134.

Apte, S., Andersen, L., Andrewartha, J., Angel, B., Shearer, D., Simpson, S., Stauber, J., & Vicente-Beckett, V. (2006). Contaminant pathways in Port Curtis: Final report. *Cooperative Research Centre for Coastal Zone, Estuary and Waterway Management (Coastal CRC), Indooroopilly, Australia*, *143*.

Aranda, M., Li, Y., Liew, Y. J., Baumgarten, S., Simakov, O., Wilson, M. C., Piel, J., Ashoor, H., Bougouffa, S., Bajic, V. B., et al. (2016). Genomes of coral dinoflagellate symbionts highlight evolutionary adaptations conducive to a symbiotic lifestyle. *Scientific Reports*, *6*(1), 39734.

Armstrong, E. J., Roa, J. N., Stillman, J. H., & Tresguerres, M. (2018). Symbiont photosynthesis in giant clams is promoted by V-type H^+-ATPase from host cells. *Journal of Experimental Biology*, *221:jeb177220*.

Arndt, D., Xia, J., Liu, Y., Zhou, Y., Guo, A. C., Cruz, J. A., Sinelnikov, I., Budwill, K., Nesbø, C. L., & Wishart, D. S. (2012). METAGENassist: A comprehensive web server for comparative metagenomics. *Nucleic Acids Research*, *40*(W1), W88–W95.

Arnott, S. E., Yan, N., Keller, W., & Nicholls, K. (2001). The influence of drought-induced acidification on the recovery of plankton in Swan Lake (Canada). *Ecological Applications*, *11*(3), 747–763.

Arora, P. K., & Bae, H. (2014). Bacterial degradation of chlorophenols and their derivatives. *Microbial Cell Factories*, *13*, 1–17.

Ates, M., Demir, V., Arslan, Z., Camas, M., & Celik, F. (2016). Toxicity of engineered nickel oxide and cobalt oxide nanoparticles to *Artemia salina* in seawater. *Water, Air, & Soil Pollution*, *227*(3), 70.

Augustin, R., Schröder, K., Murillo Rincón, A. P., Fraune, S., Anton-Erxleben, F., Herbst, E.-M., Wittlieb, J., Schwentner, M., Grötzinger, J., Wassenaar, T. M., et al. (2017). A secreted antibacterial neuropeptide shapes the microbiome of *Hydra*. *Nature communications*, *8*(1), 698.

Avendaño-Herrera, R., Toranzo, A. E., & Magariños, B. (2006). Tenacibaculosis infection in marine fish caused by *Tenacibaculum maritimum*: A review. *Diseases of Aquatic Organisms*, *71*(3), 255–266.

Baedke, J., Fábregas-Tejeda, A., & Nieves Delgado, A. (2020). The holobiont concept before Margulis. *Journal of Experimental Zoology Part B: Molecular and Developmental Evolution*, *334*(3), 149–155.

Bai, J., Li, H., & Zhao, Y. (2009). Bacterial distribution at different stations in the Northern Yellow Sea. *Acta Microbiologica Sinica*, *49*(3), 343–350.

Baker, A. C. (2004). Symbiont diversity on coral reefs and its relationship to bleaching resistance and resilience. In *Coral Health and Disease* (pp. 177–194). Springer.

Banaszak, A. T., Santos, M. G. B., LaJeunesse, T., & Lesser, M. (2006). The distribution of mycosporine-like amino acids (MAAs) and the phylogenetic identity of symbiotic dinoflagellates in cnidarian hosts from the Mexican Caribbean. *Journal of Experimental Marine Biology and Ecology*, *337*(2), 131–146.

Barneah, O., Weis, V., Perez, S., & Benayahu, Y. (2004). Diversity of dinoflagellate symbionts in Red Sea soft corals: Mode of symbiont acquisition matters. *Marine Ecology Progress Series*, *275*, 89–95.

Bastidas, C., & Garcia, E. (2004). Sublethal effects of mercury and its distribution in the coral *Porites astreoides*. *Marine Ecology Progress Series*, *267*, 133–143.

Baştürk, M. N., Christa, G., & de Vries, J. (2025). Kleptoplasty: Solar-powered sea slugs house stolen plastids in kleptosomes. *Current Biology*, *35*(17), R840–R842.

Baumgartner, F. A., & Toth, G. B. (2014). Abundance and size distribution of the sacoglossan *Elysia viridis* on co-occurring algal hosts on the Swedish west coast. *PLoS One*, *9*(3), e92472.

Bay, L. K., Doyle, J., Logan, M., & Berkelmans, R. (2016). Recovery from bleaching is mediated by threshold densities of background thermo-tolerant symbiont types in a reef-building coral. *Royal Society Open Science*, *3*(6), 160322.

Bayat, Z., Hassanshahian, M., & Hesni, M. A. (2015). Enrichment and isolation of crude oil degrading bacteria from some mussels collected from the Persian Gulf. *Marine Pollution Bulletin*, *101*(1), 85–91.

Bayer, T., Neave, M. J., Alsheikh-Hussain, A., Aranda, M., Yum, L. K., Mincer, T., Hughen, K., Apprill, A., & Voolstra, C. R. (2013). The microbiome of the Red Sea coral *Stylophora pistillata* is dominated by tissue-associated *Endozoicomonas* bacteria. *Applied and Environmental Microbiology*, *79*(15), 4759–4762.

Bayliss, S. L., Scott, Z. R., Coffroth, M. A., & terHorst, C. P. (2019). Genetic variation in *Breviolum antillogorgium*, a coral reef symbiont, in response to temperature and nutrients. *Ecology and Evolution*, *9*(5), 2803–2813.

Bergh, R. (1870). Malacologische untersuchungen. in: C. semper, reisen im archpel der philippinen. *Wiss. Res.*, *2*(14), 603–645.

Bergh, R. (1896). Eolidiens d'amboine. *Revue Suisse de Zoologie*, *4*(2), 385–394.

Bickell-Page, L. R. (1989). Autotomy of cerata by the nudibranch *Melibe leonina* (Mollusca): Ultrastructure of the autotomy plane and neural correlate of the behaviour. *Philosophical Transactions of the Royal Society of London. B, Biological Sciences*, *324*(1222), 149–172.

Bida, I., Moliszewska, E., Matik, K., Ślusarczyk, A., Pawliczek, D., Havryliuk, O., Hovorukha, V., & Tashyrev, O. (2025). The resistance of biohumus microbiome to cobalt and nickel compounds. *Scientific Reports*, *15*(1), 10437.

Bielmyer, G., Brix, K., Capo, T., & Grosell, M. (2005). The effects of metals on embryo-larval and adult life stages of the sea urchin, *Diadema antillarum*. *Aquatic Toxicology*, *74*(3), 254–263.

Bisanz, J. E. (2018). *qiime2R: Importing QIIME2 artifacts and associated data into R sessions* [v0.99].

Biscéré, T., Ferrier-Pagès, C., Gilbert, A., Pichler, T., & Houlbrèque, F. (2018). Evidence for mitigation of coral bleaching by manganese. *Scientific Reports*, *8*(1), 16789.

Blewett, T. A., Dow, E. M., Wood, C. M., McGeer, J. C., & Smith, D. S. (2018). The role of dissolved organic carbon concentration and composition on nickel toxicity to early life-stages of the blue mussel *Mytilus edulis* and purple sea urchin *Strongylocentrotus purpuratus*. *Ecotoxicology and Environmental Safety*, *160*, 162–170.

Blewett, T. A., & Leonard, E. M. (2017). Mechanisms of nickel toxicity to fish and invertebrates in marine and estuarine waters. *Environmental Pollution*, *223*, 311–322.

Blewett, T. A., Smith, D. S., Wood, C. M., & Glover, C. N. (2016). Mechanisms of nickel toxicity in the highly sensitive embryos of the sea urchin *Evechinus chloroticus*, and the modifying effects of natural organic matter. *Environmental Science & Technology*, *50*(3), 1595–1603.

Böhringer, N., Fisch, K. M., Schillo, D., Bara, R., Hertzer, C., Grein, F., Eisenbarth, J.-H., Kaligis, F., Schneider, T., Wägele, H., et al. (2017). Antimicrobial potential of bacteria associated with marine sea slugs from North Sulawesi, Indonesia. *Frontiers in Microbiology*, *8*, 1092.

Bolyen, E., Rideout, J. R., Dillon, M. R., Bokulich, N. A., Abnet, C. C., Al-Ghalith, G. A., Alexander, H., Alm, E. J., Arumugam, M., Asnicar, F., et al. (2019). Reproducible, interactive, scalable and extensible microbiome data science using QIIME 2. *Nature Biotechnology*, *37*(8), 852–857.

Bonaventura, R., Costa, C., Deidda, I., Zito, F., & Russo, R. (2022). Gene expression analysis of the stress response to lithium, nickel, and zinc in paracentrotus lividus embryos. *Toxics*, *10*(6), 325.

Bordenstein, S., & Theis, K. (2008). Host biology in light of the microbiome: Ten principles of holobionts and hologenomes. *PLoS Biology*, *13*(8), 1–23.

Borgstein, N. M., Burgués Palau, L., Parodi, B. A., & Laetz, E. M. (2024b). Unraveling the Phidiana paradox: *Phidiana lynceus* can retain algal symbionts but its nocturnal tendencies prevent benefits from photosynthesis. *Symbiosis*, *92*(2), 245–255.

Borgstein, N. M., van der Meij, S. E., Christa, G., & Laetz, E. M. (2024a). Potential energetic and oxygenic benefits to unstable photosymbiosis in the cladobranch slug, *Berghia stephanieae* (nudibranchia, aeolidiidae). *Marine Biology Research*, *20*(1-2), 45–58.

Bourne, D. G., Garren, M., Work, T. M., Rosenberg, E., Smith, G. W., & Harvell, C. D. (2009). Microbial disease and the coral holobiont. *Trends in Microbiology*, *17*(12), 554–562.

Bourne, D. G., Morrow, K. M., & Webster, N. S. (2016). Insights into the coral microbiome: Underpinning the health and resilience of reef ecosystems. *Annual Review of Microbiology*.

Brading, P., Warner, M. E., Smith, D. J., & Suggett, D. J. (2013). Contrasting modes of inorganic carbon acquisition amongst *Symbiodinium* (Dinophyceae) phylotypes. *New Phytologist*, *200*(2), 432–442.

Bray, J. R., & Curtis, J. T. (1957). An ordination of the upland forest communities of southern Wisconsin. *Ecological Monographs*, *27*(4), 326–349.

Britstein, M., Cerrano, C., Burgsdorf, I., Zoccarato, L., Kenny, N. J., Riesgo, A., Lalzar, M., & Steindler, L. (2020). Sponge microbiome stability during environmental acquisition of highly specific photosymbionts. *Environmental Microbiology*, *22*(8), 3593–3607.

Brocco French, K. I. (2024). With a little help from their friends: Marine Invertebrate Microbiomes in the Face of Global Change. *Diss. University of California, Irvine*.

Brooks, P. R., Browne, M. A., Benedetti-Cecchi, L., Lyons, D. A., & Crowe, T. P. (2023). A response-surface approach into the interactive effects of multiple stressors reveals new insights into complex responses. *Frontiers in Marine Science*, *10*, 1169677.

Brown, A. L., Sharp, K., & Apprill, A. (2022). Reshuffling of the coral microbiome during dormancy. *Applied and Environmental Microbiology*, *88*(23), e01391–22.

Brown, J. W., Berg, O. H., Boutko, A., Stoerck, C., Boersma, M. A., & Frost, W. N. (2024). Division of labor for defensive retaliation and preemption by the peripheral and central nervous systems in the nudibranch *Berghia*. *Current Biology*, *34*(10), 2175–2185.

Buckingham, M., D'Angelo, C., Chalk, T. B., Foster, G., Johnson, K., Connelly, Z., Olla, C., Saeed, M., & Wiedenmann, J. (2022). Impact of nitrogen (n) and phosphorus (p) enrichment and skewed n: P stoichiometry on the skeletal formation and microstructure of symbiotic reef corals. *Coral Reefs*, *41*(4), 1147–1159.

Budinoff, C. R., Dunlap, J. R., Hadden, M., & Buchan, A. (2011). *Marivita roseacus* sp. nov., of the family Rhodobacteraceae, isolated from a temperate estuary and an emended description of the genus *Marivita*. *The Journal of General and Applied Microbiology*, *57*(5), 259–267.

Bunse, C., Koch, H., Breider, S., Simon, M., & Wietz, M. (2021). Sweet spheres: Succession and CAZyme expression of marine bacterial communities colonizing a mix of alginate and pectin particles. *Environmental Microbiology*, *23*(6), 3130–3148.

Burghardt, I., Evertsen, J., Johnsen, G., & Wägele, H. (2005). Solar powered seaslugs - Mutualistic symbiosis of aeolid nudibranchia (Mollusca, Gastropoda, Opisthobranchia) with *Symbiodinium*. *Symbiosis*.

Burghardt, I., & Gosliner, T. M. (2006). *Phyllodesmium rudmani* (Mollusca: Nudibranchia: Aeolidoidea), a new solar powered species from the Indo-West Pacific with data on its symbiosis with zooxanthellae. *Zootaxa*, *1308*(1), 31–47.

Burghardt, I., Schrödl, M., & Wägele, H. (2008). Three new solar-powered species of the genus *Phyllodesmium* Ehrenberg, 1831 (Mollusca: Nudibranchia: Aeolidioidea) from the tropical Indo-Pacific, with analysis of their photosynthetic activity and notes on biology. *Journal of Molluscan Studies*, *74*(3), 277–292.

Burghardt, I., Stemmer, K., & Wägele, H. (2008). Symbiosis between *Symbiodinium* (Dinophyceae) and various taxa of Nudibranchia (Mollusca: Gastropoda), with analyses of long-term retention. *Organisms Diversity & Evolution*, *8*(1), 66–76.

Burghardt, I., & Wägele, H. (2014). The symbiosis between the 'solar-powered'nudibranch *Melibe engeli* Risbec, 1937 (Dendronotoidea) and *Symbiodinium* sp. (Dinophyceae). *Journal of Molluscan Studies*, *80*(5), 508–517.

Burgués Palau, L., Senna, G., & Laetz, E. M. (2024). Crawl away from the light! Assessing behavioral and physiological photoprotective mechanisms in tropical solar-powered sea slugs exposed to natural light intensities. *Marine Biology*, *171*(2), 50.

Burn, R. (1962). Descriptions of victorian nudibranchiate Mollusca, with a comprehensive review of the Eolidacea. *Memoirs of the National Museum of Victoria, Melbourne*, *25*, 95–128.

Bushnell, B., Rood, J., & Singer, E. (2017). BBMerge–accurate paired shotgun read merging via overlap. *PloS one*, *12*(10), e0185056.

Butler, C. C., Turnham, K. E., Lewis, A. M., Nitschke, M. R., Warner, M. E., Kemp, D. W., Hoegh-Guldberg, O., Fitt, W. K., van Oppen, M. J., & LaJeunesse, T. (2023). Formal recognition of host-generalist species of dinoflagellate (*Cladocopium*, Symbiodiniaceae) mutualistic with Indo-Pacific reef corals. *Journal of Phycology*, *59*(4), 698–711.

Byrne, M. (2012). Global change ecotoxicology: Identification of early life history bottlenecks in marine invertebrates, variable species responses and variable experimental approaches. *Marine Environmental Research*, *76*, 3–15.

Callahan, B. J., McMurdie, P. J., Rosen, M. J., Han, A. W., Johnson, A. J. A., & Holmes, S. P. (2016). DADA2: High-resolution sample inference from Illumina amplicon data. *Nature Methods*, *13*(7), 581–583.

Camacho, C., Coulouris, G., Avagyan, V., Ma, N., Papadopoulos, J., Bealer, K., & Madden, T. L. (2009). BLAST+: Architecture and applications. *BMC Bioinformatics*, *10*, 1–9.

Cammack, R. (1988). Nickel in metalloproteins. In *Advances in inorganic chemistry* (pp. 297–333, Vol. 32). Elsevier.

Campbell, A. L., Mangan, S., Ellis, R. P., & Lewis, C. (2014). Ocean acidification increases copper toxicity to the early life history stages of the polychaete *Arenicola marina* in artificial seawater. *Environmental Science & Technology*, *48*(16), 9745–9753.

Caron, D. (2000). Symbiosis and mixotrophy among pelagic microorganisms. *Microbial ecology of the oceans*, 495–523.

Carriker, M. R. (2001). Embryogenesis and organogenesis of veligers and early juveniles. In *Developments in Aquaculture and Fisheries Science* (pp. 77–115, Vol. 31). Elsevier.

Cartaxana, P., Morelli, L., Cassin, E., Havurinne, V., Cabral, M., & Cruz, S. (2023). Prey species and abundance affect growth and photosynthetic performance of the polyphagous sea slug *Elysia crispata*. *Royal Society Open Science*, *10*, 230810.

Cartaxana, P., Morelli, L., Jesus, B., Calado, G., Calado, R., & Cruz, S. (2019). The photon menace: Kleptoplast protection in the photosynthetic sea slug *Elysia timida*. *Journal of Experimental Biology*, *222:jeb202580*.

Cartaxana, P., Rey, F., LeKieffre, C., Lopes, D., Hubas, C., Spangenberg, J. E., Escrig, S., Jesus, B., Calado, G., Domingues, R., Kühl, M., Calado, R., Meibom, A., & Cruz, S. (2021). Photosynthesis from stolen chloroplasts can support sea slug reproductive fitness. *Proceedings of the Royal Society B*, *288*.

Cartaxana, P., Morelli, L., Quintaneiro, C., Calado, G., Calado, R., & Cruz, S. (2018). Kleptoplast photoacclimation state modulates the photobehaviour of the solar-powered sea slug *Elysia viridis*. *Journal of Experimental Biology*, *221*(12).

Cartaxana, P., Trampe, E., Kühl, M., & Cruz, S. (2017). Kleptoplast photosynthesis is nutritionally relevant in the sea slug *Elysia viridis*. *Scientific Reports*, *7*(1), 7714.

Casalduero, F. G., & Muniain, C. (2008). The role of kleptoplasts in the survival rates of *Elysia timida* (Risso, 1818):(Sacoglossa: Opisthobranchia) during periods of food shortage. *Journal of Experimental Marine Biology and Ecology*, *357*(2), 181–187.

Cerbino, G. N., Traglia, G. M., Ayala Nuñez, T., Parmeciano Di Noto, G., Ramírez, M. S., Centrón, D., Iriarte, A., & Quiroga, C. (2023). Comparative genome analysis of the genus *Shewanella* unravels the association of key genetic traits with known and potential pathogenic lineages. *Frontiers in Microbiology*, *14*, 1124225.

Chan, C. X., Vaysberg, P., Price, D. C., Pelletreau, K. N., Rumpho, M. E., & Bhattacharya, D. (2018). Active host response to algal symbionts in the sea slug *Elysia chlorotica*. *Molecular biology and evolution*, *35*(7), 1706–1711.

Chan, H. Y., Chang, Y.-W., Chen, L.-S., Nishida, K., & Shao, Y. T. (2022). The effect of environmental factors on spatial-temporal variation of heterobranch sea slug community in northern Taiwan. *Frontiers in Marine Science*, *9*, 1042961.

Chen, M.-C., Cheng, Y.-M., Hong, M.-C., & Fang, L.-S. (2004). Molecular cloning of rab5 (aprab5) in *Aiptasia pulchella* and its retention in phagosomes harboring live zooxanthellae. *Biochemical and Biophysical Research Communications*, *324*(3), 1024–1033.

Chen, M.-C., Cheng, Y.-M., Sung, P.-J., Kuo, C.-E., & Fang, L.-S. (2003). Molecular identification of rab7 (aprab7) in *Aiptasia pulchella* and its exclusion from phagosomes harboring Zooxanthellae. *Biochemical and Biophysical Research Communications*, *308*(3), 586–595.

Chiarelli, R., & Roccheri, M. C. (2014). Marine invertebrates as bioindicators of heavy metal pollution.

Choi, H. M., Schwarzkopf, M., Fornace, M. E., Acharya, A., Artavanis, G., Stegmaier, J., Cunha, A., & Pierce, N. A. (2018). Third-generation *in situ* hybridization chain reaction: Multiplexed, quantitative, sensitive, versatile, robust. *Development*, *145*(12), dev165753.

Christa, G. (2023). Kleptoplasty. *Current Biology*, *33*, 465–467.

Christa, G., Händeler, K., Schäberle, T. F., König, G. M., & Wägele, H. (2014a). Identification of sequestered chloroplasts in photosynthetic and non-photosynthetic sacoglossan sea slugs (Mollusca, Gastropoda). *Frontiers in Zoology*, *11*, 15.

Christa, G., Pütz, L., Sickinger, C., Melo Clavijo, J., Laetz, E. M., Greve, C., & Serôdio, J. (2018). Photoprotective non-photochemical quenching does not prevent kleptoplasts from net photoinactivation. *Frontiers in Ecology and Evolution*, *6*, 121.

Christa, G., Zimorski, V., Woehle, C., Tielens, A. G. M., Wägele, H., Martin, W. F., & Gould, S. B. (2014b). Plastid-bearing sea slugs fix CO2 in the light but do not require photosynthesis to survive. *Proceedings of the Royal Society B*, *281*.

Christa, G., Händeler, K., Kück, P., Vleugels, M., Franken, J., Karmeinski, D., & Wägele, H. (2015). Phylogenetic evidence for multiple independent origins of functional kleptoplasty in Sacoglossa (Heterobranchia, Gastropoda). *Organisms Diversity & Evolution*, *15*(1), 23–36.

Clavijo, J. M., Sickinger, C., Bleidißel, S., Gasparoni, G., Tierling, S., Preisfeld, A., & Christa, G. (2022). The nudibranch *Berghia stephanieae* (Valdés, 2005) is not able to initiate a functional symbiosome-like environment to maintain *Breviolum minutum* (JE Parkinson & LaJeunesse 2018). *Frontiers in Marine Science*, *9*, 934307.

Cocks, W. (1852). New species of mollusca. *Naturalist*, *2*(1).

Connor, P. (1972). Acute toxicity of heavy metals to some marine larvae. *Marine Pollution Bulletin*, *3*(12), 190–192.

Córdoba-Tovar, L., Marrugo-Negrete, J., Barón, P. R., & Díez, S. (2022). Drivers of biomagnification of Hg, As and Se in aquatic food webs: A review. *Environmental Research*, *204*, 112226.

Correia, A. T., Motta, E., Daniel, D., Nunes, B., & Neves, J. (2025). Ecotoxicological effects of environmentally relevant concentrations of nickel nanoparticles on aquatic organisms from three trophic levels: Insights from oxidative stress biomarkers. *Journal of Xenobiotics*, *15*(4), 112.

Cowen, R. (1988). The role of algal symbiosis in reefs through time. *Palaios*, 221–227.

Criswell, K. E., & Gillis, J. A. (2020). Resegmentation is an ancestral feature of the gnathostome vertebral skeleton. *Elife*, *9*, e51696.

Cruz, S., & Cartaxana, P. (2022). Kleptoplasty: Getting away with stolen chloroplasts. *PLoS Biol*, *20*.

Cruz, S., Calado, R., Serôdio, J., & Cartaxana, P. (2013). Crawling leaves: Photosynthesis in sacoglossan sea slugs. *Journal of Experimental Botany*, *64*(13), 3999–4009.

Cruz, S., LeKieffre, C., Cartaxana, P., Hubas, C., Thiney, N., Jakobsen, S., Escrig, S., Jesus, B., Kühl, M., Calado, R., et al. (2020). Functional kleptoplasts intermediate incorporation of carbon and nitrogen in cells of the Sacoglossa sea slug *Elysia viridis*. *Scientific Reports*, *10*(1), 10548.

Cunning, R., Gates, R. D., & Edmunds, P. J. (2017). Using high-throughput sequencing of ITS2 to describe *Symbiodinium* metacommunities in St. John, US Virgin Islands. *PeerJ*, *5*, e3472.

Cunning, R., Silverstein, R. N., & Baker, A. C. (2015). Investigating the causes and consequences of symbiont shuffling in a multi-partner reef coral symbiosis

under environmental change. *Proceedings of the Royal Society B: Biological Sciences*, *282*(1809), 20141725.

Curdt, F., Schupp, P. J., & Rohde, S. (2022). Light availability affects the symbiosis of sponge specific cyanobacteria and the common blue aquarium sponge (*Lendenfeldia chondrodes*). *Animals*, *12*(10), 1283.

Curry, T. M., Peña, M. J., & Urbanowicz, B. R. (2023). An update on xylan structure, biosynthesis, and potential commercial applications. *The Cell Surface*, 100101.

Curson, A. R., Liu, J., Bermejo Martínez, A., Green, R. T., Chan, Y., Carrión, O., Williams, B. T., Zhang, S.-H., Yang, G.-P., Bulman Page, P. C., et al. (2017). Dimethylsulfoniopropionate biosynthesis in marine bacteria and identification of the key gene in this process. *Nature Microbiology*, *2*(5), 1–9.

Curtis, E., Moseley, J., Racicot, R., & Wright, R. M. (2023). Bacterial microbiome variation across symbiotic states and clonal lines in a cnidarian model. *Frontiers in Marine Science*.

Curtis, N., Massey, S., Schwartz, J., Maugel, T., & Pierce, S. (2005). The intracellular, functional chloroplasts in adult sea slugs (*Elysia crispata*) come from several algal species, and are also different from those in juvenile slugs. *Microscopy and Microanalysis*, *11*(S02), 1194–1195.

Dagdag, O., Quadri, T. W., Haldhar, R., Kim, S.-C., Daoudi, W., Berdimurodov, E., Akpan, E. D., & Ebenso, E. E. (2023). An overview of heavy metal pollution and control. *Heavy metals in the environment: Management strategies for global pollution*, 3–24.

Dall'Olio, L. R., Beran, A., Flander-Putrle, V., Malej, A., & Ramšak, A. (2022). Diversity of dinoflagellate symbionts in scyphozoan hosts from shallow environments: The Mediterranean Sea and Cabo Frio (Rio de Janeiro, Brazil). *Frontiers in Marine Science*, *9*, 867554.

Dana, J. D. (1846). *United states exploring expedition during the years 1838-1842: Atlas zoophytes* (Vol. 7). Lea; Blanchard.

Dang, K. V., Pierangelini, M., Roberty, S., & Cardol, P. (2019). Alternative photosynthetic electron transfers and bleaching phenotypes upon acute heat stress in *Symbiodinium* and *Breviolum* spp.(Symbiodiniaceae) in culture. *Frontiers in Marine Science*, *6*, 656.

Daniels, C. A., Baumgarten, S., Yum, L. K., Michell, C. T., Bayer, T., Arif, C., Roder, C., Weil, E., & Voolstra, C. R. (2015). Metatranscriptome analysis of the reef-building coral *Orbicella faveolata* indicates holobiont response to coral disease. *Frontiers in Marine Science*, *2*, 62.

Dave, G., & Xiu, R. (1991). Toxicity of mercury, copper, nickel, lead, and cobalt to embryos and larvae of zebrafish, *Brachydanio rerio*. *Archives of Environmental Contamination and Toxicology*, *21*, 126–134.

Davies, S. W., Moreland, K. N., Wham, D. C., Kanke, M. R., & Matz, M. V. (2020). *Cladocopium* community divergence in two *Acropora* coral hosts across multiple spatial scales. *Molecular Ecology*, *29*(23), 4559–4572.

Davis, J., Fricke, W. F., Hamann, M. T., Esquenazi, E., Dorrestein, P. C., & Hill, R. T. (2013). Characterization of the bacterial community of the chemically defended Hawaiian sacoglossan *Elysia rufescens*. *Applied and Environmental Microbiology*, *79*(22), 7073–7081.

Davison, H. R., Hurst, G. D., & Siozios, S. (2023). *'Candidatus* Megaira 'are diverse symbionts of algae and ciliates with the potential for defensive symbiosis. *Microbial Genomics*, *9*(3), 000950.

Davy, S. K., Allemand, D., & Weis, V. M. (2012). Cell biology of cnidarian-dinoflagellate symbiosis. *Microbiology and Molecular Biology Reviews*, *76*, 229–261.

de Barros Marangoni, L. F., Marques, J. A., Duarte, G. A. S., Pereira, C. M., Calderon, E. N., e Castro, C. B., & Bianchini, A. (2017). Copper effects on biomarkers associated with photosynthesis, oxidative status and calcification in the Brazilian coral *Mussismilia harttii* (Scleractinia, Mussidae). *Marine Environmental Research*, *130*, 248–257.

de Oliveira, B. F. R., Freitas-Silva, J., Sánchez-Robinet, C., & Laport, M. S. (2020). Transmission of the sponge microbiome: Moving towards a unified model. *Environmental Microbiology Reports*, *12*(6), 619–638.

de Souza, M. R., Caruso, C., Ruiz-Jones, L., Drury, C., Gates, R., & Toonen, R. J. (2022). Community composition of coral-associated Symbiodiniaceae differs across fine-scale environmental gradients in Kāne ʻohe bay. *Royal Society Open Science*, *9*(9), 212042.

de Vries, J., Habicht, J., Woehle, C., Huang, C., Christa, G., Wägele, H., Nickelsen, J., Martin, W. F., & Gould, S. B. (2013). Is ftsH the key to plastid longevity in sacoglossan slugs? *Genome Biology and Evolution*, *5*, 2540–2548.

de Vries, J., Rauch, C., Christa, G., & Gould, S. B. (2014). A sea slug's guide to plastid symbiosis. *Acta Societatis Botanicorum Poloniae*, *83*, 415–421.

de Vries, J., Woehle, C., Christa, G., Wägele, H., Tielens, A. G. M., Jahns, P., & Gould, S. B. (2015). Comparison of sister species identifies factors underpinning plastid compatibility in green sea slugs. *Proceedings of the Royal Society B*, *282*.

De Schamphelaere, K. A., Koene, J. M., Heijerick, D. G., & Janssen, C. R. (2008). Reduction of growth and haemolymph Ca levels in the freshwater snail *Lymnaea stagnalis* chronically exposed to cobalt. *Ecotoxicology and Environmental Safety*, *71*(1), 65–70.

De Vries, J., Rauch, C., Christa, G., & Gould, S. B. (2014). A sea slug's guide to plastid symbiosis. *Acta Societatis Botanicorum Poloniae*, *83*(4).

Dean, A. D., Minter, E. J., Sørensen, M. E., Lowe, C. D., Cameron, D. D., Brockhurst, M. A., & Wood, A. J. (2016). Host control and nutrient trading in a photosynthetic symbiosis. *Journal of theoretical biology*, *405*, 82–93.

Decelle, J. (2013). New perspectives on the functioning and evolution of photosymbiosis in plankton: Mutualism or parasitism? *Communicative & Integrative Biology*, *6*(4), e24560.

D'elia, C., Domotor, S., & Webb, K. (1983). Nutrient uptake kinetics of freshly isolated zooxanthellae. *Marine Biology*, *75*, 157–167.

Delle Chiaie, S. (1841). Descrizione e notomia degli animali invertebrati della sicilia citeriore: Osservati vivi negli anni 1822-1830/da s. delle chiale. *Museum of Comparative Zoology–Biodiversity Heritage Library digitization project*.

Devezas, T. (2025). Prospective and analytical forecasting analysis of the currently identified as the most critical materials for the energy transition.

Devine, S. P., Pelletreau, K. N., & Rumpho, M. E. (2012). 16S rDNA-based metagenomic analysis of bacterial diversity associated with two populations of the kleptoplastic sea slug *Elysia chlorotica* and its algal prey *Vaucheria litorea*. *The Biological Bulletin*, *223*(1), 138–154.

Diaz, M. C., Thacker, R. W., Rützler, K., & Piantoni Dietrich, C. (2007). Two new haplosclerid sponges from Caribbean Panama with symbiotic filamentous cyanobacteria, and an overview of sponge-cyanobacteria associations. *Porifera research: Biodiversity, innovation and sustainability*.

Dikow, R. B. (2011). Genome-level homology and phylogeny of *Shewanella* (Gammaproteobacteria: Iteromonadales: Shewanellaceae). *BMC Genomics*, *12*, 1–14.

Diner, R. E., Allard, S. M., & Gilbert, J. A. (2024). Host-associated microbes mitigate the negative impacts of aquatic pollution. *Msystems*, *9*(10), e00868–24.

Dishaw, L. J., Flores-Torres, J., Lax, S., Gemayel, K., Leigh, B., Melillo, D., Mueller, M. G., Natale, L., Zucchetti, I., De Santis, R., et al. (2014). The gut of geographically disparate *Ciona intestinalis* harbors a core microbiota. *PLoS One*, *9*(4), e93386.

Dittami, S. M., Arboleda, E., Auguet, J.-C., Bigalke, A., Briand, E., Cárdenas, P., Cardini, U., Decelle, J., Engelen, A. H., Eveillard, D., et al. (2021). A community perspective on the concept of marine holobionts: Current status, challenges, and future directions. *PeerJ*, *9*, e10911.

Dixon, P. (2003). VEGAN, a package of R functions for community ecology. *Journal of Vegetation Science*, *14*(6), 927–930.

Djeghri, N., Pondaven, P., Stibor, H., & Dawson, M. N. (2019). Review of the diversity, traits, and ecology of zooxanthellate jellyfishes. *Marine Biology*, *166*(11), 147.

Doepke, H., Herrmann, K., & Schuett, C. (2012). Endobacteria in the tentacles of selected cnidarian species and in the cerata of their nudibranch predators. *Helgoland Marine Research*, *66*(1), 43–50.

Doering, T., Wall, M., Putchim, L., Rattanawongwan, T., Schroeder, R., Hentschel, U., & Roik, A. (2021). Towards enhancing coral heat tolerance: A "microbiome transplantation" treatment using inoculations of homogenized coral tissues. *Microbiome*, *9*(1), 102.

Donat, J. R., & Bruland, K. W. (1988). Direct determination of dissolved cobalt and nickel in seawater by differential pulse cathodic stripping voltammetry preceded by adsorptive collection of cyclohexane-1, 2-dione dioxime complexes. *Analytical Chemistry*, *60*(3), 240–244.

Dos Reis, L. L., de Abreu, C. B., Gebara, R. C., Rocha, G. S., Longo, E., Mansano, A. d. S., & Melão, M. d. G. G. (2024). Isolated and combined effects of cobalt and nickel on the microalga *Raphidocelis subcapitata*. *Ecotoxicology*, *33*(1), 104–118.

Douglas, A. (2003). Coral bleaching–How and why? *Marine Pollution Bulletin*, *46*(4), 385–392.

Duchassaing de Fonbressin, P., & Michelotti, G. (1860). Mémoire sur les Coralliaires des Antilles.

Džunková, M., La Clair, J. J., Tyml, T., Doud, D., Schulz, F., Piquer-Esteban, S., Porcel Sanchis, D., Osborn, A., Robinson, D., Louie, K. B., Bowen, B. P., Bowers, R. M., Lee, J., Arnau, V., Díaz-Villanueva, W., Stepanauskas, R., Gosliner, T., Date, S. V., Northen, T. R., … Woyke, T. (2023). Synthase-selected sorting approach identifies a beta-lactone synthase in a nudibranch symbiotic bacterium. *Microbiome*, *11*(130).

Edmunds, M. (1966). Protective mechanisms in the Eolidacea (Mollusca Nudibranchia). *Zoological Journal of the Linnean Society*, *46*(308), 27–71.

Eitinger, T., Suhr, J., Moore, L., & Smith, J. A. C. (2005). Secondary transporters for nickel and cobalt ions: Theme and variations. *Biometals*, *18*, 399–405.

Elfeky, H. H., Hanora, A., & Solyman, S. M. (2023). Bioactivity of bacteria associated with Red Sea nudibranchs and whole genome sequence of *Nocardiopsis dassonvillei* RACA-4. *Marine Genomics*, *67*, 101004.

Emery, M. A., Beavers, K. M., Van Buren, E. W., Batiste, R., Dimos, B., Pellegrino, M. W., & Mydlarz, L. D. (2024). Trade-off between photosymbiosis and innate immunity influences cnidarian's response to pathogenic bacteria. *Proceedings of the Royal Society B*, *291*(2032), 20240428.

Environment and Climate Change Canada. (2017). Screening assessment Cobalt and Cobalt-Containing substances [Accessed: 2024-12-04].

Epstein, H. E., Brown, T., Akinrinade, A. O., McMinds, R., Pollock, F. J., Sonett, D., Smith, S., Bourne, D. G., Carpenter, C. S., Knight, R., et al. (2025). Evidence for microbially-mediated tradeoffs between growth and defense throughout coral evolution. *Animal Microbiome*, *7*(1), 1.

Eren, A. M., Morrison, H. G., Lescault, P. J., Reveillaud, J., Vineis, J. H., & Sogin, M. L. (2015). Minimum entropy decomposition: Unsupervised oligotyping for sensitive partitioning of high-throughput marker gene sequences. *The ISME Journal*, *9*(4), 968–979.

European Commission. (2018). European Union risk assessment report on nickel, nickel sulphate, nickel carbonate, nickel chloride, nickel dinitrate. Protection Agency on behalf of the European Union, Copenhagen, Denmark. *Final report May 2008. Prepared by Danish Environmental*.

Evertsen, J., & Johnsen, G. (2009). *In vivo* and *in vitro* differences in chloroplast functionality in the two north atlantic sacoglossans (Gastropoda, Opisthobranchia) *Placida dendritica* and *Elysia viridis*. *Marine Biology*, *156*, 847–859.

Falkowski, P. G., Dubinsky, Z., Muscatine, L., & McCloskey, L. (1993). Population control in symbiotic corals. *Bioscience*, *43*(9), 606–611.

Fay, S., Weber, M., & Lipps, J. (2009). The distribution of *Symbiodinium* diversity within individual host Foraminifera. *Coral Reefs*, *28*, 717–726.

Fernandez, J.-M., Ouillon, S., Chevillon, C., Douillet, P., Fichez, R., & Le Gendre, R. (2006). A combined modelling and geochemical study of the fate of terrigenous inputs from mixed natural and mining sources in a coral reef lagoon (New Caledonia). *Marine Pollution Bulletin*, *52*(3), 320–331.

FitzPatrick, S., Liberatore, K., Garcia, J., Burghardt, I., Colman, D., Moquin, S., Takacs-Vesbach, C., & Shepherd, U. (2012). *Symbiodinium* diversity in the soft coral *Heteroxenia* sp. and its nudibranch predator *Phyllodesmium lizardensis*. *Coral Reefs*, *31*, 895–905.

Foroutan, R., Oujifard, A., Papari, F., & Esmaeili, H. (2019). Calcined *Umbonium vestiarium* snail shell as an efficient adsorbent for treatment of wastewater containing Co (II). *3 Biotech*, *9*(3), 78.

Forskål, P. (1775). *Descriptiones animalium, avium, amphibiorum, piscium, insectorum, vermium: Quae in itinere orientali observavit*. ex officina Mölleri.

Fragoso ados Santos, H., Duarte, G. A. S., Rachid, C. T. d. C., Chaloub, R. M., Calderon, E. N., Marangoni, L. F. d. B., Bianchini, A., Nudi, A. H., Do Carmo, F. L., Van Elsas, J. D., et al. (2015). Impact of oil spills on coral reefs can be reduced by bioremediation using probiotic microbiota. *Scientific Reports*, *5*(1), 18268.

Frankenbach, S., Luppa, Q., Serôdio, J., Greve, C., Bleidissel, S., Melo Clavijo, J., Laetz, E. M., Preisfeld, A., & Christa, G. (2021). Kleptoplasts are continuously digested during feeding in the plastid-bearing sea slug *Elysia viridis*. *Journal of Molluscan Studies*, *87*(3), eyab022.

Frankenbach, S., Melo Clavijo, J., Brück, M., Bleidißel, S., Simon, M., Gasparoni, G., Lo Porto, C., Laetz, E. M., Greve, C., Donath, A., et al. (2023). Shedding light on starvation in darkness in the plastid-bearing sea slug *Elysia viridis* (Montagu, 1804). *Marine Biology*, *170*(7), 89.

Frisch, K., Småge, S. B., Brevik, Ø. J., Duesund, H., & Nylund, A. (2018). Genotyping of *Tenacibaculum maritimum* isolates from farmed Atlantic salmon in Western Canada. *Journal of Fish Diseases*, *41*(1), 131–137.

Fritts-Penniman, A. L., Gosliner, T. M., Mahardika, G. N., & Barber, P. H. (2020). Cryptic ecological and geographic diversification in coral-associated nudibranchs. *Molecular Phylogenetics and Evolution*, *144*, 106698.

Fujise, L., Nitschke, M. R., Frommlet, J. C., Serôdio, J., Woodcock, S., Ralph, P. J., & Suggett, D. J. (2018). Cell cycle dynamics of cultured coral endosymbiotic microalgae (*Symbiodinium*) across different types (species) under alternate light and temperature conditions. *Journal of Eukaryotic Microbiology*, *65*(4), 505–517.

Funkhouser, L. J., & Bordenstein, S. R. (2013). Mom knows best: The universality of maternal microbial transmission. *PLoS Biology*, *11*(8), e1001631.

Gall, J. E., Boyd, R. S., & Rajakaruna, N. (2015). Transfer of heavy metals through terrestrial food webs: A review. *Environmental Monitoring and Assessment*, *187*(4), 201.

Gao, Y., Zhang, Y., Liu, J., & Kong, H. (2013). Metabolism and subcellular distribution of anthracene in tall fescue (*Festuca arundinacea* Schreb.) *Plant and Soil*, *365*, 171–182.

Gardner, S. G., Camp, E. F., Smith, D. J., Kahlke, T., Osman, E. O., Gendron, G., Hume, B. C., Pogoreutz, C., Voolstra, C. R., & Suggett, D. J. (2019). Coral microbiome diversity reflects mass coral bleaching susceptibility during the 2016 El Niño heat wave. *Ecology and Evolution*, *9*(3), 938–956.

Gascoigne, T. (1977). Sacoglossan teeth. *Malacologia*, *16*, 101–105.

Gashkina, N. A. (2024). Metal toxicity: Effects on energy metabolism in fish. *International Journal of Molecular Sciences*, *25*(9), 5015.

Gasteiger, E., Hoogland, C., Gattiker, A., Duvaud, S., Wilkins, M. R., Appel, R. D., & Bairoch, A. (2005). Protein identification and analysis tools on the ExPASy server. *The Proteomics Protocols Handbook*, 571–607.

Gatidou, G., Stasinakis, A. S., & Iatrou, E. I. (2015). Assessing single and joint toxicity of three phenylurea herbicides using *Lemna minor* and *Vibrio fischeri* bioassays. *Chemosphere*, *119*, S69–S74.

Gautam, P. K., Gautam, R. K., Banerjee, S., Chattopadhyaya, M., & Pandey, J. (2016). Heavy metals in the environment: Fate, transport, toxicity and remediation technologies. *Nova Sci Publishers*, *60*, 101–130.

Gayoso, A., Lopez, R., Xing, G., Boyeau, P., Valiollah Pour Amiri, V., Hong, J., Wu, K., Jayasuriya, M., Mehlman, E., Langevin, M., et al. (2022). A Python library for probabilistic analysis of single-cell omics data. *Nature Biotechnology*, *40*(2), 163–166.

Gerwick, W. H., & Fenner, A. M. (2013). Drug Discovery from Marine Microbes. *Microbial Ecology*, *65*, 800–806.

Girden, E. R. (1992). *ANOVA: Repeated measures*. Sage.

Giroux, M. S., Reichman, J. R., Langknecht, T., Burgess, R. M., & Ho, K. T. (2022). Environmental RNA as a tool for marine community biodiversity assessments. *Scientific Reports*, *12*(1), 17782.

Gissi, F., Reichelt-Brushett, A. J., Chariton, A. A., Stauber, J. L., Greenfield, P., Humphrey, C., Salmon, M., Stephenson, S. A., Cresswell, T., & Jolley, D. F. (2019). The effect of dissolved nickel and copper on the adult coral *Acropora muricata* and its microbiome. *Environmental Pollution*, *250*, 792–806.

Gissi, F., Stauber, J. L., Binet, M. T., Golding, L. A., Adams, M. S., Schlekat, C. E., Garman, E. R., & Jolley, D. F. (2016). A review of nickel toxicity to marine and estuarine tropical biota with particular reference to the South East Asian and Melanesian region. *Environmental Pollution*, *218*, 1308–1323.

Gissi, F., Stauber, J. L., Binet, M. T., Trenfield, M. A., Van Dam, J. W., & Jolley, D. F. (2018). Assessing the chronic toxicity of nickel to a tropical marine gastropod and two crustaceans. *Ecotoxicology and Environmental Safety*, *159*, 284–292.

Gissi, F., Wang, Z., Batley, G. E., Leung, K. M., Schlekat, C. E., Garman, E. R., & Stauber, J. L. (2020). Deriving a chronic guideline value for nickel in tropical

and temperate marine waters. *Environmental Toxicology and Chemistry*, *39*(12), 2540–2551.

González, A., Osorio, H., Romero, S., Méndez, P., Sepúlveda, M., Laporte, D., Gutierrez-Cutiño, M., Santander, R., Castro-Nallar, E., & Moenne, A. (2022). Transcriptomic analyses reveal increased expression of dioxygenases, monooxygenases, and other metabolizing enzymes involved in anthracene degradation in the marine alga *Ulva lactuca*. *Frontiers in Plant Science*, *13*, 955601.

González, A., Vidal, C., Espinoza, D., & Moenne, A. (2021). Anthracene induces oxidative stress and activation of antioxidant and detoxification enzymes in *Ulva lactuca* (Chlorophyta). *Scientific Reports*, *11*(1), 7748.

Goodheart, J. A., Bazinet, A. L., Valdés, Á., Collins, A. G., & Cummings, M. P. (2017). Prey preference follows phylogeny: Evolutionary dietary patterns within the marine gastropod group Cladobranchia (Gastropoda: Heterobranchia: Nudibranchia). *BMC Evolutionary Biology*, *17*, 1–14.

Goodheart, J. A., & Bely, A. E. (2017). Sequestration of nematocysts by divergent cnidarian predators: Mechanism, function, and evolution. *Invertebrate Biology*, *136*(1), 75–91.

Goodheart, J. A., Bleidißel, S., Schillo, D., Strong, E. E., Ayres, D. L., Preisfeld, A., Collins, A. G., Cummings, M. P., & Wägele, H. (2018). Comparative morphology and evolution of the cnidosac in Cladobranchia (Gastropoda: Heterobranchia: Nudibranchia). *Frontiers in Zoology*, *15*, 1–18.

Goodheart, J. A., Fiorenza, R., Rio, R., Lopez-Anido, R. N., Martin, N. J., Herrlinger, T. J., Tarvin, R. D., & Lyons, D. C. (2025). A subset of conserved phagocytic genes are likely used for the intracellular theft of cnidarian stinging organelles in nudibranch gastropods. *EvoDevo*.

Goodheart, J. A., Rio, R. A., Taraporevala, N. F., Fiorenza, R. A., Barnes, S. R., Morrill, K., Jacob, M. A. C., Whitesel, C., Masterson, P., Batzel, G. O., et al. (2024). A chromosome-level genome for the nudibranch gastropod *Berghia stephanieae* helps parse clade-specific gene expression in novel and conserved phenotypes. *BMC Biology*, *22*(1), 9.

Gopalakrishnan, S., Thilagam, H., & Raja, P. (2007). Toxicity of heavy metals on embryogenesis and larvae of the marine sedentary polychaete *Hydroides elegans*. *Archives of Environmental Contamination and Toxicology*, *52*(2), 171–178.

Gorman, L. M., Tivey, T. R., Raymond, E. H., Ashley, I. A., Oakley, C. A., Grossman, A. R., Weis, V. M., & Davy, S. K. (2025). Stability of the cnidarian–dinoflagellate symbiosis is primarily determined by symbiont cell-cycle arrest. *Proceedings of the National Academy of Sciences*, *122*(14), e2412396122.

Gornik, S. G., Bergheim, B. G., Morel, B., Stamatakis, A., Foulkes, N. S., & Guse, A. (2021). Photoreceptor diversification accompanies the evolution of anthozoa. *Molecular Biology and Evolution*, *38*, 1744–1760.

Goudriaan, M., Zeghal, E., Witte, H., Vaksmaa, A., & Niemann, H. (2024). Differentiation of bacterial communities on five common plastics after six days of exposure to Caribbean coastal waters. *Environmental Advances*, *16*, 100518.

Goulet, T. L., & Coffroth, M. A. (2004). The genetic identity of dinoflagellate symbionts in Caribbean octocorals. *Coral Reefs*, *23*, 465–472.

Goulet, T. L., Lucas, M. Q., & Schizas, N. V. (2019). Symbiodiniaceae genetic diversity and symbioses with hosts from shallow to mesophotic coral ecosystems. *Mesophotic Coral Ecosystems*, 537–551.

Goulet, T. L., Simmons, C., & Goulet, D. (2008). Worldwide biogeography of *Symbiodinium* in tropical octocorals. *Marine Ecology Progress Series*, *355*, 45–58.

Guillén Matus, D. G., Donaghy, C. M., Vijayan, N., Lane, Z. T., Howell, M., Glavin, G. G., Angeles-Boza, A. M., Nyholm, S. V., & Balunas, M. J. (2024). Multi-omics analysis reveals important role for microbial-derived metabolites from *Botryllus schlosseri* in metal interactions. *ASM Journals*, 2024–11.

Guiry, M. D. (2024). How many species of algae are there? A reprise. Four kingdoms, 14 phyla, 63 classes and still growing. *Journal of Phycology*, *60*(2), 214–228.

Hackstadt, A. J., & Hess, A. M. (2009). Filtering for increased power for microarray data analysis. *BMC Bioinformatics*, *10*, 1–12.

Halliwell, B., & Gutteridge, J. M. (1985). Free radicals in biology and medicine.

Hamada, M., Schröder, K., Bathia, J., Kürn, U., Fraune, S., Khalturina, M., Khalturin, K., Shinzato, C., Satoh, N., & Bosch, T. C. (2018). Metabolic co-dependence drives the evolutionarily ancient *Hydra–Chlorella* symbiosis. *Elife*, *7*, e35122.

Händeler, K., Wägele, H., Wahrmund, U., Rüdinger, M., & Knoop, V. (2010). Slugs' last meals: Molecular identification of sequestered chloroplasts from different algal origins in Sacoglossa (Opisthobranchia, Gastropoda). *Molecular Ecology Resources*, *10*, 968–978.

Händeler, K., Grzymbowski, Y. P., Krug, P. J., & Wägele, H. (2009). Functional chloroplasts in metazoan cells-a unique evolutionary strategy in animal life. *Frontiers in Zoology*, *6*, 1–18.

Händeler, K., & Wägele, H. (2007). Preliminary study on molecular phylogeny of Sacoglossa and a compilation of their food organisms. *Bonner Zoologische Beiträge*, *55*(3/4), 231–254.

Hardefeldt, J. M., & Reichelt-Brushett, A. J. (2015). Unravelling the role of zooxanthellae in the uptake and depuration of an essential metal in *Exaiptasia pallida*; an experiment using a model cnidarian. *Marine Pollution Bulletin*, *96*(1-2), 294–303.

Hartman, L. M., van Oppen, M. J. H., & Blackall, L. L. (2020). Microbiota characterization of *Exaiptasia diaphana* from the Great Barrier Reef. *Animal Microbiome*, *2*(1), 1–14.

Havurinne, V., Handrich, M., Antinluoma, M., Khorobrykh, S., Gould, S. B., & Tyystjärvi, E. (2021). Genetic autonomy and low singlet oxygen yield support kleptoplast functionality in photosynthetic sea slugs. *Journal of Experimental Botany*, *erab216*.

Hawes, C., & Cobb, A. (1980). The effects of starvation on the symbiotic chloroplasts in *Elysia viridis*: A fine structural study. *New Phytologist*, 375–379.

Hayashi, M., & Nakano, H. (2024). Staging of post-settlement growth in the nudibranch *Hypselodoris festiva*. *Scientific Reports*, *14*(1), 16157.

Hayward, P. J., & Ryland, J. S. (2017). *Handbook of the marine fauna of North-West Europe*. Oxford University Press.

Heidelberg, J. F., Paulsen, I. T., Nelson, K. E., Gaidos, E. J., Nelson, W. C., Read, T. D., Eisen, J. A., Seshadri, R., Ward, N., Methe, B., et al. (2002). Genome sequence of the dissimilatory metal ion–reducing bacterium *Shewanella oneidensis*. *Nature Biotechnology*, *20*(11), 1118–1123.

Hennige, S., Suggett, D., Warner, M., McDougall, K., & Smith, D. (2009). Photobiology of *Symbiodinium* revisited: Bio-physical and bio-optical signatures. *Coral Feefs*, *28*(1), 179–195.

Hernandez-Agreda, A., Gates, R. D., & Ainsworth, T. D. (2017). Defining the core microbiome in corals' microbial soup. *Trends in Microbiology*, *25*(2), 125–140.

Herrera Sarrias, M., Ziegler, M., Voolstra, C. R., & Aranda, M. (2017). Laboratory-Cultured Strains of the Sea Anemone *Exaiptasia* Reveal Distinct Bacterial Communities. *Frontiers in Marine Science*.

Hikosaka-Katayama, T., Koike, K., Yamashita, H., Hikosaka, A., & Koike, K. (2012). Mechanisms of maternal inheritance of dinoflagellate symbionts in the acoelomorph worm *Waminoa litus*. *Zoological Science*, *29*(9), 559–567.

Hill, M., Allenby, A., Ramsby, B., Schönberg, C., & Hill, A. (2011). *Symbiodinium* diversity among host clionaid sponges from caribbean and pacific reefs: evidence of heteroplasmy and putative host-specific symbiont lineages. *Molecular Phylogenetics and Evolution*, *59*(1), 81–88.

Hinde, R., & Smith, D. (1975). The role of photosynthesis in the nutrition of the mollusc *Elysia viridis*. *Biological Journal of the Linnean Society*, *7*(2), 161–171.

Hinde, R., & Smith, D. (1972). Persistence of functional chloroplasts in *Elysia viridis* (Opisthobranchia, Sacoglossa). *Nature New Biology*, *239*(88), 30–31.

Hirokane, Y., Miyamoto, A., Kitaura, J., Nakano, R., Hirano, Y. M., Kawane, M., & Yusa, Y. (2022). Phylogeny and evolution of functional chloroplast retention in sacoglossan sea slugs (Gastropoda: Heterobranchia). *Organisms Diversity & Evolution*, *22*, 419–429.

Hirose, E. (2015). Ascidian photosymbiosis: Diversity of cyanobacterial transmission during embryogenesis. *Genesis*, *53*(1), 121–131.

Hirose, E., Neilan, B. A., Schmidt, E. W., Murakami, A., Gault, P., et al. (2009). Enigmatic life and evolution of *Prochloron* and related cyanobacteria inhabiting colonial ascidians. *Handbook on Cyanobacteria*, 161–189.

Hochart, C., Paoli, L., Ruscheweyh, H.-J., Salazar, G., Boissin, E., Romac, S., Poulain, J., Bourdin, G., Iwankow, G., Moulin, C., et al. (2023). Ecology of Endozoicomonadaceae in three coral genera across the Pacific Ocean. *Nature Communications*, *14*(1), 3037.

Hoegh-Guldberg, O., & Jones, R. J. (1999). Photoinhibition and photoprotection in symbiotic dinoflagellates from reef-building corals. *Marine Ecology Progress Series*, *183*, 73–86.

Hollants, J., Leliaert, F., Verbruggen, H., De Clerck, O., & Willems, A. (2013). Host specificity and coevolution of Flavobacteriaceae endosymbionts within the siphonous green seaweed *Bryopsis*. *Molecular Phylogenetics and Evolution*, *67*(3), 608–614.

Hou, D., Jia, X., Wang, L., McGrath, S. P., Zhu, Y.-G., Hu, Q., Zhao, F.-J., Bank, M. S., O'Connor, D., & Nriagu, J. (2025). Global soil pollution by toxic metals threatens agriculture and human health. *Science*, *388*(6744), 316–321.

Howells, E. J., Vaughan, G., Work, T. M., Burt, J., & Abrego, D. (2020). Annual outbreaks of coral disease coincide with extreme seasonal warming. *Coral Reefs*, *39*, 771–781.

Hu, M., Zheng, X., Fan, C.-M., & Zheng, Y. (2020). Lineage dynamics of the endosymbiotic cell type in the soft coral *Xenia*. *Nature*, *582*(7813), 534–538.

Hume, B. C., D'Angelo, C., Burt, J. A., & Wiedenmann, J. (2018). Fine-scale biogeographical boundary delineation and sub-population resolution in the *Symbiodinium* thermophilum coral symbiont group from the Persian/Arabian Gulf and Gulf of Oman. *Frontiers in Marine Science*, *5*, 138.

Hume, B. C., Smith, E. G., Ziegler, M., Warrington, H. J., Burt, J. A., LaJeunesse, T., Wiedenmann, J., & Voolstra, C. R. (2019). SymPortal: A novel analytical framework and platform for coral algal symbiont next-generation sequencing ITS2 profiling. *Molecular Ecology Resources*, *19*(4), 1063–1080.

Hume, B. C., Voolstra, C. R., Arif, C., D'Angelo, C., Burt, J. A., Eyal, G., Loya, Y., & Wiedenmann, J. (2016). Ancestral genetic diversity associated with the rapid spread of stress-tolerant coral symbionts in response to Holocene climate change. *Proceedings of the National Academy of Sciences*, *113*(16), 4416–4421.

Hunt, J. W., Anderson, B. S., Phillips, B. M., Tjeerdema, R. S., Puckett, H. M., Stephenson, M., Tucker, D. W., & Watson, D. (2002). Acute and chronic toxicity of nickel to marine organisms: Implications for water quality criteria. *Environmental Toxicology and Chemistry: An International Journal*, *21*(11), 2423–2430.

Hwang, C. Y., Bae, G. D., Yih, W., & Cho, B. C. (2009). *Marivita cryptomonadis* gen. nov., sp. nov. and *Marivita litorea* sp. nov., of the family Rhodobacteraceae, isolated from marine habitats. *International Journal of Systematic and Evolutionary Microbiology*, *59*(7), 1568–1575.

Iglic, K. L. (2011). *Diss: Trace metal limitation and its role in oxidative stress of coral algal symbionts; implications for thermally induced coral bleaching events*. The University of Western Ontario (Canada).

International Energy Agency. (2021). The Role of Critical World Energy Outlook Special Report Minerals in Clean Energy Transitions. World Energy Outlook Special Report [Accessed: 2024-12-04].

Ip, Y. K., Teng, G. C. Y., Boo, M. V., Poo, J. S. T., Hiong, K. C., Kim, H., Wong, W. P., & Chew, S. F. (2020). Symbiodiniaceae dinoflagellates express urease in three subcellular compartments and upregulate its expression levels *in situ* in three organs of a giant clam (*Tridacna squamosa*) during illumination. *Journal of Phycology*, *56*(6), 1696–1711.

Jaishankar, M., Tseten, T., Anbalagan, N., Mathew, B. B., & Beeregowda, K. N. (2014). Toxicity, mechanism and health effects of some heavy metals. *Interdisciplinary Toxicology*, *7*(2), 60.

Jékely, G. (2009). Evolution of phototaxis. *Philosophical Transactions of the Royal Society B: Biological Sciences*, *364*, 2795–2808.

Jensen, K. R. (1997). Evolution of the Sacoglossa (Mollusca, Opisthobranchia) and the ecological associations with their food plants. *Evolutionary Ecology*, *11*(3), 301–335.

Jeong, H., Byeon, E., Kim, D.-H., Maszczyk, P., & Lee, J.-S. (2023). Heavy metals and metalloid in aquatic invertebrates: A review of single/mixed forms, combination with other pollutants, and environmental factors. *Marine Pollution Bulletin*, *191*, 114959.

Jimbo, M., Koike, K., Sakai, R., Muramoto, K., & Kamiya, H. (2005). Cloning and characterization of a lectin from the octocoral *Sinularia lochmodes*. *Biochemical and Biophysical Research Communications*, *330*(1), 157–162.

Jinkerson, R. E., Russo, J. A., Newkirk, C. R., Kirk, A. L., Chi, R. J., Martindale, M. Q., Grossman, A. R., Hatta, M., & Xiang, T. (2022). Cnidarian-Symbiodiniaceae symbiosis establishment is independent of photosynthesis. *Current Biology*, *32*, 2402–2415.e4.

Johansson, K.-E., & Pettersson, B. (2002). Taxonomy of Mollicutes. *Molecular biology and pathogenicity of Mycoplasmas*, 1–29.

Johnson, R. F., & Gosliner, T. M. (2012). Traditional taxonomic groupings mask evolutionary history: A molecular phylogeny and new classification of the chromodorid nudibranchs. *Plos one*, *7*(4), e33479.

Jomova, K., Alomar, S. Y., Nepovimova, E., Kuca, K., & Valko, M. (2025). Heavy metals: Toxicity and human health effects. *Archives of Toxicology*, *99*(1), 153–209.

Jones, A. M., Berkelmans, R., van Oppen, M. J., Mieog, J. C., & Sinclair, W. (2008). A community change in the algal endosymbionts of a scleractinian coral following a natural bleaching event: Field evidence of acclimatization. *Proceedings of the Royal Society B: Biological Sciences*, *275*(1641), 1359–1365.

Kalaji, H. M., Schansker, G., Ladle, R. J., Goltsev, V., Bosa, K., Allakhverdiev, S. I., Brestic, M., Bussotti, F., Calatayud, A., Dąbrowski, P., et al. (2014). Frequently asked questions about *in vivo* chlorophyll fluorescence: Practical issues. *Photosynthesis Research*, *122*(2), 121–158.

Karmeinski, D., Meusemann, K., Goodheart, J. A., Schroedl, M., Martynov, A., Korshunova, T., Wägele, H., & Donath, A. (2021). Transcriptomics provides a robust framework for the relationships of the major clades of cladobranch sea slugs (Mollusca, Gastropoda, Heterobranchia), but fails to resolve the position of the enigmatic genus Embletonia. *BMC Ecology and Evolution*, *21*(1), 226.

Katharios, P., Seth-Smith, H. M., Fehr, A., Mateos, J. M., Qi, W., Richter, D., Nufer, L., Ruetten, M., Guevara Soto, M., Ziegler, U., et al. (2015). Environmental marine pathogen isolation using mesocosm culture of sharpsnout seabream: Striking genomic and morphological features of novel *Endozoicomonas* sp. *Scientific Reports*, *5*(1), 17609.

Kawafune, K., Hongoh, Y., Hamaji, T., Sakamoto, T., Kurata, T., Hirooka, S., Miyagishima, S.-y., & Nozaki, H. (2015). Two different rickettsial bacteria invading *Volvox carteri*. *PLoS One*, *10*(2), e0116192.

Keller-Costa, T., Lago-Lestón, A., Saraiva, J., Toscan, R., Silva, S., Gonçalves, J., Cox, C. J., Kyrpides, N., Nunes da Rocha, U., & Costa, R. (2021). Metagenomic insights into the taxonomy, function, and dysbiosis of prokaryotic communities in octocorals. *Microbiome*, *9*, 1–21.

Kempf, S. C. (1984). Symbiosis between the zooxanthella *Symbiodinium* (= *Gymnodinium*) *microadriaticum* (Freudenthal) and four species of nudibranchs. *The Biological Bulletin*, *166*(1), 110–126.

Kempf, S. C. (1991). A 'primitive'symbiosis between the aeolid nudibranch *Berghia verrucicornis* (A. Costa, 1867) and a zooxanthella. *Journal of Molluscan Studies*, *57*(Supplement_Part_4), 75–85.

Khan, B., Ho, K. T., & Burgess, R. M. (2020). Application of biomarker tools using bivalve models toward the development of adverse outcome pathways for contaminants of emerging concern. *Environmental Toxicology and Chemistry*, *39*(8), 1472–1484.

Kiene, R. P., Linn, L. J., & Bruton, J. A. (2000). New and important roles for DMSP in marine microbial communities. *Journal of Sea Research*, *43*(3-4), 209–224.

Killam, D., Das, S., Martindale, R. C., Gray, K. E., Paytan, A., & Junium, C. K. (2023). Photosymbiosis and nutrient utilization in giant clams revealed by nitrogen isotope sclerochronology. *Geochimica et Cosmochimica Acta*, *359*, 165–175.

Kimbrough, K. L. (2008). An assessment of two decades of contaminant monitoring in the nation's coastal zone.

Kirk, A. L., Clowez, S., Lin, F., Grossman, A. R., & Xiang, T. (2020). Transcriptome reprogramming of Symbiodiniaceae *Breviolum minutum* in response to casein amino acids supplementation. *Frontiers in Physiology*, *11*, 574654.

Kirso, U., & Irha, N. (1998). Role of algae in fate of carcinogenic polycyclic aromatic hydrocarbons in the aquatic environment. *Ecotoxicology and Environmental Safety*, *41*(1), 83–89.

Klussmann-Kolb, A., Dinapoli, A., Kuhn, K., Streit, B., & Albrecht, C. (2008). From sea to land and beyond–new insights into the evolution of euthyneuran Gastropoda (Mollusca). *BMC Evolutionary Biology*, *8*(1), 57.

Kodžoman, K., Clavijo, J. M., Sickinger, C., & Christa, G. (2023). Funktionale Kleptoplastie in Meeresnacktschnecken: Schnecken, die gerne Algen wären? *Biologie in unserer Zeit-BiuZ*, *53*(2), 155–163.

Krieger-Liszkay, A. (2005). Singlet oxygen production in photosynthesis. *Journal of Experimental Botany*, *56*(411), 337–346.

Kristiana, R., Sibero, M. T., Farisa, M. Y., Ayuningrum, D., Dirgantara, D., Hanafi, M., Radjasa, O. K., Sabdono, A., & Trianto, A. (2019). Antibacterial potential of nudibranch-associated bacteria from Saparua and Nusa Laut Islands, Indonesia. *Biodiversitas Journal of Biological Diversity*, *20*(7).

Kristof, A., & Klussmann-Kolb, A. (2010). Neuromuscular development of *Aeolidiella stephanieae* Valdéz, 2005 (mollusca, gastropoda, nudibranchia). *Frontiers in Zoology*, *7*(1), 5.

Kruskal, W. H., & Wallis, W. A. (1952). Use of ranks in one-criterion variance analysis. *Journal of the American Statistical Association*, *47*(260), 583–621.

Kuehn, E., Clausen, D. S., Null, R. W., Metzger, B. M., Willis, A. D., & Özpolat, B. D. (2022). Segment number threshold determines juvenile onset of germline cluster expansion in *Platynereis dumerilii*. *Journal of Experimental Zoology Part B: Molecular and Developmental Evolution*, *338*(4), 225–240.

Kuek, F. W., Motti, C. A., Zhang, J., Cooke, I. R., Todd, J. D., Miller, D. J., Bourne, D. G., & Raina, J.-B. (2022). DMSP production by coral-associated bacteria. *Frontiers in Marine Science*, *9*.

Kükenthal, W. (1913). *Alcyonaria des Roten Meeres*. K. k. Hof-u. Staatsdr., Hölder.

Kumar, P., Gacem, A., Ahmad, M. T., Yadav, V. K., Singh, S., Yadav, K. K., Alam, M. M., Dawane, V., Piplode, S., Maurya, P., et al. (2022). Environmental and human health implications of metal (loid) s: Source identification, contamination, toxicity, and sustainable clean-up technologies. *Frontiers in environmental science*, *10*, 949581.

Kuniya, N., Jimbo, M., Tanimoto, F., Yamashita, H., Koike, K., Harii, S., Nakano, Y., Iwao, K., Yasumoto, K., & Watabe, S. (2015). Possible involvement of Tachylectin-2-like lectin from *Acropora tenuis* in the process of *Symbiodinium* acquisition. *Fisheries Science*, *81*(3), 473–483.

Kvennefors, E. C. E., Leggat, W., Hoegh-Guldberg, O., Degnan, B. M., & Barnes, A. C. (2008). An ancient and variable mannose-binding lectin from the coral *Acropora millepora* binds both pathogens and symbionts. *Developmental & Comparative Immunology*, *32*(12), 1582–1592.

Kvennefors, E. C. E., Leggat, W., Kerr, C. C., Ainsworth, T. D., Hoegh-Guldberg, O., & Barnes, A. C. (2010). Analysis of evolutionarily conserved innate immune components in coral links immunity and symbiosis. *Developmental & Comparative Immunology*, *34*(11), 1219–1229.

Laetz, E. M., Moris, V. C., Moritz, L., Haubrich, A. N., & Wägele, H. (2017b). Photosynthate accumulation in solar-powered sea slugs-starving slugs survive due to accumulated starch reserves. *Frontiers in Zoology*, *14*, 1–9.

Laetz, E. M., Rühr, P. T., Bartolomaeus, T., Preisfeld, A., & Wägele, H. (2017a). Examining the retention of functional kleptoplasts and digestive activity in sacoglossan sea slugs. *Organisms Diversity & Evolution*, *17*, 87–99.

Laetz, E. M., & Wägele, H. (2019). Comparing amylose production in two solar-powered sea slugs: The sister taxa *Elysia timida* and *E. cornigera* (Heterobranchia: Sacoglossa). *Journal of Molluscan Studies*, *85*, 166–171.

LaJeunesse, T. (2002). Diversity and community structure of symbiotic dinoflagellates from Caribbean coral reefs. *Marine Biology*, *141*, 387–400.

LaJeunesse, T., Parkinson, J. E., Gabrielson, P. W., Jeong, H. J., Reimer, J. D., Voolstra, C. R., & Santos, S. R. (2018). Systematic revision of Symbiodiniaceae highlights the antiquity and diversity of coral endosymbionts. *Current Biology*, *28*(16), 2570–2580.

Lampert, K. P. (2016). *Cassiopea* and its zooxanthellae. *The cnidaria, past, present and future: The world of medusa and her sisters*, 415–423.

Lange, R., & Marshall, D. (2017). Ecologically relevant levels of multiple, common marine stressors suggest antagonistic effects. *Scientific Reports*, *7*(1), 6281.

Laoye, B., Olagbemide, P., Ogunnusi, T., & Akpor, O. (2025). Heavy metal contamination: Sources, health impacts, and sustainable mitigation strategies with insights from nigerian case studies. *F1000Research*, *14*, 134.

Laroche, O., Wood, S. A., Tremblay, L. A., Lear, G., Ellis, J. I., & Pochon, X. (2017). Metabarcoding monitoring analysis: The pros and cons of using co-extracted environmental DNA and RNA data to assess offshore oil production impacts on benthic communities. *PeerJ*, *5*, e3347.

Laurillard, C. L. (1832). *In: Iconographie du règne animal de g. cuvier, ou représentation d'après nature de l'une des espèces les plus remarquables, et souvent non encore figurées, de chaque genre d'animaux. avec un texte descriptif mis au courant de la science: Ouvrage pouvant servir d'atlas à tous les traités de zoologie* (Vol. 4). JB Baillière.

Leal, M. C., Nunes, C., Alexandre, D., Da Silva, T. L., Reis, A., Dinis, M. T., & Calado, R. (2012). Parental diets determine the embryonic fatty acid profile of the tropical nudibranch *Aeolidiella stephanieae*: The effect of eating bleached anemones. *Marine Biology*, *159*, 1745–1751.

Leal, M. C., Rey, F., Ferreira, G. D., Domingues, M. R., & Calado, R. (2022). Inter-individual variability of early life stages of a model marine invertebrate with a bi-phasic life cycle is shaped by contrasting oceanographic conditions. *Frontiers in Marine Science*, *9*, 984569.

Lee, S. Y., Jeong, H. J., & Lajeunesse, T. (2020). *Cladocopium infistulum* sp. nov. (Dinophyceae), a thermally tolerant dinoflagellate symbiotic with giant clams from the western Pacific Ocean. *Phycologia*, *59*(6), 515–526.

Lehel, J., Magyar, M., Palotás, P., Abonyi-Tóth, Z., Bartha, A., & Budai, P. (2023). To eat or not to eat? Food safety aspects of essential metals in seafood. *Foods*, *12*(22), 4082.

Lehtovirta-Morley, L. E. (2018). Ammonia oxidation: Ecology, physiology, biochemistry and why they must all come together. *FEMS microbiology letters*, *365*(9), fny058.

Lesser, M. (2019). Phylogenetic signature of light and thermal stress for the endosymbiotic dinoflagellates of corals (family Symbiodiniaceae). *Limnology and Oceanography*, *64*(5), 1852–1863.

Lesser, M., Falcón, L. I., Rodríguez-Román, A., Enríquez, S., Hoegh-Guldberg, O., & Iglesias-Prieto, R. (2007). Nitrogen fixation by symbiotic cyanobacteria provides a source of nitrogen for the scleractinian coral *Montastraea cavernosa*. *Marine Ecology Progress Series*, *346*, 143–152.

Lesser, M., Stat, M., & Gates, R. (2013). The endosymbiotic dinoflagellates (*Symbiodinium* sp.) of corals are parasites and mutualists. *Coral Reefs*, *32*, 603–611.

Levin, R. A., Beltran, V. H., Hill, R., Kjelleberg, S., McDougald, D., Steinberg, P. D., & Van Oppen, M. J. (2016). Sex, scavengers, and chaperones: Transcriptome secrets of divergent *Symbiodinium* thermal tolerances. *Molecular Biology and Evolution*, *33*(9), 2201–2215.

Li, J., Shao, Z., Cheng, K., Yang, Q., Ju, H., Tang, X., Zhang, S., & Li, J. (2025). Coral-associated Symbiodiniaceae exhibit host specificity but lack phylosymbiosis, with *Cladocopium* and *Durusdinium* showing different cophylogenetic patterns. *New Phytologist*, *247*(1), 309–324.

Li, J., Zhang, Y., Sun, J., Thompson, F., & Zhang, Y. (2023). Interaction between marine invertebrates and symbiotic microbes in a changing environment: Community structure and ecological functions.

Li, Q., Tintut, Y., Demer, L. L., Vazquez-Padron, R. I., Bendeck, M. P., & Hsu, J. J. (2024). Collagen VIII in Vascular Diseases. *Matrix Biology*.

Li, T., Lin, X., Yu, L., Lin, S., Rodriguez, I. B., & Ho, T.-Y. (2020). RNA-seq profiling of *Fugacium kawagutii* reveals strong responses in metabolic processes and symbiosis potential to deficiencies of iron and other trace metals. *Science of the Total Environment*, *705*, 135767.

Liao, I. J.-Y., Sakagami, T., Lewin, T. D., Bailly, X., Hamada, M., & Luo, Y.-J. (2025). Animal–chlorophyte photosymbioses: Evolutionary origins and ecological diversity. *Biology Letters*, *21*(7), 20250250.

Liu, H., Stephens, T. G., González-Pech, R. A., Beltran, V. H., Lapeyre, B., Bongaerts, P., Cooke, I., Aranda, M., Bourne, D. G., Forêt, S., et al. (2018). *Symbiodinium* genomes reveal adaptive evolution of functions related to coral-dinoflagellate symbiosis. *Communications Biology*, *1*(1), 95.

Lo, R., Dougan, K. E., Chen, Y., Shah, S., Bhattacharya, D., & Chan, C. X. (2022). Alignment-free analysis of whole-genome sequences from Symbiodiniaceae reveals different phylogenetic signals in distinct regions. *Frontiers in Plant Science*, *13*, 815714.

Lovén, S. L. (1846). *Index molluscorum: Litora scandinaviæ occidentalia habitantium. faunæ prodromum*. PA Norstedt.

Lu, S. C. (2013). Glutathione synthesis. *Biochimica et Biophysica Acta (BBA)-General Subjects*, *1830*(5), 3143–3153.

Luter, H. M., Andersen, M., Versteegen, E., Laffy, P., Uthicke, S., Bell, J. J., & Webster, N. S. (2020). Cross-generational effects of climate change on the microbiome of a photosynthetic sponge. *Environmental Microbiology*, *22*(11), 4732–4744.

Ma, Y. J., Hein, E., Munthe-Fog, L., Skjoedt, M.-O., Bayarri-Olmos, R., Romani, L., & Garred, P. (2015). Soluble collectin-12 (CL-12) is a pattern recognition molecule initiating complement activation via the alternative pathway. *The Journal of Immunology*, *195*(7), 3365–3373.

Macomber, L., & Hausinger, R. P. (2011). Mechanisms of nickel toxicity in microorganisms. *Metallomics*, *3*(11), 1153–1162.

Maeda, T., Hirose, E., Chikaraishi, Y., Kawato, M., Takishita, K., Yoshida, T., Verbruggen, H., Tanaka, J., Shimamura, S., Takaki, Y., Tsuchiya, M., Iwai, K., & Maruyama, T. (2012). Algivore or phototroph? *Plakobranchus ocellatus* (Gastropoda) continuously acquires kleptoplasts and nutrition from multiple algal species in nature. *PLoS ONE*, *7*, e42024.

Maeda, T., Takahashi, S., Yoshida, T., Shimamura, S., Takaki, Y., Nagai, Y., Toyoda, A., Suzuki, Y., Arimoto, A., Ishii, H., et al. (2021). Chloroplast acquisition without the gene transfer in kleptoplastic sea slugs, *Plakobranchus ocellatus*. *Elife*, *10*, e60176.

Mahadevan, P., & Middlebrooks, M. L. (2020). Bacterial diversity in the *clarki* ecotype of the photosynthetic sacoglossan, *Elysia crispata*. *MicrobiologyOpen*, *9*(9), e1098.

Maire, J., Blackall, L. L., & van Oppen, M. J. (2021). Microbiome characterization of defensive tissues in the model anemone *Exaiptasia diaphana*. *BMC Microbiology*, *21*(1), 152.

Maire, J., Tandon, K., Collingro, A., van de Meene, A., Damjanovic, K., Gotze, C. R., Stephenson, S., Philip, G. K., Horn, M., Cantin, N. E., et al. (2023). Colocalization and potential interactions of *Endozoicomonas* and Chlamydiae in

microbial aggregates of the coral *Pocillopora acuta*. *Science Advances*, *9*(20), eadg0773.

Malcolm, H., & April, H. (2012). The magnesium inhibition and arrested phagosome hypotheses: New perspectives on the evolution and ecology of *Symbiodinium* symbioses. *Biological Reviews*, *87*(4), 804–821.

Mansfield, K. M., & Gilmore, T. D. (2019). Innate immunity and cnidarian-Symbiodiniaceae mutualism. *Developmental & Comparative Immunology*, *90*, 199–209.

Marin, A., Di Marzo, V., & Cimino, G. (1991). A histological and chemical study of the cerata of the opisthobranch mollusc *Tethys fimbria*. *Marine Biology*, *111*(3), 353–358.

Marín, A., & Ros, J. (2004). Chemical defenses in Sacoglossan Opisthobranchs: Taxonomic trends and evolutionary implications. *Scientia Marina*, *68*(S1), 227–241.

Markich, S. J. (2017). Sensitivity of the glochidia (larvae) of freshwater mussels (Bivalvia: Unionida: Hyriidae) to cadmium, cobalt, copper, lead, nickel and zinc: Differences between metals, species and exposure time. *Science of the Total Environment*, *601*, 1427–1436.

Martens, J.-H., Barg, H., Warren, M., & Jahn, D. (2002). Microbial production of vitamin B12. *Applied Microbiology and Biotechnology*, *58*(3), 275–285.

Martin, R., Walther, P., & Tomaschko, K.-H. (2015). Variable retention of kleptoplast membranes in cells of sacoglossan sea slugs: Plastids with extended, shortened and non-retained durations. *Zoomorphology*, *134*(4), 523–529.

Martinez, S., Grover, R., & Ferrier-Pagès, C. (2022). Symbiont starvation affects the stability of the coral–Symbiodiniaceae symbiosis. *Frontiers in Marine Science*, *9*, 979563.

Martinez-Pita, I., Garcia, F., & Pita, M.-L. (2005). Fatty acid composition and utilization in developing eggs of some marine nudibranchs (Mollusca: Gastropoda: Opistobranchia) from southwest Spain. *Journal of Shellfish Research*, *24*(4), 1209–1216.

Maselli, M., Anestis, K., Klemm, K., Hansen, P. J., & John, U. (2021). Retention of prey genetic material by the kleptoplastidic ciliate *Strombidium cf. basimorphum*. *Frontiers in Microbiology*, *12*, 694508.

Masindi, V., & Muedi, K. L. (2018). Environmental contamination by heavy metals. *Heavy metals*, *10*(4), 115–133.

Matthews, J. L., Crowder, C. M., Oakley, C. A., Lutz, A., Roessner, U., Meyer, E., Grossman, A. R., Weis, V. M., & Davy, S. K. (2017). Optimal nutrient exchange and immune responses operate in partner specificity in the cnidarian-dinoflagellate symbiosis. *Proceedings of the National Academy of Sciences*, *114*(50), 13194–13199.

Matthews, J. L., Hoch, L., Raina, J.-B., Pablo, M., Hughes, D. J., Camp, E. F., Seymour, J. R., Ralph, P. J., Suggett, D. J., & Herdean, A. (2023). Symbiodiniaceae photophysiology and stress resilience is enhanced by microbial associations. *Scientific Reports*, *13*(1), 20724.

McCauley, M., Goulet, T., Jackson, C., & Loesgen, S. (2023). Systematic review of cnidarian microbiomes reveals insights into the structure, specificity, and fidelity of marine associations. *Nature Communications*, *14*(1), 4899.

McDevitt-Irwin, J. M., Baum, J. K., Garren, M., & Vega Thurber, R. L. (2017). Responses of coral-associated bacterial communities to local and global stressors. *Frontiers in Marine Science*, *4*, 262.

McDougall, D. R., Toone, T. A., & Jeffs, A. G. (2022). Natural heavy metal concentrations in seawater as a possible cause of low survival of larval mussels. *Journal of Trace Elements in Medicine and Biology*, *74*, 127071.

McFall-Ngai, M., Hadfield, M. G., Bosch, T. C., Carey, H. V., Domazet-Lošo, T., Douglas, A. E., Dubilier, N., Eberl, G., Fukami, T., Gilbert, S. F., et al. (2013). Animals in a bacterial world, a new imperative for the life sciences. *Proceedings of the National Academy of Sciences*, *110*(9), 3229–3236.

Mebane, C. A., Eakins, R. J., Fraser, B. G., & Adams, W. J. (2015). Recovery of a mining-damaged stream ecosystem. *Elementa*, *3*.

Meehan, W. J., & Ostrander, G. K. (1997). Coral bleaching: A potential biomarker of environmental stress. *Journal of Toxicology and Environmental Health, Part A Current Issues*, *50*(6), 529–552.

Melo Clavijo, J., Donath, A., Serôdio, J., & Christa, G. (2018). Polymorphic adaptations in metazoans to establish and maintain photosymbioses. *Biological Reviews*, *93*(4), 2006–2020.

Melo Clavijo, J., Frankenbach, S., Fidalgo, C., Serôdio, J., Donath, A., Preisfeld, A., & Christa, G. (2020). Identification of scavenger receptors and thrombospondin-type-1 repeat proteins potentially relevant for plastid recognition in Sacoglossa. *Ecology and Evolution*, *10*(21), 12348–12363.

Melo Clavijo, J., Sickinger, C., Bleidißel, S., Gasparoni, G., Tierling, S., Preisfeld, A., & Christa, G. (2022). The nudibranch *Berghia stephanieae* (Valdés, 2005) is not able to initiate a functional symbiosome-like environment to maintain *Breviolum minutum* (JE Parkinson & LaJeunesse 2018). *Frontiers in Marine Science*.

Mendoza, M., Rocha, S., Troncoso, J., Posada, D., & Canchaya, C. (2023). Transcriptomic landscape of the kleptoplastic sea slug *Elysia viridis*. *Journal of Molluscan Studies*, *89*(1), eyad001.

Merrot, P., Juillot, F., Noël, V., Lefebvre, P., Brest, J., Menguy, N., Guigner, J.-M., Blondeau, M., Viollier, E., Fernandez, J.-M., et al. (2019). Nickel and iron partitioning between clay minerals, Fe-oxides and Fe-sulfides in lagoon sediments from New Caledonia. *Science of the Total Environment*, *689*, 1212–1227.

Meunier, V., Geissler, L., Bonnet, S., Rädecker, N., Perna, G., Grosso, O., Lambert, C., Rodolfo-Metalpa, R., Voolstra, C. R., & Houlbrèque, F. (2021). Microbes support enhanced nitrogen requirements of coral holobionts in a high CO2 environment. *Molecular Ecology*, *30*(22), 5888–5899.

Meyer, J. S., Lyons-Darden, T., Garman, E. R., Middleton, E. T., & Schlekat, C. E. (2020). Toxicity of nanoparticulate nickel to aquatic organisms: Review and recommendations for improvement of toxicity tests. *Environmental Toxicology and Chemistry*, *39*(10), 1861–1883.

Meyer, J. L., Paul, V. J., & Teplitski, M. (2014). Community shifts in the surface microbiomes of the coral *Porites astreoides* with unusual lesions. *PLoS One*, *9*(6), e100316.

Miller, J. A., & Byrne, M. (2000). Ceratal autotomy and regeneration in the aeolid nudibranch *Phidiana crassicornis* and the role of predators. *Invertebrate biology*, *119*(2), 167–176.

Mitoh, S., & Yusa, Y. (2021). Extreme autotomy and whole-body regeneration in photosynthetic sea slugs. *Current Biology*, *31*(5), R233–R234.

Miyake, S., Ngugi, D. K., & Stingl, U. (2016). Phylogenetic diversity, distribution, and cophylogeny of giant bacteria (*Epulopiscium*) with their surgeonfish hosts in the Red Sea. *Frontiers in Microbiology*, *7*, 285.

Miyamoto, A., Sakai, A., Nakano, R., & Yusa, Y. (2015). Phototaxis of sacoglossan sea slugs with different photosynthetic abilities: A test of the 'crawling leaves' hypothesis. *Marine Biology*, *162*, 1343–1349.

Mohamed, A. R., Ochsenkühn, M. A., Kazlak, A. M., Moustafa, A., & Amin, S. A. (2023). The coral microbiome: Towards an understanding of the molecular mechanisms of coral–microbiota interactions. *FEMS Microbiology Reviews*, *47*(2), fuad005.

Mohamed, A., Cumbo, V., Harii, S., Shinzato, C., Chan, C., Ragan, M., Bourne, D., Willis, B., Ball, E., Satoh, N., et al. (2016). The transcriptomic response of the coral *Acropora digitifera* to a competent *Symbiodinium* strain: The symbiosome as an arrested early phagosome. *Molecular Ecology*, *25*(13), 3127–3141.

Mojiri, A., Zhou, J. L., Ohashi, A., Ozaki, N., & Kindaichi, T. (2019). Comprehensive review of polycyclic aromatic hydrocarbons in water sources, their effects and treatments. *Science of the Total Environment*, *696*, 133971.

Montalbetti, E., Biscéré, T., Ferrier-Pagès, C., Houlbrèque, F., Orlandi, I., Forcella, M., Galli, P., Vai, M., & Seveso, D. (2021). Manganese benefits heat-stressed corals at the cellular level. *Frontiers in Marine Science*, *8*, 681119.

Monteiro, E. A., Güth, A. Z., Banha, T. N., Sumida, P. Y., & Mies, M. (2019). Evidence against mutualism in an aeolid nudibranch associated with Symbiodiniaceae dinoflagellates. *Symbiosis*, *79*, 183–189.

Moore, E. J., & Gosliner, T. (2014). Additions to the genus *Phyllodesmium*, with a phylogenetic analysis and its implications to the evolution of symbiosis. *The Veliger*, *51*, 237–251.

Moore, E. J., & Gosliner, T. M. (2011). Molecular phylogeny and evolution of symbiosis in a clade of Indopacific nudibranchs. *Molecular Phylogenetics and Evolution*, *58*(1), 116–123.

Morris, L. A., Voolstra, C. R., Quigley, K. M., Bourne, D. G., & Bay, L. K. (2019). Nutrient availability and metabolism affect the stability of coral–symbiodiniaceae symbioses. *Trends in Microbiology*, *27*(8), 678–689.

Mulrooney, S. B., & Hausinger, R. P. (2003). Nickel uptake and utilization by microorganisms. *FEMS Microbiology Reviews*, *27*(2-3), 239–261.

Murakami, T., Segawa, T., Dial, R., Takeuchi, N., Kohshima, S., & Hongoh, Y. (2017). Bacterial microbiota associated with the glacier ice worm is dominated by both worm-specific and glacier-derived facultative lineages. *Microbes and Environments*, *32*(1), 32–39.

Muscatine, L., Falkowski, P., Porter, J., & Dubinsky, Z. (1984). Fate of photosynthetic fixed carbon in light-and shade-adapted colonies of the symbiotic coral *Stylophora pistillata*. *Proceedings of the Royal Society of London. Series B. Biological Sciences*, *222*(1227), 181–202.

Muscatine, L., & Porter, J. W. (1977). Reef corals: Mutualistic symbioses adapted to nutrient-poor environments. *Bioscience*, *27*(7), 454–460.

Naryono, E. (2023). Nickel mine exploitation in Indonesia, between a blessing and a disaster of environmental damage. *Center for Open Science*, 1–22.

Naz, S., Habib, S. S., Arshad, M., Majeed, S., Acar, Ü., Kesbiç, O. S., Mohany, M., Aragona, F., & Fazio, F. (2025). Human health risk of heavy metal biomagnification: Trophic transfer patterns in aquatic ecosystems. *Journal of Trace Elements in Medicine and Biology*, 127704.

Neave, M. J., Apprill, A., Ferrier-Pagès, C., & Voolstra, C. R. (2016). Diversity and function of prevalent symbiotic marine bacteria in the genus *Endozoicomonas*. *Applied Microbiology and Biotechnology*, *100*, 8315–8324.

Neave, M. J., Michell, C. T., Apprill, A., & Voolstra, C. R. (2017). *Endozoicomonas* genomes reveal functional adaptation and plasticity in bacterial strains symbiotically associated with diverse marine hosts. *Scientific Reports*, *7*(1), 40579.

Nechev, J., Stefanov, K., & Popov, S. (2006). Effect of cobalt ions on lipid and sterol metabolism in the marine invertebrates *Mytilus galloprovincialis* and *Actinia equina*. *Comparative Biochemistry and Physiology Part A: Molecular & Integrative Physiology*, *144*(1), 112–118.

Neu, A. T., Allen, E. E., & Roy, K. (2021). Defining and quantifying the core microbiome: Challenges and prospects. *Proceedings of the National Academy of Sciences*, *118*(51), e2104429118.

Neubauer, E. F., Poole, A. Z., Detournay, O., Weis, V. M., & Davy, S. K. (2016). The scavenger receptor repertoire in six cnidarian species and its putative role in cnidarian-dinoflagellate symbiosis. *PeerJ*, *4*, e2692.

Neuwirth, E. (2022). *RColorBrewer: ColorBrewer Palettes* [R package version 1.1-3].

Ng, M. S., Soon, N., Afiq-Rosli, L., Kunning, I., Mana, R. R., Chang, Y., & Wainwright, B. J. (2024). Highly diverse symbiodiniaceae types hosted by corals in a global hotspot of marine biodiversity. *Microbial Ecology*, *87*(1), 92.

Ng, M. S., Soon, N., Chang, Y., & Wainwright, B. J. (2022). Bacterial and fungal co-occurrence in the nudibranch, *Pteraeolidia semperi*. *Life*, *12*(12), 1988.

Nissen, M., Shcherbakov, D., Heyer, A., Brümmer, F., & Schill, R. O. (2015). Behaviour of the plathelminth *Symsagittifera roscoffensis* under different light conditions and the consequences on the symbiotic algae *Tetraselmis convolutae*. *Journal of Experimental Biology*, *110429*.

Nitschke, M. R., Craveiro, S. C., Brandão, C., Fidalgo, C., Serôdio, J., Calado, A. J., & Frommlet, J. C. (2020). Description of *Freudenthalidium* gen. nov. and *Halluxium* gen. nov. to formally recognize clades Fr3 and H as genera in the family Symbiodiniaceae (Dinophyceae). *Journal of Phycology*, *56*(4), 923–940.

Noël, V., Morin, G., Juillot, F., Marchand, C., Brest, J., Bargar, J. R., Muñoz, M., Marakovic, G., Ardo, S., & Brown Jr, G. E. (2015). Ni cycling in mangrove sediments from New Caledonia. *Geochimica et Cosmochimica Acta*, *169*, 82–98.

Noetzel, D. C., Colsoul, B., Akcha, F., Briant, N., Le Roy, J., François, V., Stavrakakis, C., Pogoda, B., & Sokolova, I. (2025). Effect of temperature and trace metal exposure on early life stages of European flat oysters and Pacific oysters. *Marine Environmental Research*, 107376.

Norris, R. D. (2000). Pelagic species diversity, biogeography, and evolution. *Paleobiology*, *26*(S4), 236–258.

Norton, J. H., Shepherd, M. A., Long, H. M., & Fitt, W. K. (1992). The zooxanthellal tubular system in the giant clam. *The Biological Bulletin*, *183*(3), 503–506.

Oakley, C. A., Newson, G. I., Peng, L., & Davy, S. K. (2023). The *Symbiodinium* proteome response to thermal and nutrient stresses. *Plant and Cell Physiology*, *64*(4), 433–447.

Obermann, D., Bickmeyer, U., & Wägele, H. (2012). Incorporated nematocysts in *Aeolidiella stephanieae* (Gastropoda, Opisthobranchia, Aeolidoidea) mature by acidification shown by the pH sensitive fluorescing alkaloid Ageladine A. *Toxicon*, *60*(6), 1108–1116.

Ochsenkühn, M. A., Röthig, T., D'Angelo, C., Wiedenmann, J., & Voolstra, C. R. (2017). The role of floridoside in osmoadaptation of coral-associated algal endosymbionts to high-salinity conditions. *Science Advances*, *3*(8), e1602047.

Oros, A. (2025). Bioaccumulation and trophic transfer of heavy metals in marine fish: Ecological and ecosystem-level impacts. *Journal of Xenobiotics*, *15*(2), 59.

Othman, H. B., Pick, F. R., Hlaili, A. S., & Leboulanger, C. (2023). Effects of polycyclic aromatic hydrocarbons on marine and freshwater microalgae–A review. *Journal of Hazardous Materials*, *441*, 129869.

Ou, R., Huang, H., He, X., Lin, S., Ou, D., Li, W., Qiu, J., & Wang, L. (2023). Ecotoxicology of polymetallic nodule seabed mining: The effects of cobalt and nickel on phytoplankton growth and pigment concentration. *Toxics*, *11*(12), 1005.

Pallas, P. S. (1766). *Elenchus zoophytorum sistens generum adumbrationes generaliores et specierum cognitarum... descriptiones etc*. Varrentrapp.

Pasqualetti, C., Szokoli, F., Rindi, L., Petroni, G., & Schrallhammer, M. (2020). The obligate symbiont "*Candidatus Megaira polyxenophila*" has variable effects on the growth of different host species. *Frontiers in Microbiology*, *11*, 1425.

Patel, A. B., Shaikh, S., Jain, K. R., Desai, C., & Madamwar, D. (2020). Polycyclic aromatic hydrocarbons: Sources, toxicity, and remediation approaches. *Frontiers in Microbiology*, *11*, 562813.

Peixoto, R. S., Rosado, P. M., Leite, D. C. d. A., Rosado, A. S., & Bourne, D. G. (2017). Beneficial microorganisms for corals (BMC): Proposed mechanisms for coral health and resilience. *Frontiers in Microbiology*, *8*, 341.

Peters, E. C., Gassman, N. J., Firman, J. C., Richmond, R. H., & Power, E. A. (1997). Ecotoxicology of tropical marine ecosystems. *Environmental Toxicology and Chemistry*, *16*(1), 12–40.

Piel, W. (1991). Pycnogonid predation on nudibranchs and ceratal autotomy.

Pineda, M. C., McQuaid, C. D., Turon, X., Lopez-Legentil, S., Ordonez, V., & Rius, M. (2012). Tough adults, frail babies: An analysis of stress sensitivity across early life-history stages of widely introduced marine invertebrates. *PlosOne*.

Pineda, M. C., Strehlow, B., Duckworth, A., Doyle, J., Jones, R., & Webster, N. S. (2016). Effects of light attenuation on the sponge holobiont-implications for dredging management. *Scientific Reports*, *6*(1), 39038.

Pochon, X., Pawlowski, J., Zaninetti, L., & Rowan, R. (2001). High genetic diversity and relative specificity among *Symbiodinium*-like endosymbiotic dinoflagellates in soritid foraminiferans. *Marine Biology*, *139*, 1069–1078.

Pogoreutz, C., Oakley, C. A., Rädecker, N., Cárdenas, A., Perna, G., Xiang, N., Peng, L., Davy, S. K., Ngugi, D. K., & Voolstra, C. R. (2022). Coral holobiont cues prime *Endozoicomonas* for a symbiotic lifestyle. *The ISME Journal*, *16*(8), 1883–1895.

Posadas, N., Baquiran, J. I. P., Nada, M. A. L., Kelly, M., & Conaco, C. (2022). Microbiome diversity and host immune functions influence survivorship of sponge holobionts under future ocean conditions. *The ISME Journal*, *16*(1), 58–67.

Potet, M., Giambérini, L., Pain-Devin, S., Louis, F., Bertrand, C., & Devin, S. (2018). Differential tolerance to nickel between *Dreissena polymorpha* and *Dreissena rostriformis bugensis* populations. *Scientific Reports*, *8*(1), 700.

Poynton, H. C., Robinson, W. E., Blalock, B. J., & Hannigan, R. E. (2014). Correlation of transcriptomic responses and metal bioaccumulation in mytilus edulis l. reveals early indicators of stress. *Aquatic Toxicology*, *155*, 129–141.

Prazeres, M., Ainsworth, T., Roberts, T. E., Pandolfi, J. M., & Leggat, W. (2017). Symbiosis and microbiome flexibility in calcifying benthic foraminifera of the Great Barrier Reef. *Microbiome*, *5*(1), 1–11.

Pröschold, T., & Darienko, T. (2020). *Choricystis* and *Lewiniosphaera* gen. nov. (Trebouxiophyceae, Chlorophyta), two different green algal endosymbionts in freshwater sponges. *Symbiosis*, *82*(3), 175–188.

Pujalte, M. J., Lucena, T., Ruvira, M. A., Arahal, D. R., & Macián, M. C. (2014). The family rhodobacteraceae. In *The Prokaryotes*. Springer.

Pupier, C. A., Grover, R., Fine, M., Rottier, C., Van de Water, J. A., & Ferrier-Pagès, C. (2021). Dissolved nitrogen acquisition in the symbioses of soft and hard corals with Symbiodiniaceae: A key to understanding their different nutritional strategies? *Frontiers in Microbiology*, *12*, 657759.

Purser, A., Marcon, Y., & Boetius, A. (2016). Megabenthic community structure within and surrounding the DISCOL experimental area 26 years after simulated manganese nodule mining disturbance. *American Geophysical Union, Ocean Sciences Meeting*, *2016*, ME33B–03.

Pyle, G., & Couture, P. (2011). Nickel. In *Homeostasis and Toxicology of Essential Metals* (pp. 253–289, Vol. 31A). Elsevier.

Quast, C., Pruesse, E., Yilmaz, P., Gerken, J., Schweer, T., Yarza, P., Peplies, J., & Glöckner, F. O. (2012). The SILVA ribosomal RNA gene database project: Improved data processing and web-based tools. *Nucleic Acids Research*, *41*(D1), D590–D596.

Quoy, J. R. C., & Gaimard, J. P. (1833). *Zoologie IV: Zoophytes. In:Zoologie. Voyage de la corvette l'Astrolabe : exécuté par ordre du roi, pendant les années 1826-1827-1828-1829* (Vol. 5). J. Tastu, editeur-imprimeur.

R Core Team. (2021). *R: A Language and Environment for Statistical Computing*. R Foundation for Statistical Computing. Vienna, Austria.

Rädecker, N., Pogoreutz, C., Gegner, H. M., Cárdenas, A., Roth, F., Bougoure, J., Guagliardo, P., Wild, C., Pernice, M., Raina, J.-B., Meibom, A., & Voolstra, C. R. (2021). Heat stress destabilizes symbiotic nutrient cycling in corals. *Proceedings of the National Academy of Sciences*, *118*.

Rädecker, N., Pogoreutz, C., Voolstra, C. R., Wiedenmann, J., & Wild, C. (2015). Nitrogen cycling in corals: The key to understanding holobiont functioning? *Trends in Microbiology*, *23*(8), 490–497.

Raina, J.-B., Tapiolas, D., Willis, B. L., & Bourne, D. G. (2009). Coral-associated bacteria and their role in the biogeochemical cycling of sulfur. *Applied and environmental microbiology*, *75*(11), 3492–3501.

Raju, N. V., Prasanth, P., Harsha, T., Naravula, J., Srikanth, K., & Nutalapati, V. (2022). Evaluation of oxidative stress biomarkers in Pila virens exposed to spinel Co_3O_4 nanoparticles. *Materials Science and Engineering: B*, *282*, 115757.

Ramsby, B. D., & Goulet, T. L. (2019). Symbiosis and host morphological variation: Symbiodiniaceae photosynthesis in the octocoral *Briareum asbestinum* at ambient and elevated temperatures. *Coral Reefs*, *38*(2), 359–371.

Rapp, W. (1829). *Ueber die Polypen im Allgemeinen und die Actinien insbesondere* (Vol. i-iv: 1-62).

Rasmussen, J. A., Kiilerich, P., Madhun, A. S., Waagbø, R., Lock, E.-J. R., Madsen, L., Gilbert, M. T. P., Kristiansen, K., & Limborg, M. T. (2023). Co-diversification of an intestinal *Mycoplasma* and its salmonid host. *The ISME journal*, *17*(5), 682–692.

Rasmussen, J. A., Villumsen, K. R., Duchêne, D. A., Puetz, L. C., Delmont, T. O., Sveier, H., Jørgensen, L. v. G., Præbel, K., Martin, M. D., Bojesen, A. M., et al. (2021). Genome-resolved metagenomics suggests a mutualistic relationship between *Mycoplasma* and salmonid hosts. *Communications Biology*, *4*(1), 579.

Rauch, C., Jahns, P., Tielens, A. G., Gould, S. B., & Martin, W. F. (2017). On being the right size as an animal with plastids. *Frontiers in Plant Science*, *8*, 1402.

Rauch, C., Tielens, A. G., Serôdio, J., Gould, S. B., & Christa, G. (2018). The ability to incorporate functional plastids by the sea slug *Elysia viridis* is governed by its food source. *Marine Biology*, *165*(5), 82.

Rauch, C., Vries, J. d., Rommel, S., Rose, L. E., Woehle, C., Christa, G., Laetz, E. M., Wägele, H., Tielens, A. G., Nickelsen, J., et al. (2015). Why it is time to look beyond algal genes in photosynthetic slugs. *Genome Biology and Evolution*, *7*(9), 2602–2607.

Ravera, O. (2001). Monitoring of the aquatic environment by species accumulator of pollutants: A review. *Journal of Limnology*, *60*(1s), 63–78.

Ravindran, C., Lawrance, I., & Vasanth, A. J. (2022). Endosymbiotic *Symbiodinium* clades occurrence and influence on coral growth and resilience during stress. *Symbiosis*, *86*(3), 261–272.

Razin, S., Yogev, D., & Naot, Y. (1998). Molecular biology and pathogenicity of *Mycoplasmas*. *Microbiology and Molecular Biology Reviews*, *62*(4), 1094–1156.

Real, M. K. H., Varol, M., Rahman, M. S., & Islam, A. R. M. T. (2024). Pollution status and ecological risks of metals in surface water of a coastal estuary and health risk assessment for recreational users. *Chemosphere*, *348*, 140768.

Reichelt-Brushett, A. (2012). Risk assessment and ecotoxicology: Limitations and recommendations for ocean disposal of mine waste in the coral triangle. *Oceanography*, *25*(4), 40–51.

Reichelt-Brushett, A. J., & McOrist, G. (2003). Trace metals in the living and nonliving components of scleractinian corals. *Marine Pollution Bulletin*, *46*(12), 1573–1582.

Reisser, W. (1984). The taxonomy of green algae endosymbiotic in ciliates and a sponge. *British Phycological Journal*, *19*(4), 309–318.

Reynolds, J. M., Bruns, B. U., Fitt, W. K., & Schmidt, G. W. (2008). Enhanced photoprotection pathways in symbiotic dinoflagellates of shallow-water corals and other cnidarians. *Proceedings of the National Academy of Sciences*, *105*(36), 13674–13678.

Riewluang, S., & Wakeman, K. C. (2023). Biodiversity of symbiotic microalgae associated with meiofaunal marine acoels in Southern Japan. *PeerJ*, *11*, e16078.

Ripps, H., & Shen, W. (2012). Taurine: A "very essential" amino acid. *Molecular Vision*, *18*, 2673.

Risbec, J. (1937). Note préliminaire au sujet de nudibranches néo-calédoniens. *Bulletin de Museé National d'Histoire Naturelle, Paris, Ser*, *2*(9), 159–164.

Risbec, J. (1928). *Contribution a l'etude des nudibranches neo-caledoniens* (Vol. 2). Société d'éditions géographiques, maritimes et coloniales.

Risely, A. (2020). Applying the core microbiome to understand host–microbe systems. *Journal of Animal Ecology*, *89*(7), 1549–1558.

Ritchie, A. E., & Johnson, Z. I. (2012). Abundance and genetic diversity of aerobic anoxygenic phototrophic bacteria of coastal regions of the Pacific Ocean. *Applied and Environmental Microbiology*, *78*(8), 2858–2866.

Ritchie, K. B. (2011). Bacterial symbionts of corals and *Symbiodinium*. *Beneficial Microorganisms in Multicellular Life Forms*, 139–150.

Robinson, J. T., Thorvaldsdóttir, H., Winckler, W., Guttman, M., Lander, E. S., Getz, G., & Mesirov, J. P. (2011). Integrative genomics viewer. *Nature Biotechnology*, *29*(1), 24–26.

Rodriguez, I. B., Lin, S., Ho, J., & Ho, T.-Y. (2016). Effects of trace metal concentrations on the growth of the coral endosymbiont *Symbiodinium kawagutii*. *Frontiers in Microbiology*, *7*, 82.

Rohwer, F., Seguritan, V., Azam, F., & Knowlton, N. (2002). Diversity and distribution of coral-associated bacteria. *Marine Ecology Progress Series*, *243*, 1–10.

Rola, M., Frankenbach, S., Bleidissel, S., Sickinger, C., Donath, A., Frommlet, J. C., Greve, C., Serôdio, J., Preisfeld, A., Melo Clavijo, J., et al. (2022). Cladobranchia (Gastropoda, Nudibranchia) as a promising model to understand the molecular evolution of photosymbiosis in animals. *Frontiers in Marine Science*, *8*, 745644.

Romero, M., Muras, A., Mayer, C., Buján, N., Magariños, B., & Otero, A. (2014). In vitro quenching of fish pathogen *Edwardsiella tarda* AHL production using marine bacterium *Tenacibaculum* sp. strain 20J cell extracts. *Diseases of Aquatic Organisms*, *108*(3), 217–225.

Rosenberg, E., Koren, O., Reshef, L., Efrony, R., & Zilber-Rosenberg, I. (2007). The role of microorganisms in coral health, disease and evolution. *Nature Reviews Microbiology*, *5*(5), 355–362.

Rosenberg, E., & Zilber-Rosenberg, I. (2021). Reconstitution and transmission of gut microbiomes and their genes between generations. *Microorganisms*, *10*(1), 70.

Rosic, N. N., & Dove, S. (2011). Mycosporine-like amino acids from coral dinoflagellates. *Applied and Environmental Microbiology*, *77*(24), 8478–8486.

Rosset, S. L., Oakley, C. A., Ferrier-Pagès, C., Suggett, D. J., Weis, V. M., & Davy, S. K. (2021). The molecular language of the cnidarian–dinoflagellate symbiosis. *Trends in Microbiology*, *29*(4), 320–333.

Roth, M. S. (2014). The engine of the reef: Photobiology of the coral–algal symbiosis. *Frontiers in microbiology*, *5*, 422.

Röthig, T., Costa, R. M., Simona, F., Baumgarten, S., Torres, A. F., Radhakrishnan, A., Aranda, M., & Voolstra, C. R. (2016). Distinct bacterial communities associated with the coral model *Aiptasia* in aposymbiotic and symbiotic states with *Symbiodinium*. *Frontiers in Marine Science*, *3*, 234.

Röthig, T., Puntin, G., Wong, J. C., Burian, A., McLeod, W., & Baker, D. M. (2021). Holobiont nitrogen control and its potential for eutrophication resistance in an obligate photosymbiotic jellyfish. *Microbiome*, *9*(1), 127.

Rouzé, H., Lecellier, G., Saulnier, D., & Berteaux-Lecellier, V. (2016). *Symbiodinium* clades A and D differentially predispose *Acropora cytherea* to disease and *Vibrio* spp. colonization. *Ecology and Evolution*, *6*(2), 560–572.

Rudman, W. (1981). The anatomy and biology of alcyonarian-feeding aeolid opisthobranch molluscs and their development of symbiosis with zooxanthellae. *Zoological Journal of the Linnean Society*, *72*(3), 219–262.

Rudman, W. (1982). The taxonomy and biology of further aeolidacean and arminacean nudibranch molluscs with symbiotic zooxanthellae. *Zoological Journal of the Linnean Society*, *74*(2), 147–196.

Rudman, W. (1991). Further studies on the taxonomy and biology of the octocoral-feeding genus *Phyllodesmium* Ehrenberg, 1831 (Nudibranchia: Aeolidoidea). *Journal of Molluscan Studies*, *57*(2), 167–203.

Ruiz-Toquica, J., Herrera, A. F., & Medina, M. (2025). Endozoicomonas dominance and vibrionaceae stability underpin resilience in urban coral madracis auretenra. *PeerJ*, *13*, e19226.

Rumpho, M. E., Dastoor, F. P., Manhart, J. R., & Lee, J. (2006). The Kleptoplast. *The Structure and Function of Plastids*, 451–473.

Saili, K. S., Cardwell, A. S., & Stubblefield, W. A. (2021). Chronic toxicity of cobalt to marine organisms: Application of a species sensitivity distribution approach to develop international water quality standards. *Environmental Toxicology and Chemistry*, *40*(5), 1405–1418.

Sampayo, E., Dove, S., & LaJeunesse, T. (2009). Cohesive molecular genetic data delineate species diversity in the dinoflagellate genus *Symbiodinium*. *Molecular Ecology*, *18*(3), 500–519.

Santhosh, K., Kamala, K., Ramasamy, P., Musthafa, M. S., Almujri, S. S., Asdaq, S. M. B., & Sivaperumal, P. (2024). Unveiling the silent threat: Heavy metal toxicity devastating impact on aquatic organisms and DNA damage. *Marine Pollution Bulletin*, *200*, 116139.

Saravanan, P., Saravanan, V., Rajeshkannan, R., Arnica, G., Rajasimman, M., Baskar, G., & Pugazhendhi, A. (2024). Comprehensive review on toxic heavy metals in the aquatic system: Sources, identification, treatment strategies, and health risk assessment. *Environmental Research*, *258*, 119440.

Schauer, R., Bienhold, C., Ramette, A., & Harder, J. (2010). Bacterial diversity and biogeography in deep-sea surface sediments of the South Atlantic Ocean. *The ISME Journal*, *4*(2), 159–170.

Schloss, P. D., Westcott, S. L., Ryabin, T., Hall, J. R., Hartmann, M., Hollister, E. B., Lesniewski, R. A., Oakley, B. B., Parks, D. H., Robinson, C. J., et al. (2009). Introducing mothur: Open-source, platform-independent, community-supported software for describing and comparing microbial communities. *Applied and Environmental Microbiology*, *75*(23), 7537–7541.

Schmitt, V., & Wägele, H. (2011). Behavioral adaptations in relation to long-term retention of endosymbiotic chloroplasts in the sea slug *Elysia timida* (Opisthobranchia, Sacoglossa). *Thalassas*, *27*(2), 225–238.

Schrauzer, G. (1991). Cobalt in Metals and their compounds, in the environment occurrence, analysis and biological relevance. *Editor Merian EL Editorial VCH Verlagsgesellschaft Weinheim Alemania*, *879*.

Schuett, C., & Doepke, H. (2013). Endobacterial morphotypes in nudibranch cerata tips: A SEM analysis. *Helgoland Marine Research*, *67*, 219–227.

Serôdio, J., Silva, R., Ezequiel, J., & Calado, R. (2011). Photobiology of the symbiotic acoel flatworm *Symsagittifera roscoffensis*: Algal symbiont photoacclimation and host photobehaviour. *Journal of the Marine Biological Association of the United Kingdom*, *91*, 163–171.

Shannon, C. E. (1948). A mathematical theory of communication. *The Bell System Technical Journal*, *27*(3), 379–423.

Shashar, N., Cohen, Y., Loya, Y., & Sar, N. (1994). Nitrogen fixation (acetylene reduction) in stony corals: Evidence for coral-bacteria interactions. *Marine Ecology Progress Series*, 259–264.

Shick, J. M., & Dunlap, W. C. (2002). Mycosporine-like amino acids and related gadusols: Biosynthesis, accumulation, and UV-protective functions in aquatic organisms. *Annual review of Physiology*, *64*(1), 223–262.

Shinzato, C., Shoguchi, E., Kawashima, T., Hamada, M., Hisata, K., Tanaka, M., Fujie, M., Fujiwara, M., Koyanagi, R., Ikuta, T., et al. (2011). Using the *Acropora digitifera* genome to understand coral responses to environmental change. *Nature*, *476*(7360), 320–323.

Shiroyama, H., Mitoh, S., Ida, T. Y., & Yusa, Y. (2020). Adaptive significance of light and food for a kleptoplastic sea slug: Implications for photosynthesis. *Oecologia*, *194*(3), 455–463.

Sickinger, C., Bleidißel, S., Brück, M., Gasparoni, G., Tierling, S., Rauch, C., Preisfeld, A., & Christa, G. (2025a). Diversity of symbiodiniaceae (dinophyceae) in the sea slug clade cladobranchia (nudibranchia) c. sickinger et al. *Organisms Diversity & Evolution*, 1–13.

Sickinger, C., Brackwehr, S. M., Melo Clavijo, J., Gasperoni, G., Tierling, S., Preisfeld, A., & Christa, G. (2024). Microbiome origin and stress-related changes in bacterial abundance of the photosymbiotic sea slug *Berghia stephanieae* (Á. valdés, 2005). *Symbiosis*, 1–16.

Sickinger, C., Thiel, A., Bornhorst, J., Christa, G., & Preisfeld, A. (2026). Nickel and cobalt disrupt the microbiome and metabolic function of the photosymbiotic sea slug berghia stephanieae (á. valdés, 2005). *Marine Environmental Research*, 107845.

Sickinger, C., Weimann, E., Wenning, J., & Christa, G. (2025c). The phototactic behaviour of the kleptoplastic sea slug elysia viridis (montagu, 1804) is not connected to the photosynthetic activity of kleptoplasts. *Marine Biology Research*, *21*(8-10), 417–426.

Sikorskaya, T. V., Ermolenko, E. V., Ginanova, T. T., Boroda, A. V., Efimova, K. V., & Bogdanov, M. (2024). Membrane vectorial lipidomic features of coral host cells' plasma membrane and lipid profiles of their endosymbionts *Cladocopium*. *Communications Biology*, *7*(1), 878.

Silva, R. X., Cartaxana, P., & Calado, R. (2021). Prevalence and photobiology of photosynthetic dinoflagellate endosymbionts in the nudibranch *Berghia stephanieae*. *Animals*, *11*(8), 2200.

Silva, R. X., Madeira, D., Cartaxana, P., & Calado, R. (2023). Assessing the trophic impact of bleaching: The model pair *Berghia stephanieae/Exaiptasia diaphana*. *Animals*, *13*(2), 291.

Silveira, C. B., Cavalcanti, G. S., Walter, J. M., Silva-Lima, A. W., Dinsdale, E. A., Bourne, D. G., Thompson, C. C., & Thompson, F. L. (2017). Microbial processes driving coral reef organic carbon flow. *FEMS Microbiology Reviews*, *41*(4), 575–595.

Smith, E. G., Ketchum, R. N., & Burt, J. A. (2017). Host specificity of *Symbiodinium* variants revealed by an ITS2 metahaplotype approach. *The ISME Journal*, *11*(6), 1500–1503.

Sorek, M., Díaz-Almeyda, E. M., Medina, M., & Levy, O. (2014). Circadian clocks in symbiotic corals: The duet between *Symbiodinium* algae and their coral host. *Marine genomics*, *14*, 47–57.

Sørensen, M. E., Wood, A. J., Minter, E. J., Lowe, C. D., Cameron, D. D., & Brockhurst, M. A. (2020). Comparison of independent evolutionary origins reveals both convergence and divergence in the metabolic mechanisms of symbiosis. *Current Biology*, *30*(2), 328–334.

Sousa, C. S., Sun, J., & Mestre, N. C. (2024). Potential biomarkers of metal toxicity in deep-sea invertebrates–A critical review of the omics data. *Science of the Total Environment*, *951*, 175628.

Stanley Jr, G. D., & Lipps, J. H. (2011). Photosymbiosis: The driving force for reef success and failure. *The Paleontological Society Papers*, *17*, 33–59.

Stat, M., Morris, E., & Gates, R. D. (2008). Functional diversity in coral–dinoflagellate symbiosis. *Proceedings of the National Academy of Sciences*, *105*(27), 9256–9261.

Stat, M., Pochon, X., Cowie, R. O., & Gates, R. D. (2009). Specificity in communities of *Symbiodinium* in corals from Johnston Atoll. *Marine Ecology Progress Series*, *386*, 83–96.

Stévenne, C., Micha, M., Plumier, J.-C., & Roberty, S. (2021). Corals and sponges under the light of the holobiont concept: How microbiomes underpin our understanding of marine ecosystems. *Frontiers in Marine Science*, *8*, 698853.

Stewart, F. J. (2013). Preparation of microbial community cDNA for metatranscriptomic analysis in marine plankton. In *Methods in Enzymology* (pp. 187–218, Vol. 531). Elsevier.

Stoecker, D. K., Johnson, M. D., de Vargas, C., & Not, F. (2009). Acquired phototrophy in aquatic protists. *Aquatic Microbial Ecology*, *57*(3), 279–310.

Strumpen, N. F., Rädecker, N., Pogoreutz, C., Meibom, A., & Voolstra, C. R. (2022). High light quantity suppresses locomotion in symbiotic *Aiptasia*. *Symbiosis*, *86*, 293–304.

Sun, Z., Gong, C., Ren, J., Zhang, X., Wang, G., Liu, Y., Ren, Y., Zhao, Y., Yu, Q., Wang, Y., et al. (2020). Toxicity of nickel and cobalt in Japanese flounder. *Environmental Pollution*, *263*, 114516.

Sunagawa, S., DeSantis, T. Z., Piceno, Y. M., Brodie, E. L., DeSalvo, M. K., Voolstra, C. R., Weil, E., Andersen, G. L., & Medina, M. (2009). Bacterial diversity and white plague disease-associated community changes in the caribbean coral *Montastraea faveolata*. *The ISME Journal*, *3*(5), 512–521.

Swain, T. D., Chandler, J., Backman, V., & Marcelino, L. (2017). Consensus thermotolerance ranking for 110 *Symbiodinium* phylotypes: An exemplar utilization of a novel iterative partial-rank aggregation tool with broad application potential. *Functional Ecology*, *31*(1), 172–183.

Taguchi, S., & Kinzie Iii, R. (2001). Growth of zooxanthellae in culture with two nitrogen sources. *Marine Biology*, *138*, 149–155.

Tandon, K., Lu, C.-Y., Chiang, P.-W., Wada, N., Yang, S.-H., Chan, Y.-F., Chen, P.-Y., Chang, H.-Y., Chiou, Y.-J., Chou, M.-S., et al. (2020). Comparative genomics: Dominant coral-bacterium *Endozoicomonas acroporae* metabolizes dimethylsulfoniopropionate (DMSP). *The ISME Journal*, *14*(5), 1290–1303.

Taylor, J. D., Cottingham, S. D., Billinge, J., & Cunliffe, M. (2014). Seasonal microbial community dynamics correlate with phytoplankton-derived polysaccharides in surface coastal waters. *The ISME Journal*, *8*(1), 245–248.

Teugels, B., Bouillon, S., Veuger, B., Middelburg, J., & Koedam, N. (2008). Kleptoplasts mediate nitrogen acquisition in the sea slug *Elysia viridis*. *Aquatic Biology*, *4*(1), 15–21.

The Metals Company. (2023). Summary report nickel and cobalt mining impact on terrestrial carbon sinks in Sulawesi, Indonesia and Katanga, DRC.

Thinesh, T., Meenatchi, R., Jose, P. A., Kiran, G. S., & Selvin, J. (2019). Differential bleaching and recovery pattern of southeast Indian coral reef to 2016 global mass bleaching event: Occurrence of stress-tolerant symbiont *Durusdinium* (Clade D) in corals of Palk Bay. *Marine Pollution Bulletin*, *145*, 287–294.

Thomas, N. J., Coates, C. J., & Tang, K. W. (2023). Environmental constraints on the photosynthetic rate of the marine flatworm *Symsagittifera roscoffensis*. *Journal of Experimental Marine Biology and Ecology*, *558*, 151830.

Thornhill, D. J., Lajeunesse, T., & Santos, S. R. (2007). Measuring rDNA diversity in eukaryotic microbial systems: How intragenomic variation, pseudogenes, and PCR artifacts confound biodiversity estimates. *Molecular Ecology*, *16*(24), 5326–5340.

Thornhill, D. J., Lewis, A. M., Wham, D. C., & LaJeunesse, T. (2014). Host-specialist lineages dominate the adaptive radiation of reef coral endosymbionts. *Evolution*, *68*(2), 352–367.

Tivey, T. R., Parkinson, J. E., Mandelare, P. E., Adpressa, D. A., Peng, W., Dong, X., Mechref, Y., Weis, V. M., & Loesgen, S. (2020). N-linked surface glycan biosynthesis, composition, inhibition, and function in cnidarian-dinoflagellate symbiosis. *Microbial Ecology*, *80*(1), 223–236.

Tolleter, D., Seneca, F. O., DeNofrio, J. C., Krediet, C. J., Palumbi, S. R., Pringle, J. R., & Grossman, A. R. (2013). Coral bleaching independent of photosynthetic activity. *Current Biology*, *23*(18), 1782–1786.

Trapnell, C. (2015). Defining cell types and states with single-cell genomics. *Genome Research*, *25*(10), 1491–1498.

Tremblay, P., Grover, R., Maguer, J. F., Legendre, L., & Ferrier-Pagès, C. (2012). Autotrophic carbon budget in coral tissue: A new 13C-based model of photosynthate translocation. *Journal of Experimental Biology*, *215*(8), 1384–1393.

Trench, R. K. (1969). Chloroplasts as functional endosymbionts in the mollusc *Tridachia crispata* (Bërgh), (Opisthobranchia, Sacoglossa). *Nature*, *222*(5198), 1071–1072.

Trench, R., Boyle, J. E., & Smith, D. (1974). The association between chloroplasts of *Codium fragile* and the mollusc *Elysia viridis*-III. Movement of photosynthetically fixed 14C in tissues of intact living *E. viridis* and in *Tridachia crispata*. *Proceedings of the Royal Society of London. Series B. Biological Sciences*, *185*(1081), 453–464.

Turley, S., Dietschy, J., Arias, I., et al. (1988). The liver: Biology and pathobiology. *Arias, IM, Jakoby, WB, Popper, H., Schachter, D., Shafritz, DS, Eds*, 617–641.

Turnbaugh, P. J., Ley, R. E., Hamady, M., Fraser-Liggett, C. M., Knight, R., & Gordon, J. I. (2007). The human microbiome project. *Nature*, *449*(7164), 804–810.

Tyler-Walters, H., & Williams, E. (2023). Sensitivity Assessment of Contaminant Pressures - Oyster species – Evidence Review. MarLIN (Marine Life Information Network). *Marine Biological Association of the UK, Plymouth*, 170.

United Nations, Department of Economic and Social Affairs. (2015a). Sustainable development goals (sdgs): Goal 12 - responsible consumption and production [Accessed: 2026-01-06].

United Nations, Department of Economic and Social Affairs. (2015b). Sustainable development goals (sdgs): Goal 14 - life below water [Accessed: 2026-01-06].

US Geological Survey. (2023). Mineral Commodity Summaries 2023 [Accessed: 2024-12-04].

Valdés, Á. (2005). A new species of *Aeolidiella* Bergh, 1867 (Mollusca: Nudibranchia: Aeolidiidae) from the Florida Keys, USA. *Veliger*, *47*(3), 218–223.

van Oppen, M. J., & Berkelmans, R. (2006). The role of zooxanthellae in the thermal tolerance of corals: A 'nugget of hope' for coral reefs in an era of climate change. *Proceedings of the Royal Society B: Biological Sciences*.

Van Alstyne, K., Dominique, V., & Muller-Parker, G. (2009). Is dimethylsulfoniopropionate (DMSP) produced by the symbionts or the host in an anemone–zooxanthella symbiosis? *Coral Reefs*, *28*, 167–176.

Van Dam, R., Harford, A., Houston, M., Hogan, A., & Negri, A. (2008). Tropical marine toxicity testing in Australia: A review and recommendations. *Australasian Journal of Ecotoxicology*, *14*(2/3), 55–88.

Van Steenkiste, N. W., Stephenson, I., Herranz, M., Husnik, F., Keeling, P. J., & Leander, B. S. (2019). A new case of kleptoplasty in animals: Marine flatworms steal functional plastids from diatoms. *Science Advances*, *5*(7), eaaw4337.

Vega de Luna, F., Dang, K.-V., Cardol, M., Roberty, S., & Cardol, P. (2019). Photosynthetic capacity of the endosymbiotic dinoflagellate *Cladocopium* sp. is preserved during digestion of its jellyfish host *Mastigias papua* by the anemone *Entacmaea medusivora*. *FEMS Microbiology Ecology*, *95*(10), fiz141.

Veldhuizen, E. J., van Eijk, M., & Haagsman, H. P. (2011). The carbohydrate recognition domain of collectins. *The FEBS journal*, *278*(20), 3930–3941.

Venn, A. A., Loram, J. E., & Douglas, A. E. (2008). Photosynthetic symbioses in animals. *Journal of experimental botany*, *59*(5), 1069–1080.

Vieira, S., Calado, R., Coelho, H., & Serôdio, J. (2009). Effects of light exposure on the retention of kleptoplastic photosynthetic activity in the sacoglossan mollusc *Elysia viridis*. *Marine Biology*, *156*, 1007–1020.

Virtanen, P., Gommers, R., Oliphant, T. E., Haberland, M., Reddy, T., Cournapeau, D., Burovski, E., Peterson, P., Weckesser, W., Bright, J., van der Walt, S. J., Brett, M., Wilson, J., Millman, K. J., Mayorov, N., Arj, N., Jones, E., Kern, R., Larson, E., … van Mulbregt P. SciPy. (2020). Scipy 1.0: Fundamental algorithms for scientific computing in python. *Nature Methods*, *17*, 261–272.

Voolstra, C. R., Raina, J.-B., Dörr, M., Cárdenas, A., Pogoreutz, C., Silveira, C. B., Mohamed, A. R., Bourne, D. G., Luo, H., Amin, S. A., et al. (2024). The coral microbiome in sickness, in health and in a changing world. *Nature Reviews Microbiology*, *22*(8), 460–475.

Voolstra, C. R., & Ziegler, M. (2020). Adapting with microbial help: Microbiome flexibility facilitates rapid responses to environmental change. *BioEssays*, *42*(7), 2000004.

Wägele, H. (2004). Potential key characters in Opisthobranchia (Gastropoda, Mollusca) enhancing adaptive radiation. *Organisms Diversity & Evolution*, *4*(3), 175–188.

Wägele, H., & Klussmann-Kolb, A. (2005). Opisthobranchia (Mollusca, Gastropoda)–more than just slimy slugs. Shell reduction and its implications on defence and foraging. *Frontiers in Zoology*, *2*, 1–18.

Wägele, H., Raupach, M. J., Burghardt, I., Grzymbowski, Y., & Händeler, K. (2010). Solar powered seaslugs (Opisthobranchia, Gastropoda, Mollusca): Incorporation of photosynthetic units: A key character enhancing radiation? *Evolution in action: Case studies in adaptive radiation, speciation and the origin of biodiversity*, 263–282.

Wägele, H., Vonnemann, V., & Wägele, J. (2003). Toward a phylogeny of the Opisthobranchia. *Molecular systematics and phylogeography of mollusks*, 185–228.

Wägele, H., & Willan, R. C. (2000). Phylogeny of the Nudibranchia. *Zoological Journal of the Linnean Society*, *130*(1), 83–181.

Wang, Y., Li, Q., Yun, X., Zhou, J., & Wang, J. (2022). A review on the ecotoxicological effects of heavy metals on aquatic organisms. *Journal of Earth Sciences & Environmental Studies*, *6*(2), 148–161.

Wang, Z., Gerstein, M., & Snyder, M. (2009). RNA-Seq: A revolutionary tool for transcriptomics. *Nature Reviews Genetics*, *10*(1), 57–63.

Weaver, S., & Clark, K. (1981). Light intensity and color preferences of five ascoglossan (= sacoglossan) molluscs (Gastropoda: Opisthobranchia): A comparison of chloroplast-symbiotic and aposymbiotic species. *Marine & Freshwater Behaviour & Phy*, *7*(4), 297–306.

Webster, N. S., Cobb, R. E., Soo, R., Anthony, S. L., Battershill, C. N., Whalan, S., & Evans-Illidge, E. (2011). Bacterial community dynamics in the marine sponge *Rhopaloeides odorabile* under *in situ* and *ex situ* cultivation. *Marine Biotechnology*, *13*, 296–304.

Wecker, P., Fournier, A., Bosserelle, P., Debitus, C., Lecellier, G., & Berteaux-Lecellier, V. (2015). Dinoflagellate diversity among nudibranchs and sponges from French Polynesia: Insights into associations and transfer. *Comptes Rendus. Biologies*, *338*(4), 278–283.

Weis, V. M., Davy, S. K., Hoegh-Guldberg, O., Rodriguez-Lanetty, M., & Pringle, J. R. (2008). Cell biology in model systems as the key to understanding corals. *Trends in Ecology & Evolution*, *23*(7), 369–376.

Weisburg, W. G., Barns, S. M., Pelletier, D. A., & Lane, D. J. (1991). 16S ribosomal DNA amplification for phylogenetic study. *Journal of Bacteriology*, *173*(2), 697–703.

Wickham, H. (2016). *ggplot2: Elegant Graphics for Data Analysis*. Springer-Verlag New York.

Wickham, H., Averick, M., Bryan, J., Chang, W., McGowan, L. D., François, R., Grolemund, G., Hayes, A., Henry, L., Hester, J., Kuhn, M., Pedersen, T. L., Miller, E., Bache, S. M., Müller, K., Ooms, J., Robinson, D., Seidel, D. P., Spinu, V., … Yutani, H. (2019). Welcome to the tidyverse. *Journal of Open Source Software*, *4*(43), 1686.

Wickham, H., Hester, J., Chang, W., & Bryan, J. (2022). *devtools: Tools to Make Developing R Packages Easier* [R package version 2.4.5].

Wiegel, J., Tanner, R., Rainey, F. A., et al. (2006). An introduction to the family Clostridiaceae. *The Prokaryotes*, *4*, 654–678.

Wood, C. M., Farrell, A. P., & Brauner, C. J. (2012). *Homeostasis and toxicology of essential metals* (Vol. 1). Academic Press.

Wood-Charlson, E. M., & Weis, V. M. (2009). The diversity of C-type lectins in the genome of a basal metazoan, *Nematostella vectensis*. *Developmental & Comparative Immunology*, *33*(8), 881–889.

Xiang, N., Rädecker, N., Pogoreutz, C., Cárdenas, A., Meibom, A., Wild, C., Gärdes, A., & Voolstra, C. R. (2022). Presence of algal symbionts affects denitrifying bacterial communities in the sea anemone *Aiptasia* coral model. *ISME Communications*, *2*(1), 105.

Xu, L.-L., McIlroy, S. E., Ni, Y., Guibert, I., Chen, J., Rocha, U., Baker, D. M., & Panagiotou, G. (2025). Chemical pollution drives taxonomic and functional shifts in marine sediment microbiome, influencing benthic metazoans. *ISME Communications*, ycae141.

Yamamoto, S., Hirano, Y. M., Hirano, Y. J., Trowbridge, C. D., Akimoto, A., Sakai, A., & Yusa, Y. (2013). Effects of photosynthesis on the survival and weight retention of two kleptoplastic sacoglossan opisthobranchs. *Journal of the Marine Biological Association of the United Kingdom*, *93*, 209–215.

Yee, D. P., Juery, C., Toullec, G., Catacora-Grundy, A., Lekieffre, C., Wangpraseurt, D., & Decelle, J. (2025). Physiology and metabolism of eukaryotic microalgae involved in aquatic photosymbioses. *New Phytologist*.

Yorifuji, M., Takeshima, H., Mabuchi, K., Watanabe, T., & Nishida, M. (2015). Comparison of *Symbiodinium* dinoflagellate flora in sea slug populations of the *Pteraeolidia ianthina* complex. *Marine Ecology Progress Series*, *521*, 91–104.

Yuyama, I., & Higuchi, T. (2014). Comparing the effects of symbiotic algae (*Symbiodinium*) clades C1 and D on early growth stages of *Acropora tenuis*. *PLoS One*, *9*(6), e98999.

Zeeshan, M., Murugadas, A., Ghaskadbi, S., Ramaswamy, B. R., & Akbarsha, M. A. (2017). Ecotoxicological assessment of cobalt using *Hydra* model: ROS, oxidative stress, DNA damage, cell cycle arrest, and apoptosis as mechanisms of toxicity. *Environmental Pollution*, *224*, 54–69.

Zhang, J., Song, L., Pedersen, D. V., Li, A., Lambris, J. D., Andersen, G. R., Mollnes, T. E., Ma, Y. J., & Garred, P. (2020). Soluble collectin-12 mediates C3-independent docking of properdin that activates the alternative pathway of complement. *Elife*, *9*, e60908.

Zhou, Z., Zhao, S., Ni, J., Su, Y., Wang, L., & Xu, Y. (2018). Effects of environmental factors on c-type lectin recognition to zooxanthellae in the stony coral *Pocillopora damicornis*. *Fish & Shellfish Immunology*, *79*, 228–233.

Zhukova, N. V., & Eliseikina, M. G. (2012). Symbiotic bacteria in the nudibranch mollusk *Dendrodoris nigra*: Fatty acid composition and ultrastructure analysis. *Marine Biology*, *159*, 1783–1794.

Zhukova, N. V., Eliseikina, M. G., Balakirev, E. S., & Ayala, F. J. (2022). Multiple bacterial partners in symbiosis with the nudibranch mollusk *Rostanga alisae*. *Scientific Reports*, *12*, 169.

Zverlov, V. V., Kellermann, J., & Schwarz, W. H. (2005). Functional subgenomics of *Clostridium thermocellum* cellulosomal genes: Identification of the major catalytic components in the extracellular complex and detection of three new enzymes. *Proteomics*, *5*(14), 3646–3653.

Acknowledgements

The work presented in this dissertation was carried out over the course of four years. Four years full of discovery, learning, laughter, and the occasional moment of doubt. Looking back, I realise that this journey was never a solitary one, and I am deeply grateful to all the people who have supported, inspired, and accompanied me along the way.

First and foremost, I would like to express my sincere gratitude to Prof. Dr. Angelika Preisfeld, my doctoral supervisor, for her continuous support, guidance, and trust. Thank you for giving me the freedom to explore my own ideas while always being there with advice, patience, and encouragement. Your belief in my work made this thesis possible.

My heartfelt thanks also go to Prof. Dr. Gregor Christa, who has played an important role in my scientific journey from the very beginning. You were the one who first introduced me to the fascinating world of photosymbiosis during my very first research project and have continued to support me ever since, from Bonn to Aveiro and finally to Wuppertal. Your enthusiasm for science and your energy have been a constant source of motivation and inspiration.

I would also like to thank all members of the Zoology working group at the BUW, especially Sabine Stratmann, Dr. Nadine Domröse, Max Stutzenberger, and Pia Münninghoff. Sharing the past years of teaching, preparing courses together, and facing the everyday challenges of academic life has been a genuine pleasure.

A very special thank you goes to my fellow PhD students and lab companions Dr. Jenny Melo Clavijo, Max Fischer, Jonas Dreesmann, and Marcellina Rola. Thank you for every lunch break filled with scientific discussions, laughter, and shared frustrations about experiments that did not go as planned. I am grateful for your friendship, your help, and the sense of community we built together, it made all the difference. A very warm thank you also goes to all the students I supervised during my PhD and contributed in so many ways to this work. I hope that working on this research was at least a little bit of fun and maybe even inspired some of you to see the beauty of the fascinating world of sea slugs.

I also want to thank the many wonderful women I met during my scientific path. Above all Dr. Jessica Goodheart, Dr. Sofia Paz Sedano, Rebecca Lopez-Anido and Lina Raubold. Our time together in New York was unforgettable and reminded me of what truly matters in science: curiosity, creativity, and the joy of discovery. Thank you for bringing back the spark and for showing me that science can be both brilliant and fun. My deepest gratitude also goes to Prof. Dr. Heike Wägele, who first sparked my fascination for sea slugs and welcomed me into her research group when I was still a bachelor student. Without your early encouragement and support, I might never have followed this path. You planted the seed for everything that came after, and I will always be thankful for that.

Finally, I would like to thank all the colleagues that I had the chance to collaborate with during the course of this project and contributed to the work here presented: Dr. Sabrina Bleidißel, Dr. Gilles Gasparoni, Dr. Sascha Tierling, Dr. Cessa Rauch, Prof. Dr. Julia Bornhorst and Dr. Alicia Thiel. I am deeply grateful for your valuable feedback, insightful discussions, and the time and expertise you shared. Your input greatly enriched the quality and depth of this work.

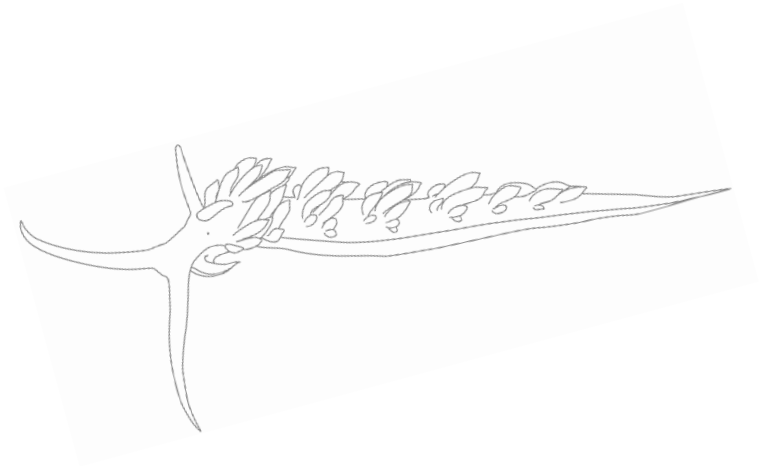

Declaration of Authorship

Hiermit erkläre ich, dass ich, Corinna Sickinger:

- die von mir eingereichte Dissertation selbständig und ohne fremde Hilfe verfasst habe,
- nur die in der Dissertation angegebenen Hilfsmittel benutzt und alle wörtlich oder inhaltlich übernommenen Stellen als solche unter Angabe der Quelle gekennzeichnet habe,
- die Dissertation weder in der vorliegenden noch in ähnlicher Form bei anderen Hochschulen oder wissenschaftichen Instituten vorgelegt habe und
- bislang keine Promotionsversuche unternommen habe.

Ich bin damit einverstanden, dass meine Dissertation wissenschaftlich interessierten Personen oder Institutionen zur Einsichtnahme zur Verfügung gestellt werden kann.

Wuppertal,

Corinna Sickinger